# Design, Synthesis, and Preclinical Evaluation of Radiolabeled Bombesin Analogues for the Diagnosis and Targeted Radiotherapy of Bombesin-receptor Expressing Tumors

**Inauguraldissertation**

zur

Erlangung der Würde eines Doktors der Philosophie

vorgelegt der

Philosophisch-Naturwissenschaftlichen Fakultät

der Universität Basel

von

Hanwen Zhang

aus Beijing, Volksrepublik China

Basel, 2007

Genehmigt von der Philosophisch-Naturwissenschaftlichen Fakultät auf Antrag von

Prof. Dr. Helmut R. Maecke

Prof. Dr. Helma Wennemers (Korreferentin)

Basel, den 10. Mai 2005

Prof. Dr. Hans-Jakob Wirz (Dekan)

# ACKNOWLEDGEMENTS

This work was performed in the Division of Radiological Chemistry, Department of Radiology, University Hospital Basel, Switzerland, from December 2000 to April 2005, and was supported financially by the Swiss National Science Foundation, Mallinckrodt Med, and the "Amt für Ausbildungsbeiträge".

First, I would like to express my appreciation to my supervisor, Prof. Dr. Helmut R. Maecke, for giving me the opportunity to perform this work in the lab, and also for his guidance and support, especially for his great kindness, not only pertaining to my studies, but also in practical matters for my personal life.

I thank Prof. Dr. Helma Wennemers that she was willing to take the responsibility to work on my thesis as a co-referee even though she was very busy on her own work when I was going to graduate.

This work is clearly interdisciplinary and was only possible due to strong cooperation with our lab co-partners. I am very grateful to them:

Prof. Reubi and his technician, Ms. Beatrice Waser (Division of Cell Biology and Experimental Cancer Research, Institute of Pathology, University of Bern) who kindly helped us during the whole four years to determine the binding affinity to the receptors expressed on tissue; Prof. Reubi's cooperation was especially beneficial for me.

Dr. Ilse Novak-Hofer and Dr. Michael Honer (Center for Radiopharmaceutical Sciences, Paul Scherrer Institute) who kindly supplied $^{64/67}$Cu, performed microPET imaging with $^{64}$Cu-labeled peptide.

Dr. Jochen Schumacher and his co-workers (Department of Diagnostic and Therapeutic Radiology, German Cancer Research Center, Heidelberg) who tested two of the $^{68}$Ga-labeled peptides using PET imaging in his lab;

PD Dr. Anna Seelig and her group (Department of Biophysical Chemistry, Biocenter of the University of Basel) who kindly allowed me to use their CD-instrument for determining the secondary structure of peptides in her lab and subsequently showed me how to perform the measurement and helped to evaluate the data.

Dr. Theodosia Maina and her group (Institute of Radioisotopes-Radiodiagnostic Products, National Center for Scientific Research "Demokritos", Athens) who provided experimental cooperation and valuable communication.

I deeply thank the mass spectrometry team of Novartis AG (Basel) for gratuitous analytical support; in particular, Dieter Staab and Dr. Ueli Ramseier helped me to analyze a large amount of samples with MALDI.

And I also thank the animal lab staff: Ulrich Schneider, Heinz Künzi, Thomas Aerni, Esther Vögtli, Sybille Hugi, Rodrigo Recinos, Marcus Ceramella, Catherine Meyer, and Nicole Caviezel (University Hospital Basel) who carefully and kindly took care of the animals.

I thank Prof. J. Mueller-Brand, head of the Institute of Nuclear Medicine, and the clinical staff for their kind help in scanning tumor-bearing animals. I am grateful to the clinical group in our lab for helping me to order many materials for my studies, especially Pia Powell, Daniela Biondo, Priska Preisig, Karin Hinni and Nadia Mutter. I give my thanks to Dr. Christian Waldherr, Dr. Jianhua Chen, Dr. Martin Walter and Dr. Damian Wild for their valuable help in performing animal experiments.

Special thanks go to postdoc Jörg Simon Schmitt, Sandrine Fraysse-Phisbien and Simona Ciobanu for their kind support on my relative projects. Many thanks also to all the present and past members of the lab: Mihaela Ginj, Patricia Dos Santos Antunes, Valerie Hinard, Sibylle Tschumi, Stephan Good, Daniel Storch, Michi Frischknecht, Klaus-Peter Eisenwiener, for providing a very enjoyable working atmosphere. It has been a great pleasure working in the lab and having valuable discussions with them.

I also would like to thank Evelyn Peters for correcting my pronunciation with great patience, and her kind help for proof-reading my thesis and one of my published papers. I thank Claudine Pfister for her hard work on the manuscript preparation and grammar correction.

I am grateful to all my Chinese friends, who made my stay in Basel extremely delightful due to their valuable discussions, communication and encouragement.

Last but not least, I would like to thank my family for their love and encouragement, especially my wife, her great support and companionship during my PhD study in Basel, Switzerland.

## Table of Contents

# Part I: INTRODUCTION

## 1.1 Background

Since its inception, a main attraction of nuclear medicine has been the potential application of radioactive tracer principles to "follow" organ function and metabolic pathways under physiological and pathological conditions. Since two or more decades, the advent and progress of molecular biology have led to the development of a new approach for imaging and therapy, the so-called molecular nuclear medicine, which specifically localizes the target in vivo, like the relationship between a "key" and a "lock".

The first introduction of radioimmunodetection (RAID) and radioimmunotherapy (RAIT) was the use of isotopes conjugated to intact monoclonal antibodies (MoAbs) (1), which were considered as potentially ideal agents to target specific antigens for the following reasons: they are stable in blood, typically have nanomolar affinity to their targets, their bonding and nonbonding domains are separated physically, and they tolerate conjugation to chemotherapeutic agents or radioisotopes. After 20 years of pursuing this direction (2), RAIT has started to play a role in the treatment of hematopoietic neoplasms, especially in the therapy of non-Hodgkin's lymphomas. Several drawbacks were encountered during the application of MoAbs in treating solid tumors: modest response rates in patients with solid tumors, poor accumulation in tissues, slow blood clearance with unfavorable target visualization, and generation of human anti-mouse antibodies (HAMA). For example, the US Food and Drug Administration approved $^{111}$In-labeled ProstaScint (3) for pretreatment evaluation of metastatic prostate adenocarcinoma in high-risk patients and post-prostatectomy assessment of recurrent disease in patients with a rising prostate-specific antigen level; however, the patient receives a relatively high irradiation dose due to the prolonged circulation. The same MoAb-conjugate labeled with $^{90}$Y was used as a therapeutic agent by Kahn et al (4). They found that RAIT for occult metastastic prostate cancer at a dose of 333 MBq/m$^2$ body surface did not lower serum PSA, but caused significant hematologic toxicity in patients.

Therefore, it is necessary and challenging to develop a more efficient approach to overcome the drawbacks in the use of radioconjugated antibodies, and especially, for targeted radiotherapy of minimal or micrometastatic disease. Up to now, a number of approaches for treating solid tumors have been prompted to improve the radiation dose delivered and to achieve the ultimate goal: the delivery of tumoricidal doses while sparing normal tissue. Among these approaches, the peptide/receptor system has been the most outstanding method.

### 1.2 Peptide and receptor system

In fundamental biological processes, peptides are more important elements than any other class of molecules, designed by nature for stimulating, inhibiting, or regulating numerous biological functions through their respective receptors. The molecular basis for the use of radiopeptides was found to be that peptide receptors are overexpressed by certain tumors (5). Before a peptide can be used in nuclear medicine, it has to be modified to carry radioisotopes to the target, and at the same time, still maintain its high, biological activity. The clinical impact of radiolabeled peptides is at the diagnostic level: *in vivo* receptor scintigraphy for the localization of tumors and their metastases; and at the therapeutic level: peptide receptor mediated radiotherapy of tumors emerges as an important treatment option. Despite the fact that the investigation of radiopeptides appeared to be only a small niche in the very large field of oncology, the targeting of overexpressed peptide receptors in tumors by small peptides has become a very strong focus of interest in nuclear medicine (6). At the 100-year anniversary of nuclear medicine, Henry Wagner named the peptide approach in nuclear oncology as one of the most promising fields for the next decade; gastroenterologists and endocrinologists are also attracted by the concept of peptide receptor targeting.

Compared to antibodies, peptides are smaller-sized molecules containing fewer than 100 amino acids with a molecular mass of <10 000 Da; and “small peptides” refers to peptides with fewer

than 30 amino acids or a molecular mass of <3500 Da, which has proved most favorable in nuclear medicine. Small peptides display high specific affinity to their receptors. Peptides show a lower (or no) antigenicity, faster clearance, and more rapid penetration of tissue and tumor than MoAbs; furthermore, they can be synthesized, modified and stabilized more easily and less expensively.

Table 1 Peptides, their functions and the target diseases and/or cell expressing receptors[a]

| Peptide | Function | Target/disease/receptor |
|---|---|---|
| Bombesin (BN) | CNS[b] & GI tract activity. Suppresses feeding in rats | Glioblastoma, SCLC, prostate, breast, gastric, colon and pancreatic CA |
| CCK-B[c]/gastrin | Gallbladder contraction/acid secretion | SCLC, GI tumors, ovarian cancer, medullary thyroid CA, homology to VIP receptors |
| Epidermal growth factor (7) | Growth promoter | Breast CA, glioblastoma, head and neck, renal cell tumors |
| GRP | Gastrin secretion | GRP/neuromedin B, see Bombesin |
| α-MSH | Regulation of skin pigmentation | Melanoma cells |
| Somatostatin & its analogues | Growth hormone release inhibiting factor | Neuroendocrine tumors, SCLC, breast CA, lymphoma, subtypes 1-5 |
| VIP | Vasodilator, growth promoter, immunomodulator | Subtypes 1 & 2, epithelial tumors, breast CA, Colon CA, NSCLC, pancreatic CA, prostate, bladder and ovarian CA |

[a] Compiled from Okarvi (8), Reubi (9-11) and Heasley (12).

[b] CNS=central nervous system, GI=gastrointestinal, SCLC=small cell lung cancer, CA=cancer and NSCLC=Non-small cell lung cancer.

[c] CCK=cholecystokinin, GRP=gastrin releasing peptide, VIP=Vasoactive Intestinal Peptide, and α-MSH= α-melanocyte stimulating hormone.

Up to now, there are over 850 well-characterized endogenous peptides from which a suitable peptide or its analogues can be chosen for an intended application (13, 14). Peptide receptors are located on the plasma membrane and, upon binding of a ligand, allow for the internalization of the receptor-ligand complex. Radionuclides coupled to tumor specific peptides are currently under development, preclinical investigation and in clinical trials. Table 1 (13) shows a selected list of peptides, their functions, and target cells that are presently under investigation as radiopeptides. Among these radiopeptides, the most outstanding example is the analogues of

somatostatin. Some somatostatin derivatives have become commercially-available, FDA-approved drugs (6, 15), such as $^{111}$In-DTPA-OctreoScan®, a somatostatin receptor binder, that is well established for the diagnosis of neuroendocrine tumors. NeoTect, another approved somatostatin-receptor-binding analogue labeled with $^{99m}$Tc shows good specificity for lung cancer detection. Octreotide and its analogues labeled with $^{111}$In, $^{90}$Y, $^{64}$Cu or $^{177}$Lu are under study for the treatment of patients and present promising results (16-18). Especially in high doses, the $^{90}$Y-labeled [DOTA-Tyr$^3$]octreotide has the capacity to reduce or at least stabilize the tumor size, which usually results in a remarkable improvement of life quality. All these results have led to a growth in the development of radiolabeled peptides for diagnostic and therapeutic application in oncology. In particular, it has fascinated many researchers to develop bombesin (BN) conjugated radioligands for BN receptors (15, 19) because BN and its receptors are associated with many types of human cancer (20, 21).

### 1.3 Bombesin and its receptors (Table 2)

Table 2 Bombesin and its receptor subtypes

| Subtype | Native Peptide | | Origin |
|---|---|---|---|
| NMB-R | Neuromedin B (NMB) | Gly-**Asn-Leu-Trp-Ala-Thr-Gly-His-Phe-Met-$NH_2$** | Mammalian |
| GRP-R | Gastrin Releasing Peptide (GRP) | Val-Pro-Leu-Pro-Ala-Gly-Gly-Gly-Thr-Val-Leu-Thr-Lys-Met-Tyr-Pro-Arg-Gly-Asn-**His-Trp-Ala-Val-Gly-His-Leu-Met-$NH_2$** | Mammalian |
| BRS-3 | | Not identified | Mammalian |
| BRS-4 | Bombesin (BN) | Pyr-Glp-Gln-Arg-Leu-Gly-Asn-**Gln-Trp-Ala-Val-Gly-His-Leu-Met-$NH_2$** | Amphibian |
| | | Pyr-Glp-Gln-Arg-Leu-Gly-Asn-**Gln-Trp-Ala-Val-Gly-His-Phe-Met-$NH_2$** | |

The sequences for the native peptides that bind to the mammalian bombesin receptor subtypes NMB-R and GRP-R and the amphibian bombesin receptor subtype BRS-4 are represented. Two distinct forms of the peptide bombesin have been identified for the BRS-4 receptor subtype differing by either -Leu$^{13}$- or -Phe$^{13}$-. A high affinity native peptide has not been identified for the mammalian bombesin receptor subtype BRS-3.

In 1971, Anastasi et al (22) initiated the investigation of the bombesin (BN) receptor system with the isolation of the tetradecapeptide bombesin from the skin of the frog Bombina bombina. The mammalian counterpart of bombesin, a 27 amino acid peptide called gastrin releasing peptide (GRP) was isolated from the porcine stomach by McDonald et al in 1979 (23). Successively, based on a stimulating effect on rat uterus contraction, Minamino et al purified neuromedin B (NMB), which is structurally related to ranatensin, from the porcine spinal cord (24) in 1983.

The bombesin receptor family currently comprises four receptor subtypes of which three have been identified from mammalian origin. These subtypes are classified as the NMB preferring receptor (NMB-R), the GRP preferring receptor (GRP-R) whose density in human cancer is very high, the orphan BN receptor subtype-3 (BRS-3), and the BN receptor subtype 4 (BRS-4) that was isolated and characterized only in amphibian animals. Up to now, the native peptide ligand showing high binding affinity to the BRS-3 subtype has not yet been identified.

### 1.4 Pan-bombesin ligands

BN receptors have been shown to be overexpressed in various major human cancers like prostate, breast and small cell lung cancer (21): 26 of 26 prostate cancers, 41 of 57 breast cancers, and 5 of 5 gastrinomas expressed predominantly GRP receptors; 11 of 24 intestinal, 1 of 26 bronchial, and 1 of 1 thymic carcinoids had preferentially NMB receptors; 9 of 26 bronchial carcinoids, 1 large cell neuroendocrine lung carcinoma, and 4 of 9 small cell lung carcinomas had preferentially BRS-3 receptors, whereas 3 of 9 small cell lung carcinomas had GRP receptors. It is also interesting that renal cell carcinomas had GRP receptors in 6 of 16 cases and BRS-3 receptors in 4 of 16 cases. These data show that each BN receptor subtype may be overexpressed on different types of tumors, and the same type of tumor may co-express more than one BN receptor subtype, indicating that universal bombesin analogues have the potential to

visualize these tumors with high incidence. A universal ligand, [D-Tyr$^{6}$, βAla$^{11}$, Phe$^{13}$, Nle$^{14}$]BN (6-14), which has high affinity to all receptor subtypes, was developed by Mantey et al (25) and Prahan et al (26).

These findings prompted me to develop conjugates based on a slightly modified (Thi$^{13}$ vs. Phe$^{13}$) universal BN ligand [D-Tyr$^{6}$, βAla$^{11}$, Phe$^{13}$, Nle$^{14}$] BN (6-14), to label them with $^{111}$In, $^{177}$Lu and $^{90}$Y for targeting BN receptor-expressing tumors and to evaluate their biological behavior (27). Meanwhile, based on [D-Tyr$^{6}$, βAla$^{11}$, Phe$^{13}$, Nle$^{14}$]BN (6-14), Moody et al (28) developed a camptothecin-bombesin (CPT-BN) conjugate via a labile linker with site-specific cytotoxicity. CPT-L2-BA3, one of these CPT-BN analogues displayed high affinity to all three BN receptor subtypes and functioned as a full agonist for each subtype. [$^{125}$I]-CPT-L2-BA3 rapidly internalized into cells expressing each BN receptor profile and subsequently into cytoplasmic compartments. HPLC analysis of the internalized ligands showed that 40% were intact, 25% were metabolized by releasing free CPT, and 35% were metabolized to other breakdown products. CPT-L2-BA3 inhibited the growth of NCIH1299 non-small cell lung cancer cells and was cytotoxic for cells transfected with each class of BN receptors. However, it had significantly less effect in cells lacking BN receptors. These results indicate that CPT-L2-BA3 is a potent agonist that is cytotoxic for cells overexpressing any of the three BN receptor classes and might be a useful prototype to explore the effectiveness of delivering tumor-specific cytotoxics.

### 1.5 BN analogues focusing on GRP-R

The expression of GRP-R (the mammalian counterpart of BN receptors) (29) in primary prostatic invasive carcinoma was present in 100% of the tissues tested (30 of 30 cases), and in 83% of these cases, GRP receptor expression was determined to be high or very high (>1000 dpm/mg). More interestingly, of 26 patients with high-grade prostatic intraepithelial neoplasia, all but one showed high to very high densities of GRP receptors. It was also demonstrated that 4 out of 7 of

androgen independent prostate cancer bone metastases were GRP receptor positive. Halmos et al (30) examined the binding of radioiodinated bombesin to the membrane obtained from 100 individual human breast carcinomas and found significant GRP receptor expression in 33% of these samples.

Apart from prostate carcinoma, GRP receptors were also overexpressed in other types of tumors. For example, 50 of 68 breast tumors (74%) expressed GRP receptors, the relative mean density being 9,819±530 dpm/mg tissue (31); and 16 of 19 gastrointestinal stromal tumors (GIST) expressed GRP receptors having a density of 7864±9629 dpm/mg tissue (32). These results clearly make the GRP receptor an attractive target for diagnostic and therapeutic purposes.

### 1.5.1 Radiopeptides derived from the untruncated BN analogues

Up to now, different research groups have coupled chelators to [$Lys^3$]-BN. For example, diaminedithiol (DADT) was conjugated to the side-chain amine of $Lys^3$ by Baidoo et al (33) in 1998. Their results demonstrated that these conjugates had high affinity for the GRP receptor in rat brain cortex membranes with $K_i$ values of 3.5-7.4 nM by using [$^{125}$I-$Tyr^4$]-BN as a radioligand. *In vivo* biodistribution analysis showed little uptake in non-target tissue, with excretion being primarily via the hepatobiliary pathway. Recently, Chen et al (34) used DOTA to replace DTPA to couple with [$Lys^3$]BN for the labeling with $^{64}$Cu. Their results showed specific binding affinity ($IC_{50}$ value: 2.2±0.5nM) to PC-3 cells by using [$^{125}$I-$Tyr^4$]-BN as a radioligand and accumulation in human prostate adenocarcinoma xenografts (androgen-independent PC-3 tumor: 5.62±0.08 %ID/g at 0.5h p.i.). Breeman et al (35) reported on the design and development of radiolabeled BN conjugates based on BN for the labeling with $^{111}$In, e.g. DTPA-[$Pro^1$, $Tyr^4$]BN. Their data showed that these ligands had high affinity for the GRP receptor in 7315b rat pituitary tumor cell membranes, and *in vitro* internalization inherent to agonistic binding and high uptake in rat pituitary tumors.

### 1.5.2 Truncated BN analogues labeled with different radioisotopes

GRP and bombesin share amidated C terminus sequence homology (36) in the final 7 amino acids, -Trp-Ala-Val-Gly-His-Leu-Met-$NH_2$. Deletion of the N-terminus sequence $pGlu^1$-$Gln^2$-$Arg^3$-$Leu^4$-$Gly^5$- from the BN molecule caused practically no loss of affinity and intrinsic activity, but further shortening of BN gave rise to a gradual reduction of both parameters. On the other hand, deletion of only two ($Leu^{13}$-$Met^{14}$) or three ($His^{12}$-$Leu^{13}$-$Met^{14}$) amino acids from the C-terminus afforded BN fragments with low affinities (BN(1-12) and BN(1-11)) and, in the case of BN(1-11), also a reduced intrinsic activity. GRP and its two fragments GRP(14-27) and acetyl-GRP(20-27)) exhibited the same intrinsic activity as BN, and these two fragments were found to be either as potent or slightly more potent than BN itself. The sequence $His^{12}$-$Leu^{13}$-$Met^{14}$-$NH_2$ seems to be critical to fully activate BN receptors; and the sequence BN(7-14) was regarded to be sufficient for the specific binding interaction with the gastrin-releasing peptide receptor (36).

Gali et al (37) developed and demonstrated the *in vivo* stability of $^{99m}Tc$/$^{188}Re(V)$-$P_2S_2$-5-Ava-BN(7-14). The $IC_{50}$ value of $ReO_2$-$P_2S_2$-5-Ava-BN(7-14) to Swiss 3T3 fibroblasts reached 0.8±0.4 nM by using the native [$^{125}I$-$Tyr^4$]-BN as radioligand. Furthermore, preliminary biodistribution assays in PC-3 tumor bearing SCID mice (SCID = Severely Compromised Immunodeficient) showed a tumor uptake of 4.7±0.8 %ID/g at 1h. However, this is still no further report of clinical trial from a therapeutic application of $^{188}Re$-labeled peptides.

La Bella et al introduced an "organometallic" labeling strategy to conjugate $^{99m}Tc$ to BN analogues (38). Despite its high affinity to GRP receptors ($IC_{50}$: 2.0nM), [$^{99m}Tc(CO)_3$-Nα-histidinyl acetate]-BN(7-14) localizes rather poorly in PC-3 tumors (0.6±0.1% ID/g, 1.5h p.i.).

Smith et al (39) reported on the *in vitro*/*in vivo* evaluation of [$^{99m}Tc$(**X**)$(CO)_3$-Dpr-SSS-BN(7-14)] (Dpr=2,3-Diaminopropionic Acid, X=$H_2O$ or $P(CH_2OH)_3$) in GRP receptor specific tissue.

These $^{99m}$Tc(I)-labeled conjugates retained high binding affinity (0.9±0.2nM) and specific targeting of PC-3 xenografts (3.7±0.9%ID/g at 1h p.i.).

Hoffman et al (40) showed that the *in vivo* uptake of [$^{111}$In]-DOTA-8-Aoc-BN(7-14) in human prostate PC-3 xenografted flank tumors was 3.63±1.11 %ID/g at 1h and that affinity for PC-3 cells *in vitro* was high. Pre-clinical evaluation of $^{177}$Lu-DOTA-8-Aoc-BN(7-14) by Smith et al (41) exhibited an $IC_{50}$ of 0.5±0.1nM in GRP receptor-expressing PC-3 tumor cells. Receptor-mediated tumor targeting of the PC-3 xenografted SCID mice resulted in tumor uptake and retention values of 4.22±1.09 %ID/g, 3.03±0.91%ID/g, and 1.54±1.14%ID/g at 1h, 4h, and 24h, respectively. Rogers et al (42) labeled the same ligand with $^{64}$Cu for PET imaging. This radiotracer bound to PC-3 cells with a $K_d$ of 6.1±2.5nM. Its biodistribution in PC-3 xenografted athymic mice showed significantly lower tumor/non-target ratios despite the fact that the tumor accumulation was similar to that of the same peptide labeled with $^{177}$Lu.

Recently, Chen et al (43) reported that [$^{177}$Lu]-AMBA (DOTA-Gly-[4-aminobenzoyl]-BN (7-14)) has high affinity to two human BN receptor subtypes (NMB-R: 0.9nM, and GRP-R: 0.8nM), and does not bind to the BRS-3 receptor (>1μM). Its biodistribution showed high uptake in PC-3 tumors (at 1h: 5.5%ID/g, and at 24h: 3.4±0.9%ID/g).

According to these published data, conjugated BN(7-14) analogues have exhibited high affinity to the human GRP receptor (PC-3 cells). However, all accumulations in PC-3 tumors were relatively low and the ratios between tumor and background or kidneys were not high either.

### 1.5.3 Influence of spacers between BN (7-14) and chelator on biological characteristics

According to our unpublished data, a chelator which is directly coupled to the peptide will lead to a significant loss of binding affinity to GRP receptors. Therefore, it was necessary to insert a spacer between the peptide and the chelate. Based on the sequence of BN (7-14), Smith et al (44) constructed [$^{99m}$Tc-$N_3S$]-**X**-BN (7-14) ($N_3S$=dimethylglycyl-L-seryl-L-cysteinylglycinamide. **X:**

0-Carbon, β-Ala (β-alanine), 5-Ava (5-aminovaleric acid), 8-Aoc (8-aminooctanoic acid), or 11-Aun (11-aminoundecanoic acid)) to study the flexibility of designed $^{99m}$Tc-labeled BN analogues that retain high specific affinity to GRP receptors. They reported that the hydrocarbon spacer group could be varied from at least 3 to 8 carbon atoms in length without compromising the binding affinity to GRP receptors (0.52±0.25 to 1.00±0.20 nM against PC-3 cells). Biodistribution in SCID mice showed 2.1±0.5% ID/g uptake (1h p.i.) of $^{99m}$Tc-$N_3$S-5-Ava-BN (7-14) in receptor-mediated PC-3 tumors. A similar *in vitro* and *in vivo* evaluation of a series of $^{111}$In-DOTA-**X**-BN(7-14) analogues (**X**: 0 Carbon, β-Ala, 5-Ava, 8-Aoc or 11-Aun) was recently reported by Hoffman et al (40). These conjugates (3, 5, or 8-carbon spacer moieties) also exhibited high binding affinity for GRP receptors in human PC-3 cells ($IC_{50}$ values ranged from 0.6-2.1 nM). *In vivo* biodistribution studies demonstrated that the analogues (**X**=5-Ava or 8-Aoc) had high specific localization in the pancreas (a naturally GRP receptor expressing organ) and efficient clearance from the blood primarily *via* the renal/urinary pathway. The uptake of $^{111}$In-DOTA-8-Aoc-BN(7-14) in human prostate PC-3 xenografted flank tumors was 3.63±1.11%ID/g at 1h. These results suggested that the construction of [$^{111}$In]-DOTA-**X**-BN (7-14) (**X** is a tether of either 5 or 8 carbons in length) might form the basis for developing radiometallated diagnostic or therapeutic radiopharmaceuticals for the targeting of GRP receptor expressing cancers. According to these two studies (40, 44), Smith and Hoffman only focused on the influence of the hydrocarbon spacer between peptide and the chelator, studying and comparing the binding affinity and uptake in human prostate PC-3 xenografted tumors.

### 1.5.4 Radiolabeled antagonistic BN analogues

[D-Phe$^6$]BN(6-13)NHEt and [D-Tyr$^6$]BN(6-13)NHEt have been reported to be high-affinity BN receptor antagonists by Wang *et al* (45) and Jensen *et al* (46), respectively. Breeman WAP et al (35) developed DTPA-[Tyr$^5$, D-Phe$^6$]BN(5-13)NHEt and DTPA-[Tyr$^6$]BN(6-13)NHEt for

labeling with $^{111}$In. Compared to their nonchelated peptides, the $IC_{50}$ values of both ligands are reduced by a factor of 5.5 and 21.5 towards 7315b rat pituitary tumor cell membranes. When DTPA was directly coupled to [D-Phe$^6$]BN(6-13)NHEt, its binding affinity to human prostate cancer tissue was weakened significantly (unpublished data in our and Prof. Reubi's group). Recently, Nock et al (47) reported on $^{99m}$Tc-Demobesin 1 (*[$^{99m}$Tc-N4$^{0-1}$, bzlg$^0$, (D)Phe$^6$, Leu-NHEt$^{13}$, desMet$^{14}$]BN(6-14)*), which exhibited high binding affinity to PC-3 cells. Receptor-mediated tumor uptake in Swiss nu/nu mice bearing human PC-3 xenografts reached up to 16.2±3.1% ID/g at 1h p.i., which is by far the highest uptake in this tumor model by any bombesin based radioligand; however, it also showed high uptake in the liver.

Comparing their binding affinities, it seemed that the negatively charged chelator (DTPA) directly coupled to antagonistic BN analogue led to a loss of binding affinity, whereas the positively charged chelator (N4) improved the binding affinity and afforded a high accumulation in the tumor. These results indicate that the charge at the N-terminus might be a key factor for determining the pharmacological characteristics of BN derivatives.

### 1.5.5 Modification on the 11$^{th}$ position of BN analogues and its biological influences

In 1997, Mantey et al (48) predicted that the important substitution site in the universal ligand ([D-Tyr$^6$, βAla$^{11}$, Phe$^{13}$, Nle$^{14}$] BN (6-14)) is β-alanine in the eleventh position of bombesin. In 2001, the same group published (49) their BRS-3 selective ligands resulting from the βAla$^{11}$ substitution with conformationally restricted amino acids in the prototype ligand [D-Tyr$^6$, βAla$^{11}$, Phe$^{13}$, Nle$^{14}$] BN (6-14) or its D-Phe$^6$ analogue. Two of their synthesized peptides with an (*R*)- or (*S*)-amino-3-phenylpropionic acid substitution for βAla$^{11}$ in the prototype ligand had the highest selectivity for the hBRS-3 over the mammalian BN receptors and did not interact with receptors for other gastrointestinal hormones/neurotransmitters. The results of molecular modeling implied that these two selective BRS-3 ligands had a unique conformation of β-amino acids (11$^{th}$

position). Recently, they (50) replaced βAla$^{11}$ with Apa (3-amino-phenylpropionic acid) derivatives resulting in a much more selective ligand. For example, [D-Tyr$^{6}$, Apa-4Cl$^{11}$, Phe$^{13}$, Nle$^{14}$]BN(6-14), retained high affinity for hBRS-3 (*K*i = 8 nM) and had enhanced selectivity (>230-fold) for hBRS-3 over hGRP-R and hNMB-R.

According to their data, Mantey et al focused mainly on the study of the selectivity of BN (6-14) analogues for hBRS-3 receptors, and evaluated the binding affinities and internalization rates into cells expressing all BN receptor subtypes separately.

In our previous study (27), carnosinase has been proved to be the responsible enzyme to cleave the bond between βAla$^{11}$ and His$^{12}$. All these data suggest that the modification of βAla$^{11}$ changes the peptide conformation, binding affinity and the stability of BN analogues.

### 1.5.6 Potential radiolabeled BN ligands for clinical trials

In designing radiometal-based radiopeptides for cancer, important factors to be considered include the half-life of the radiometal, the mode of decay, and the cost and availability of the isotope. For diagnostic imaging, $^{99m}$Tc, $^{123}$I, $^{67}$Ga and $^{111}$In were used for SPECT imaging and $^{18}$F, $^{64}$Cu and $^{68}$Ga for PET imaging. The half-life of these radionuclides is long enough to allow accumulation in the tumor of the patient while allowing clearance from the body at a relatively rapid rate. The ideal therapeutic radiopeptides should localize at cancerous foci with high specificity, while producing minimal or tolerable radiation damage to normal tissues. Particle-emitting radionuclides are effective for delivering localized cytotoxic doses of ionizing radiation (51). They include β-particle emitters ($^{90}$Y, $^{177}$Lu, $^{186/188}$Re, $^{153}$Sm, $^{64/67}$Cu, $^{131}$I etc), α-particle emitters ($^{211}$At and $^{212}$Bi) and Auger-electrons (52).

By using $^{99m}$Tc-RP527 ([$^{99m}$Tc-$N_3S$]-Gly-5-Ava-BN (7-14), $IC_{50}$(GRP-R): 1.0±0.2nM, PC-3 tumor bearing mice: 2.1±0.5%ID/g at 1h p.i.), Van de Wiele et al (53) published a first study about prostate (n=4) and breast cancer (n=6) patients: the results showed that $^{99m}$Tc-RP527

specifically visualized four of six breast and one of four prostate carcinomas. Since $^{99m}$Tc-Demobesin 1 (*[$^{99m}$Tc-N4$^{0-1}$, bzlg$^{0}$, (D)Phe$^{6}$, Leu-NHEt$^{13}$, desMet$^{14}$]BN(6-14)*) (47) has shown a high affinity to GRP receptors and very high accumulation in PC-3 tumor bearing mice, this ligand was also planned for a patient study, but until now, no data have been reported in the literature.

# Part II: RATIONALE, HYPOTHESIS, AND GOALS

Although radiolabeled bombesin (BN) analogues may be valuable vehicles for delivering radioisotopes to target tumors, there are a few key obstacles to be overcome for their use as oncology drugs like somatostatin derivatives. Ideal BN analogues must tolerate optimization for labeling with the desired radioisotopes, while retaining affinity to their receptors, as well as high internalization into cells, slow efflux from cells, survival in the circulation, and high accumulation in the targeted tumor. In this work, I studied the influence on the pharmacological behavior when BN analogues were optimized to satisfy these requirements.

## 2.1 Pan-Bombesin analogues

### ***Background 1***

As various major human cancers have been shown to overexpress different BN receptor subtypes (21), there is a promising possibility to utilize one pan-bombesin radioligand for the diagnosis and targeted radionuclide therapy of all of these BN receptor-expressing tumors. A universal ligand, D-Phe(or D-Tyr)-Gln-Trp-Ala-Val-βAla-His-Phe-Nle-$NH_2$, has proved to bind to all BN receptor subtypes with high affinity (25, 26) and may be modified for radiolabeling with different radioisotopes. As it is known that the His-Leu peptide bond of the BN analogue (AA-Gln-Trp-Ala-Val-Gly-His-Leu-Met-$NH_2$) is hydrolyzed by peptidase (54), I assumed that this peptidase might also be responsible for cleaving the His-Phe peptide bond of the universal ligand. The strategy of substituting $Phe^{13}$ by the non-natural amino acid (Thi) was used to increase the *in vivo* stability.

### ***Step 1***

DTPA(or DOTA)-GABA-D-Tyr-Gln-Trp-Ala-Val-βAla-His-Thi-Nle-$NH_2$ ligand (GABA= γ-aminobutyric acid) was designed and synthesized for evaluating its biological and pharmacological properties [Paper 1].

## ***Background 2***

According to our unpublished data, the chelator that was directly coupled to the peptide led to a significant loss of binding affinity towards GRP receptors. Therefore it was necessary to insert a spacer between the peptide and the chelator in order to retain a high binding affinity. Furthermore, the type of spacer may influence the pharmacological properties.

## ***Step 2***

Different spacers (Fig. 1) with various chain-lengths were introduced to study their influence on the pharmacological properties [Manuscript 1 and Paper 2].

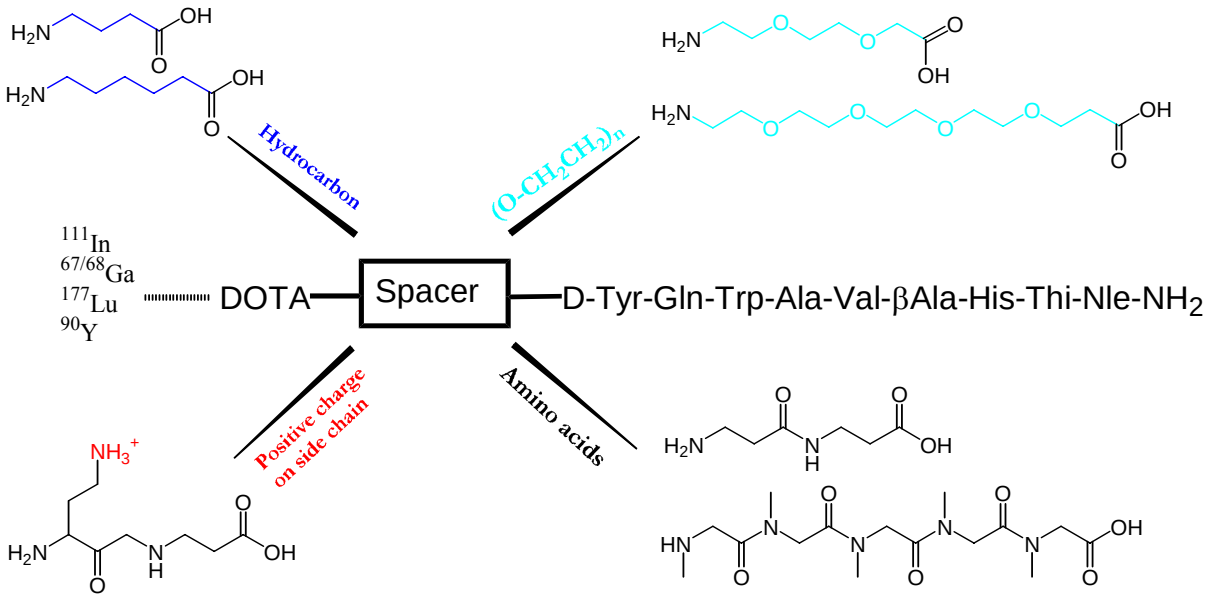


Fig. 1 Differing-spacer modified BN analogues

## ***Goal***

I aimed to develop a pan-bombesin radioligand for labeling with $^{67/68}$Ga, $^{111}$In, $^{177}$Lu, and $^{90}$Y, and to further test it for receptor affinity, receptor subtype profile, uptake and efflux in cells, biodistribution, and metabolic stability.

## 2.2 Modification of the 11th position in bombesin analogues

### ***Background***

1). According to the study of pan-bombesin ([$^{111}$In]-DTPA(or DOTA)-GABA-D-Tyr-Gln-Trp-Ala-Val-βAla-His-Thi-Nle-$NH_2$), carnosinase is responsible for cleaving the bond between βAla$^{11}$ and His$^{12}$. This bond also has been identified as the weakest bond [Paper 1]. This implies that βAla$^{11}$-His$^{12}$ is a very important site for the determination of the stability of BN analogues in serum. In addition, from the published study of D-Tyr-Gln-Trp-Ala-Val-βAla-His-Phe-Nle-$NH_2$ (48, 49), the substitution of β-alanine might change its secondary structure and lead to the BN receptor-selective ligand.

2). The literature (55-57) shows that the azaglycine may influence and stabilize the peptide conformation because the rotation of the N-N bond is restricted by the lone nitrogen pairs approximately perpendicular to one another. From unpublished data (Reubi, Schmitt and Maecke), the introduction of azaglycine on the 11$^{th}$ position of the BN analogue has a slight influence on binding affinity.

3). Based on the [D-Tyr$^6$, β-Ala$^{11}$, Phe$^{13}$, Nle$^{14}$] BN (6-14) (25, 26, 58, 59) or BN (6-14) (60), D-Phe$^6$ or D-Tyr$^6$ is important for keeping the affinity to the GRP receptor, even though BN(7-14) was considered to sufficiently keep biological activity (19, 36, 61).

### ***Goal***

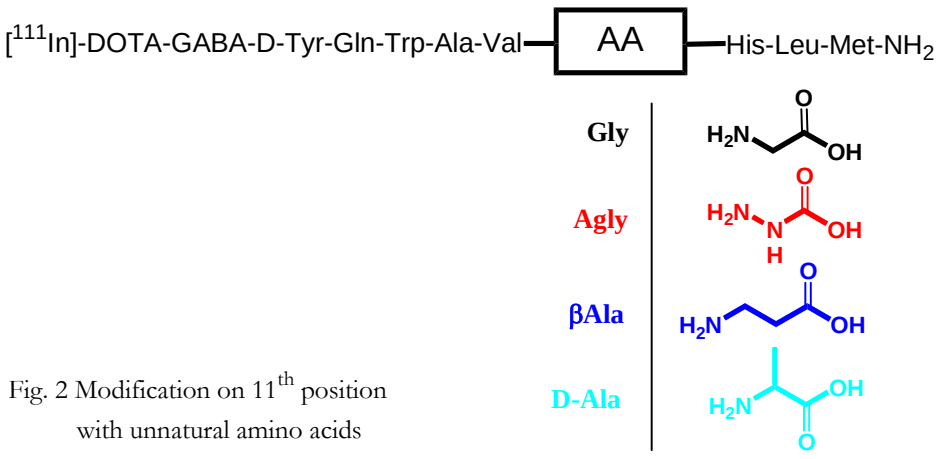


Fig. 2 Modification on 11$^{th}$ position with unnatural amino acids

These findings prompted me to modify the 11$^{th}$ position with azaglycine, D-alanine and β-alanine in the prototype of [D-Tyr$^6$]-BN(6-14) (Fig. 2). The influence on the serum stability and other biological characteristics were studied [Manuscript 2].

## 2.3 Radiocopper-conjugated BN analogue for PET imaging and targeted radiotherapy

### *Background*

1). Positron emission tomography (PET) has become an attractive diagnostic tool in nuclear medicine since 2-deoxy-2-[$^{18}$F]fluoro-D-glucose ($^{18}$FDG) became a commercially available drug. However, the challenge in the use of $^{18}$FDG is its short half-life ($t_{1/2}$ = 110 min), which requires its synthesis to be conducted either at the cyclotron production site or in institutions situated in close proximity (within 1-2 h travel time). Compared to $^{18}$F, $^{64}$Cu (62) has a longer physical half-life ($t_{1/2}$ =12.7h) and may be produced in large amounts of radioactivity by biomedical cyclotrons for distribution to far-away PET centers. Furthermore, $^{64}$Cu has therapeutic potential because of its low energy $\beta^-$ and electron capture (63-65).

2). Copper-67 ($t_{1/2}$ = 61.9h) is a low energy β-emitter that is very suitable for irradiation of small metastases (66, 67). Furthermore, $^{67}$Cu also emits low energy photons, which is particularly useful for pretherapeutic, diagnostic imaging with a γ-camera.

3). Radiocopper was conjugated to small bioactive molecules via bifunctional chelates, such as DOTA (1,4,7,10-tetraaza-1,4,7,10-tetraazacyclododecane)-acetic acid) and CPTA (4-(1,4,8,11-tetraaza-1-yl)-methyl benzoic acid). When the complex was formed between copper and chelate under physiological conditions, the [Cu$^{II}$-DOTA]-peptide was negatively charged (-1) and the [Cu$^{II}$-CPTA]-peptide complex was positively charged (+2) (Fig. 3). Up to now, nothing has been known about the influence of different charges on the pharmacological properties of BN analogues.

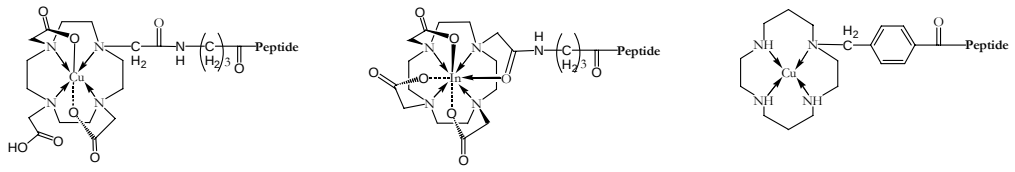


Fig. 3 Metal complexes display different charges under physiological conditions

4). Since hippurane has been shown to facilitate kidney clearance, I assume that a hippurane like structure between chelate and peptide as a spacer may enhance kidney clearance. This structure was formed by modification of CPTA with glycine (Fig. 4).

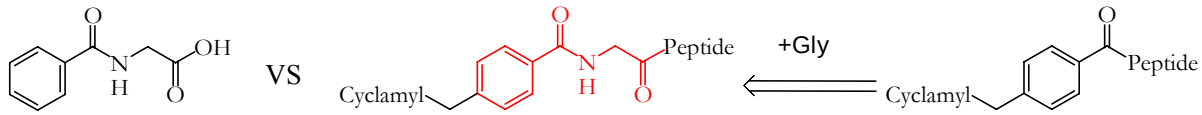


hippurane hippurane like structure

Fig. 4 Hippurane-like structure is formed in BN analogue

5). According to our previously unpublished data (Reubi, Schmitt, Chen and Maecke), the replacement of methionine by norleucine at the 14$^{th}$ position of BN did not change the binding affinity of the peptide because there is little structural difference (-S- versus -$CH_2$-) between these two amino acids. Since β-emission may lead to the radiolytic oxidation of methionine, it seems worthwhile to substitute methionine with norleucine.

## ***Goal***

[$^{64/67}$Cu]-conjugated BN analogues were designed for PET imaging and targeted radiotherapy. Furthermore, $^{64/67}$Cu-labeled peptides were used to study the influence of different charges at the N-terminus, of the hippurane-like structure, and of the modification on the 14$^{th}$ position [Manuscript 3].

## 2.4 Design and evaluation of a clinically potential BN analogue: [$^{68}$Ga/$^{177}$Lu]-DOTA-PESIN

### ***Background***

1). The first radiolabeled BN analogue used in a preliminary patient study was $^{99m}$Tc-RP527. The results indicate that BN analogues can be applied for the diagnosis of hGRP receptor expressing tumors in humans. Comparing the preclinical data of $^{99m}$Tc-RP527 and $^{99m}$Tc-Demobesin 1, the latter (47) displayed more promising characteristics than $^{99m}$Tc-RP527, such as higher accumulation in the tumor. However, these two $^{99m}$Tc-labeled BN derivatives showed relatively low tumor/background ratios, even though $^{99m}$Tc-Demobesin 1 was highly accumulated in PC-3 bearing xenografts. In consideration of these drawbacks, it was necessary to design a novel ligand for improving the tumor-to-background ratios without influencing the tumor uptake.

2). $^{68}$Ga ($t_{1/2}$=67.6min) has become more and more attractive as a PET nuclide, which is eluted from a $^{68}$Ge/$^{68}$Ga generator (68). As the parent radionuclide $^{68}$Ge has a very long half-life (270.8 days), the $^{68}$Ge/$^{68}$Ga generator can afford $^{68}$Ga every four hours and last at least one year. Thus the cost of $^{68}$Ga may become very low. Furthermore, $^{68}$Ga can be available worldwide by the installation of $^{68}$Ge/$^{68}$Ga generators, which are independent of cyclotron irradiation whenever a patient requires PET diagnosis.

3). $^{177}$Lu is a suitable radioisotope for the therapy of small-size primary tumors and metastases (69). However, for the $^{177}$Lu-conjugated BN analogue, the high tumor-to-kidney ratio is the most important factor to achieve a successful therapy of GRP receptor-expressing tumors because side effect on kidneys is frequently a major problem when patients receive high-dose treatment.

4). According to my previous study, poly(ethylene oxide) as a spacer decreases kidney uptake.

## ***Goal***

Based on the advantages of $^{68}Ga/^{177}Lu$, my aim was to design a $^{68}Ga/^{177}Lu$-conjugated BN analogue for PET imaging and targeted radiotherapy [Manuscript 4]. [$^{68}Ga/^{177}Lu$]-DOTA-$PEG_4$-BN(7-14) (DOTA-PESIN) may overcome the above-mentioned drawbacks of $^{99m}Tc$-BN analogues and afford desirable pharmacological properties such as high specific accumulation in the tumor, quick visualization of tumors, and high tumor-to-blood and tumor-to-kidney ratios *in vivo*.

# Part III: SUMMARY OF RESEARCH

### 3.1 Evaluation of pan-bombesin derivatives (Paper 1)

#### *Background*

[D-Tyr$^{6}$, βAla$^{11}$, Phe$^{13}$, Nle$^{14}$] BN (6-14) has been shown to bind to all BN receptor subtypes with fairly high affinity. When conjugated to DOTA/DTPA and labeled with a radioisotope, this peptide may be promising for the diagnosis and targeted therapy of a variety of human tumors including prostate, breast cancer, and gastrointestinal stromal tumors (GIST). However, it has been shown that BN is hydrolyzed by **CD10** (common acute lymphoblastic leukemia antigen)/**NEP** (neutral endopeptidase **24.11**) at the His-Leu peptide bond (54). It is reasonable to assume that this metalloprotease may also cleave the His-Phe peptide bond in the prototype of [D-Tyr$^{6}$, βAla$^{11}$, Phe$^{13}$, Nle$^{14}$] BN (6-14). To increase its *in-vivo* stability, phenylalanine (Phe$^{13}$) was replaced by thienylalanine (Thi), a synthetic amino acid. The subsequent evaluation of these two ligands indicated a similar biological behavior, such as the binding affinity toward hGRP receptors (1.2±0.3 nM (Phe$^{13}$) versus 1.0±0.2 nM (Thi$^{13}$)).

#### *Synthesis and radiolabeling*

All BN analogues involved in my thesis were synthesized on Rink amide MBHA resin using Fmoc strategy. After purification with preparative HPLC, overall yields of the peptide were approximately 30% based on the removal of the first Fmoc group. The pure chelator-conjugated peptide and metallated peptide (purity >97%) were identified by MS/MALDI and analyzed with analytical HPLC.

The DTPA-conjugated peptide was labeled with $^{111}$In by incubation at room temperature. The DOTA-conjugated peptide was labeled with $^{111}$In, $^{90}$Y, and $^{177}$Lu at elevated temperature (95°C, 15-25 min). Labeling yields of >98% at specific activities of >37 GBq μmol$^{-1}$ were achieved.

#### *Binding affinity*

The binding affinity profiles were determined *in vitro* using receptor autoradiography, as described in the literature (21, 70). Human tumors were selected that had previously been shown

to express predominantly one single bombesin receptor subtype; namely either the neuromedin B receptor, gastrin-releasing peptide receptor, or the BRS-3 receptor. Using [$^{125}$I-D-Tyr$^{6}$, βAla$^{11}$, Phe$^{13}$, Nle$^{14}$] BN (6-14) as radioligand, the $IC_{50}$ values of [$In^{III}$]-BZH1 (*[$In^{III}$]-DTPA-GABA-[D-Tyr$^{6}$, βAla$^{11}$, Thi$^{13}$, Nle$^{14}$] BN (6-14)*) and [$Y^{III}$]-BZH2 (*[$Y^{III}$]-DOTA-GABA-[D-Tyr$^{6}$, βAla$^{11}$, Thi$^{13}$, Nle$^{14}$] BN (6-14)*) were measured in competitive binding experiments with successive tissue sections containing tumors expressing either the GRP receptor, NMB receptor or BRS-3 receptor. The results showed that both [$In^{III}$]-BZH1 and [$Y^{III}$]-BZH2 had a high affinity to the GRP receptor, and a medium affinity to the NMB receptor and the BRS-3 receptor. The $IC_{50}$ values of [$In^{III}$]-BZH1 were 3.47±0.32 nM to the GRP receptor, 10.5±3.03nM to the NMB receptor, and 41.7±22.2nM to the BRS-3 receptor. The $IC_{50}$ values of [$Y^{III}$]-BZH2 were 1.40±0.10 nM to the GRP receptor, 4.93±1.03 nM to the NMB receptor and 10.7±4.2 nM to the BRS-3 receptor [Paper 1, Table 1].

### ***Internalization and externalization***

The internalization of the peptide was studied in AR4-2J and PC-3 cells. The results showed fast internalization rates for both $^{111}$In-labeled BZH1 and BZH2 [Paper 1, Fig 5]. Compared to $^{111}$In-BZH2 $^{177}$Lu/$^{90}$Y-labeled BZH2 exhibited a similar internalization rate [Paper 1, Fig 6]. Internalization was specific and receptor mediated as shown by a blocking experiment in the presence of 0.57 μM unlabeled BZH2. The kinetics of the externalization of both peptides [Paper 1, Fig 7] showed that within 2 h, 45% of [$^{111}$In]-BZH1 and 30% of [$^{111}$In]-BZH2 were released from the AR4-2J cells. [$^{111}$In]-BZH1 was used as a leading peptide to identify the structural composition of externalized peptide. Following 2 h of internalization and acid wash of the surface bound peptide, the radioactivity that externalized within 30 min already consisted of approximately 50% intact peptide and 50% $^{111}In(DTPA)^{2-}$ as the only metabolite. At 4 h, the externalized radioactivity consisted of 12.5% intact peptide and 87.5% $^{111}In(DTPA)^{2-}$; whereas at 24 h, only $^{111}In(DTPA)^{2-}$ was found.

## ***Biodistribution***

Biodistribution studies [Paper 1, Table 3, Fig 8] were performed with Lewis rats bearing the AR4-2J rat pancreatic tumor using the $^{111}$In-labeled peptides. Both [$^{111}$In]-BZH1 and [$^{111}$In]-BZH2 displayed rapid blood clearance with less than 0.02% ID/g and 0.01% ID/g, respectively, remaining in blood at 4h. Fast clearance from the GRP-R negative tissues except the kidneys was found as well. [$^{111}$In]-BZH1 and [$^{111}$In]-BZH2 show high uptake values in the AR4-2J tumor and in the GRP-R positive organs (4 h: tumor, 1.71±0.51% ID/g vs. 0.72±0.22% ID/g; pancreas, 3.92±0.86% ID/g vs. 1.96±0.67% ID/g). *In-vivo* competition experiments using 50 µg BZH2 co-injected with [$^{111}$In]-BZH1 (data for [$^{111}$In]-BZH2 in brackets) resulted in an >93% (89%) reduction of tumor uptake and also in a reduction of the uptake in normal GRP-R positive organs (>97% reduction for both radiopeptides in the pancreas). The pharmacokinetics of $^{177}$Lu-BZH2 was very similar to those of $^{111}$In-BZH2. These radioligands showed a relatively fast washout from AR4-2J tumor and GRP receptor positive organs.

## ***Pioneer clinical study***

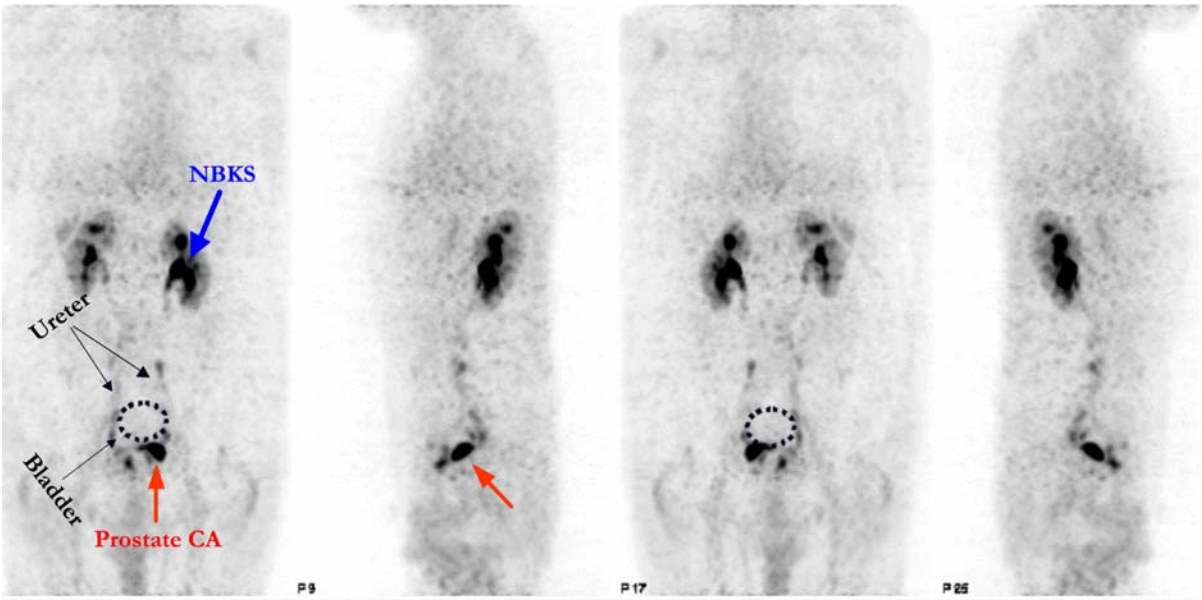


Fig. 5 PET imaging of prostate cancer patient with [$^{68}$Ga]-BZH2 at 1h p.i. (Hofmann et al, MH, Hannover, unpublished result)

Hoffmann et al (MH, Hannover) performed a patient study (5 cases) by using [$^{68}$Ga]-BZH2; it showed that [$^{68}$Ga]-BZH2 visualizes the tumor quickly (Fig. 5). Paganelli et al (IEO, Milan) performed a clinical trial with $^{111}$In-labeled BZH1 and BZH2. Their results (personal communication) show that the tumor is well localized. However, the radioactivity was released from the target relatively quickly (within 24h). These data indicate that the rapid release from the tumor may make little sense when [$^{90}$Y/$^{177}$Lu]-BZH2 is used for targeted radiotherapy.

**Why was radiolabeled BN analogue released from the tumor quickly? Unstable?**

***Stability and metabolites***

The study of the stability in human serum was performed to find out why $^{111}$In-labeled BZH1 or BZH2 cannot be residualized in the tumor. A consecutive reaction ( $A \xrightarrow{k1} B \xrightarrow{k2} C + D$ ) was assumed to calculate the disappearance of intact peptide ($[A] = 100 \cdot e^{-k1t}$) as well as the formation and disappearance of the metabolite ($[B] = 100 \cdot k_1/(k_1 - k_2) \cdot (e^{-k2t} - e^{-k1t})$). According to this reaction model, the stability of the intact peptide and the first metabolite in fresh human serum was calculated ($t_{1/2}$=0.693/$k_i$).

The metabolic stability results show that $^{111}$In-labeled BZH1 or BZH2 are not stable in the human serum ($t_{1/2}$=2.0-2.3h) [Paper 1, Table 2]. Furthermore, the βAla$^{11}$-His$^{12}$ bond is the weakest bond in the prototype of [$^{111}$In]-DTPA-GABA-[D-Tyr$^6$, βAla$^{11}$, Thi$^{13}$, Nle$^{14}$] BN (6-14) since the cleavage site of βAla$^{11}$-His$^{12}$ was identified as the first metabolite by analytical HPLC [Paper 1, Fig 2, 3 and 4]. Subsequently, this metabolite was decomposed at the Gln$^7$-Trp$^8$ peptide bond and at the chelate-GABA. Incubation in the presence of EDTA or βAla-His (carnosine) slowed down the metabolic process distinctly, indicating that carnosinase may be the active enzyme, thus supporting the finding that the first enzymatic cleavage was between βAla$^{11}$-His$^{12}$ [Paper 1, Fig 4]. In addition, the substitution of Phe$^{13}$ by Thi$^{13}$ increases the stability by a factor of 1.5 *(unpublished in paper 1)*.

***Implication:*** Stabilizing BN analogue!

### 3.2 Spacer modified pan-bombesin analogues (Manuscript 1 and Paper 2)

#### *Background*

Preliminary results from our laboratory showed that direct coupling of the chelator to the peptide led to a significant loss of binding affinity towards GRP receptors. Therefore it was necessary to insert a spacer between the peptide and the chelator in order to retain a high binding affinity. Furthermore, based on the assumption that the type of spacer would influence the pharmacological properties, different spacers with various chain-lengths (Fig. 1) were introduced to study the supposed influence, including GABA (γ-aminobutyric acid), Ahx (6-aminohexanoic acid), $PEG_2$ (8-amino-3,6-dioxaoctanoic acid), $PEG_4$ (15-amino-4,7,10,13-tetraoxapentadecanoic acid), $\beta Ala_2$ (di-β-alanine), D-Dab-βAla and $Sar_5$ (pentasarcosine). The positive charge on the side chain was introduced by using diaminobutanoic acid (Dab) as amino acid spacer.

#### *Binding affinity*

The results showed that all conjugates have a relatively high affinity ($IC_{50}$ value: 0.8- 6.3nM. *Ref.: Table 3*) to the human GRP receptor expressed in human prostate cancer by using [$^{125}$I-Tyr$^4$] BN as a radioligand. The different chain lengths of the spacers had an effect on the binding affinity of their corresponding conjugates. For example, for the spacer of the hydrocarbon type, five methylene groups (Ahx: 0.8±0.1nM) afforded a better binding affinity to the hGRP receptor than three (GABA: 2.2±0.2nM), which is consistent with other published results (40, 44). For the spacer of the ethylene oxide type, on the other hand, four ethylene oxide groups ($PEG_4$: 6.3±1.3nM) showed a lower affinity than two ($PEG_2$: 2.1±0.8nM). Considering the influence of length among all types of spacers, the longer spacers ($PEG_4$ and $Sar_5$) led to a lower binding affinity for the human GRP receptor than the shorter spacers (GABA, Ahx, $PEG_2$, $\beta Ala_2$, and D-Dab-βAla). In addition, the positive charge on the side chain (Dab) did not improve the binding affinity.

## ***Internalization***

Since AR4-2J (rat pancreatic tumor) cells and PC-3 (human prostate cancer) cells express GRP receptors, internalization was studied with both cell lines. In PC-3 cells, all spacer-modified conjugates displayed a similar internalization rate, which is not consistent with their corresponding affinity (human GRP-Rs). On the other hand, in AR4-2J cells, the longer spacers ($Sar_5$ and $PEG_4$) result in a slower internalization rate than the shorter ones. These results imply that the GRP receptor expressed on rat cells is different from the GRP receptor expressed on human cells [Manuscript 1, Fig 4]. Among all spacer-modified conjugates, only longer spacer-modified ($Sar_5$ and $PEG_4$) analogues displayed a significantly different internalization rate between these two cell types (Table 3). Thus it was expected that these two ligands would show a lower affinity to the mouse/rat GRP receptor than to the human GRP receptor. However, the results obtained from [$Y^{III}$]-DOTA-$PEG_4$-BZH were contrary to my expectation (*$IC_{50}$ values: 0.20±0.00 nM (AR4-2J cell membrane)* ***vs*** *3.93±1.23nM (PC-3 cell membrane); 0.46±0.03 nM (mouse pancreas tissue)* ***vs*** *6.3±1.3nM (human prostate cancer tissue)*) (71).

Table. 3 Internalization rate of [$^{111}$In]-DOTA-**Spacer**-BZH‡ after 6h incubation and corresponding binding affinities to human GRP receptor.

| Spacer | $IC_{50}$ (nM)† | PC-3 cells<br>% of added radioligands per 1 million cells | AR4-2J | Difference |
|---|---|---|---|---|
| $Sar_5$ | 5.7±1.4 (3) | 38.1±1.3 | 22.4±1.7 | 15.7 |
| $PEG_4$ | 6.3±1.3 (5) | 35.8±0.7 | 19.7±0.2 | 16.1 |
| $\beta Ala_2$ | 2.5±0.4 (3) | 30.7±1.6 | 24.0±0.9 | 6.7 |
| Ahx | 0.8±0.1 (3) | 36.4±0.5 | 33.9±1.6 | 2.5 |
| GABA | 2.2±0.2 (3) | 35.8±0.9 | 36.1±0.2 | -0.3 |
| $PEG_2$ | 2.1±0.8 (3) | 33.5±0.6 | 37.1±2.9 | -4.4 |
| D-Dab-βAla | 2.1±0.9 (3) | 31.7±1.6 | 36.6±1.9 | -5.1 |

†: Binding affinity study was performed on human prostate cancer by using [$^{125}$I-$Tyr^4$] BN as radioligand;
‡: DOTA-**Spacer**-D-Tyr-Gln-Trp-Ala-Val-βAla-His-Thi-Nle-$NH_2$

Is another factor influencing the internalization rate into murine cells? The p-glycoprotein (mdr1 expression) may influence internalization, especially for peptides containing sarcosine or the ethylene oxide group because they may be excreted from cells by mdr1. The density of mdr1 expression on murine cells is higher than that on human cells (72). This may explain why longer spacer-modified conjugates ($Sar_5$ and $PEG_4$) display abnormal trends in the AR4-2J cells.

### ***PET imaging and biodistribution***

AR4-2J tumor bearing nude mice were used for PET imaging. The results show that [$^{68}$Ga]-DOTA-$PEG_2$-BZH visualizes the AR4-2J tumor quickly [Paper 2, Fig 5].

Biodistribution studies [Manuscript 1, Table 5 and Fig 5] of these spacer-modified BN analogues were performed with Lewis rats bearing the AR4-2J pancreatic tumor. All of the [$^{111}$In]-DOTA-spacer-BZH ligands displayed a rapid clearance from blood and from the GRP-R negative tissues with the exception of the kidneys. All derivatives showed high uptake in the AR4-2J tumor and in the GRP-R positive organs. For example, among the tested derivatives (4h p.i.), [$^{111}$In]-DOTA-GABA-BZH (BZH2) has the lowest uptake in the AR4-2J tumor (0.82±0.06% ID/g), and [$^{111}$In]-DOTA-$PEG_4$-BZH the highest (1.55±0.25% ID/g). On the other hand, they show a reverse tendency in the kidney (1.51±0.61% ID/g vs 0.76±0.18% ID/g). The kinetics of $^{111}$In-labeled $Sar_5$/GABA modified conjugates show that the $Sar_5$ derivative has a much higher accumulation in AR4-2J tumor and pancreas.

From biodistribution results, the $Sar_5$ and $PEG_4$ modified peptides show higher accumulation in the AR4-2J tumor even though both have a slower internalization rate into AR4-2J cells than other spacers. Do different spacers between peptide and chelator influence the *in vivo* stability and thus affect the accumulation in the tumor?

### ***Stability***

To answer the above-mentioned question, stability in serum was determined as described in *Chapter 3.1*. The results show that with increasing length of the spacers, the $^{111}$In-labeled

conjugates showed an increasing stability ($t_{1/2}$ = 2.3h to 33.6h) in fresh human serum [Manuscript 1, Table 4]. This may explain why $Sar_5$ or $PEG_4$-modified peptides ($PEG_4$=15-amino-4,7,10,13-tetraoxapentadecanoic acid) show high accumulation in the AR4-2J tumor despite their slower internalization rate. However, since the spacer is distant from the weakest bond ($\beta Ala^{11}$-$His^{12}$), it is still not clear how spacers influence the *in vivo* stability. Does the linear BN analogue form secondary structures in the serum, thus shortening the distance between the spacer and the weakest bond?

## ***Secondary structure***

To understand the structural basis of the above-mentioned biological differences, I analyzed the secondary structure of spacer-modified pan-BN analogues. All of the [$Y^{III}$]-DOTA-spacer-BZH ligands, dissolved in PBS buffer (60 µM), were measured with circular dichroism (CD) at room temperature. The CD spectra showed that [$Y^{III}$]-DOTA-$Sar_5$-BZH significantly differs from the other conjugates, having a typical curve of a α-helix [Manuscript 1, Fig. 6]. The results from further evaluation of all spectra (Anna Seelig group) [Manuscript 1, Table 6] show that the main form of their secondary structure in PBS buffer is random coil varying from 40.8% to 67.9%. (D)Dab-βAla and $Sar_5$ may form about 1 helical turn; especially, the most stable ligand, DOTA-$Sar_5$-BZH, might form 1 helical turn. For GABA, Ahx, $PEG_2$ and $PEG_4$ derivatives, there is practically no α-helix or β-turn structure. These results indicate that the spacer may partially affect the peptide secondary structure, especially for $Sar_5$ (pentasarcosine).

## ***Implication***

- Poly(ethylene oxide) group as spacer decreases the kidney uptake;
- Pentasarcosine as spacer increases stability;
- GRP receptor expressed on human tumor cells differs from GRP receptor expressed on the murine cells.

## 3.3 Modification on the 11$^{th}$ position of [$^{111}$In]-DOTA-GABA-[D-Tyr$^{6}$]BN(6-14) for studying the influence on metabolic stability and probing species differences (Manuscript 2)

### ***Background***

Based on D-Tyr-Gln-Trp-Ala-Val-βAla-His-Phe-Nle-$NH_2$, Mantey et al (48-50) reported that the substitution of β-alanine may change its secondary structure, and lead a pan-ligand to become a BRS-3 receptor-selective ligand. In the experiments discussed in *Chapter 3.1*, carnosinase is responsible for cleaving the bond between βAla$^{11}$ and His$^{12}$ which was identified as the weakest bond in [$^{111}$In]-DTPA(or DOTA)-GABA-D-Tyr-Gln-Trp-Ala-Val-βAla-His-Thi-Nle-$NH_2$. These results imply that it may be worthwhile to optimize the pharmacological properties through modification on the 11$^{th}$ position of the BN analogue.

Since according to the literature (25, 26, 58-60) D-Phe$^{6}$ or D-Tyr$^{6}$ seem to keep the affinity to the GRP receptor even though the BN(7-14) was considered to have sufficient biological activity for the GRP receptor (19), [D-Tyr$^{6}$]-BN(6-14) was chosen as a peptide model for the 11$^{th}$ position modification. Glycine (Gly$^{11}$) was substituted by β-alanine (βAla), D-Ala, or azaglycine (Agly)[Manuscript 2, Fig. 1]. It may be possible that D-Ala and Agly may not only increase the stability, but also influence the peptide conformation.

### ***Stability***

The stability of [$^{111}$In]-DOTA-GABA-[D-Tyr$^{6}$, **X**$^{11}$] BN (6-14) was determined in serum, as described in *Chapter 3.1*. The results show that the stability in human serum increased due to this substitution. The Agly analogue is the most stable among these four ligands. The half-lives ($t_{1/2}$) of the corresponding peptides in human serum varied from 2.9±0.5 h (Gly) to 14.1±1.5 h (Agly) [Manuscript 2, Table 3]. However, the degree of stabilization is insufficient, most likely because other peptide bonds are susceptible to degradation by proteolytic enzymes.

## ***Binding affinity***

Using [$^{125}$I-Tyr$^{4}$] BN as GRP receptor-preferring radioligand, competition binding assays on cryostat sections of human prostate tumors and mouse pancreas were conducted for [In$^{III}$]-DOTA-GABA-[D-Tyr$^{6}$, **X**$^{11}$] BN (6-14). The $IC_{50}$ values of these compounds for the mouse GRP receptor were between 0.5±0.2nM and 5.8±2.2nM, and for the human GRP receptor between 11.5±2.6nM and 96±13nM [Manuscript 2, Table 2]. Although there appears to be a high interspecies homology of >90% between human and mouse GRP receptors (73), [In$^{III}$]-DOTA-GABA-[D-Tyr$^{6}$, Agly$^{11}$] BN (6-14) showed the highest affinity difference (96-fold) between human and mouse GRP receptors. The reason may be that human and mouse GRP receptor prefer to bind to the ligand that has different conformation, but the conformation of Agly analogue can not be changed because the rotation of the N-N bond between Val$^{10}$-Agly$^{11}$ is restricted by the lone nitrogen pairs approximately perpendicular to each other (55). On the other hand, as the other three ligands cannot restrict the conformation, it is to be expected that they have less difference of affinity than the Agly derivative (the differences for βAla, Gly and D-Ala derivatives are 25, 9.6 and 7.1 fold, respectively).

## ***Secondary structure analysis***

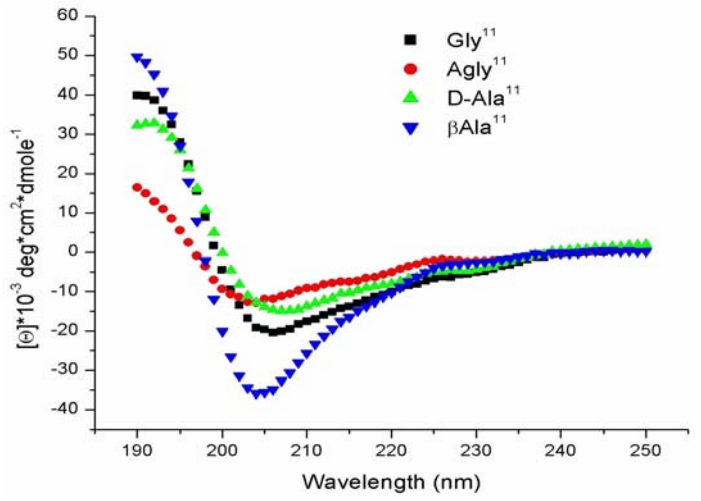


Fig. 6 Circular dichroism spectra of 60 μM [In$^{III}$]-DOTA-GABA-[D-Tyr$^{6}$, **X**$^{11}$] BN (6-14) (**X**=Gly, Agly, βAla and D-Ala) in TFE/PBS (7:3), The concentration was calibrated with UV (280nm, ε=6890).

To probe whether the secondary structure is changed due to modifying the 11$^{th}$ position with Agly and D-Ala, all of the [In$^{III}$]-DOTA-GABA-[D-Tyr$^{6}$, **X**$^{11}$] BN(6-14) ligands were dissolved in trifluoroethanol (TFE)/0.1M phosphate buffer (pH=7.4) solution (v/v=7/3), then measured with circular dichroism (CD). Their CD spectra (Fig. 6) displayed that their main secondary structure still is random coil and there is no significant difference of secondary structure, indicating that the secondary structures difference of random coil may be detectable only when BN analogues bind to the GRP receptors.

***Internalization and externalization***

Generally, the internalization rate of these serial ligands into PC-3 cells (human receptor) was faster than into AR4-2J cells (rat receptor). For the Agly analogue, the difference of internalization rate into these two cell lines was only 3% (6h incubation), whereas for the D-Ala$^{11}$ analogue, it was 13.7%, which was the highest difference found among these four ligands [Manuscript 2, Fig 2].

The reason for these results may be that the binding affinity and the receptor density on the cells together determine the internalization rate. The GRP receptor density in PC-3 cells ($2.5\times10^{5}$ *receptor sites per cell* (42)) is higher than in AR4-2J cells (*Singh et al* (74): $1.5\times10^{5}$; *Schuhmacher et al* (75): $0.97\times10^{5}$). For the Agly analogue, the binding affinity to the PC-3 tumor is by a factor of 96 lower than to the mouse pancreas; for the D-Ala analogue only by a factor of 7.1. These two factors may result in the above-mentioned difference of internalization rate.

All radio-labeled ligands were released from PC-3 cells with a similar rate (P = 0.98) except [$^{111}$In]-DOTA-GABA-[D-Tyr$^{6}$, D-Ala$^{11}$] BN(6-14) which had a relative faster washout (P = 0.04). [Manuscript 2, Fig 3].

## ***Biodistribution***

Biodistribution was performed in normal rats and double-tumor (AR4-2J and PC-3) bearing nude mice, respectively. The respective biodistribution in normal rats [Manuscript 2, Table 4] show that the accumulation of βAla or Agly derivatives in the GRP-receptor positive pancreas is higher than that of the Gly or D-Ala analogues, which is consistent with their affinity. The uptake in the kidney is also dependable to their corresponding affinity, implying that the kidney may be a mouse GRP receptor positive organ. In the double-tumor bearing mice, the uptake of all the radiotracers in the PC-3 tumors was significantly lower than in the AR4-2J tumor, which is in accordance with their relative binding affinities [Manuscript 2, Table 5]. All of these *in vivo* results showed that the accumulation in the target was not determined by the internalization rate, but by the binding affinity to the GRP receptor. When the ligands had a similar affinity to the receptor, the ligand that is more stable in serum displays a higher accumulation in the target.

## ***Implication***

- Stabilizing a single peptide bond is not sufficient to afford a stable BN analogue;
- The BN analogue may display a different interaction with the GRP receptor when it is obtained from different species.

## 3.4 $^{64/67}$Cu-conjugated BN analogues for targeted PET imaging and radiotherapy of BN receptor expressing tumors (Manuscript 3)

### *Background*

Copper-64 and copper-67 have become attractive (Table 4) for radiolabelling proteins and peptides (42, 64-67) for both diagnosis and therapy because of their suitable physical properties. Especially, copper-64 has been identified as an emerging positron emitter (62) also showing therapeutic potential because of its low energy $\beta^-$ and electron capture (63, 64). Copper-67 ($t_{1/2}$ = 61.9h) is a low energy beta-emitter that is very suitable for irradiation of small metastases. $^{67}$Cu also emits low energy photons, particularly useful for pretherapeutic diagnostic imaging with a γ-camera. All these advantages prompted me to develop radiocopper-conjugated BN analogues for PET imaging and targeted radiotherapy of BN receptor positive tumors.

Table 4 Physical properties and potential applications of a range of copper isotopes (76)

| Isotope | Half-life | Imaging (emission, energy [a], abundance) | Therapy (energy [a], range in tissue) | Application |
|---|---|---|---|---|
| $^{60}$Cu | 20 min | PET ($\beta^+$, 873 keV; 93%) | | Radiolabelling of small molecules for repeat studies under different physiological conditions |
| $^{61}$Cu | 3.3 h | PET ($\beta^+$, 527 keV; 62%) | | Radiolabelling small molecules |
| $^{62}$Cu | 9.74 min | PET ($\beta^+$, 1315 keV; 98%) | | Repeat studies under different physiological conditions |
| **$^{64}$Cu** | 12.7 h | PET ($\beta^+$, 278 keV; 19%) | $\beta^-$; 190 keV; 0.95 mm | Radiolabelling small molecules, peptides and antibodies |
| $^{66}$Cu | 5.4 min | | $\beta^-$; 1109 keV; 5.6 mm | Radiolabelling small molecules for therapy |
| **$^{67}$Cu** | 62 h | SPECT (91, 7%; 93 keV, 16%; 185, 48%) | $\beta^-$; 121 keV; 0.61 mm | Radiolabelling peptides and antibodies |

[a]: Average energy of the most non-penetrating radiation.

In addition, different charges were introduced to the N-terminus of the peptide by using [$In^{III}$/$Cu^{II}$-DOTA] and [$Cu^{II}$-CPTA]. The [$In^{III}$-DOTA]-peptide forms a neutral complex, whereas the [$Cu^{II}$-DOTA]-peptide is a negatively charged, and the [$Cu^{II}$-CPTA]-peptide a two-fold positively charged BN derivative [Manuscript 3, scheme 1].

### ***Binding affinity***

Using [$^{125}$I-Tyr$^{4}$] BN as radioligand, competitive binding assays were performed with human cancerous tissue and mouse pancreas tissue as a source of GRP-receptors. The positively charged ligand, [$Cu^{II}$]-BZH5, had significantly higher affinity to human GRP receptors than the negatively charged ([$Cu^{II}$]-BZH4) or neutral ([$In^{III}$]-BZH4) peptide [Manuscript 3, Table 2], indicating that the charge at the N-terminus is a main factor for determining the affinity to human GRP receptors. These results also imply the use of DOTA as a bifunctional chelator for conjugating $^{64}$Cu to BN analogues is not a good choice. This effect can explain why the positively charged [$^{99m}$Tc]Demobesin 1 (47) exhibited such a high affinity to the GRP receptor and high accumulation in PC-3 tumors, whereas $^{64}$Cu-labeled DOTA-Aoc-BN (7-14) (42) and DOTA-[Lys$^{3}$]BN (34) showed relatively low affinities and poor uptake. Interestingly, the differently charged peptides ([$Cu^{II}$]-BZH4, [$In^{III}$]-BZH4 and [$Cu^{II}$]-BZH5) displayed only a slight difference in affinity for the mouse GRP receptors [Manuscript 3, Table 2], demonstrating that the mouse GRP receptor is only slightly sensitive to the charge at the N-terminus.

Substitution of Nle$^{14}$ ([$Cu^{II}$]-BZH5) by Met$^{14}$ ([$Cu^{II}$]-BZH6) causes the $IC_{50}$ value (for the hGRP-R) to drop from 3.2±0.5nM to 1.0±0.2nM, whereas it had no influence on the $IC_{50}$ values for the mouse pancreas (0.6±0.2nM vs 0.8±0.2nM) [Manuscript 3, Table 2]. When D-Tyr$^{6}$ of [$Cu^{II}$]-BZH6 was removed to become [$Cu^{II}$]-BZH7, the $IC_{50}$ values improved by a factor of 2.5 (human receptor) and 4 (mouse receptor), respectively, achieving the highest binding affinity [Manuscript 3, Table 2] by far which we have found among more than 100 BN analogues. A hippurane-like structure between the cyclamyl group and [βAla$^{11}$] BN (7-14) ([$Cu^{II}$]-BZH8) decreases the binding affinity to human GRP-R and mouse GRP-R by a factor of 4 [Manuscript 3, Table 2].

### ***Receptor subtype profile of [$Cu^{II}$]-BZH7***

The most promising peptide, [$Cu^{II}$]-BZH7, was studied with respect to the bombesin receptor subtype profile using human cancerous tissue expressing predominantly a single bombesin

receptor subtype. It was very exciting to find that [$Cu^{II}$]-BZH7 had high binding affinity to all 3 human receptor subtypes (0.40±0.10 nM to NMB-R; 0.35±0.05 nM to GRP-R and 1.8±0.4 nM to BRS-3) compared to [D-$Tyr^6$, $\beta Ala^{11}$, $Phe^{13}$, $Nle^{14}$] BN (6-14) or [$Y^{III}$]-BZH2 (25-27) even though their peptide sequences differ significantly. After analyzing the structural differences of DOTA-Gly-[4-aminobenzoyl]-BN (7-14) *(binding to NMB-R and GRP-R* (43)) and BZH7 *(cyclam-(4-methylbenzoyl)-[$\beta Ala^{11}$]BN (7-14): binding to all three subtypes*), we may conclude that the benzoyl group is a key structural feature to keep high affinity to the NMB receptor and $\beta Ala^{11}$ for maintaining high affinity to the BRS-3 receptor.

### ***Stability***

The stability in human fresh serum is also performed as described in *Chapter 3.1*. The different chelate complexes (In-DOTA: [$^{111}$In]-BZH4 and Cu-CPTA: [$^{64}$Cu]-BZH5) do not show a different stability (0.61±0.11h versus 0.55±0.11h) [Manuscript 3, Table 3]. The substitution of $Nle^{14}$ by Met improves stability significantly (Table 5). [$^{64}$Cu]-CPTA-[$\beta Ala^{11}$] BN (7-14) and [$^{64}$Cu]-CPTA-[$\beta Ala^{11}$] BN (7-14) show similar stability in serum ($t_{1/2}$: 5.1±1.7h vs 4.5±1.2h).

In addition, compared to our previously designed panbombesin-ligand (BZH2: [$^{111}$In]-DOTA-GABA-[D-$Tyr^6$, β-$Ala^{11}$, $Thi^{13}$, $Nle^{14}$] BN(6-14)) (27), [$^{111}$In]-BZH4 (DOTA-GABA-[D-$Tyr^6$, β-$Ala^{11}$, $Nle^{14}$]BN(6-14)) has less stability in serum by a factor of 3.5. The stability sequence on the $13^{th}$ position of the BN analogues is Thi > Phe > Leu.

### ***Internalization and externalization***

The internalization and externalization experiments were studied with PC-3 cells. All of the $^{64}$Cu-labeled conjugates and [$^{111}$In]-BZH4 showed fast specific cell-uptake [Manuscript 3, Fig 1], in particular, [$^{64}$Cu]-BZH5 and [$^{64}$Cu]-BZH7 internalize very efficiently into PC-3 cells (Table 5). The other ligands, [$^{64}$Cu]-BZH6, [$^{64}$Cu]-BZH8, and [$^{111}$In]-BZH4, are listed in decreasing order of internalization rate. Efflux results [Manuscript 3, Fig 2] showed that [$^{64}$Cu]-BZH7 has the slowest

and [$^{111}$In]-BZH4 the fastest externalization rate, which is consistent with their affinities to hGRP-R. To identify the composition of externalized peptide, [$^{111}$In]-BZH4 is used as a leading peptide. Following 2 h of internalization and acid wash, the externalized radioactivity consists of approximately 84% metabolites and 16% intact peptide after 2h incubation.

These results indicate that high binding affinity correlates with rapid internalization and relatively slow washout from PC-3 cells among this series of ligands except [$^{64}$Cu]-BZH5.

Table 5 Structure relationships with peptide biological properties

| Peptide | $t_{1/2}$(h) | $IC_{50}$ (nM) | Int. | Ext. |
|---|---|---|---|---|
| [$^{111}$In]-BZH4<br>DOTA-GABA-[D-Tyr$^{6}$, βAla$^{11}$, Nle$^{14}$]BN(6-14) | 0.61±0.11 | 41.5±2.5 | 36.0±1.8 | 58.8±1.4 |
| [$^{64}$Cu]-BZH5<br>CPTA-[D-Tyr$^{6}$, βAla$^{11}$, Nle$^{14}$]BN(6-14) | 0.55±0.11 | 3.2±0.5 | 77.9±4.1 | 49.1±1.6 |
| [$^{64}$Cu]-BZH6<br>CPTA-[D-Tyr$^{6}$, βAla$^{11}$]BN(6-14) | 0.92±0.17 | 1.0±0.2 | 64.5±4.4 | 44.9±1.5 |
| [$^{64}$Cu]-BZH7<br>CPTA-[βAla$^{11}$]BN(7-14) | 5.1±1.7 | 0.42±0.13 | 84.6±2.3 | 36.1±2.3 |
| [$^{64}$Cu]-BZH8<br>CPTA-[Gly$^{6}$, βAla$^{11}$]BN(6-14) | 4.5±1.2 | 1.8±0.6 | 46.1±2.3 | 48.2±0.3 |
| Note: $t_{1/2}$: stability in serum; $IC_{50}$: binding affinity of metallated peptide to human GRP receptor; Int: internalization rate into PC-3 cells at 6h incubation (% of added peptide); Ext.: externalization rate from PC-3 cells at 8h incubation (% of 2h internalized activity). | | | | |

## ***Biodistribution and microPET imaging***

Rapid internalization and good trapping (residualization) of the radioactivity is important for a potentially successful targeted radiotherapy. To further evaluate these $^{64}$Cu labeled peptides, biodistribution studies were performed with athymic nude female mice bearing the PC-3 human prostate tumor [Manuscript 3, Table 4]. [$^{64}$Cu]-BZH5, [$^{64}$Cu]-BZH6, [$^{64}$Cu]-BZH7 and [$^{64}$Cu]-BZH8 all displayed a similarly rapid blood clearance varying from 0.142% ID/g to 0.182% ID/g at 4h. Like copper labeled antibody fragments or somatostatin analogues (64, 67), $^{64}$Cu-labeled BN analogues are also excreted through the liver and kidneys. The four radiolabeled ligands showed high specific uptake in the human prostate tumor xenograft and in the mouse GRP-R positive organs. These results appear to be superior to those of [$^{64}$Cu]-DOTA-Aoc-BN (7-14) (42) and

[$^{64}$Cu]-DOTA-[Lys$^{3}$]BN (34). In particular, [$^{64}$Cu]-BZH7 showed the highest accumulation in the PC-3 tumor and the lowest uptake in the liver among these conjugates [Manuscript 3, Table 5], which correlated with its very high binding affinity to GRP receptors. The pharmacokinetics of [$^{64}$Cu]-BZH7 showed an early high accumulation in the tumor (11.2±1.5 %ID/g at 1h p.i.). The uptake in the tumor dropped to 6.63±0.80 %ID/g at 4h and 4.14±0.55 %ID/g at 24h, respectively. As a consequence of its favorable properties, [$^{64}$Cu]-BZH7 visualized the PC-3 tumor very well with MicroPET imaging at 3h post injection [Manuscript 3, Fig 4]. A high accumulation of radioactivity was observed in the pancreas, liver and kidney as well. When the mouse was sacrificed at 23h post injection, the uptake in the PC-3 tumor was 3 %ID/g and the tumor-to-kidney ratio was 2.

### ***Enhancing kidney clearance***

The co-injection of [Cu$^{II}$]-BZH7 led to a somewhat increased uptake in the liver and, conversely, the uptake in the kidney was blocked partly [Manuscript 3, Table 5]. This is an indication that the BN receptor may be expressed in the mouse kidney. Dumesny et al (77) also reported that the mRNA of GRP receptor was identified in the rat kidney.

The hippurane-like spacer molecule definitely facilitates clearance through the kidney [Manuscript 3, Fig 3]. Still, the tumor-to-kidney ratio did not improve using this molecule as the GRP-receptor binding affinity of BN also decreased and concomitantly the uptake in the tumor.

Furthermore, attempts to influence the accumulation of radioactivity in the kidneys also involved co-injection of lysine. The results show that lysine has no effect on either the kidney uptake or the tumor-to-kidney ratio.

### ***Implication***

- Benzoyl group may be important to keep affinity to NMB-R and GRP-R.

## 3.5 Design and evaluation of [$^{67/68}$Ga, $^{177}$Lu]-DOTA-PESIN for clinical trial (Manuscript 4)

### ***Background***

The first radiolabeled BN analogue to be performed in a preliminary patient study was $^{99m}$Tc-RP527 (53). The results indicated that BN analogues can be applied for the diagnosis of hGRP receptor expressing tumors. The development of $^{99m}$Tc-labeled BN analogues (47, 53) for the targeting of GRP-R expressing tumors has been intensive.

However, when BN analogues are labeled with $^{68}$Ga (for PET imaging) and $^{177}$Lu (for therapy), they have to be redesigned so as to satisfy certain requirements, especially a higher tumor-to-kidney ratio than $^{99m}$Tc-labeled BN analogues. According to the study in *Chapter 3.2*, the ethylene oxide group can facilitate kidney clearance [Manuscript 1, Table 5] and partially increase stability in serum [Manuscript 1, Table 4], DOTA-PESIN (*DOTA-PEG$_4$-BN(7-14), PEG$_4$=15-amino-4,7,10,13-tetraoxapentadecanoic acid*) [Manuscript 4, Fig 1] was designed.

### ***Preparation of radiolabeled DOTA-PESIN***

DOTA-PESIN was labeled with $^{68}$Ga and $^{177}$Lu rapidly at elevated temperature ($^{68}$Ga: 90°C, 10min; $^{177}$Lu: 95°C, 15 min). The radio-oxidized [$^{177}$Lu]-DOTA-PESIN was reduced to 2% from 26% in the presence of 400 μg methionine per 370 MBq $^{177}$Lu, and radio-labeling yields of ≥98% at very high specific activity (>85 GBq μmol$^{-1}$) were achieved. It is not necessary to add methionine for labeling with $^{67/68}$Ga because the radiolytic oxidation of [$^{67/68}$Ga]-DOTA-PESIN was < 2%, and the specific activity was >129 GBq μmol$^{-1}$ for $^{68}$Ga and >12 GBq μmol$^{-1}$ for $^{67}$Ga, respectively.

### ***In vitro evaluation***

Using [$^{125}$I-Tyr$^4$] BN as radioligand, competitive binding assays were performed with human cancerous tissue and mouse pancreas tissue as a source of GRP-receptors. The $IC_{50}$ value of

DOTA-PESIN was 9.5±3.4 nM, for [$Lu^{III}$]-DOTA-PESIN 6.1±3.0nM, and for [$Ga^{III}$]- DOTA-PESIN 6.6±0.1 nM [Manuscript 4, Table 1].

Internalization and externalization experiments were executed with PC-3 cells. For internalization study, the results show that radiolabeled DOTA-PESIN rapidly internalized into PC-3 cells ($^{177}$Lu: 39.1±1.1% and $^{67}$Ga: 43.7±1.8% at 6 h incubation) [Manuscript 4, Fig 2]. As for the efflux, following 2h of internalization of [$^{67}$Ga/$^{177}$Lu]-DOTA-PESIN and acid wash, 52.5±1.6% of the total internalized still remained in PC-3 cells after 20 h incubation [Manuscript 4, Fig 3].

***In-vivo evaluation***

Biodistribution studies of [$^{67}$Ga/$^{177}$Lu]-DOTA-PESIN were performed on athymic nude female mice bearing PC-3 tumor. [$^{67}$Ga/$^{177}$Lu]-DOTA-PESIN displayed rapid clearance from blood and GRP-R negative tissues [Manuscript 4, Table 2]. Radiolabeled DOTA-PESIN is excreted through the kidney. Both radiotracers also showed high uptake in the human prostate tumor and in the mouse GRP-R positive organs [Manuscript 4, Table 2]. For example, mouse pancreas uptake of [$^{67}$Ga]-DOTA-PESIN is 65.3±8.7 %ID/g at 1h; and accumulation in the tumor is 14.8±2.5 %ID/g. This result was as high as that of $^{99m}$Tc-Demobesin 1 in the same type of tumor bearing animals (16.0±3.0 %ID/g). The uptake of $^{99m}$Tc-Demobesin 1 in the liver is 12.5-fold higher than that of [$^{67}$Ga]-DOTA-PESIN (8.0±1.6%ID/g vs 0.64±0.15%ID/g).

Co-injection of lysine did not reduce the kidney uptake, and the ratio between tumor and kidney remained unchanged, which is similar to the finding that lysine had no effect on [$^{64/67}$Cu]-BZH7. The kinetics of [$^{67}$Ga]-DOTA-PESIN showed high initial accumulation, and still was 6.76±0.29 %ID/g at 24h. [$^{177}$Lu]-DOTA-PESIN displayed similar kinetics. All kinetic results show that with the increase of time post injection the tumor-to-background ratios also increased (Table 6). Interestingly, the $^{177}$Lu-labeled peptide was released more rapidly from the pancreas and kidney than from the tumor [Manuscript 4, Fig 4].

Scintigraphy ([$^{177}$Lu]-DOTA-PESIN: 4h, 24h, 48h and 72h) and PET imaging ([$^{68}$Ga]-DOTA-PESIN: 1h p.i.) confirmed the results of tissue biodistribution [Manuscript 4, Fig 5 and 6].

Table 6 Radioactivity ratios between PC-3 tumor and other organs of $^{67}$Ga, $^{177}$Lu-labeled DOTA-PESIN in PC-3 tumor bearing female athymic nude mice [8≥**n**≥4]

| Time (h) | Blood | | Muscle | | Kidney | | Liver | |
|---|---|---|---|---|---|---|---|---|
| | $^{67}$Ga | $^{177}$Lu | $^{67}$Ga | $^{177}$Lu | $^{67}$Ga | $^{177}$Lu | $^{67}$Ga | $^{177}$Lu |
| 1 | 31 | | 62 | | 2.4 | | 23 | |
| 4 | 81 | 201 | 209 | 147 | 2.6 | 1.7 | 22 | 36 |
| 24 | 211 | 215 | 237 | 387 | 2.4 | 2.5 | 23 | 43 |
| 48 | | 476 | | 488 | | 3.1 | | 52 |
| 72 | | 715 | | 486 | | 3.6 | | 48 |

## ***Ongoing and outlook of DOTA-PESIN***

The further treatment of PC-3 tumors in mice with [$^{177}$Lu]-DOTA-PESIN is ongoing, the preliminary results show that tumor growth has been significantly prevented by injection of 37 MBq [$^{177}$Lu]-DOTA-PESIN compared to the control group.

According to the above-mentioned merits, it is highly promising to apply radiolabeled DOTA-PESIN in a clinical study of patients with GRP receptor or NMB receptor expressing tumors, the pioneer clinical trial has been proposed.

# Part IV: CONCLUSION AND OUTLOOK

## 4.1 Conclusion

### *General*

BN analogues have been developed for labeling with $^{111}$In, $^{67/68}$Ga, $^{64/67}$Cu, $^{177}$Lu and $^{90}$Y, which may be of use for diagnostic imaging (PET and SPECT) and targeted radionuclide therapy. This study mainly focuses on the spacers between peptide and chelator [Paper 1 and 2, Manuscript 1], the modification of bombesin itself [Manuscript 1, 2, and 3], and the positive charge at the N-terminus [Manuscript 3]. Through the evaluation of the binding affinity, internalization rate, efflux, and biodistribution in animals, some of these ligands have been selected for a preliminary clinical trial.

### *Influence on binding affinity of BN analogues to human GRP receptors*

**1). Modifying the peptide itself**

- The substitution of Leu$^{13}$ by Phe and Thi, respectively, afforded an affinity in the order of Thi ≈ Phe >> Leu;
- The replacement of Met$^{14}$ by Nle decreased affinity;
- The modification of Gly$^{11}$ with βAla, D-Ala, and Agly resulted in the sequence of Gly ≈ βAla > D-Ala > Agly.

**2). Synthetic amino acid or natural amino acid between chelator and peptide**

- D-Tyr or Gly between CPTA and [βAla$^{11}$] BN(7-14) led to a significant loss of affinity;
- Spacers between DOTA and [D-Tyr$^{6}$, βAla$^{11}$, Thi$^{13}$, Nle$^{14}$] BN (6-14) showed a different affinity in the order of Ahx > GABA ≈ $PEG_2$ ≈ $βAla_2$ ≈ (D)Dab-βAla > $PEG_4$ ≈ $Sar_5$.

**3). Different charges introduced into BN analogue**

- A positive charge at the N-terminus of the BN analogue improved the affinity significantly;

- A positive charge at the side chain had no effect on the affinity;
- A negative charge at the N-terminus of the BN analogue decreased the affinity significantly.

***Binding affinity of outstanding BN analogues***

- [$Cu^{II}$]-CPTA-[βAla$^{11}$] BN (7-14) not only showed by far the highest binding affinity (sub-nanomolar) to human and mouse GRP receptors among more than 100 BN analogues, but also the highest affinity to NMB receptors, as well as high affinity to BRS-3 receptors;
- [$In^{III}$]-DOTA-GABA-[D-Tyr$^{6}$, Agly$^{11}$] BN (6-14) showed a significantly different affinity to human GRP receptor and to mouse GRP receptor (96-fold difference).

***Stability in serum***

**1). Modifying the peptide itself**

- The substitution of Leu$^{13}$ by Phe and Thi, respectively, led to increased stability in the order: Thi > Phe > Leu;
- The replacement of Met$^{14}$ by Nle decreased stability;
- The modification of Gly$^{11}$ with βAla, D-Ala, and Agly resulted in the following sequence: Agly > D-Ala ≈ βAla > Gly.

**2). Synthetic amino acid or natural amino acid between chelator and peptide**

- D-Tyr or between CPTA and [βAla$^{11}$] BN(7-14) led to a significant loss of affinity, however, Gly had a slight influence;
- Spacers between DOTA and [D-Tyr$^{6}$, βAla$^{11}$, Thi$^{13}$, Nle$^{14}$] BN (6-14) showed a different stability in the order of $Sar_5$ > D-Dab-βAla > $PEG_4$ ≈ $βAla_2$ > $PEG_2$ ≈ Ahx > GABA.

***Internalization and externalization of outstanding BN analogues***

- [$^{64}$Cu]-CPTA-[βAla$^{11}$] BN (7-14) displayed the highest internalization rate into and the slowest externalization rate from the PC-3 cells.

***Biodistribution***

**1). Increasing tumor uptake**

- High affinity led to a high uptake in the tumor, e.g. [$^{64}$Cu]-CPTA-[βAla$^{11}$] BN (7-14);
- Poly(ethylene oxide) as spacer resulted in high tumor uptake even though it may also decrease the affinity of the ligand, e.g. [$^{68}$Ga/$^{177}$Lu]-DOTA-PESIN.

**2). Enhancing kidney clearance**

- A poly(ethylene oxide) group as spacer between peptide and chelator facilitated the kidney clearance;
- A hippurane-like spacer molecule decreased the kidney uptake;
- Coinjection of lysine had no influence on the kidney uptake.

**Up to now, the most promising BN analogue for PET imaging and therapy is [$^{68}$Ga/$^{177}$Lu]-DOTA-PESIN!**

## 4.2 Outlook

***Preliminary patient study***

- It would be stimulating to carry out a clinical trial with the promising [$^{64}$Cu]-BZH7 (CPTA-[βAla$^{11}$] BN (7-14)) and [$^{177}$Lu/$^{68}$Ga]-DOTA-PESIN for PET imaging and targeted radionuclide therapy of BN receptor-expressing cancers.

***Improving the pharmacological properties of BN analogues***

- To avoid the increased uptake in the liver due to positive charge, it is necessary to further modify CPTA for introducing only one positive charge at the N-terminus of a BN analogue;
- A positive charge is introduced into DOTA-PESIN for improving binding affinity by revising DOTA;
- To facilitate sufficient kidney clearance, a further optimization of the molecular spacer is required, such as by varying the length of poly(ethylene oxide) group and hippurane-like molecular structure.

***Stabilizing BN analogue***

- Since the modification of the 11$^{th}$ or 13$^{th}$ position of BN analogue had no significant effect on the biological properties, it may be worthwhile to further modify the other decomposed peptide bonds by using synthetic amino acid;
- Cyclic BN analogues may be designed for a global stabilization of BN analogues.

# Part V: REFERENCES

1. Goldenberg, D. M., DeLand, F., Kim, E., Bennett, S., Primus, F. J., van Nagell, J. R., Jr., Estes, N., DeSimone, P., and Rayburn, P. Use of radiolabeled antibodies to carcinoembryonic antigen for the detection and localization of diverse cancers by external photoscanning. N Engl J Med, *298:* 1384-1386, 1978.
2. Goldenberg, D. M. Advancing role of radiolabeled antibodies in the therapy of cancer. Cancer Immunol Immunother, *52:* 281-296, 2003.
3. Ellis, R. J., Kim, E., and Foor, R. Role of ProstaScint for brachytherapy in localized prostate adenocarcinoma. Expert Rev Mol Diagn, *4:* 435-441, 2004.
4. Kahn, D., Austin, J. C., Maguire, R. T., Miller, S. J., Gerstbrein, J., and Williams, R. D. A phase II study of [$^{90}$Y] yttrium-capromab pendetide in the treatment of men with prostate cancer recurrence following radical prostatectomy. Cancer Biother Radiopharm, *14:* 99-111, 1999.
5. Reubi, J. C. Peptide receptors as molecular targets for cancer diagnosis and therapy. Endocr Rev, *24:* 389-427, 2003.
6. Okarvi, S. M. Peptide-based radiopharmaceuticals: future tools for diagnostic imaging of cancers and other diseases. Med Res Rev, *24:* 357-397, 2004.
7. Laskin, J. J. and Sandler, A. B. Epidermal growth factor receptor: a promising target in solid tumours. Cancer Treat Rev, *30:* 1-17, 2004.
8. Okarvi, S. M. Recent developments in $^{99m}$Tc-labelled peptide-based radiopharmaceuticals: an overview. Nucl Med Commun, *20:* 1093-1112, 1999.
9. Reubi, J. C. In vitro identification of vasoactive intestinal peptide receptors in human tumors: implications for tumor imaging. J Nucl Med, *36:* 1846-1853, 1995.
10. Reubi, J. C. Neuropeptide receptors in health and disease: the molecular basis for in vivo imaging. J Nucl Med, *36:* 1825-1835, 1995.

11. Reubi, J. C. Regulatory peptide receptors as molecular targets for cancer diagnosis and therapy. Q J Nucl Med, *41:* 63-70, 1997.

12. Heasley, L. E. Autocrine and paracrine signaling through neuropeptide receptors in human cancer. Oncogene, *20:* 1563-1569, 2001.

13. Weiner, R. E. and Thakur, M. L. Radiolabeled peptides in the diagnosis and therapy of oncological diseases. Appl Radiat Isot, *57:* 749-763, 2002.

14. Signore, A., Annovazzi, A., Chianelli, M., Corsetti, F., Van de Wiele, C., and Watherhouse, R. N. Peptide radiopharmaceuticals for diagnosis and therapy. Eur J Nucl Med, *28:* 1555-1565, 2001.

15. Krenning, E. P., Kwekkeboom, D. J., Valkema, R., Pauwels, S., Kvols, L. K., and De Jong, M. Peptide receptor radionuclide therapy. Ann N Y Acad Sci, *1014:* 234-245, 2004.

16. Heppeler, A., Froidevaux, S., Eberle, A. N., and Maecke, H. R. Receptor targeting for tumor localisation and therapy with radiopeptides. Curr Med Chem, *7:* 971-994, 2000.

17. Ginj, M. and Maecke, H. R. Radiometallo-labeled peptides in tumor diagnosis and therapy. Met Ions Biol Syst, *42:* 109-142, 2004.

18. Sosabowsky, J., Melendez-Alafort, L., and Mather, S. Radiolabelling of peptides for diagnosis and therapy of non-oncological diseases. Q J Nucl Med, *47:* 223-237, 2003.

19. Hoffman, T. J., Quinn, T. P., and Volkert, W. A. Radiometallated receptor-avid peptide conjugates for specific in vivo targeting of cancer cells. Nucl Med Biol, *28:* 527-539, 2001.

20. Preston, S. R., Miller, G. V., and Primrose, J. N. Bombesin-like peptides and cancer. Crit Rev Oncol Hematol, *23:* 225-238, 1996.

21. Reubi, J. C., Wenger, S., Schmuckli-Maurer, J., Schaer, J. C., and Gugger, M. Bombesin receptor subtypes in human cancers: detection with the universal radioligand $^{125}$I-[D-Tyr$^{6}$, beta-Ala$^{11}$, Phe$^{13}$, Nle$^{14}$] bombesin(6-14). Clin Cancer Res, *8:* 1139-1146, 2002.

22. Anastasi, A., Erspamer, V., and Bucci, M. Isolation and structure of bombesin and alytesin, 2 analogous active peptides from the skin of the European amphibians Bombina and Alytes. Experientia, *27:* 166-167, 1971.

23. McDonald, T. J., Jornvall, H., Nilsson, G., Vagne, M., Ghatei, M., Bloom, S. R., and Mutt, V. Characterization of a gastrin releasing peptide from porcine non-antral gastric tissue. Biochem Biophys Res Commun, *90:* 227-233, 1979.

24. Smith, C. J., Volkert, W. A., and Hoffman, T. J. Gastrin releasing peptide (GRP) receptor targeted radiopharmaceuticals: a concise update. Nucl Med Biol, *30:* 861-868, 2003.

25. Mantey, S. A., Weber, H. C., Sainz, E., Akeson, M., Ryan, R. R., Pradhan, T. K., Searles, R. P., Spindel, E. R., Battey, J. F., Coy, D. H., and Jensen, R. T. Discovery of a high affinity radioligand for the human orphan receptor, bombesin receptor subtype 3, which demonstrates that it has a unique pharmacology compared with other mammalian bombesin receptors. J Biol Chem, *272:* 26062-26071, 1997.

26. Pradhan, T. K., Katsuno, T., Taylor, J. E., Kim, S. H., Ryan, R. R., Mantey, S. A., Donohue, P. J., Weber, H. C., Sainz, E., Battey, J. F., Coy, D. H., and Jensen, R. T. Identification of a unique ligand which has high affinity for all four bombesin receptor subtypes. Eur J Pharmacol, *343:* 275-287, 1998.

27. Zhang, H., Chen, J., Waldherr, C., Hinni, K., Waser, B., Reubi, J. C., and Maecke, H. R. Synthesis and evaluation of bombesin derivatives on the basis of pan-bombesin peptides labeled with indium-111, lutetium-177, and yttrium-90 for targeting bombesin receptor-expressing tumors. Cancer Res, *64:* 6707-6715, 2004.

28. Moody, T. W., Mantey, S. A., Pradhan, T. K., Schumann, M., Nakagawa, T., Martinez, A., Fuselier, J., Coy, D. H., and Jensen, R. T. Development of high affinity camptothecin-bombesin conjugates that have targeted cytotoxicity for bombesin receptor-containing tumor cells. J Biol Chem, *279:* 23580-23589, 2004.

29. Markwalder, R. and Reubi, J. C. Gastrin-releasing peptide receptors in the human prostate: relation to neoplastic transformation. Cancer Res, *59:* 1152-1159, 1999.

30. Halmos, G., Wittliff, J. L., and Schally, A. V. Characterization of bombesin/gastrin-releasing peptide receptors in human breast cancer and their relationship to steroid receptor expression. Cancer Res, *55:* 280-287, 1995.

31. Reubi, J. C., Gugger, M., and Waser, B. Co-expressed peptide receptors in breast cancer as a molecular basis for in vivo multireceptor tumour targeting. Eur J Nucl Med Mol Imaging, *29:* 855-862, 2002.

32. Reubi, J. C., Korner, M., Waser, B., Mazzucchelli, L., and Guillou, L. High expression of peptide receptors as a novel target in gastrointestinal stromal tumours. Eur J Nucl Med Mol Imaging, *31:* 803-810, 2004.

33. Baidoo, K. E., Lin, K. S., Zhan, Y., Finley, P., Scheffel, U., and Wagner, H. N., Jr. Design, synthesis, and initial evaluation of high-affinity technetium bombesin analogues. Bioconjug Chem, *9:* 218-225, 1998.

34. Chen, X., Park, R., Hou, Y., Tohme, M., Shahinian, A. H., Bading, J. R., and Conti, P. S. microPET and autoradiographic imaging of GRP receptor expression with $^{64}$Cu-DOTA-[Lys$^3$]bombesin in human prostate adenocarcinoma xenografts. J Nucl Med, *45:* 1390-1397, 2004.

35. Breeman, W. A., Hofland, L. J., de Jong, M., Bernard, B. F., Srinivasan, A., Kwekkeboom, D. J., Visser, T. J., and Krenning, E. P. Evaluation of radiolabelled

bombesin analogues for receptor-targeted scintigraphy and radiotherapy. Int J Cancer, *81:* 658-665, 1999.

36. Guard, S., Watling, K. J., and Howson, W. Structure-activity requirements of bombesin for gastrin-releasing peptide- and neuromedin B-preferring bombesin receptors in rat brain. Eur J Pharmacol, *240:* 177-184, 1993.

37. Gali, H., Hoffman, T. J., Sieckman, G. L., Owen, N. K., Katti, K. V., and Volkert, W. A. Synthesis, characterization, and labeling with $^{99m}$Tc/$^{188}$Re of peptide conjugates containing a dithia-bisphosphine chelating agent. Bioconjug Chem, *12:* 354-363, 2001.

38. La Bella, R., Garcia-Garayoa, E., Langer, M., Blauenstein, P., Beck-Sickinger, A. G., and Schubiger, P. A. In vitro and in vivo evaluation of a $^{99m}$Tc(I)-labeled bombesin analogue for imaging of gastrin releasing peptide receptor-positive tumors. Nucl Med Biol, *29:* 553-560, 2002.

39. Smith, C. J., Sieckman, G. L., Owen, N. K., Hayes, D. L., Mazuru, D. G., Kannan, R., Volkert, W. A., and Hoffman, T. J. Radiochemical investigations of gastrin-releasing peptide receptor-specific [$^{99m}$Tc(X)$(CO)_3$-Dpr-Ser-Ser-Ser-Gln-Trp-Ala-Val-Gly-His-Leu-Met-$(NH_2)$] in PC-3, tumor-bearing, rodent models: syntheses, radiolabeling, and in vitro/in vivo studies where Dpr = 2,3-diaminopropionic acid and X = $H_2O$ or $P(CH_2OH)_3$. Cancer Res, *63:* 4082-4088, 2003.

40. Hoffman, T. J., Gali, H., Smith, C. J., Sieckman, G. L., Hayes, D. L., Owen, N. K., and Volkert, W. A. Novel series of $^{111}$In-labeled bombesin analogs as potential radiopharmaceuticals for specific targeting of gastrin-releasing peptide receptors expressed on human prostate cancer cells. J Nucl Med, *44:* 823-831, 2003.

41. Smith, C. J., Gali, H., Sieckman, G. L., Hayes, D. L., Owen, N. K., Mazuru, D. G., Volkert, W. A., and Hoffman, T. J. Radiochemical investigations of $^{177}$Lu-DOTA-8-Aoc-BBN[7-14]$NH_2$: an in vitro/in vivo assessment of the targeting ability of this new

radiopharmaceutical for PC-3 human prostate cancer cells. Nucl Med Biol, *30:* 101-109, 2003.

42. Rogers, B. E., Bigott, H. M., McCarthy, D. W., Della Manna, D., Kim, J., Sharp, T. L., and Welch, M. J. MicroPET imaging of a gastrin-releasing peptide receptor-positive tumor in a mouse model of human prostate cancer using a $^{64}$Cu-labeled bombesin analogue. Bioconjug Chem, *14:* 756-763, 2003.

43. Chen, J., Nguyen, H., Metcalfe, E., Eaton, S., Arunachalam, T., Raju, N., Cappelletti, E., Lattuada, L., Cagnolini, A., Maddalena, M., Lantry, L. E., Nunn, A., Swenson, R. E., Tweedle, M. F., and Linder, K. E. Formulation and in Vitro Metabolism Studies with $^{177}$Lu-AMBA; a Radiotherapeutic Compound that Targets Gastrin Releasing Peptide Receptors. *In:* Annual Congress of the EANM, Helsinki, 2004, pp. S281.

44. Smith, C. J., Gali, H., Sieckman, G. L., Higginbotham, C., Volkert, W. A., and Hoffman, T. J. Radiochemical investigations of $^{99m}$Tc-$N_3$S-X-BBN[7-14]$NH_2$: an in vitro/in vivo structure-activity relationship study where X = 0-, 3-, 5-, 8-, and 11-carbon tethering moieties. Bioconjug Chem, *14:* 93-102, 2003.

45. Wang, L. H., Coy, D. H., Taylor, J. E., Jiang, N. Y., Kim, S. H., Moreau, J. P., Huang, S. C., Mantey, S. A., Frucht, H., and Jensen, R. T. Desmethionine alkylamide bombesin analogues: a new class of bombesin receptor antagonists with potent antisecretory activity in pancreatic acini and antimitotic activity in Swiss 3T3 cells. Biochemistry, *29:* 616-622, 1990.

46. Jensen, R. T. and Coy, D. H. Progress in the development of potent bombesin receptor antagonists. Trends Pharmacol Sci, *12:* 13-19, 1991.

47. Nock, B., Nikolopoulou, A., Chiotellis, E., Loudos, G., Maintas, D., Reubi, J. C., and Maina, T. [$^{99m}$Tc]Demobesin 1, a novel potent bombesin analogue for GRP receptor-targeted tumour imaging. Eur J Nucl Med Mol Imaging, *30:* 247-258, 2003.

48. Mantey, S. A., Weber, H. C., Sainz, E., Akeson, M., Ryan, R. R., Pradhan, T. K., Searles, R. P., Spindel, E. R., Battey, J. F., Coy, D. H., and Jensen, R. T. Discovery of a high affinity radioligand for the human orphan receptor, bombesin receptor subtype 3, which demonstrates that it has a unique pharmacology compared with other mammalian bombesin receptors. J Biol Chem, *272:* 26062-26071, 1997.

49. Mantey, S. A., Coy, D. H., Pradhan, T. K., Igarashi, H., Rizo, I. M., Shen, L., Hou, W., Hocart, S. J., and Jensen, R. T. Rational design of a peptide agonist that interacts selectively with the orphan receptor, bombesin receptor subtype 3. J Biol Chem, *276:* 9219-9229, 2001.

50. Mantey, S. A., Coy, D. H., Entsuah, L. K., and Jensen, R. T. Development of bombesin analogs with conformationally restricted amino acid substitutions with enhanced selectivity for the orphan receptor human bombesin receptor subtype 3. J Pharmacol Exp Ther, *310:* 1161-1170, 2004.

51. Volkert, W. A. and Hoffman, T. J. Therapeutic radiopharmaceuticals. Chem Rev, *99:* 2269-2292, 1999.

52. O'Donoghue, J. A. and Wheldon, T. E. Targeted radiotherapy using Auger electron emitters. Phys Med Biol, *41:* 1973-1992, 1996.

53. Van de Wiele, C., Dumont, F., Vanden Broecke, R., Oosterlinck, W., Cocquyt, V., Serreyn, R., Peers, S., Thornback, J., Slegers, G., and Dierckx, R. A. Technetium-99m RP527, a GRP analogue for visualisation of GRP receptor-expressing malignancies: a feasibility study. Eur J Nucl Med, *27:* 1694-1699, 2000.

54. Shipp, M. A., Tarr, G. E., Chen, C. Y., Switzer, S. N., Hersh, L. B., Stein, H., Sunday, M. E., and Reinherz, E. L. CD10/neutral endopeptidase 24.11 hydrolyzes bombesin-like peptides and regulates the growth of small cell carcinomas of the lung. Proc Natl Acad Sci U S A, *88:* 10662-10666, 1991.

55. Hill, D. J., Mio, M. J., Prince, R. B., Hughes, T. S., and Moore, J. S. A field guide to foldamers. Chem Rev, *101:* 3893-4012, 2001.

56. Lee, H. J., Ahn, I. A., Ro, S., Choi, K. H., Choi, Y. S., and Lee, K. B. Role of azaamino acid residue in beta-turn formation and stability in designed peptide. J Pept Res, *56:* 35-46, 2000.

57. Tyndall, J. D., Pfeiffer, B., Abbenante, G., and Fairlie, D. P. Over one hundred peptide-activated G protein-coupled receptors recognize ligands with turn structure. Chem Rev, *105:* 793-826, 2005.

58. Darker, J. G., Brough, S. J., Heath, J., and Smart, D. Discovery of potent and selective peptide agonists at the GRP-preferring bombesin receptor (BB2). J Pept Sci, *7:* 598-605, 2001.

59. Weber, D., Berger, C., Heinrich, T., Eickelmann, P., Antel, J., and Kessler, H. Systematic optimization of a lead-structure identities for a selective short peptide agonist for the human orphan receptor BRS-3. J Pept Sci, *8:* 461-475, 2002.

60. Lin, J. T., Coy, D. H., Mantey, S. A., and Jensen, R. T. Comparison of the peptide structural requirements for high affinity interaction with bombesin receptors. Eur J Pharmacol, *294:* 55-69, 1995.

61. Horwell, D. C., Howson, W., Naylor, D., Osborne, S., Pinnock, R. D., Ratcliffe, G. S., and Suman-Chauhan, N. Alanine scan and N-methyl amide derivatives of Ac-bombesin[7-14]. Development of a proposed binding conformation at the neuromedin B (NMB) and gastrin releasing peptide (GRP) receptors. Int J Pept Protein Res, *48:* 522-531, 1996.

62. Smith, S. V. Molecular imaging with copper-64. J Inorg Biochem, *98:* 1874-1901, 2004.

63. Lewis, M. R., Wang, M., Axworthy, D. B., Theodore, L. J., Mallet, R. W., Fritzberg, A. R., Welch, M. J., and Anderson, C. J. In vivo evaluation of pretargeted $^{64}$Cu for tumor imaging and therapy. J Nucl Med, *44:* 1284-1292, 2003.

64. Lewis, J. S., Lewis, M. R., Cutler, P. D., Srinivasan, A., Schmidt, M. A., Schwarz, S. W., Morris, M. M., Miller, J. P., and Anderson, C. J. Radiotherapy and dosimetry of $^{64}$Cu-TETA-Tyr$^3$-octreotate in a somatostatin receptor-positive, tumor-bearing rat model. Clin Cancer Res, *5:* 3608-3616, 1999.

65. Wang, M., Caruano, A. L., Lewis, M. R., Meyer, L. A., VanderWaal, R. P., and Anderson, C. J. Subcellular localization of radiolabeled somatostatin analogues: implications for targeted radiotherapy of cancer. Cancer Res, *63:* 6864-6869, 2003.

66. Novak-Hofer, I. and Schubiger, P. A. Copper-67 as a therapeutic nuclide for radioimmunotherapy. Eur J Nucl Med Mol Imaging, *29:* 821-830, 2002.

67. Novak-Hofer, I., Zimmermann, K., and Schubiger, P. A. Peptide linkers lead to modification of liver metabolism and improved tumor targeting of copper-67-labeled antibody fragments. Cancer Biother Radiopharm, *16:* 469-481, 2001.

68. Meyer, G. J., Macke, H., Schuhmacher, J., Knapp, W. H., and Hofmann, M. $^{68}$Ga-labelled DOTA-derivatised peptide ligands. Eur J Nucl Med Mol Imaging, *31:* 1097-1104, 2004.

69. Schmitt, A., Bernhardt, P., Nilsson, O., Ahlman, H., Kolby, L., Maecke, H. R., and Forssell-Aronsson, E. Radiation therapy of small cell lung cancer with $^{177}$Lu-DOTA-Tyr$^3$-octreotate in an animal model. J Nucl Med, *45:* 1542-1548, 2004.

70. Fleischmann, A., Laderach, U., Friess, H., Buechler, M. W., and Reubi, J. C. Bombesin receptors in distinct tissue compartments of human pancreatic diseases. Lab Invest, *80:* 1807-1817, 2000.

71. Maina, T., Nock, B., Zhang, H., Nikolopoulou, A., Reubi, J. C., and Maecke, H. R. Interspecies differences during comparative evaluation of [$^{111}$In]Z070 and [$^{99m}$Tc]Demobesin 1 in rat or human origin GRP-R-expressing cells and animal models. J Nucl Med, *46*, 2005.

72. Seelig, A. A general pattern for substrate recognition by P-glycoprotein. Eur J Biochem, *251:* 252-261, 1998.

73. Giladi, E., Nagalla, S. R., and Spindel, E. R. Molecular cloning and characterization of receptors for the mammalian bombesin-like peptides. J Mol Neurosci, *4:* 41-54, 1993.

74. Singh, P., Draviam, E., Guo, Y. S., and Kurosky, A. Molecular characterization of bombesin receptors on rat pancreatic acinar AR42J cells. Am J Physiol, *258:* G803-809, 1990.

75. Schuhmacher, J., Zhang, H., Doll, J., Macke, H. R., Matys, R., Hauser, H., Henze, M., Haberkorn, U., and Eisenhut, M. GRP Receptor-Targeted PET of a Rat Pancreas Carcinoma Xenograft in Nude Mice with a $^{68}$Ga-Labeled Bombesin(6-14) Analog. J Nucl Med, *46:* 691-699, 2005.

76. Fichna, J. and Janecka, A. Synthesis of target-specific radiolabeled peptides for diagnostic imaging. Bioconjug Chem, *14:* 3-17, 2003.

77. Dumesny, C., Whitley, J. C., Baldwin, G. S., Giraud, A. S., and Shulkes, A. Developmental expression and biological activity of gastrin-releasing peptide and its receptors in the kidney. Am J Physiol Renal Physiol, *287:* F578-585, 2004.

# Part VI: APPENDIX

*Paper 1*

# Synthesis and Evaluation of Bombesin Derivatives on the Basis of Pan-Bombesin Peptides Labeled with Indium-111, Lutetium-177, and Yttrium-90 for Targeting Bombesin Receptor-Expressing Tumors

**Hanwen Zhang,[1] Jianhua Chen,[1] Christian Waldherr,[1] Karin Hinni,[1] Beatrice Waser,[2] Jean Claude Reubi[2] and Helmut R Maecke[1]**

[1]Division of Radiological Chemistry, Institute of Nuclear Medicine, Department of Radiology, University Hospital, Basel;
[2]Division of Cell Biology and Experimental Cancer Research, Institute of Pathology, University of Berne, Berne, Switzerland

Published in:
*Cancer Research* 2004, 64: 6707-6715

[CANCER RESEARCH 64, 6707–6715, September 15, 2004]

# Synthesis and Evaluation of Bombesin Derivatives on the Basis of Pan-Bombesin Peptides Labeled with Indium-111, Lutetium-177, and Yttrium-90 for Targeting Bombesin Receptor-Expressing Tumors

**Hanwen Zhang,[1] Jianhua Chen,[1] Christian Waldherr,[1] Karin Hinni,[1] Beatrice Waser,[2] Jean Claude Reubi,[2] and Helmut R. Maecke[1]**

*[1]Division of Radiological Chemistry, Institute of Nuclear Medicine, Department of Radiology, University Hospital, Basel; and [2]Division of Cell Biology and Experimental Cancer Research, Institute of Pathology, University of Berne, Berne, Switzerland*

## ABSTRACT

**Bombesin receptors are overexpressed on a variety of human tumors like prostate, breast, and lung cancer. The aim of this study was to develop radiolabeled (Indium-111, Lutetium-177, and Yttrium-90) bombesin analogues with affinity to the three bombesin receptor subtypes for targeted radiotherapy. The following structures were synthesized: diethylenetriaminepentaacetic acid-γ-aminobutyric acid-[D-Tyr$^6$, β-Ala$^{11}$, Thi$^{13}$, Nle$^{14}$] bombesin (6–14) (BZH1) and 1,4,7,10-tetraazacyclododecane-*N*,*N*′,*N*″,*N*‴-tetraacetic acid-γ-aminobutyric acid-[D-Tyr$^6$, β-Ala$^{11}$, Thi$^{13}$, Nle$^{14}$] bombesin (6–14) (BZH2). [$^{111}$In]-BZH1 and in particular [$^{90}$Y]-BZH2 were shown to have high affinity to all three human bombesin receptor subtypes with binding affinities in the nanomolar range. In human serum metabolic cleavage was found between β-Ala$^{11}$ and His$^{12}$ with an approximate half-life of 2 hours. The metabolic breakdown was inhibited by EDTA and β-Ala$^{11}$-His$^{12}$ (carnosine) indicating that carnosinase is the active enzyme.**

**Both $^{111}$In-labeled peptides were shown to internalize into gastrin-releasing peptide-receptor–positive AR4–2J and PC-3 cells with similar high rates, which were independent of the radiometal. The biodistribution studies of [$^{111}$In]-BZH1 and [$^{111}$In]-BZH2 ([$^{177}$Lu]-BZH2) in AR4–2J tumor-bearing rats showed specific and high uptake in gastrin-releasing peptide-receptor–positive organs and in the AR4–2J tumor. A fast clearance from blood and all of the nontarget organs except the kidneys was found. These radiopeptides were composed of the first pan-bombesin radioligands, which show great promise for the early diagnosis of tumors bearing not only gastrin-releasing peptide-receptors but also the other two bombesin receptor subtypes and may be of use in targeted radiotherapy of these tumors.**

## INTRODUCTION

The development of ligand-targeted therapeutics in anticancer therapy including drug-ligand conjugates has gained momentum in recent years (1). Systemic cytotoxic chemotherapy shows little selectivity and is limited by potentially serious side effects. One strategy to improve the lack of selectivity is to couple therapeutics to vectors like monoclonal antibodies, their fragments, or even smaller molecules (2). The cytotoxic drug part of conjugates used in ligand-targeted therapeutics is often composed of a therapeutic radiometal encapsulated by its bifunctional chelator.

A very promising group of small targeting ligands is composed of regulatory peptides (3). A high number of peptide receptors were shown to be overexpressed in various human tumors (4). They are promising targets for molecular imaging and targeted therapy of cancer, because they are located on the plasma membrane and, upon binding of a ligand, the receptor-ligand complex is internalized. These findings were the basis for the development of diagnostic and therapeutic radiopeptides useful in peptide receptor scintigraphy and targeted radiotherapy (5–10). Among the most relevant peptide receptors, the bombesin receptors are of major interest, because they were found to be overexpressed in various important cancers like prostate (11, 12), breast (13, 14), and small cell lung cancer (15). The human counterparts of bombesin, namely gastrin-releasing peptide (16) and neuromedin B (17), have been found in mammalian tissue. They bind to different bombesin receptor subtypes, such as the neuromedin B preferring receptor (BB1 receptor; ref. 18), the gastrin-releasing peptide preferring receptor (BB2; ref. 19), as well as the orphan bombesin receptor subtype-3 (BB3 receptor; ref. 20) and the BB4 receptor (21). The BB1, BB2, and BB3 receptors have been shown recently to be overexpressed on different human tumors (22). Gastrin-releasing peptide receptors were predominantly expressed in human prostate cancer (100%), gastrinoma (100%), and breast cancer (70%), whereas concomitant expression of gastrin-releasing peptide receptor (33%) and BB3 receptor (40%) were found in small cell lung cancer. Also gastrin-releasing peptide receptor (40%) and BB3 (25%) were found concomitantly in renal cell carcinoma. Preferential expression of BB1 was found in intestinal carcinoids (11 of 24), and bronchial carcinoids had preferential BB3 receptor expression (9 of 26).

These findings provide a possibility to apply bombesin-like peptides as a vehicle for delivering cytotoxic drugs (23–25) into tumor cells. In addition, radiolabeling may allow us to diagnose and treat these tumors (10, 26–37). The sequence bombesin(7–14) was regarded to be sufficient for the specific binding interaction with the gastrin-releasing peptide receptor (38, 39). Therefore, most radiolabeled bombesin-like peptides are based on the sequence bombesin (7–14) (10, 28–31, 33–35). For example, different conjugates were developed using bifunctional chelators for labeling with $^{99m}$Tc, like $N_2S_2$ (29), $N_3S$ (31), $N_\alpha$-histidinyl acetate (35), and diaminopropionic acid (36), using the carbonyl approach. Also, diethylenetriaminepentaacetic acid (DTPA) and 1,4,7,10-tetraazacyclododecane-*N*,*N*′,*N*″,*N*‴-tetraacetic acid (DOTA) were coupled to this sequence for labeling with hard Lewis acid radiometals like $^{111}$In, $^{67,\ 68}$Ga, $^{90}$Y, and the lanthanides. Some $^{99m}$Tc-labeled peptides have been or are currently being investigated in gastrin-releasing peptide receptor-positive tumors in patients (30, 31, 33).

Recently, a universal ligand, (D-Tyr$^6$, β-Ala$^{11}$, Phe$^{13}$, Nle$^{14}$) bombesin (6–14), has been developed by Mantey *et al.* (40) and Pradhan *et al.* (41), which has high affinity to all of the bombesin receptor subtypes. The finding that not only the gastrin-releasing peptide receptor is overexpressed on human tumors but in some cases also neuromedin B and BB3 receptor subtypes prompted us to develop conjugates based on the slightly modified (Thi$^{13}$ *versus* Phe$^{13}$) universal bombesin ligand [D-Tyr$^6$, β-Ala$^{11}$, Phe$^{13}$, Nle$^{14}$] bombesin (6–14) that can be labeled with hard Lewis acid-type metallic

Received 12/09/03; revised 4/22/04; accepted 7/8/04.

**Grant support:** Supported analytically by Novartis and financially by the Swiss National Science Foundation (Grant Nr. 3100A0–100390), by the Amt für Ausbildungsbeiträge (H. Zhang), the Commission for Technology and Innovation (KTI-project 4668–1 EUS), and by Mallinckrodt Med.

The costs of publication of this article were defrayed in part by the payment of page charges. This article must therefore be hereby marked *advertisement* in accordance with 18 U.S.C. Section 1734 solely to indicate this fact.

**Requests for reprints:** Helmut Maecke, Division of Radiological Chemistry, Institute of Nuclear Medicine, Department of Radiology, University Hospital, Petersgraben 4, CH-4031 Basel, Switzerland. Phone: 41-61-265-46-99; Fax: 41-61-265-55-59; E-mail: hmaecke@uhbs.ch.

radionuclides like $^{111}$In, $^{90}$Y, and $^{177}$Lu. The Thi$^{13}$ *versus* Phe$^{13}$ modification was done because preliminary data from our laboratory have shown an increased metabolic stability of this peptide over the Phe$^{13}$ analogue. We studied these (radio)metallopeptides with regard to the bombesin receptor subtype profile. The internalization rate of the two chelated peptides, labeled with the indicated radiometals, into AR4–2J (rat pancreatic tumor cells bearing the gastrin-releasing peptide receptor) and PC-3 (human prostate cancer cell line) cells was studied as well. We also report on the metabolic stability in human blood serum and the identification of metabolites. In addition, the biodistribution of the $^{111}$In-labeled peptides was studied. This work is the first one of a pan-bombesin ligand aimed at radiotargeted diagnosis and therapy.

## MATERIALS AND METHODS

**Chemicals.** All chemicals were obtained from commercial sources and used without additional purification. DOTA-tris(tBu ester) was commercially available (Macrocyclics, Dallas, TX) or was synthesized according to Heppeler *et al.* (42). DTPA(tris-tBu) was received from Mallinckrodt Medical (Dr. Ananth Srinivasan, St. Louis, MO). Rink amide MBHA resin and all of the Fmoc-protected amino acids were commercially available from NovaBiochem (Läufelfingen, Switzerland). [$^{111}$In]$Cl_3$ was purchased from Mallinckrodt Medical (Petten, the Netherlands), [$^{90}$Y]$Cl_3$ from Perkin-Elmer Life Sciences Inc. (Boston, MA), and [$^{177}$Lu]$Cl_3$ from I.D.B. (Petten, the Netherlands). Electrospray ionization mass spectroscopy was carried out with a Finnigan SSQ 7000 spectrometer or fast atom bombardment mass spectroscopy with a VG 70SE spectrometer and matrix-assisted laser desorption ionization-mass spectrometry measurements on a Voyager sSTR equipment with a Nd:YAG laser (Applied Biosystems, Framingham, NY). Analytical high-performance liquid chromatography (HPLC) was performed on a Hewlett Packard 1050 HPLC system with a multiwavelength detector and a flow-through Berthold LB 506 Cl $\gamma$-detector using a Macherey-Nagel Nucleosil 120 $C_{18}$ column. Preparative HPLC was performed on a Metrohm HPLC system LC-CaDI 22–14 with a Macherey-Nagel VP 250/21 Nucleosil 100–5 $C_{18}$ column. Quantitative gamma counting was performed on a COBRA 5003 $\gamma$-system well counter from Packard Instruments. Solid-phase peptide synthesis was performed on a semiautomatic peptide synthesizer commercially available from Rink Combichem (Bubendorf, Switzerland). The cell culture medium was DMEM with 10% FCS from Bioconcept.

**Synthesis.** The peptide synthesis was performed on a semiautomatic peptide synthesizer according to a general procedure described previously (ref. 43; Fig. 1). Standard Fmoc chemistry was used throughout (44); the peptide was assembled on a Rink amide MBHA resin. Trt and tBu were used as protecting groups of His and D-Tyr, respectively, and Boc for Trp. The chelators were coupled as follows. Three equivalents DTPA(tBu)$_3$ were preincubated with *N*,*N*′-diisopropylcarbodiimide in 1-methyl-2-pyrrolidone for 30 min and incubated with the resin-assembled peptide until the 2,4,6-trinitrobenzenesulfonic acid test was negative (~3 hours). DOTA(tBu)$_3$ was coupled as described (43). The peptide chelator conjugates were cleaved from the resin and deprotected by incubation with trifluoroacetic acid—thioanisole–water 92:6:2 for 4 to 6 hours at room temperature and precipitated in isopropyl ether–petroleum ether (1:1). The crude peptide-chelator conjugate was purified by preparative HPLC (Macherey-Nagel Nucleosil 100–5 $C_{18}$, flow: 15 mL/min; eluents: A = 0.1% trifluoroacetic acid in water and B = acetonitrile; nonlinear gradient: 0 min, 70% A; 10 min, 50% A). Mass spectrometry [(−)electrospray ionization, matrix-assisted laser desorption ionization] was used to determine the composition of the conjugates.

**The Potential Metabolites.** Diethylenetriaminepentaacetic acid-$\gamma$-aminobutyric acid (DTPA-GABA), DTPA-GABA-D-Tyr, DTPA-GABA-D-Tyr-Gln, DTPA-GABA-D-Tyr-Gln-Trp, DTPA-GABA-D-Tyr-Gln-Trp-Ala-Val, DTPA-GABA-D-Tyr-Gln-Trp-Ala-Val-$\beta$-Ala, and DTPA-GABA-D-Tyr-Gln-Trp-Ala-Val-$\beta$-Ala-His were synthesized in parallel using the same protocol as described above.

**[In$^{III}$]-BZH1.** The metal complex was synthesized according to the methods described previously (42). A mixture of DTPA-GABA-[D, Tyr$^6$, $\beta$-Ala$^{11}$, Thi$^{13}$, Nle$^{14}$] BN(6–14) (BZH1; 0.5 $\mu$mol) in 500 $\mu$L of 0.4 mol/L sodium acetate buffer (pH 5.0) was incubated with 1.5 $\mu$mol $InCl_3 \cdot 5H_2O$ in 0.04 mol/L HCl for 1 h at room temperature and purified over a SepPak $C_{18}$ cartridge preconditioned with 10 mL of EtOH and 10 mL of water. The cartridge was eluted with 10 mL of water followed by 3 mL of methanol resulting in [$^{111}$In]-BZH1 after evaporation of the methanol. The final product was analyzed by analytical HPLC; the purity was ≥97%. Mass spectrometry [matrix-assisted laser desorption ionization, *m*/*z* (%)]: 1711.0 (100, $[M+H]^+$), 1732.9 (25, $[M+Na]^+$).

[Y$^{III}$]-DOTA-GABA-[D-Tyr$^6$, $\beta$-Ala$^{11}$, Thi$^{13}$, Nle$^{14}$] BN (6–14) (BZH2) was synthesized using $Y(NO_3)_3 \cdot 5H_2O$ as described above except that the incubation was at 95°C for 20 to 25 minutes. The final product was analyzed by analytical HPLC; the purity was >95%. Mass spectrometry (matrix-assisted laser desorption ionization; *m*/*z* (%)):1696.8 (100, $[M+H]^+$), 1718.8 (20, $[M+Na]^+$), 1734.8 (10, $[M+K]^+$).

**Preparation of the Radiotracer.** [$^{111}$In]-BZH1 was prepared by dissolving 10 $\mu$g of BZH1 (6.25 nmol) in sodium acetate buffer [300 $\mu$L and 0.4 mol/L (pH 5.0)] and by incubation with $^{111}InCl_3$ (3 to 6 mCi) for 1 hour at room temperature. A 1.5 molar excess of $InCl_3 \cdot 5H_2O$ was added and the final solution incubated again at room temperature for 1 hour. Subsequently, radiometalated peptides were purified using a SepPak $C_{18}$ cartridge as described above affording a very pure $^{111}$In/$^{nat}$In-labeled ligand for internalization studies. For biodistribution and serum stability studies, the labeling was performed accordingly without the addition of cold $InCl_3 \cdot 5H_2O$. For injection the solution was prepared by dilution with 0.9% NaCl (0.1% bovine serum albumin) to afford the radioligand solution.

[$^{90}$Y/$^{111}$In/$^{177}$Lu]-BZH2 were prepared and purified accordingly by heating at 95°C for 20 to 25 minutes; $Y(NO_3)_3 \cdot 5H_2O$, $Lu(NO_3)_3 \cdot 6H_2O$, and $InCl_3 \cdot 5H_2O$ were used.

**Serum Stability and Identification of Metabolites.** To 1 mL of freshly prepared human serum, previously equilibrated in a 5% $CO_2$ (95% air) environment at 37°C, we added 0.6 nmol $^{111}$In-labeled BZH1 or BZH2 standard solution. The mixture was incubated in a 5% $CO_2$, 37°C environment. At different time points, 50-$\mu$L aliquots (in triplicate) were removed and treated with 60 $\mu$L of EtOH. Samples were then cooled (4°C) and centrifuged for 15 min at 500 × *g* and 4°C to precipitate serum proteins. Fifty $\mu$L of supernatant were removed for activity counting in a $\gamma$-well counter, the sediment was washed twice with 1 mL of EtOH and counted, and the activity in the supernatant was compared with the activity in the pellet to give the percentage of peptides not bound to proteins or radiometal transferred to serum proteins. The supernatant was analyzed with HPLC (eluents: A = 0.1% trifluoroacetic acid in water and B = acetonitrile; gradient: 0 to 45 minutes, 95% to 60% A; 45 to 46 minutes, 100% B; 46 to 49 minutes, 100% B; 50 minutes, 95% A) to determine relative amounts of metabolites.

The data points were fitted using origin 6 (Microcal Software, Inc., Northampton, MA), assuming a consecutive reaction (Eq. A) and Eq. B and C to calculate the disappearance of intact peptide A as well as the formation and disappearance of metabolite B, respectively.

$$A \xrightarrow{k1} B \xrightarrow{k2} C + D \tag{A}$$

$$[A] = 100 \cdot e^{-k1t} \tag{B}$$

$$[B] = 100 \cdot \frac{k1}{k1 - k2} \cdot (e^{-k2t} - e^{-k1t}) \tag{C}$$

To identify the metabolites, [$^{111}$In]-BZH1 was used as the leading peptide. The extracted supernatant, obtained as described above, was co-injected with the potential "metabolites," synthesized as described above. The metabolism in serum was studied by the addition of EDTA (2.4 mmol/L) or carnosine (22.4 mmol/L) to [$^{111}$In]-BZH1 serum solutions.

**Binding Affinity and Receptor Subtype Profile.** The binding affinity profiles of [In$^{III}$]-BZH1 and [Y$^{III}$]-BZH2 for the three bombesin receptor subtypes were determined *in vitro* using receptor autoradiography. Human tumors were selected that had been shown previously to express predominantly one single bombesin receptor subtype, namely either neuromedin B receptor, gastrin-releasing peptide receptor or $BB_3$ receptor. $IC_{50}$ were measured in

competitive binding experiments performed with increasing concentrations of [$In^{III}$]-BZH1, [$Y^{III}$]-BZH2 and [D-$Tyr^6$, $\beta$-$Ala^{11}$, $Phe^{13}$, $Nle^{14}$]bombesin(6–14; as reference) in successive tissue sections containing tumors expressing either gastrin-releasing peptide-receptors, neuromedin B receptors or BB3 receptors, using [$^{125}$I-D-$Tyr^6$, $\beta$-$Ala^{11}$, $Phe^{13}$, $Nle^{14}$]bombesin(6–14) as universal radioligand, as described in detail previously (22, 45).

**Cell Culture.** AR4–2J rat pancreatic tumor cells and PC-3 cells were cultured in Dulbecco's minimal essential medium (DMEM). DMEM was supplemented with vitamins, essential and nonessential amino acids, L-glutamine, antibiotics (penicillin/streptomycine), fungicide (amprotencine) and 10% fetal calf serum (FCS) as described elsewhere (46).

**Internalization and Externalization (Efflux) Studies.** Internalization and externalization experiments were performed in 6-well plates as indicated in a previous publication (46). The procedure was the same for both cell lines. Briefly, the cells were washed twice with the internalization medium and allowed to adjust to the medium for 1 h at 37°C. Approximately 1.8 kBq (0.25 pmol) of radioligand were added to the medium and the cells ($10^6$ cells per well) and incubated (in triplicates) for 0.5, 1, 2, 4 and 6 h at 37°C, 5% $CO_2$, with or without excess of cold BZH2 (150 $\mu$L of a 5.8 $\mu$mol/L solution, final concentration of cold BZH2 was 0.58 $\mu$mol/L) to determine nonspecific internalization. The final volume was 1.5 ml. At appropriate time points the internalization was stopped by removal of the medium followed by washing the cells with ice-cold solution composed of 0.9% NaCl/0.01 mol/L $Na_2HPO_4$/0.01 M $KH_2PO_4$ (pH 7.2). Cells were then treated 5 min (twice) with glycine buffer (0.05 mol/L glycine solution, pH adjusted to 2.8 with 1 mol/L HCl) to distinguish between cell surface-bound (acid releasable) and internalized (acid resistant) radioligand. Finally, cells were detached from the plates by incubation with 1 mol/L NaOH for 10 min at 37°C, and the radioactivity was measured in a $\gamma$-counter.

For externalization studies, the AR4–2J cells were allowed to internalize the radioligands for periods of 2 h and were then exposed to an acid wash, as described in the previous section, to dissociate cell-surface-bound radioligand. One ml of culture medium was added to each well, cells were incubated at 37°C in a 5% $CO_2$ environment and externalization of the cell-incorporated radioactivity was studied at different times. The culture medium was collected and measured for radioactivity.

**Biodistribution Experiments in AR4–2J Tumor Bearing Lewis Rats.** Lewis male rats were implanted subcutaneously with 10 millions AR4–2J tumor cells, which were freshly expanded in a sterilized solution of 0.9% NaCl/0.01 mol/L $Na_2HPO_4$/0.01 mol/L $KH_2PO_4$ (pH 7.2).

Fourteen days after inoculation the tumors weighed 0.3–1.2 g and the rats were injected into the back leg vein with 0.1 $\mu$g radiolabeled peptides (about 0.5 MBq $^{111}$In or 0.9 MBq $^{177}$Lu), diluted in NaCl (0.1% bovine serum albumin, pH 7.4, total injected volume = 200 $\mu$L). For the determination of nonspecific uptake in tumor or receptor positive organs, a group of 4 animals was injected with a mixture of 0.1 $\mu$g radiolabeled peptide/50 $\mu$g BZH2 in 0.9% NaCl solution (injected volume, 225 $\mu$L). At 4 h, 24 h, 48 h, and 72 h rats (in groups of 4–11 rats) were sacrificed, and organs of interest were collected, rinsed of excess blood, blotted, weighed and counted in a $\gamma$-counter. The percentage of injected dose per gram (% ID/g) was calculated for each tissue. The total counts injected per animal were determined by extrapolation from counts of an aliquot taken from the injected solution as a standard.

All animal experiments were performed in compliance with the Swiss regulation for animal treatment (Bundesamt für Veterinärwesen, approval no. 789).

## RESULTS

**Synthesis and Labeling.** BZH1 and BZH2 (Fig. 1) were synthesized using Fmoc strategy affording an overall yield of approximately 30% based on the removal of the first Fmoc group; the purity analyzed by HPLC was $\geq$ 97%. BZH1 was labeled with $^{111}$In by incubation at room temperature (1 h incubation, pH 5, 0.4 mol/L sodium acetate buffer). BZH2 was labeled with $^{111}$In, $^{90}$Y, and $^{177}$Lu at elevated temperature (95°C, 20–25 min). In all cases, labeling yields of $\geq$ 98% at specific activities of $>$37 GBq $\mu$mol$^{-1}$ were achieved.

**Receptor Binding Affinity and the Receptor Subtype Profile.** Table 1 shows the bombesin receptor subtype binding profile of the 2 new metallopeptides. As reference peptide [D-$Tyr^6$, $\beta$-$Ala^{11}$, $Phe^{13}$, $Nle^{14}$] bombesin(6–14) was used, which binds with high affinity to all 3 bombesin receptor subtypes. Although less potent than the reference peptide, the 2 new bombesin analogues still have retained high affinity to all three receptor subtypes. The $IC_{50}$ values of [$In^{III}$]-BZH1 are 3.47 $\pm$ 0.32 nM to the gastrin-releasing peptide receptor, 10.5 $\pm$ 3.03 nM to the neuromedin B receptor, and 41.7 $\pm$ 22.2 nM to the BB3 receptor. The respective values for [$Y^{III}$]-BZH2 are 1.40 $\pm$ 0.10 nM, 4.93 $\pm$ 1.03 nM, and 10.7 $\pm$ 4.2 nM.

**Stability in Human Serum and Identification of Metabolites.** After incubation of the radiolabeled peptides with fresh serum, three metabolites were determined using HPLC and radiometric analysis. The proteic fraction obtained as pellet contained $<$5% of radioactivity. [$^{111}$In]-BZH1 was metabolized to [$^{111}$In]-DTPA-GABA-D-Tyr-Gln-Trp-Ala-Val-$\beta$-Ala (corresponding to B) due to the cleavage between $\beta$-$Ala^{11}$ and $His^{12}$, and then this metabolite decomposed to [$^{111}$In]-DTPA-GABA-D-Tyr-Gln (C) and [$^{111}$In]-DTPA (D; Fig. 2). These metabolites were identified using reverse-phase HPLC by co-injection of presynthesized chelator-conjugated peptides. The similarity of HPLC elution times indicates that [$^{111}$In]-BZH2 is metabolized to the same breakdown products. There was no indication of radiometal transfer to serum proteins during incubation studies.

Fig. 3 shows the kinetics of metabolic degradation of [$^{111}$In]-BZH1 and [$^{111}$In]-BZH2. Curve fitting data gave rate parameters for the disappearance of intact peptides (A, A′) and the built-up of metabolites (B, C, D; B′, C′, D′).

The respective half-lives for [$^{111}$In]-BZH1 and [$^{111}$In]-BZH2 were determined to 2.0 hours and 2.3 hours; however, the first metabolite B′ of [$^{111}$In]-BZH2 was more stable than B of [$^{111}$In]-BZH1, and their half-lives of disappearance are 26 hours and 46 hours, respectively (Table 2). When carnosine or EDTA were incubated together with [$^{111}$In]-BZH1 in serum, [$^{111}$In]-BZH1 is significantly more stable than without these inhibitors (Fig. 4).

**Internalization and Externalization Studies.** Both $^{111}$In-labeled radiopeptides showed a fast cell uptake, which did not reach a plateau within 6 hours of incubation at 37°C in AR4–2J cells (Figs. 5 and 6). Internalization was strongly reduced in the presence of 0.57 $\mu$mol/L unlabeled BZH2 (data not shown). Nonspecific internalization was $<$1% of the added activity. The surface bound peptide (acid removable) was $<$7% of the added activity (data not shown). BZH2 labeled with different radioisotopes ($^{111}$In, $^{177}$Lu, and $^{90}$Y) exhibited the same internalization rates (Fig. 5). [$^{111}$In]-BZH1 was internalized by AR4–2J and PC-3 cells with a similar kinetics (Fig. 4). Preliminary studies using *in vitro* receptor autoradiography showed that AR4–2J and PC-3 tumors express predominantly the gastrin-releasing peptide receptor.[3]

The kinetics of externalization of both peptides was studied with cells exposed for 2 hours to the radioligand as described for internalization. Within 2 hours, 45% of [$^{111}$In]-BZH1 and 30% of [$^{111}$In]-BZH2 were released from the AR4–2J cells. The efflux of [$^{111}$In]-BZH1 was faster than that of [$^{111}$In]-BZH2 (Fig. 7). To identify the composition of externalized peptide, [$^{111}$In]-BZH1 was used as a leading peptide. The externalized radioactivities corresponded to the intact peptide and one metabolite [$^{111}$In(DTPA)]$^{2-}$, identified by HPLC using co-injection.

Upon 2 hours of internalization and acid wash, the externalized radioactivity already after 30 min consisted of $\sim$50% [$^{111}$In-(DTPA)]$^{2-}$ as the only metabolite and 50% intact radiolabeled pep-

[3] J. C. Reubi, unpublished observations.

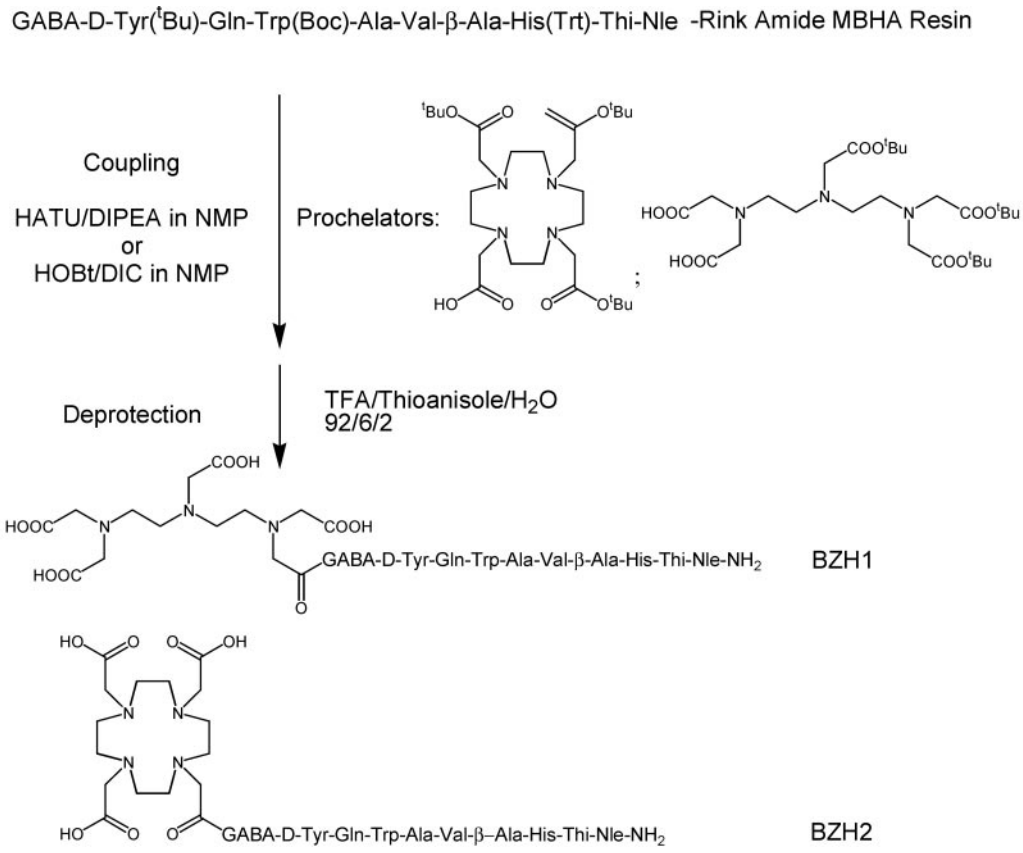


Fig. 1. GABA-D-Tyr(tBu)-Gln-Trp(Boc)-Ala-Val-β-Ala-His(Trt)-Thi-Nle -Rink Amide MBHA Resin.

tide. At 4 hours, the externalized radioactivity consisted of the metabolite $[^{111}In(DTPA)]^{2-}$ (87.5%) and intact peptide (12.5%), whereas at 24 hours, only the metabolite was found.

**Animal Biodistribution Studies.** Results from biodistribution studies using the $^{111}In$-labeled peptides performed with Lewis rats bearing the AR4–2J pancreatic tumor are presented in Table 3 as the percentage of injected dose per gram of tissue (% ID/g). Tumor uptake and retention of [$^{111}In$]-BZH2 is also shown in Fig. 8.

Both [$^{111}In$]-BZH1 and [$^{111}In$]-BZH2 displayed rapid blood clearance with <0.02% ID/g and 0.01% ID/g at 4 hours, respectively. Fast clearance from the gastrin-releasing peptide receptor-negative tissues except the kidneys was found as well. [$^{111}In$]-BZH1 and [$^{111}In$]-BZH2 show high uptake values in the AR4–2J tumor and in the gastrin-releasing peptide receptor-positive organs, *e.g.*, at 4 hours: tumor, 1.71 ± 0.51% ID/g *versus* 0.79 ± 0.07% ID/g; and pancreas, 3.92 ± 0.86% ID/g *versus* 2.63 ± 0.59% ID/g. The tumor uptake of [$^{111}In$]-BZH2 dropped from 0.79 ± 0.07% ID/g at 4 hours to 0.44 ± 0.07% ID/g at 24 hours, 0.42 ± 0.05 at 48 hours, and 0.33 ± 0.08 at 72 hours. The respective pancreas values are 2.63 ± 0.59 at 4 hours, 2.13 ± 0.68 at 24 hours, 2.07 ± 0.22 at 48 hours, and 1.65 ± 0.32 at 72 hours.

*In vivo* competition experiments using 50 μg of BZH2 co-injected with [$^{111}In$]-BZH1 (data for [$^{111}In$]-BZH2 in brackets) resulted in a >93% (89%) reduction of tumor uptake and also in a reduction of the uptake in normal gastrin-releasing peptide receptor-positive organs (>97% for both radiopeptides in the pancreas). Also, the uptake in other organs could be blocked to a high degree: stomach 84% (65%), bowel 72% (82%), and adrenals 73% (66%). The injection of the blocking dose had no significant influence on the uptake in nontarget organs except the kidneys where the uptake decreased by a factor of 1.5 on blocking. Due to the fast clearance of both peptides, high tumor–background ratios were found (Table 3).

$^{111}In$ was used as a surrogate of $^{90}Y$ for studying the pharmacokinetics of BZH2, because the latter is a pure β-emitter. This is the strategy most often used in such studies, although there may be some differences between the two due to structural differences (47, 48). Therefore, we also studied [$^{177}Lu$]-BZH2 as a radiotherapeutic peptide radiopharmaceutical. $^{177}Lu$ is a low energy β-emitter that has two γ-lines at 133 keV (7%) and 208 keV (11%) allowing convenient localization. The organ uptake values of [$^{177}Lu$]-BZH2 were very similar to those of [$^{111}In$]-BZH2. The values for the most important organs are: tumor 0.67 ± 0.04% ID/g (4 hours) and 0.42 ± 0.03% ID/g (24 hours); pancreas 2.39 ± 0.24% ID/g (4 hours) and 1.92 ± 0.25% ID/g (24 hours); and kidneys 1.17 ± 0.37% ID/g (4 hours) and 0.54 ± 0.07% ID/g (24 hours).

Table 1 *Affinity profiles ($IC_{50}$) for human BB1-BB3 receptors of the bombesin analogues [$In^{III}$]-BZH1 and [$Y^{III}$]-BZH2*

| Peptide | BB1 (NMB-R) | BB2 (GRP-R) | BB3-R |
|---|---|---|---|
| [D-Tyr$^6$, β-Ala$^{11}$, Phe$^{13}$, Nle$^{14}$]BN (6–14) | 1.01 ± 0.06 (5) | 0.68 ± 0.05 (5) | 1.73 ± 0.64 (3) |
| [$In^{III}$]-BZH1 | 10.5 ± 3.03 (3) | 3.47 ± 0.32 (3) | 41.7 ± 22.2 (3) |
| [$Y^{III}$]-BZH2 | 4.93 ± 1.03 (3) | 1.40 ± 0.10 (3) | 10.7 ± 4.2 (3) |

NOTE. The $IC_{50}$ values (nM ± SE) are in triplicates. The number of independent studies are in brackets.

Abbreviations: BN, bombesin; NMB, neuromedin B; R, receptor; GRP, gastrin-releasing peptide.

## DISCUSSION

This study describes two very promising pan-bombesin peptidic ligands for radiolabeling with diagnostic and therapeutic radiometals.

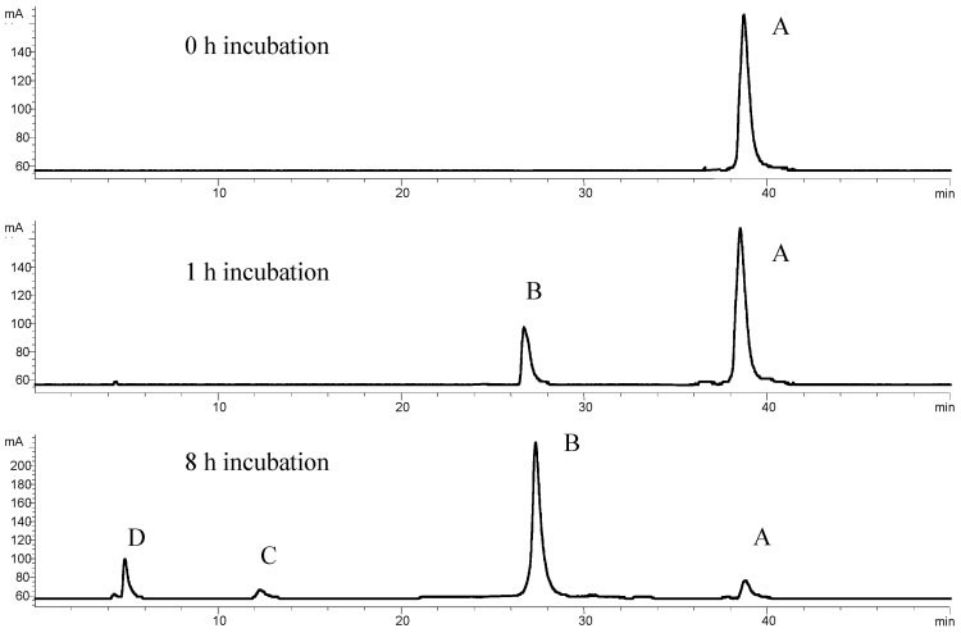


Fig. 2. HPLC elution profile of [$^{111}$In]-BZH1 after incubation with fresh human serum, immediately after incubation, $t_R$ = 38.7 min; 1 hour after incubation, $t_R$ ([$^{111}$In]-BZH1) = 38.6 minutes, $t_R$ (metabolite B) = 27.3 min; 8 hours after incubation, $t_R$ ([$^{111}$In]-BZH1) = 38.7 minutes, $t_R$ (metabolite B) = 27.5 minutes, $t_R$ (metabolite C) = 12.3 minutes, $t_R$ (metabolite D) = 5.1 minutes.

They may be used for targeted diagnosis and radiotherapy of bombesin receptor-positive tumors like prostate and breast cancer.

A variety of radiopeptides are currently being developed for the targeting of tumors (5–10). Those based on bombesin are of interest, because bombesin receptors were shown to be overexpressed on a variety of frequently occurring tumors like breast cancer and prostate cancer. In addition, Markwalder and Reubi (11) not only found a massive gastrin-releasing peptide receptor overexpression in invasive prostate cancer tissue but also in the early stage of the disease, *i.e.*, the prostatic intraepithelial neoplasia, which may open the possibility to localize an early event in prostate carcinogenesis.

Many reports on bombesin-based radiopeptides have been published recently (26–36), but there has been no study thus far on radiopeptides based on pan-bombesin ligands. These may be of interest, because not only the gastrin-releasing peptide (BB2)-receptor but also BB1-receptor and BB3-receptor were found to be overexpressed on human tumors as well (22).

In our present study we evaluated the slightly modified pan-bombesin ligand [D-Tyr$^6$, $\beta$-Ala$^{11}$, Phe$^{13}$, Nle$^{14}$] bombesin(6–14) developed by the Jensen group (40, 41), by attaching DTPA(BZH1) and DOTA(BZH2) via a GABA spacer to the octapeptide. The chelators allow a high specific activity labeling with $^{111}$In (DTPA). DOTA chelates a large number of radiometals with extremely high kinetic stability like $^{68}$Ga for PET-studies; $^{111}$In for SPECT; and $^{90}$Y, $^{177}$Lu, and other lanthanides for therapeutic applications.

The receptor binding profiles of [In$^{III}$]-BZH1 and [Y$^{III}$]-BZH2 to the three bombesin receptor subtypes BB1, BB2, and BB3 were tested on human tumor specimen preferentially expressing each of the three receptor subtypes. Both metallopeptides show high binding affinity to the gastrin-releasing peptide receptor and slightly

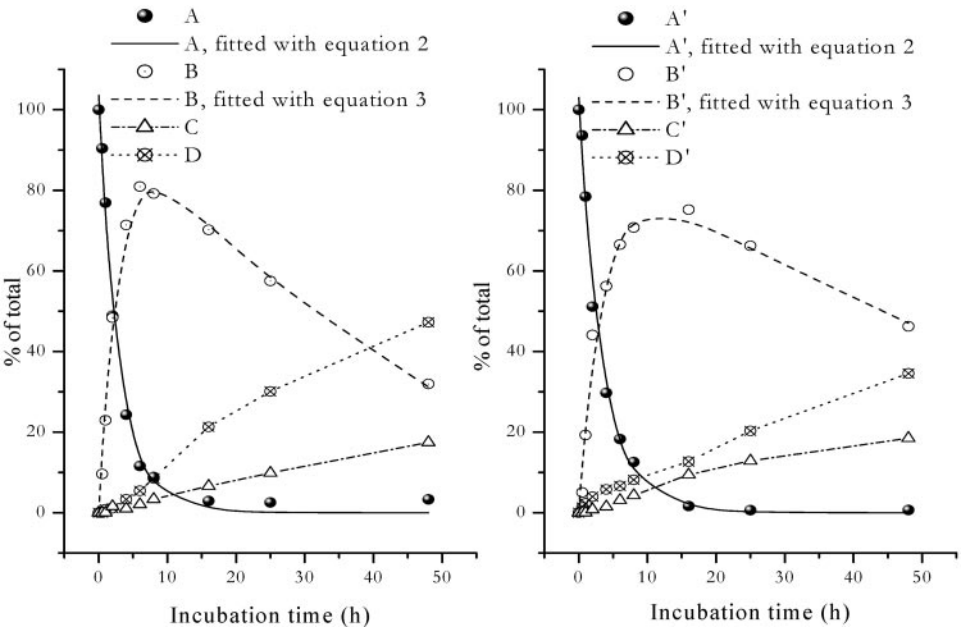


Fig. 3. Comparison of kinetic stability of [$^{111}$In]-BZH1 (*left*) and [$^{111}$In]-BZH2 (*right*) in fresh human serum. Percentage of total peptide after different incubation times with serum under 37°C, 5% $CO_2$, the concentration is 0.6 nmol radiolabeled peptide per mL serum.

Table 2 *Calculation of serum stabilities according to the equations 2 and 3; A means intact radiolabeled peptide; B represents their first metabolites*

| | Equation 2 ($A$) $= 100 \cdot e^{-k1t}$ | | Equation 3 (B) $= 100 \cdot k1/k1 - k2 \cdot (e^{-k2t} - e^{k1t})$ | | |
|---|---|---|---|---|---|
| Radioligand | $k_1$ ($h^{-1}$) | $t^1_{1/2}$ (h) | $k_1$ ($h^{-1}$) | $k_2$ ($h^{-1}$) | $t^2_{1/2}$ (h) |
| [$^{111}$In]-BZH1 | 0.35 ± 0.02 | 2.0 | 0.32 ± 0.03 | 0.026 ± 0.001 | 26 |
| [$^{111}$In]-BZH2 | 0.30 ± 0.02 | 2.3 | 0.27 ± 0.04 | 0.014 ± 0.003 | 46 |

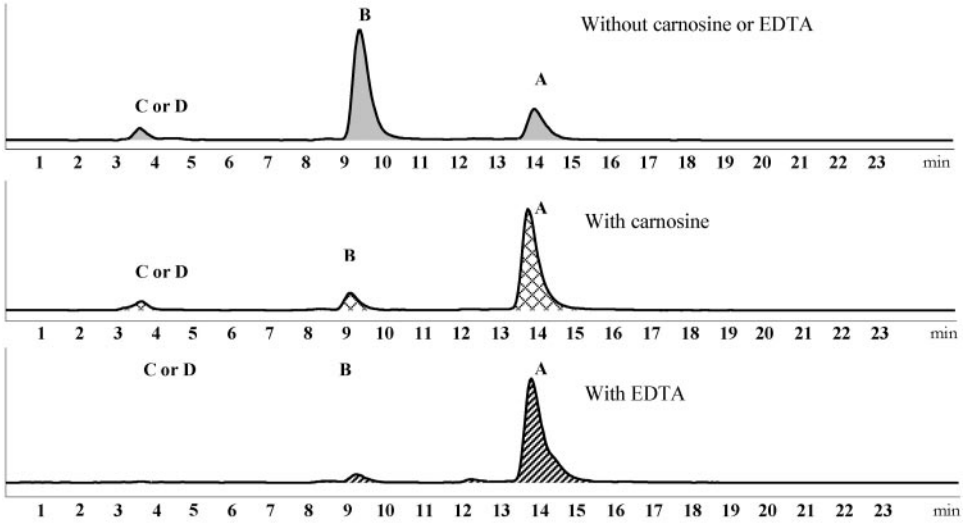


Fig. 4. HPLC elution profile of [$^{111}$In]-BZH1 after 4-hour incubation with fresh human serum and in the presence of carnosine and EDTA, respectively.

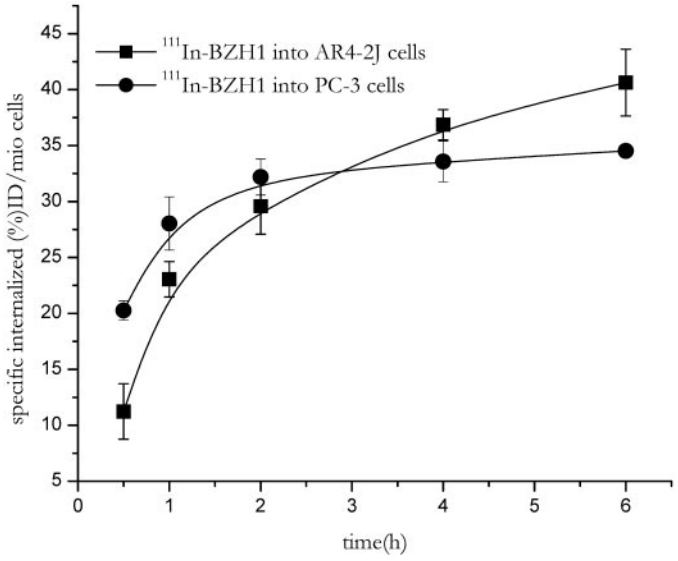


Fig. 5. Comparison of the internalization rate of [$^{111}$In]-BZH1 into rat pancreatic tumor AR4–2J (■) cells and human PC-3 (●) cells. Data result from two independent experiments with triplicates in each experiment and are expressed as specific internalization; *bars,* ±SD.

lower binding affinities to BB1 receptor and BB3 receptor. The [$Y^{III}$]-DOTA-derivative shows a distinctly and significantly higher binding affinity to all three of the receptor subtypes compared with the [$In^{III}$]-DTPA-analogue. We assume that this is due to the extra negative charge at the $NH_2$ terminus, which was shown to lower the binding affinity of bombesin-based radiopeptides.[4]

Both radiopeptides internalize rapidly, and no significant difference could be found between the two when labeled with $^{111}$In. In addition, no significant difference was observed when different radionuclides ([$^{111}$In/$^{90}$Y/$^{177}$Lu]-BZH2) were used with the DOTA-based peptide, indicating that there are no structural differences among these three radiopeptides.

For an optimized use of radiopharmaceuticals in targeted radiotherapy, not only an efficient internalization is of importance but also the trapping (residualization) of the radioactivity adds to the potential success of the treatment via targeted radiotherapy. Therefore, we studied the externalization of [$^{111}$In]-BZH1 as well as the identity of the externalized radioactivity. The rate of efflux of both compounds was shown to be rather fast, even faster for [$^{111}$In]-BZH1 than for [$^{111}$In]-BZH2. The externalized radioactivity consisted preferentially of [$^{111}$In(DTPA)]$^{2-}$ as the only metabolite. This is in contrast to the metabolites found when incubated in human serum, and it is also in

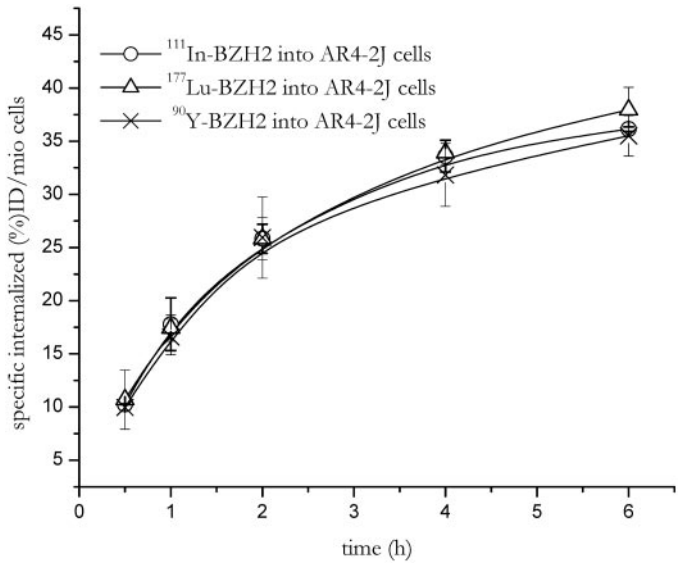


Fig. 6. Comparison of the internalization rate of [$^{111}$In]-BZH2 (○), [$^{90}$Y]-BZH2 (×) and [$^{177}$Lu]-BZH2 (△) into AR4–2J cells. Data result from two independent experiments with triplicates in each experiment and are expressed as specific internalization; *bars,* ±SD.

[4] Unpublished observations.

contrast to the chelator-conjugated somatostatin analogues that show only intact externalized peptide at least within the first 4 hours of externalization (43). At present we have no information on the particular enzymes responsible for the metabolism inside the cell.

An additional important aspect for the suitability of a radiopeptide used in targeted radiotherapy is its metabolic stability in human serum. High metabolic stability allows the radiopeptide to reach the target intact and in optimal concentrations. Both peptides were studied in the form of their $^{111}$In-labeled versions in fresh human serum. Fig. 2 shows the disappearance kinetics of the two radiopeptides and the build-up and decay of the first metabolite (B). The metabolic stability of both radiopeptides is relatively low with half-lives of 2.0 hours for [$^{111}$In]-BZH1 and 2.3 hours for [$^{111}$In]-BZH2, respectively. The curve fitting procedure gave similar results for $k_1$ ($k_1'$) independent of whether it was derived from the disappearance of A or the build-up and decay of the first intermediate B. Whereas the $k_1$-values show little difference between the two radiopeptides, the rate of metabolic decay of the intermediate is influenced by the chelate. Reverse-phase HPLC analysis of the metabolites along with co-injection of the predefined metabolites allowed an identification of the decay products.

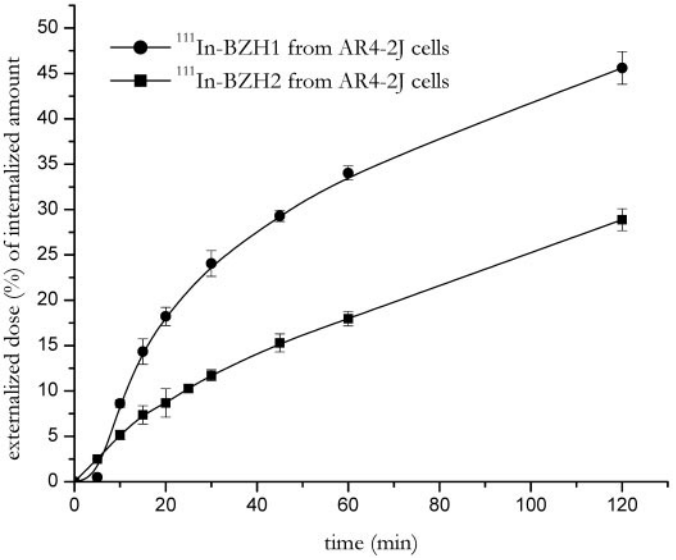


Fig. 7. Comparison of the externalization rate from AR4–2J after 2 hours of internalization and acid wash of [$^{111}$In]-BZH1(●) and [$^{111}$In]-BZH2(■); *bars,* ±SD.

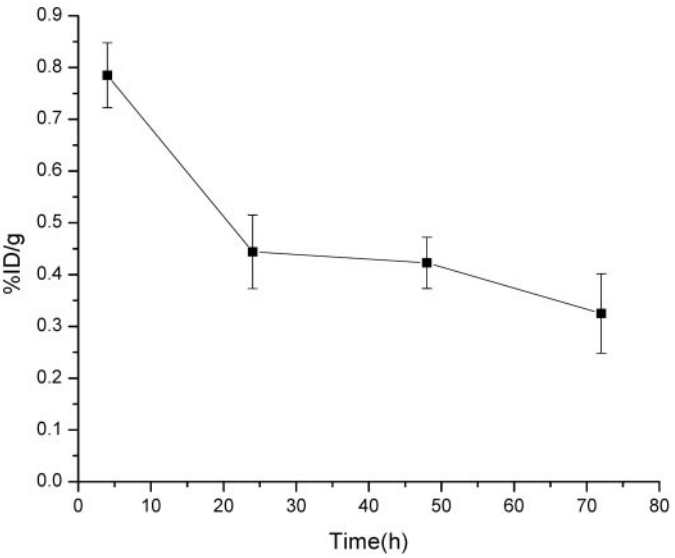


Fig. 8. Tumor retention of $^{111}$In-BZH2 inAR4–2J tumor-bearing rats. The uptake is given in percentage of injected dose per g (*%ID/g*) tumor at 4 hours, 24 hours, 48 hours, and 72 hours.

The definition of the cleavage sites and the characterization of the metabolites are of importance, because this knowledge allows us to define and synthesize peptides of enhanced metabolic stability. Because of lack of reliable access to liquid chromatography/mass spectrometry, we mainly relied on the synthesis of potential metabolites and their co-injection using reverse-phase HPLC and radiometric detection. This procedure allowed us to define the first degradation site of both peptides between β-Ala$^{11}$ and His$^{12}$ and the second degradation site between Gln$^7$ and Trp$^8$. The question arises as to which enzyme may be responsible for the processing of this amino acid sequence. A first experiment adding EDTA to the human serum/radiopeptide mixture slowed down the metabolic degradation distinctly indicating that the responsible enzyme is a metalloenzyme. The addition of a large excess of carnosine (β-Ala-His), a dipeptide, which

Table 3 *Biodistribution analyses [% ID/g ± SD, n = 4] and tissue ratios of [$^{111}$In]-BZH1 and [$^{111}$In]-BZH2 in AR4-2J tumor-bearing Lewis rats*

| | [$^{111}$In]-BZH1 (4h) | | [$^{111}$In]-BZH2 (4h) | | | |
|---|---|---|---|---|---|---|
| Site | Unblocked | Blocked* | Unblocked | Blocked* | [$^{111}$In]-BZH1 (24h)† | [$^{111}$In]-BZH2 (24h)† |
| Blood | 0.016 ± 0.003 | 0.010 ± 0.003 | 0.008 ± 0.001 | 0.007 ± 0.001 | 0.005 ± 0.001 | 0.002 ± 0.000 |
| Muscle | 0.010 ± 0.001 | 0.007 ± 0.003 | 0.008 ± 0.001 | 0.008 ± 0.001 | 0.008 ± 0.002 | 0.005 ± 0.000 |
| Pancreas | 3.92 ± 0.86 | 0.09 ± 0.02 | 2.63 ± 0.59 | 0.05 ± 0.01 | 2.43 ± 0.34 | 2.13 ± 0.68 |
| Bowel | 0.33 ± 0.09 | 0.09 ± 0.05 | 0.22 ± 0.04 | 0.04 ± 0.00 | 0.18 ± 0.06 | 0.09 ± 0.03 |
| Spleen | 0.05 ± 0.01 | 0.03 ± 0.01 | 0.04 ± 0.00 | 0.04 ± 0.00 | 0.04 ± 0.01 | 0.03 ± 0.00 |
| Liver | 0.05 ± 0.01 | 0.04 ± 0.01 | 0.07 ± 0.01 | 0.06 ± 0.00 | 0.03 ± 0.01 | 0.03 ± 0.01 |
| Stomach | 0.21 ± 0.06 | 0.04 ± 0.02 | 0.11 ± 0.01 | 0.04 ± 0.01 | 0.12 ± 0.02 | 0.06 ± 0.02 |
| Adrenals | 0.08 ± 0.01 | 0.02 ± 0.01 | 0.07 ± 0.01 | 0.02 ± 0.00 | 0.06 ± 0.01 | 0.06 ± 0.01 |
| Kidney | 1.15 ± 0.22 | 0.77 ± 0.21 | 1.19 ± 0.29 | 0.90 ± 0.09 | 0.79 ± 0.12 | 0.78 ± 0.16 |
| Lung | 0.03 ± 0.01 | 0.02 ± 0.01 | 0.03 ± 0.01 | 0.02 ± 0.00 | 0.02 ± 0.00 | 0.01 ± 0.00 |
| Heart | 0.01 ± 0.00 | 0.01 ± 0.00 | 0.01 ± 0.00 | 0.01 ± 0.00 | 0.01 ± 0.00 | 0.01 ± 0.00 |
| Bone | 0.02 ± 0.00 | 0.01 ± 0.00 | 0.01 ± 0.00 | 0.01 ± 0.00 | 0.02 ± 0.00 | 0.01 ± 0.00 |
| Tumor | 1.71 ± 0.51 | 0.12 ± 0.02 | 0.79 ± 0.06 | 0.09 ± 0.00 | 0.72 ± 0.22 | 0.44 ± 0.07 |
| | | | Tumor—normal tissue radioactivity ratios | | | |
| Tumor/blood | 107 | | 99 | | 144 | 220 |
| Tumor/muscle | 171 | | 99 | | 90 | 88 |
| Tumor/liver | 34 | | 11 | | 24 | 15 |
| Tumor/kidney | 1.5 | | 0.66 | | 0.91 | 0.56 |

NOTES. Results are the mean of groups of 4 animals (except for the tumor, pancreas, and kidney of [$^{111}$In]-BZH2, where 11 animals were studied).
* Blocked by injecting 50 μg BZH2 together with radiopeptide.
† Unblocked.

is cleaved by carnosinase (49), competitively inhibits the metabolic process (Fig. 3). Therefore, we assume that carnosinase, which is present in human serum, is the enzyme cleaving the peptide at $\beta$-Ala$^{11}$-His$^{12}$. This result also supports the finding that the first enzymatic cleavage occurs between these 2 amino acids.

In biodistribution studies, a strong accumulation of all of the radiotracers in bombesin receptor-positive tissues and the xenografted tumor was observed. As a tumor model the AR4–2J rat pancreatic carcinoma cell line was used, which is known to express high levels of bombesin receptors (50). Lewis rats bearing the AR4–2J solid tumor showed a high and specific uptake of both $^{111}$In-labeled peptides as well as [$^{177}$Lu]-BZH2 in the tumor (and other bombesin receptor-bearing organs and tissues like the pancreas, the stomach, and the intestines). The blood clearance of both radiopeptides is very fast with $<$0.015% ID/g remaining in the blood at 4 hours. Somewhat unexpectedly, the uptake in receptor-positive organs was higher for [$^{111}$In]-BZH1 compared with [$^{111}$In]-BZH2 by almost a factor of 2, although the latter has a higher binding affinity to all three of the receptor subtypes, and the rate of internalization is comparable for the two. BZH2 was developed for radiolabeling with therapeutic radionuclides like $^{90}$Y and the lanthanides. $^{111}$In was used as a surrogate of $^{90}$Y, because it can be followed and measured with more certainty than the pure $\beta$-emitter $^{90}$Y. The two show similar chemistry; nevertheless, some differences in the pharmacokinetics of radiopharmaceuticals labeled with the two and studied in comparison have been reported. $^{177}$Lu, another therapeutic radiometal [$\beta_{energy}$ = 0.49 MeV; $\gamma$-emissions 133 keV (7%); 208 keV (11%)], shows great promise in targeted radiotherapy. Therefore, we studied the biodistribution of [$^{177}$Lu]-BZH2. There was no significant difference between [$^{111}$In]-BZH2 and [$^{177}$Lu]-BZH2 indicating that we may expect similar results with [$^{90}$Y]-BZH2.

The competitive binding studies with cold peptides clearly demonstrated that the uptake of both radiopeptides in relevant target tissues is specific and receptor mediated. The residence times of both peptides in the tumor are not very long; this may originate from a somewhat low metabolic stability in the respective cells and may parallel the relatively low serum stability. Relatively fast tumor washout was also found for other radiometal-labeled, bombesin-based radiopeptides, for instance, $^{99m}$Tc-labeled bombesin(7–14) derivatives (34, 35). The identification of the "weakest" peptide bond at $\beta$-Ala$^{11}$-His$^{12}$ will help to improve the stability in future developments.

Tumor–normal tissue radioactivity ratios were very high for both radiopeptides. Ratios of tumor–blood of and tumor–muscle of $>$100 indicate that an early scintigraphic detection with a low background should be feasible. These ratios are higher than for other bombesin-based radiopeptides published recently using the PC-3 (33, 34, 36) and AR4–2J (51) tumor mouse model and argue for an early human use of these compounds. For instance, the tumor–muscle ratio for $^{99m}$Tc-RP527 [*N*,*N*-dimethyl-Gly-Ser-Cys-Gly-5-aminovaleric acid-bombesin(7–14)] in a AR4–2J mouse tumor model was 23.5 at 4 hours and 73 at 24 hours. Our values of 171 (for $^{111}$In-BZH1) and 103 (for $^{111}$In-BZH2) at 4 hours and 90 (98) at 24 hours compare well with these data. In addition, both radioligands appear to interact with the human gastrin-releasing peptide receptor (PC-3 cell line; $2.5 \pm 0.6 \times 10^5$ gastrin-releasing peptide receptor-binding sites per cell; ref. 52) in a way very similar to that with the rat gastrin-releasing peptide receptor ($\sim 1.5 \times 10^5$ gastrin-releasing peptide receptor binding sites per cell; ref. 50). Indeed, first clinical applications in breast and prostate cancer patients, if labeled with $^{68}$Ga or $^{111}$In, showed very promising tumor localizations. Because we do not expect that the performance with the therapeutic radionuclides is much different, [$^{90}$Y, $^{177}$Lu]-BZH2 may already be good candidates for targeted radiotherapy in patients. However, because the localization of neuromedin B receptor and BB3 receptor in normal human tissues is virtually unexplored, one cannot yet exclude the appearance of unwanted side effects related to yet unknown physiologic bombesin targets. In addition, one may argue that $^{177}$Lu with its long physical half-life of 6.65 days may not be the ideal therapeutic radionuclide considering the relatively low metabolic stability of the two radiopeptides. $^{90}$Y (half-life = 64 hours) and other radiolanthanides like $^{166}$Ho (half-life = 27 hours) or $^{149}$Pm (half-life = 53 hours), which also can be labeled to the DOTA-modified peptides, may be more suitable.

## ACKNOWLEDGMENTS

We thank Evelyn Peter for reviewing the English grammar.

## REFERENCES

1. Allen TM. Ligand-targeted therapeutics in anticancer therapy. Nat Rev Cancer 2002;2:750–63.
2. Maison W, Frangioni JV. Improved Chemical Strategies for the Targeted Therapy of Cancer. Angew Chem Int Ed Engl 2003;42:4726–8.
3. Reubi JC. Peptide receptors as molecular targets for cancer diagnosis and therapy. Endocr Rev 2003;24:389–427.
4. Reubi JC. Neuropeptide receptors in health and disease: the molecular basis for in vivo imaging. J Nucl Med 1995;36:1825–35.
5. Behr TM, Behe M, Becker W. Diagnostic applications of radiolabeled peptides in nuclear endocrinology. Q J Nucl Med 1999;43:268–80.
6. Breeman WA, de Jong M, Kwekkeboom DJ, et al. Somatostatin receptor-mediated imaging and therapy: basic science, current knowledge, limitations and future perspectives. Eur J Nucl Med 2001;28:1421–9.
7. Heppeler A, Froidevaux S, Eberle AN, Maecke HR. Receptor targeting for tumor localisation and therapy with radiopeptides. Curr Med Chem 2000;7:971–94.
8. Liu S, Edwards DS. $^{99m}$Tc-Labeled Small Peptides as Diagnostic Radiopharmaceuticals. Chem Rev 1999;99:2235–68.
9. Okarvi SM. Recent developments in $^{99m}$Tc-labelled peptide-based radiopharmaceuticals: an overview. Nucl Med Commun 1999;20:1093–112.
10. Hoffman TJ, Quinn TP, Volkert WA. Radiometallated receptor-avid peptide conjugates for specific in vivo targeting of cancer cells. Nucl Med Biol 2001;28:527–39.
11. Markwalder R, Reubi JC. Gastrin-releasing peptide receptors in the human prostate: relation to neoplastic transformation. Cancer Res 1999;59:1152–9.
12. Sun B, Halmos G, Schally AV, Wang X, Martinez M. Presence of receptors for bombesin/gastrin-releasing peptide and mRNA for three receptor subtypes in human prostate cancers. Prostate 2000;42:295–303.
13. Gugger M, Reubi JC. Gastrin-releasing peptide receptors in non-neoplastic and neoplastic human breast. Am J Pathol 1999;155:2067–76.
14. Halmos G, Wittliff JL, Schally AV. Characterization of bombesin/gastrin-releasing peptide receptors in human breast cancer and their relationship to steroid receptor expression. Cancer Res 1995;55:280–7.
15. Toi-Scott M, Jones CL, Kane MA. Clinical correlates of bombesin-like peptide receptor subtype expression in human lung cancer cells. Lung Cancer 1996;15:341–54.
16. McDonald TJ, Jornvall H, Tatemoto K, Mutt V. Identification and characterization of variant forms of the gastrin-releasing peptide (GRP). FEBS Lett 1983;156:349–56.
17. Minamino N, Kangawa K, Matsuo H. Neuromedin B: a bombesin like peptide identified in porcine spinal cord. Biochem Biophys Res Commun 1983;114:542–8.
18. Von Schrenck T, Heinz-Erian P, Moran T, Mantey SA, Gardner J, Jensen R. Neuromedin B receptor in esophagus: evidence for subtypes of bombesin receptors. Am J Physiol 1989;256:G747–58.
19. Spindel ER, Giladi E, Brehm P, Goodman RH, Segerson TP. Cloning and functional characterization of a complementary DNA encoding the murine fibroblast bombesin/gastrin-releasing peptide receptor. Mol Endocrinol 1990;4:1956–63.
20. Fathi Z, Corjay MH, Shapira H, et al. BRS-3: a novel bombesin receptor subtype selectively expressed in testis and lung carcinoma cells. J Biol Chem 1993;268:5979–84.
21. Nagalla SR, Barry BJ, Creswick KC, Eden P, Taylor JT, Spindel ER. Cloning of a receptor for amphibian [Phe$^{13}$]bombesin distinct from the receptor for gastrin-releasing peptide: identification of a fourth bombesin receptor subtype (BB4). Proc Natl Acad Sci USA 1995;92:6205–9.
22. Reubi JC, Wenger S, Schmuckli-Maurer J, Schaer JC, Gugger M. Bombesin receptor subtypes in human cancers: detection with the universal radioligand $^{125}$I-[D-TYR$^6$, beta-ALA$^{11}$, PHE$^{13}$, NLE$^{14}$] bombesin(6–14). Clin Cancer Res 2002;8:1139–46.
23. Schally AV, Nagy A. Cancer chemotherapy based on targeting of cytotoxic peptide conjugates to their receptors on tumors. Eur J Endocrinol 1999;141:1–14.
24. Nagy A, Armatis P, Cai RZ, Szepeshazi K, Halmos G, Schally AV. Design, synthesis, and in vitro evaluation of cytotoxic analogs of bombesin-like peptides containing doxorubicin or its intensely potent derivative, 2-pyrrolinodoxorubicin. Proc Natl Acad Sci USA 1997;94:652–6.
25. Szereday Z, Schally AV, Nagy A, et al. Effective treatment of experimental U-87MG human glioblastoma in nude mice with a targeted cytotoxic bombesin analogue, AN-215. Br J Cancer 2002;86:1322–7.

26. Hu F, Cutler CS, Hoffman T, Sieckman G, Volkert WA, Jurisson SS. Pm-149 DOTA bombesin analogs for potential radiotherapy. in vivo comparison with Sm-153 and Lu-177 labeled DO3A-amide-betaAla-BBN(7–14)NH(2). Nucl Med Biol 2002;29: 423–30.
27. Breeman WA, De Jong M, Bernard BF, et al. Pre-clinical evaluation of [$^{111}$In-DTPA-Pro$^{1}$, Tyr$^{4}$]bombesin, a new radioligand for bombesin-receptor scintigraphy. Int J Cancer 1999;83:657–63.
28. Karra SR, Schibli R, Gali H, et al. $^{99m}$Tc-labeling and in vivo studies of a bombesin analogue with a novel water-soluble dithiadiphosphine-based bifunctional chelating agent. Bioconjug Chem 1999;10:254–60.
29. Baidoo KE, Lin KS, Zhan Y, Finley P, Scheffel U, Wagner HN Jr. Design, synthesis, and initial evaluation of high-affinity technetium bombesin analogues. Bioconjug Chem 1998;9:218–25.
30. Scopinaro F, De Vincentis G, Varvarigou AD, et al. $^{99m}$Tc-bombesin detects prostate cancer and invasion of pelvic lymph nodes. Eur J Nucl Med Mol Imaging 2003;30: 1378–82.
31. Van de Wiele C, Dumont F, Dierckx RA, et al. Biodistribution and dosimetry of $^{99m}$Tc-RP527, a gastrin-releasing peptide (GRP) agonist for the visualization of GRP receptor-expressing malignancies. J Nucl Med 2001;42:1722–7.
32. Gali H, Hoffman TJ, Sieckman GL, Owen NK, Katti KV, Volkert WA. Synthesis, characterization, and labeling with $^{99m}$Tc/$^{188}$Re of peptide conjugates containing a dithia-bisphosphine chelating agent. Bioconjug Chem 2001;12:354–63.
33. Van de Wiele C, Dumont F, Vanden Broecke R, et al. Technetium-99m RP527, a GRP analogue for visualisation of GRP receptor-expressing malignancies: a feasibility study. Eur J Nucl Med 2000;27:1694–9.
34. Nock B, Nikolopoulou A, Chiotellis E, et al. [$^{99m}$Tc]Demobesin 1, a novel potent bombesin analogue for GRP receptor-targeted tumour imaging. Eur J Nucl Med Mol Imaging 2003;30:247–58.
35. La Bella R, Garcia-Garayoa E, Bahler M, et al. A $^{99m}$Tc(I)-postlabeled high affinity bombesin analogue as a potential tumor imaging agent. Bioconjug Chem 2002;13: 599–604.
36. Smith CJ, Sieckman GL, Owen NK, et al. Radiochemical investigations of gastrin-releasing peptide receptor-specific [$^{99m}$Tc(X)$(CO)_3$-Dpr-Ser-Ser-Ser-Gln-Trp-Ala-Val-Gly-His-Leu-Met-$(NH_2)$] in PC-3, tumor-bearing, rodent models: syntheses, radiolabeling, and in vitro/in vivo studies where Dpr = 2,3-diaminopropionic acid and X = $H_2O$ or $P(CH_2OH)_3$. Cancer Res 2003;63:4082–8.
37. Breeman WA, de Jong M, Erion JL, et al. Preclinical comparison of $^{111}$In-labeled DTPA- or DOTA-bombesin analogs for receptor-targeted scintigraphy and radionuclide therapy. J Nucl Med 2002;43:1650–6.
38. Broccardo M, Falconieri Erspamer G, Melchiorri P, Negri L, de Castiglione R. Relative potency of bombesin-like peptides. Br J Pharmacol 1975;55:221–7.
39. Girard F, Bachelard H, St-Pierre S, Rioux F. The contractile effect of bombesin, gastrin releasing peptide and various fragments in the rat stomach strip. Eur Pharmacol 1984;102:489–97.
40. Mantey SA, Weber HC, Sainz E, et al. Discovery of a high affinity radioligand for the human orphan receptor, bombesin receptor subtype 3, which demonstrates that it has a unique pharmacology compared with other mammalian bombesin receptors. J Biol Chem 1997;272:26062–71.
41. Pradhan TK, Katsuno T, Taylor JE, et al. Identification of a unique ligand which has high affinity for all four bombesin receptor subtypes. Eur Pharmacol 1998;343:275–87.
42. Heppeler A, Froidevaux S, Maecke HR, et al. Radiometal-labelled macrocyclic chelator-derivatised somatostatin analogue with superb tumor-targeting properties and potential for receptor-mediated internal radiotherapy. Chem Eur J 1999;5:1974–81.
43. Wild D, Schmitt JS, Ginj M, et al. DOTA-NOC, a high-affinity ligand of somatostatin receptor subtypes 2, 3 and 5 for labelling with various radiometals. Eur J Nucl Med Mol Imaging 2003;30:1338–47.
44. Atherton E, Sheppard R. Fluorenylmethoxycarbonyl-polyamide solid phase peptide synthesis. General principles and development. Oxford: Oxford Information Press; 1989.
45. Fleischmann A, Laderach U, Friess H, Buechler MW, Reubi JC. Bombesin receptors in distinct tissue compartments of human pancreatic diseases. Lab Invest 2000;80: 1807–17.
46. Eisenwiener KP, Prata MI, Buschmann I, et al. NODAGATOC, a new chelator-coupled somatostatin analogue labeled with [$^{67/68}$Ga] and [$^{111}$In] for SPECT, PET, and targeted therapeutic applications of somatostatin receptor (hsst2) expressing tumors. Bioconjug Chem 2002;13:530–41.
47. Liu S, Pietryka J, Ellars CE, Edwards DS. Comparison of yttrium and indium complexes of DOTA-BA and DOTA-MBA: models for $^{90}$Y- and $^{111}$In-labeled DOTA-biomolecule conjugates. Bioconjug Chem 2002;13:902–13.
48. Maecke HR, Scherer G, Heppeler A, Hennig M. Is In-111 an ideal surrogate for Y-90? If not, why? Eur J Nucl Med 2001;28:967.
49. Teufel M, Saudek V, Ledig JP, et al. Sequence identification and characterization of human carnosinase and a closely related non-specific dipeptidase. J Biol Chem 2003;278:6521–31.
50. Singh P, Draviam E, Guo YS, Kurosky A. Molecular characterization of bombesin receptors on rat pancreatic acinar AR42J cells. Am J Physiol 1990;258:G803–9.
51. Hoffmann T, Simpson S, Smith C, et al. Accumulation and retention of Tc-99m-RP527 by GRP receptor expressing tumors in scid mice. J Nucl Med 1999;40:104P.
52. Rogers BE, Bigott HM, McCarthy DW, et al. MicroPET imaging of a gastrin-releasing peptide receptor-positive tumor in a mouse model of human prostate cancer using a $^{64}$Cu-labeled bombesin analogue. Bioconjug Chem 2003;14:756–63.

*Paper 2*

# GRP Receptor-Targeted PET Imaging of a Rat Pancreas Carcinoma Xenograft in Nude Mice with a Gallium-68 Labeled Bombesin (6-14) Analogue

**Jochen Schuhmacher, [1] Hanwen Zhang, [2] Josef Doll, [1] Helmut R Maecke, [2] Ronald Matys, [1] Harald Hauser, [1] Marcus Henze, [3] Uwe Haberkorn, [3] and Michael Eisenhut [1]**

[1]Department of Diagnostic and Therapeutic Radiology, German Cancer Research Center, Heidelberg, Germany;

[2]Division of Radiological Chemistry, Institute of Nuclear Medicine, Department of Radiology, University Hospital Basel, Switzerland;

[3]Department of Nuclear Medicine, University of Heidelberg, Heidelberg, Germany

Published in:

*The Journal of Nuclear Medicine* 2005, 46: 691-699.

# GRP Receptor-Targeted PET of a Rat Pancreas Carcinoma Xenograft in Nude Mice with a $^{68}$Ga-Labeled Bombesin(6–14) Analog

Jochen Schuhmacher, PhD[1]; Hanwen Zhang, MS[2]; Josef Doll, PhD[1]; Helmut R. Mäcke, PhD[2]; Ronald Matys, BSc[1]; Harald Hauser, BSc[1]; Marcus Henze, MD[3]; Uwe Haberkorn, MD[3]; and Michael Eisenhut, PhD[1]

*[1]Department of Diagnostic and Therapeutic Radiology, German Cancer Research Center, Heidelberg, Germany; [2]Institute of Nuclear Medicine, University Hospital Basel, Basel, Switzerland; and [3]Department of Nuclear Medicine, University of Heidelberg, Heidelberg, Germany*

Bombesin (BN), a 14-amino-acid peptide, shows high affinity for the human gastrin-releasing peptide receptor (GRP-r), which is overexpressed on several types of cancer, including prostate, breast, gastrointestinal, and small cell lung cancer. Thus, radiolabeled BN or BN analogs may prove to be specific tracers for diagnostic and therapeutic targeting of GRP-r–positive tumors in nuclear medicine. This study evaluated a novel BN analog labeled with the positron emitter $^{68}$Ga for receptor imaging with PET. **Methods:** DOTA-PEG$_2$-[D-Tyr$^6$,β-Ala$^{11}$,Thi$^{13}$,Nle$^{14}$] BN(6–14) amide (BZH3) (DOTA is 1,4,7,10-tetraazacyclododecane-*N,N′,N″,N‴*-tetraacetic acid; PEG is ethyleneglycol (2-aminoethyl)carboxymethyl ether) was synthetized using the Fmoc strategy and radiolabeled with either $^{67}$Ga or $^{177}$Lu for in vitro and biodistribution experiments. $^{68}$Ga for PET was obtained from a $^{68}$Ge/$^{68}$Ga generator. In vitro binding, internalization, and efflux were determined using the pancreatic tumor cell line AR42J. Biodistribution of the peptide as a function of time and dose was studied in AR42J tumor-bearing mice. **Results:** In vitro assays demonstrated a high affinity of $^{67}$Ga-BZH3 (dissociation constant = 0.46 nmol/L), a rapid internalization (70% of total cell-associated activity was endocytosed after a 15-min incubation), and an intracellular retention half-life ($t_{1/2}$) of the $^{67}$Ga activity of 16.5 ± 2.4 h. Biodistribution indicated a dose-dependent uptake in the tumor and a prolonged tumor residence time ($t_{1/2}$ ~ 16 h). Clearance from GRP-r–negative tissues was fast, resulting in high tumor-to-tissue ratios as early as 1 h after injection. Replacing $^{67}$Ga by $^{177}$Lu, a therapeutic radionuclide, for peptide labeling resulted in a slightly reduced (~20%) tumor uptake and tumor residence time of $^{177}$Lu-BZH3. In contrast, $^{177}$Lu decline in the pancreas was significantly accelerated by a factor of ~3 compared with that of $^{67}$Ga. PET of mice with $^{68}$Ga-BZH3 clearly delineated tumors in the mediastinal area. **Conclusion:** The promising in vivo data of $^{68}$Ga-BZH3 indicate its potential for an improved localization of GRP-r–positive tumors and also suggest its application in patients. PET may also be favorably used for GRP-r density determination, a prerequisite for therapeutic applications.

**Key Words:** bombesin analog; $^{68}$Ga; PET; gastrin-releasing peptide receptor imaging

**J Nucl Med 2005; 46:691–699**

Bombesin (BN) is an amphibian neuropeptide of 14 amino acids that shows—just as its mammalian homolog gastrin-releasing peptide (GRP)—high affinity for the human GRP receptor (GRP-r). Aside from its physiologic actions on the central nervous system (*1*) and the release of gastrointestinal hormones (*2*), BN acts as an autocrine growth stimulator in a variety of human neoplasms (*3–5*). Autoradiographic examination of malignant tissues using radioiodine-labeled BN or BN analogs demonstrated a high GRP-r expression in prostate, gastrointestinal, breast, and small cell lung cancer specimens compared with the surrounding normal tissues (*6–12*), suggesting the potential of GRP-r for a specific tumor targeting. Consequently, various radiolabeled BN analogs have been investigated and proposed for use in nuclear medicine (*13–20*). In particular, $^{90}$Y, $^{188}$Re, and $^{177}$Lu have been used to radiolabel BN analogs for potential radiotherapy applications, whereas $^{99m}$Tc and $^{111}$In labeling has been used for γ-camera imaging of GRP-r–positive tumors.

PET is the most efficient imaging method in nuclear medicine because of its option of an absolute activity determination, its better contrast resolution, and its higher detection efficiency compared with conventional γ-cameras. Thus, we have focused on the labeling of BN analogs with the short-lived positron emitter $^{68}$Ga (half-life [$t_{1/2}$] = 68 min; $\beta^+$, 88%), which is obtained from a $^{68}$Ge/$^{68}$Ga radionuclide generator. In the present study, we evaluated a novel BN analog (BZH3) derivatized with the macrocyclic chelator 1,4,7,10-tetraazacyclododecane-*N,N′,N″,N‴*-tetraacetic acid (DOTA). This ligand forms $M^{3+}$ metal chelates of high in vivo stability and can be labeled with $^{68/67}$Ga, $^{111}$In, $^{90}$Y, and $^{177}$Lu and, thus, is suitable for diagnostic and therapeutic applications as well.

Received Jun. 15, 2004; revision accepted Oct. 25, 2004.

For correspondence or reprints contact: Jochen Schuhmacher, PhD, Department of Diagnostic and Therapeutic Radiology, German Cancer Research Center, Im Neuenheimer Feld 280, D-69120 Heidelberg, Germany.

E-mail: j.schuhmacher@dkfz.de

## MATERIALS AND METHODS

### Synthesis and Radiolabeling of BZH3

All chemicals were purchased from commercial sources and used without further purification. DOTA-Tris (tBu ester) was obtained from Macrocyclics. Rink amide MBHA (4-methylbenzhydrylamine) resin and all Fmoc-protected amino acids were available from Novabiochem and Neosystem, respectively. Peptide synthesis was performed on a semiautomatic peptide synthesizer (Rink Combichem Technologies) according to general Fmoc chemistry. The peptide was assembled on a Rink amide MBHA resin. Trityl (Trt) and tBu were used as protecting groups of His and D-Tyr, respectively, and Boc was used for Trp. The spacer (Fmoc-$PEG_2$-OH [PEG is ethyleneglycol (2-aminoethyl)carboxymethyl ether]) was coupled to the chelator DOTA-Tris (tBu ester) as described previously (*21*). The peptide chelator conjugate was cleaved from the resin and deprotected by incubation with trifluoroacetic acid (TFA)/thioanisole/water, 92:6:2 for 4–6 h at room temperature, and precipitated in isopropyl ether/petroleum ether (1:1). The crude peptide-chelator conjugate was purified by preparative high-performance liquid chromatography (HPLC) on a Nucleosil 100-5 $C_{18}$ column (Macherey–Nagel) at a flow rate of 15 mL/min (eluents: A = 0.1% TFA in water and B = acetonitrile; nonlinear gradient: 0 min, 70% A; 10 min, 50% A). Mass spectometry (MS-MALDI) was used to characterize the composition of the conjugate.

$^{68}$Ga for PET was obtained from a $^{68}$Ge/$^{68}$Ga generator, which consists of a column containing a self-made phenolic ion-exchanger loaded with $^{68}$Ge and coupled in series with a small-sized anion-exchanger column (AG 1×8 $Cl^-$, mesh 200–400; Bio-Rad) to concentrate $^{68}$Ga during elution (*22*). This generator provides $^{68}$Ga with an average yield of ~60% for >1.5 y. For peptide labeling, the eluate containing ~0.5 GBq of $^{68}$Ga in 0.2 mL 0.5 mol/L HCl was evaporated to dryness and redissolved in 0.2 mL 0.1 mol/L acetate buffer (pH 4.8). After addition of 5 μL 1 mmol/L aqueous solution of BZH3, the mixture was kept for 10 min at 90°C. Uncomplexed $^{68}$Ga was separated by adsorption onto a $C_{18}$-coated silica gel cartridge (Sep-Pak; Waters Corp.) that was equilibrated with 0.1 mol/L acetate buffer (pH 6.2), whereas $^{68}$Ga-BZH3 could be eluted with 1.5 mL ethanol. After evaporation of the organic solvent, the compound was redissolved in 0.01 mol/L phosphate-buffered saline ([PBS] pH 7.) containing 0.5 mg/mL human serum albumin. The preparations were checked for bound and free $^{68}$Ga by paper chromatography using Whatman no. 1 and a mixture of methanol and 0.01 mol/L acetate buffer (pH 6.2) at a ratio of 55:45. $^{68}$Ge contamination of the $^{68}$Ga-BZH3 preparations was determined by γ-counting after a waiting period of ≥30 h, which ensures complete $^{68}$Ga decay. $^{67}GaCl_3$ and $^{177}LuCl_3$ used for in vitro and biodistribution experiments were obtained in dilute HCl from Mallinckrodt and Perkin Elmer, respectively. All labeling steps with these radionuclides were identical to that of $^{68}$Ga. The radiochemical purity of $^{67}$Ga-BZH3 was analyzed by reversed-phase HPLC using a Nucleosil 120 $C_{18}$ column (Macherey–Nagel) at a flow rate of 0.75 mL/min (eluents: A = 0.1% TFA in water; B = acetonitrile; nonlinear gradient: 0 min, 80% A; 20 min, 50% A).

### Cell Lines

For all in vivo and in vitro experiments, the AR42J cell line, derived from a rat exocrine pancreas tumor, was used. Cells were obtained from the European Collection of Cell Cultures and were grown in RPMI 1640 medium supplemented with 2 mmol/L glutamine and 10% fetal calf serum. Adherent cells were dislodged with trypsin/ethylenediaminetetraacetic acid (0.02%:0.05%, w/v) and allowed to recover for 2 h. Nonspecific binding of $^{67}$Ga-BZH3 was tested with the GRP-r–negative human breast carcinoma cell line AR-1, obtained from the Department of Gynecological Oncology (University Hospital Heidelberg, Heidelberg, Germany).

### Receptor Binding

The equilibrium binding constant, $K_a$, of $^{67}$Ga-BZH3 to the GRP-rs of AR42J cells was determined using a fixed number of $4 \times 10^5$ cells in 150 μL RPMI 1640 medium and increasing amounts, 0.033–1.056 pmol (0.055–1.76 ng), of the peptide. Cells were placed in a U-shaped 96-well plate and agitated on a gyratory shaker for 1 h in an incubator (37°C, 5% $CO_2$). Cells were washed 3 times with ice-cold RPMI 1640 medium and pellets were counted in a γ-counter. A least-squares fit from a Scatchard plot (bound activity/free activity [B/F] vs. bound activity [B]) results in a straight line, the slope of which indicates $-K_a$. The intercept of B/F with B represents the maximum concentration of peptide ($B_{max}$) bound to the GRP-rs of cells at infinite peptide excess.

### Internalization

Internalization of $^{67}$Ga-BZH3 was studied at low and high peptide-to-receptor ratios. Twenty-seven million cells in 8.1 mL medium were incubated (37°C, 5% $CO_2$) with either 0.45 or 45 pmol (0.75 or 75 ng) of the peptide. During incubation, cells were kept in suspension by gyratory shaking. After 15, 30, 60, and 120 min of incubation, six 300-μL samples, containing $1 \times 10^6$ cells and 0.0166 or 1.66 pmol of peptide, were taken, mixed with 700 μL ice-cold RPMI 1640 medium in a conical tube, and centrifuged (3 min, 500*g*). Three samples were washed twice with 1 mL ice-cold RPMI 1640 medium, and cell pellets were counted in a γ-counter. Radioactivity in the cell pellets represents surface bound together with internalized peptide. The remaining 3 samples were further incubated (5 min, 22°C) with 1 mL of an acidic buffer (pH 4.3) containing 0.15 mol/L NaCl, 0.02 mol/L NaOAc, and 2 mg/mL human serum albumin to remove surface-bound peptide (*23*). Subsequently, cells were washed twice with the acidic buffer. Radioactivity in the cell pellet was assumed to represent internalized peptide

### Efflux

Since an acid treatment of cells might unfavorably affect cell metabolism (*23*), we used an excess of unlabeled BZH3 to remove surface-bound radioactive peptide before efflux determination, which additionally blocks rebinding of internalized radioactivity released from the cells during incubation. Sixteen million cells in 4.8 mL RPMI 1640 medium were preloaded with 10 pmol of either $^{67}$Ga- or $^{177}$Lu-labeled BZH3 for 1 h at 37°C, 5% $CO_2$. Cells were washed 3 times and then resuspended in 4.8 mL medium; two 300-μL samples were taken as a control for total cell-associated activity (cell surface bound and internalized). Subsequently, 50 μL of 1 mmol/L unlabeled BZH3 were added to the remaining incubation mixture. Ten, 20, 30, 60, 90, and 120 min after the addition of unlabeled peptide, two 303-μL samples ($1 \times 10^6$ cells) were taken, diluted with 700 μL ice-cold RPMI 1640 medium, and centrifuged. Pellets were washed twice with cold medium and counted for radioactivity.

### Receptor Density

Since the receptor density of AR42J cells might decrease with increasing passages, accompanied by a reduction in cellular size

and tumorigenic activity, the binding capacity of cells was tested before each tumor inoculation. One million cells in 150 μL RPMI 1640 medium were incubated with 1.5 pmol of $^{67}$Ga-BZH3, kept in suspension for 1 h at 37°C, 5% $CO_2$, washed 3 times with cold medium, and counted for radioactivity.

### Biodistribution

Animal experiments were performed in accordance with the German laws for the protection of animals. Female Swiss CD1 *nu/nu* mice (8-wk old; Iffa Credo) had subcutaneous inoculation of $5 \times 10^6$ AR42J tumor cells (in 0.2 mL of RPMI 1640 medium) into the right thoracic wall near the shoulder. Eleven to 13 d later, tumors that weighed 100–600 mg were selected for the experiments. Mice received a tail vein injection of 0.2 mL 0.01 mol/L PBS containing 100 μg human serum albumin and the labeled compounds under investigation. Animals were anesthetized with ether, bled from the retroorbital plexus, and killed by cervical dislocation at the time points indicated. Organs were removed, weighed, and counted for radioactivity with a high-resolution germanium detector. For evaluation of a dose dependence of the tumor uptake, mice were injected with 5, 15, 45, or 135 pmol of $^{67}$Ga-BZH3 and killed 1 h after injection. Biokinetics were studied in animals receiving a 15-pmol dose of either $^{67}$Ga- or $^{177}$Lu-labeled BZH3. Mice were killed 1, 2, 4, and 24 h after injection of $^{67}$Ga-BZH3 and 1 and 24 h after injection of $^{177}$Lu-BZH3. GRP-r–blocking studies were performed using AR42J tumor-bearing male Lewis rats (body weight, 160–200 g; Iffa Credo) as described previously (*24*). Briefly, 2 groups of rats, each comprising 4 animals, were injected with either 60 pmol (0.1 μg) $^{177}$Lu-BZH3 or a mixture containing 0.1 μg $^{177}$Lu- BZH3 and 50 μg of unlabeled BZH3. Rats were killed 4 h after injection. Pancreas and tumor were dissected and counted for $^{177}$Lu activity.

### PET

AR42J tumor-bearing mice were injected with 15 pmol (0.49 MBq) $^{68}$Ga-BZH3, sacrificed 1 h after injection, and imaged with a 30-min emission scan and a 10-min transmission scan on an ECAT EXACT HR$^+$ scanner (Siemens/CTI). Images were taken in the 3-dimensional (3D) mode and reconstructed iteratively with a fully 3D algorithm from a 256 × 256 matrix for viewing transaxial, coronal, and sagittal slices of 0.57-mm thickness (*25*). Pixel size was 1.14 mm and transaxial resolution obtained was 2.8 mm. Subsequently, tumors were removed and counted for $^{68}$Ga activity.

## RESULTS

### Synthesis and Radiolabeling

BZH3 (Fig. 1) was synthesized using the Fmoc strategy affording an overall yield of 30% based on the removal of the first Fmoc group; the purity analyzed by HPLC was ≥97%. MS-MALDI confirmed the calculated exact mass of 1,669.79: m/z (%): 1,670.0 (100, $[M+H]^+$); 1,692.0 (19, $[M+Na]^+$); 1,708.9 (10, $[M+K]^+$). Labeling of BZH3 with $M^{3+}$ radionuclides took 60 min. Starting with 0.5 GBq (13.5 mCi) of $^{68}$Ga, specific activities of 37–44 MBq/nmol (1–1.2 mCi/nmol) of peptide were obtained and preparations contained <3 ppm $^{68}$Ge contamination. Labeling with commercially available $^{67}$Ga and $^{177}$Lu resulted in 20–22 and 35–40 MBq/nmol, respectively. The radiochemical purity of $^{67}$Ga-BZH3, as assessed by reversed-phase HPLC, showed a single product with a slightly reduced retention time of 12.2 min versus 12.6 min for the unlabeled BZH3. Heating to 90°C during the labeling procedure caused no detectable degradation of the peptide, a finding that has also been reported by Breeman et al. (*14*). Thus, subsequent preparations were only checked by paper chromatography for the nonchelated fraction of the radionuclide that remains at the beginning. Typically, ≥98% of the activity migrated with an $R_f$ of 0.6–0.7 corresponding to the labeled peptide.

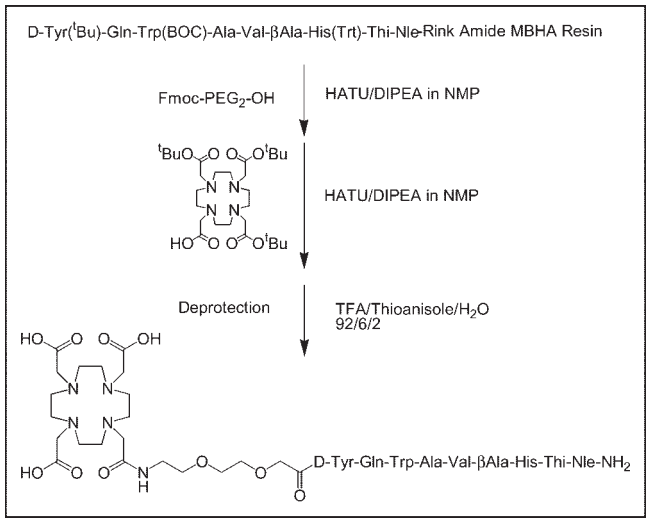


**FIGURE 1.** Synthesis of DOTA-$PEG_2$-[D-Tyr$^6$,βAla$^{11}$,Thi$^{13}$,Nle$^{14}$] BN(6–14) amide (BZH3). Thi = 3-(2-thienyl)-L-alanine; MBHA = 4-methylbenzhydrylamine; HATU = *O*-(7-azabenzotriazole-1-yl)-1,1,3,3-tetramethyluronium hexafluorophosphate; DIPEA = diisopropylethylamine; NMP = *N*-methylpyrrolidone.

### Receptor Binding

The saturation binding curve of $^{67}$Ga-BZH3 to GRP-r of AR42J cells and its Scatchard transformation are shown in Figure 2. From the Scatchard plot, a high receptor affinity $K_a$ of $2.19 \times 10^9$ L/mol was calculated, which corresponds to a dissociation constant $K_d$ of 0.46 nmol/L. Determination of $B_{max}$ resulted in $9.7 \times 10^4$ receptors per cell. Nonspecific binding of the peptide was tested with the GRP-r–negative breast carcinoma cell line AR-1 and amounted to <3.5%.

### Internalization

Internalization of $^{67}$Ga-BZH3 by AR42J cells at 2 different concentrations was followed for 2 h (Fig. 3). The fraction of internalized activity compared with total cell-associated activity (cell surface bound + internalized) was nearly identical for both the low and the high concentration and amounted to 71%–75% after a 15- and 30-min incubation and 85%–88% after a 1- and 2-h incubation. The kinetics of internalization during the first hour of incubation also were very similar. In contrast, using the low dose and a 2-h incubation, which reduced the free peptide concentration in the medium to ≤0.02 nmol/L, the internalization rate drastically decreased.

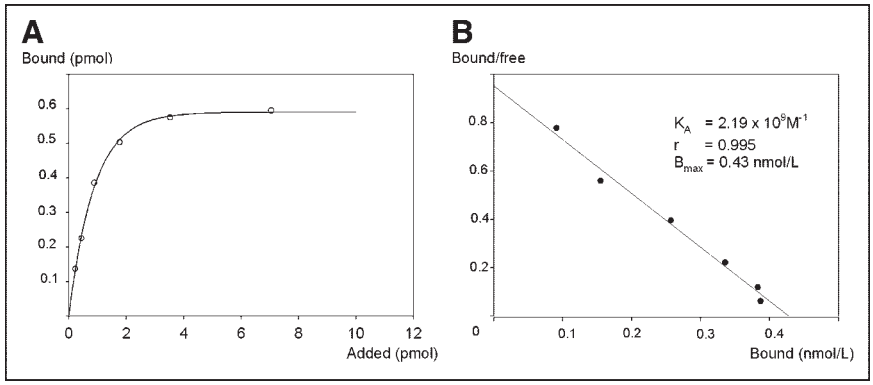


**FIGURE 2.** Saturation curve (A) and Scatchard transformation (B) of binding of increasing amounts of $^{67}$Ga-BZH3 to 4 × $10^5$ AR42J cells. Cells were incubated for 1 h. Data are means of triplicate samples and are corrected for nonspecific binding (≤3.5%).

### Efflux

Efflux of internalized radioactivity was evaluated after preloading of AR42J cells with either $^{67}$Ga- or $^{177}$Lu-labeled BZH3. Cell surface–bound peptide was removed by excess unlabeled peptide within the first minutes of incubation and amounted to ~10% of total activity, a fraction that is consistent with the results obtained in internalization experiments using an acid treatment of cells. Another ~10% was excreted during the following 2-h incubation. From a semilogarithmic plot of data, half-lives of 16.5 ± 2.4 h and 12.8 ± 1.4 h for the excretion of $^{67}$Ga and $^{177}$Lu, respectively, were calculated (Fig. 4).

### Receptor Density

Three separate tumor inoculations (dose dependence, biokinetics, and PET) were performed with AR42J cells that differ in the number of passages from 7 to 16 relating to the commercially obtained cells. No marked difference in peptide uptake was noted. The uptake amounted to 0.132, 0.145, and 0.159 pmol per $10^6$ cells, respectively.

### Biodistribution

Tumor and normal tissue uptake 1 h after the administration of increasing doses (5, 15, 45, and 135 pmol) of $^{67}$Ga-BZH3 are presented in Table 1. A dose dependence was noted in the AR42J tumor and the normal GRP-r–expressing tissues, including small intestine, colon, and pancreas. Small intestine and colon showed a continuously decreasing uptake with increasing doses. The uptake in

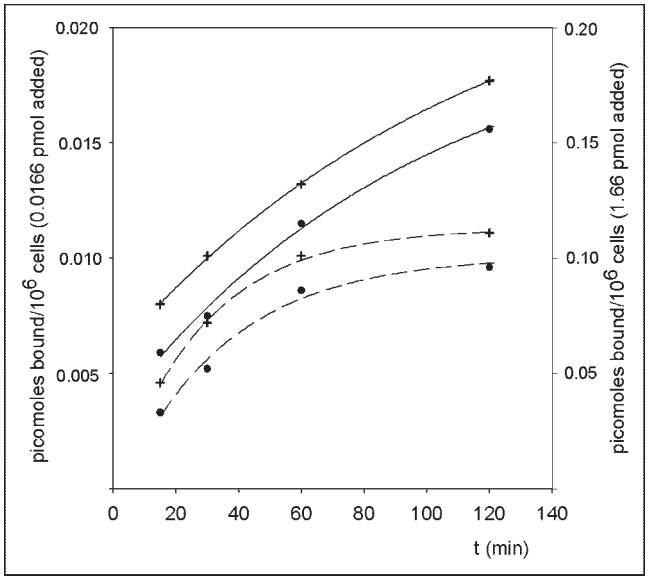


**FIGURE 3.** Internalization of $^{67}$Ga-BZH3 by 1 × $10^6$ AR42J cells in 300 μL medium containing either 0.0166 pmol (low dose, dashed line) or 1.66 pmol (high dose, solid line) of peptide. +, Total activity (cell surface bound + internalized); ●, internalized activity. Note different scaling of the *y*-axis. Data are means of triplicate samples.

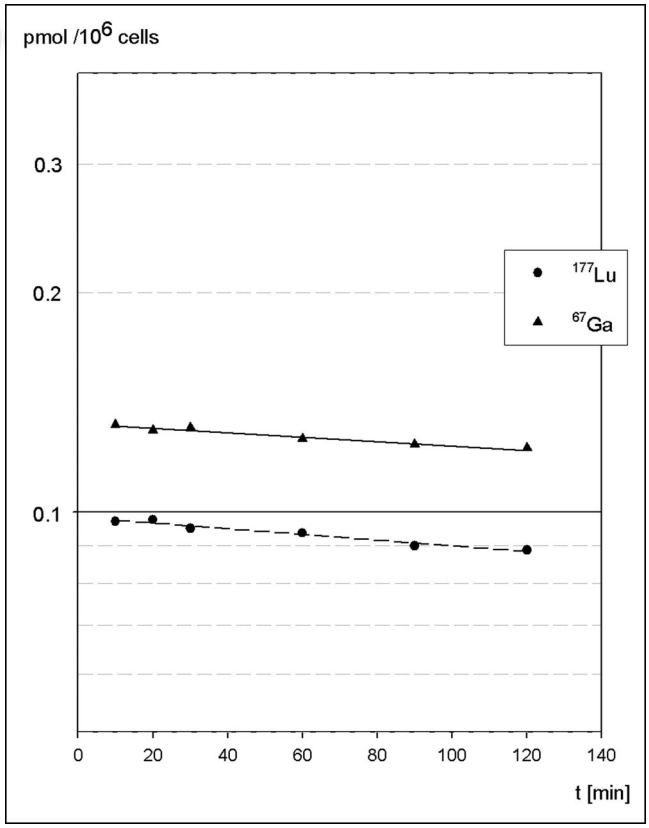


**FIGURE 4.** Semilogarithmic plot shows efflux (externalization) of radioactivity from AR42J cells preloaded with either $^{67}$Ga-BZH3 (solid line) or $^{177}$Lu-BZH3 (dashed line). Data are means of duplicate samples from 2 experiments.

**TABLE 1**
Tissue Distribution of Increasing Doses of $^{67}$Ga-BZH3 at 1 Hour After Injection in AR42J Tumor-Bearing Nude Mice

| Tissue | pmol per animal | | | |
|---|---|---|---|---|
| | 5 | 15 | 45 | 135 |
| Blood | 0.45 ± 0.12 | 0.57 ± 0.17 | 0.51 ± 0.14 | 0.53 ± 0.10 |
| Liver | 0.68 ± 0.18 | 1.12 ± 0.39 | 0.87 ± 0.23 | 0.72 ± 0.13 |
| Spleen | 2.14 ± 0.49 | 1.62 ± 0.48 | 1.82 ± 0.89 | 1.29 ± 0.54 |
| Kidneys | 6.55 ± 1.92 | 6.32 ± 2.00 | 4.52 ± 0.59 | 3.03 ± 0.45 |
| Pancreas | 35.98 ± 2.22 | 40.39 ± 2.81* | 46.06 ± 3.51* | 39.37 ± 4.57* |
| Muscle | 0.16 ± 0.05 | 0.13 ± 0.04 | 0.20 ± 0.07 | 0.20 ± 0.05 |
| Bone† | 0.37 ± 0.13 | 0.51 ± 0.22 | 0.29 ± 0.15 | 0.48 ± 0.24 |
| Lungs | 0.60 ± 0.17 | 0.63 ± 0.25 | 0.56 ± 0.15 | 0.64 ± 0.11 |
| Tumor | 7.98 ± 1.57 | 10.90 ± 1.48* | 8.00 ± 1.68* | 6.25 ± 0.80 |
| Small intestine‡ | 8.70 ± 2.39 | 7.51 ± 1.45 | 5.62 ± 0.79 | 4.00 ± 0.43 |
| Large intestine‡ | 3.94 ± 0.24 | 3.82 ± 0.49 | 2.96 ± 0.69 | 1.95 ± 0.49 |

*Significantly different ($P \leq 0.05$) from preceding group (Student *t* test).
†One femur was measured.
‡Small and large intestines were measured with content.
All data are mean percentage injected dose per gram (%ID/g) ± SD of 5 animals. Body weight of animals, 23.9 ± 1.7 g; tumor weight, 218 ± 104 mg (range, 88–388 mg); pancreas weight, 204 ± 30 mg ($n = 20$).

pancreas and tumor showed a bell-shaped dose dependence. The maxima obtained were 10.9 percentage injected dose per gram (%ID/g) for tumor and 46.1 %ID/g for pancreas after administration of a 15- and a 45-pmol dose, respectively. No dose dependence was found in blood, liver, spleen, muscle, lung, and bone. In kidneys, a significantly reduced activity was noted after the administration of the highest dose (135 pmol = 0.23 μg).

The tissue distribution of $^{67}$Ga- or $^{177}$Lu-labeled BZH3 as a function of time was determined using the 15-pmol dose (Table 2). The radioactivity in the GRP-r–expressing tissues after administration of the $^{67}$Ga-BZH3 did not significantly decrease up to 4 h after injection. From data at 1 and 24 h after injection, the average half-lives of $^{67}$Ga-BZH3 retention in pancreas and tumor of ~22 h and ~16 h could be estimated, respectively, the latter being very similar to the excretion half-life of $^{67}$Ga activity in vitro after internalization of $^{67}$Ga-BHZ3 into AR42J cells. Low activity was found in blood, liver, lung, muscle, and bone, even at 1 h after injection, and tumor-to-tissue ratios did not markedly increase after 2 h following injection (Table 3).

The difference in tumor uptake 1 h after injection between the 2 experiments using a 15-pmol dose, 10.9 %ID/g (dose dependence) versus 5.6 %ID/g (kinetics), is not

**TABLE 2**
Tissue Distribution of $^{67}$Ga- and $^{177}$Lu-BZH3 as Function of Time in AR42J Tumor-Bearing Nude Mice After Injection of 15 pmol of Peptide

| Tissue | $^{67}$Ga | | | | $^{177}$Lu | |
|---|---|---|---|---|---|---|
| | 1 h | 2 h | 4 h | 24 h | 1 h | 24 h |
| Blood | 0.25 ± 0.02 | 0.17 ± 0.03 | 0.12 ± 0.01 | 0.015 ± 0.006 | 0.51 ± 0.06 | 0.025 ± 0.006 |
| Liver | 0.47 ± 0.12 | 0.40 ± 0.05 | 0.32 ± 0.07 | 0.22 ± 0.03 | 0.62 ± 0.06 | 0.35 ± 0.05 |
| Spleen | 3.32 ± 0.90 | 3.35 ± 1.44 | 2.26 ± 1.07 | 0.83 ± 0.24 | 1.67 ± 0.17 | 0.31 ± 0.07 |
| Kidneys | 6.78 ± 0.40 | 4.49 ± 0.37 | 4.12 ± 0.70 | 1.75 ± 0.40 | 4.96 ± 0.87 | 0.72 ± 0.04 |
| Pancreas | 42.16 ± 2.30 | 37.52 ± 6.69 | 36.54 ± 5.19 | 20.75 ± 5.24 | 31.78 ± 3.69 | 3.71 ± 0.55 |
| Muscle | 0.13 ± 0.07 | 0.11 ± 0.09 | 0.04 ± 0.02 | 0.021 ± 0.009 | 0.13 ± 0.02 | 0.02 ± 0.005 |
| Bone* | 0.39 ± 0.09 | 0.29 ± 0.03 | 0.26 ± 0.06 | 0.20 ± 0.09 | 0.59 ± 0.08 | 0.79 ± 0.13 |
| Lungs | 0.31 ± 0.04 | 0.19 ± 0.04 | 0.13 ± 0.03 | 0.04 ± 0.01 | 0.45 ± 0.06 | 0.05 ± 0.02 |
| Tumor | 5.65 ± 0.73 | 6.47 ± 1.13 | 5.26 ± 1.30 | 2.10 ± 0.38 | 4.52 ± 0.57 | 1.48 ± 0.23 |
| Small intestine† | 4.74 ± 0.48 | 3.39 ± 0.38 | 1.66 ± 0.18 | 0.85 ± 0.13 | 4.62 ± 0.95 | 0.48 ± 0.15 |
| Large intestine† | 4.93 ± 1.13 | 6.78 ± 0.93 | 4.90 ± 0.52 | 1.75 ± 0.86 | 3.38 ± 1.18 | 1.22 ± 0.14 |

*One femur was measured.
†Small and large intestines were measured with content.
All data are mean %ID/g ± SD of 5 animals. Body weight of animals, 22.4 ± 2.02 g; tumor weight, 252 ± 130 mg (range, 86–612 mg); pancreas weight, 179 ± 36 mg ($n = 30$).

**TABLE 3**
Tumor-to-Tissue Ratios of $^{67}$Ga- and $^{177}$Lu-BZH3 in Tumor-Bearing Nude Mice

| | $^{67}$Ga | | | | $^{177}$Lu | |
|---|---|---|---|---|---|---|
| Tumor/organ | 1 h | 2 h | 4 h | 24 h | 1 h | 24 h |
| Blood | 22.6 ± 2.4 | 38.1 ± 8.5 | 43.8 ± 11.7 | 140 ± 81 | 8.9 ± 1.5 | 59 ± 23 |
| Liver | 12.0 ± 1.8 | 16.2 ± 1.8 | 16.4 ± 6.0 | 9.5 ± 2.3 | 7.3 ± 0.8 | 4.2 ± 1.0 |
| Spleen | 1.7 ± 0.6 | 1.8 ± 0.6 | 2.3 ± 1.0 | 2.5 ± 0.7 | 2.7 ± 0.3 | 4.8 ± 1.3 |
| Kidneys | 0.83 ± 0.05 | 1.4 ± 0.2 | 1.3 ± 0.4 | 1.2 ± 0.3 | 0.91 ± 0.28 | 2.1 ± 0.3 |
| Pancreas | 0.13 ± 0.01 | 0.17 ± 0.04 | 0.14 ± 0.05 | 0.10 ± 0.02 | 0.14 ± 0.02 | 0.40 ± 0.10 |
| Muscle | 74 ± 30 | 83 ± 26 | 131 ± 57 | 105 ± 28 | 34.8 ± 10.8 | 74 ± 39 |
| Bone | 14.5 ± 0.8 | 22.3 ± 3.9 | 20.2 ± 1.7 | 10.5 ± 1.5 | 7.7 ± 0.6 | 1.9 ± 0.5 |
| Lungs | 18.2 ± 3.1 | 34.1 ± 4.7 | 40.5 ± 15.0 | 52 ± 14 | 10.0 ± 1.5 | 30.7 ± 11.6 |

Ratios are calculated from animals of Table 2. Data are mean ± SD ($n$ = 5).

readily understood because AR42J cells used for tumor inoculation showed no difference with regard to in vitro binding and internalization of $^{67}$Ga-BZH3. A possible explanation might be that the fraction of tumor cells in relation to the total tumor mass was different, since tumors were highly hemorrhagic.

As an estimate for therapeutic applications, BZH3 was labeled with $^{177}$Lu, which is a medium-energy β-emitter ($E_{\beta\text{-max}}$ = 497 keV) with a low abundance of γ-radiation at 113 and 208 keV, and biodistribution of $^{177}$Lu-BZH3 was determined at 1 and 24 h after injection of a 15-pmol dose (Table 2). Uptake in the tumor and pancreas 1 h after injection appears to be somewhat lower compared with that of $^{67}$Ga-BZH3, 4.5 versus 5.6 %ID/g and 31.8 versus 42.1 %ID/g, respectively. The in vivo half-life of $^{177}$Lu-BZH3 in the tumor, estimated from the 1- and 24-h biodistribution data, was ~14 h and, thus, corresponds to the in vitro data of efflux. In contrast, the decline of $^{177}$Lu activity in the pancreas was significantly accelerated compared with that of the $^{67}$Ga-labeled BZH3 ($t_{1/2}$, ~7.5 vs. ~22 h).

Coadministration of excess unlabeled BZH3 in the blocking experiments reduced uptake of $^{177}$Lu-BZH3 in the pancreas of rats from 2.69 ± 0.60 %ID/g to 0.06 ± 0.01 %ID/g and in the AR42J tumor from 1.11 ± 0.31 %ID/g to 0.09 ± 0.01 %ID/g, indicating a specific and GRP-r–mediated uptake of the labeled peptide.

### PET

PET images of tumor-bearing mice obtained 1 h after injection of 15 pmol $^{68}$Ga-BZH3 are presented in Figure 5. Transaxial slices cutting the tumor and mediastinal region demonstrate a clear delineation of the tumor tissue and a low activity background in lungs, liver, and circulation. Coronal slices show the highest activity in pancreas and a nonuniform activity distribution in the duodenum, which complicates visualization of the kidneys. γ-Counting indicated an activity accumulation of 5.3 and 7.0 %ID/g in the resected tumors of the left and the right animal, respectively. Tumor weights were 200 mg (left animal) and 128 mg (right animal).

## DISCUSSION

During the past decade, the successful application of radiolabeled somatostatin analogs in nuclear medicine for diagnostics and therapy of neuroendocrine tumors has stimulated the research in receptor targeting of additional tumor types (*26*). In a recent study, Van de Wiele et al. demonstrated the feasibility of scintigraphic imaging of GRP-r–positive prostate and breast carcinoma in patients with the $^{99m}$Tc- labeled BN analog RP 527, indicating the potential of BN analogs for use in humans (*13,27*). In the present study, we investigated a novel BN analog, BZH3, for its in vitro and in vivo behavior under the aspects of improving targeting of GRP-r–positive tumors and introducing the short-lived positron emitter $^{68}$Ga for peptide labeling and, thus, to enable PET, which increases the spatial resolution and sensitivity of tumor detection compared with conventional γ-camera imaging (*28–30*). Additionally, scatter-corrected PET provides the ability to quantify biodistribution and, thus, may be favorably used for GRP-r density determination, which is a prerequisite for the appropriate selection of patients entering radiotherapy, and to control effectiveness of radiotherapy or surgical interventions.

The affinity of $^{67}$Ga-BZH3 to GRP-r of live AR42J cells showed a $K_d$ of 0.46 nmol/L, which is a factor of 3 lower

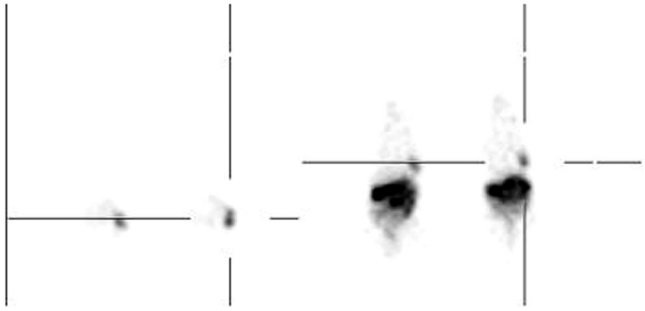

**FIGURE 5.** Iteratively reconstructed transaxial (left) and coronal (right) PET images of 2 AR42J tumor-bearing nude mice 1 h after injection of 15 pmol (0.49 MBq) $^{68}$Ga-BZH3. Tumors are located in thoracic wall. Tumor uptake and weight: left animal, 5.3 %ID/g, 200 mg; right animal, 7.0 %ID/g, 128 mg.

than that of $^{125}$I-Tyr$^4$-BN ($K_d$ = 1.6 nmol/L), which is commonly used as a standard for determination of GRP-r–specific binding. The affinity of $^{67}$Ga-BZH3 is thus comparable with that of $^{99m}$Tc-demobesin 1 ($K_d$ = 0.67 nmol/L) (*18*) and $^{111}$In-labeled DOTA-Aoc-BN(7–14) (50% inhibitory concentration = 0.6 nmol/L vs. $^{125}$I-Tyr$^4$-BN) (*15*), which are the BN analogs with the highest GRP-r affinity reported so far. Though determination of $K_d$ is independent of using live cells or cell membranes (*31*), the $B_{max}$ of 9.7 × $10^4$ receptors per cell, obtained with live AR42J cells, overestimates the number of receptors actually present on the cell surface. This can be attributed to the recycling of part of the receptors to the cell surface after internalization of the GRP-r/BN complex (*27,32*), which increases the $B_{max}$ of live cells with incubation time.

Internalization of $^{67}$Ga-BZH3 into AR42J cells suggests an agonistic nature of the peptide. The rapid and high degree of internalization—70% of total cell-associated activity was endocytosed within 15 min using both the low and the high peptide concentration—fits well with the internalization rate of the agonist $^{125}$I-Tyr$^4$-BN/GRP-r complex ($t_{1/2}$ ~ 6 min) and its independence from the peptide-to-receptor ratio (*31*).

Efflux of $^{67}$Ga and $^{177}$Lu activity from AR42J cells after internalization of labeled BZH3 showed half-lives of 13–16 h in vivo and in vitro, which are much longer than that of $^{125}$I-Tyr$^4$-BN ($t_{1/2}$ ~ 3 h) (*33*). Since lysosomal degradation of BN analogs is very rapid—after a 15 min-incubation, 80% of internalized $^{125}$I-Tyr$^4$-BN has already been metabolized (*34*)—the prolonged intracellular retention in tumor cells appears to be a specific feature of the $M^{3+}$ DOTA chelate and presumably of the linker used for coupling rather than of the peptide degradation products. This is supported by similar efflux data of $^{177}$Lu from PC-3 tumor cells using a different, but DOTA-conjugated, BN analog (*35*).

Biodistribution studies with escalating doses of $^{67}$Ga-BZH3 in tumor-bearing mice indicated a dose-dependent uptake in GRP-r–positive tissues. Intestines showed a continuously decreasing %ID/g uptake with increasing amounts of peptide, which indicates an increasing saturation of the receptors and an uptake maximum equal to or less than the lowest dose of 5 pmol per animal. In contrast, tumor and pancreas uptake peaked at the 15- and 45-pmol dose, respectively. Breeman et al. (*36*) also described such a bell-shaped, dose-dependent uptake in the pancreas of rats. These authors suggest that the initial stimulation of the %ID/g uptake with increasing amounts of peptide might be related to a clustering of the receptor/BN complexes in the cell membrane, which might be required for internalization of the complexes. Since we found no dose dependence of internalization in vitro with doses much lower than that used in biodistribution experiments, in vivo a preferential trapping of the peptide at low doses in the intestines appears to be more likely. Assuming receptor densities of pancreas > tumor > intestine—but taking into account the high absolute amount of intestinal GRP-r and a much higher blood flow in the intestines compared with the tumor tissue (*37*)—an optimum tumor uptake may be achieved only after a sufficient saturation of the intestinal GRP-r. In GRP-r–negative tissues, only kidneys showed a significantly reduced activity uptake after administration of the highest dose. This is in contrast to published results reporting no change in the kidney uptake of BN analogs in mice and rats up to a 100-μg dose (*36,37*). Thus, a slightly prolonged retention time of the small doses of $^{67}$Ga-BHZ3 in the kidneys seems to be more likely than a saturation of renal excretion by the high dose.

The clearance of $^{67}$Ga-BZH3 from the circulation and normal GRP-r–negative tissues was fast and resulted in low background activity with maximum tumor-to-tissue ratios at 2 h after injection, which meets the requirements of PET with the short-lived positron emitter $^{68}$Ga. The low liver uptake of 0.5 %ID/g versus 3–8 %ID/g observed for $^{99m}$Tc-labeled BN analogs (*17,18,33,38*) should facilitate tumor localization in the abdominal region compared with $^{99m}$Tc imaging.

Similar to somatostatin analogs, BN analogs labeled with a therapeutic radionuclide might have a potential for radiotherapy. Using the diagnostic radiolabel for calculation of the absorbed therapeutic radiation dose, a comparison of the biokinetics of the therapeutic and the diagnostic radiolabel is necessary, since a change in the $M^{3+}$ radiometal used for DOTA labeling can alter the biodistribution of a DOTA-conjugated peptide (*39*). For the couple of $^{67/68}$Ga and $^{177}$Lu (the latter has been used successfully in therapy of neuroendocrine tumors (*40*)), we found a slightly reduced (~20%) uptake of $^{177}$Lu-BZH3 in the tumor and a ~20% shortened half-life of tumor retention, whereas biodistribution and biokinetics in normal tissues were quite similar to that of $^{67}$Ga-BZH3. An exception, which might be beneficial for therapy, is the observed 3-fold accelerated clearance of pancreatic $^{177}$Lu activity. Presently, no reasonable explanation for the different kinetics of the $^{67}$Ga- and $^{177}$Lu-labeled peptide could be found. However, the data are in agreement with those reported by Smith et al. (*35*) for the washout of $^{177}$Lu activity from the pancreas of mice after administration of the $^{177}$Lu DOTA-8-Aoc-BN(7–14) analog. Nevertheless, the high initial, receptor-mediated $^{177}$Lu uptake in the pancreas has to be considered for limiting-dose calculations.

PET clearly indicated the potential of $^{68}$Ga-BZH3 for a sensitive localization of GRP-r–positive tumors in the mediastinal area. Compared with a $^{64}$Cu-labeled DOTA-BN analog ($t_{1/2}$, 12.7 h; $\beta^+$, 19%), recently proposed for PET (*37*), $^{68}$Ga-BZH3 appears to be much more favorable with regard to in vivo stability and biodistribution, in vitro data, and simplicity of radionuclide production. Detection of metastatic prostate carcinoma, especially of an invasion of pelvic lymph nodes, remains less predictable because of the enhanced intestinal and bladder background activity. On the other hand, the high GRP-r density found in most of the

prostatic neoplasms and metastases (*8*) might partially compensate these limitations.

## CONCLUSION

The $M^{3+}$ radiolabeled BN analog BZH3 evaluated in this study has shown many of the prerequisites for a successful targeting of GRP-r–positive tumors, such as a high affinity in the subnanomolar range and a rapid internalization with a prolonged intracellular retention of the $M^{3+}$ radionuclide in vitro. In vivo, high tumor-to-tissue ratios 1 h after injection and a rapid clearance of unbound peptide from GRP-r–negative, normal tissues was observed. PET has demonstrated the diagnostic potential in the tumor-bearing mouse model with $^{68}$Ga-BZH3. Additionally, the ability of PET to quantify biodistribution data should enable more accurate dose calculations for radiotherapy with $M^{3+}$ therapeutic radionuclides—for example, $^{90}$Y or $^{177}$Lu. The physiologic features together with PET and the simplicity of $^{68}$Ga production from a generator recommend $^{68}$Ga-BZH3 as a promising, versatile tool for an improved localization of GRP-r–positive tumors also in patients.

Because our generator is not commercially available, we refer the reader to a $TiO_2$-based $^{68}$Ge/$^{68}$Ga generator, which is commercially available from the Cyclotron Co. Ltd. Obninsk. Meyer et al. (*41*) have published a comparison, showing a similar suitability and efficiency of both generators.

## ACKNOWLEDGMENTS

We thank the Swiss National Science Foundation, the Swiss Commission for Technology and Innovation (KTI project 4668-1), the Deutsche Forschungsgemeinschaft (DFG grant 2901/3-1), and Mallinckrodt Medical for financial support of this work and Novartis for analytic support.

## REFERENCES

1. Martinez V, Tache Y. Bombesin and the brain-gut axis. *Peptides.* 2000;21:1617–1625.
2. Delle Fave G, Annibale B, De Magistris L, et al. Bombesin effects on human GI functions. *Peptides.* 1985;6:113–116.
3. Cuttita F, Carney DN, Mulshine J, et al. Bombesin-like peptides can function as autocrine growth factors in human small cell lung cancer. *Nature.* 1985;316:823–826.
4. Bologna MC, Festuccia C, Muzi P, Biordi L, Ciomei M. Bombesin stimulates growth of human prostatic cancer cells in vitro. *Cancer.* 1989;63:1714–1720.
5. Yano T, Pinski J, Groot K, Schally AV. Stimulation by bombesin and inhibition by bombesin/gastrin-releasing peptide antagonist RC-3095 of growth of human breast cancer cell lines. *Cancer Res.* 1992;52:4545–4547.
6. Gugger M, Reubi JC. Gastrin-releasing peptide receptors in non neoplastic and neoplastic human breast. *Am J Pathol.* 1999;155:2067–2076.
7. Reubi JC, Gugger M, Waser B. Co-expressed peptide receptors in breast cancer as a molecular basis for in vivo multireceptor tumor targeting. *Eur J Nucl Med.* 2002;29:855–862.
8. Markwalder R, Reubi JC. Gastrin releasing peptide receptors in human prostate: relation to neoplastic transformation. *Cancer Res.* 1999;59:1152–1159.
9. Reubi JC, Wenger S, Schmuckli-Maurer J, Schaer JC, Gugger M. Bombesin receptor subtypes in human cancers: detection with the universal radioligand $^{125}$I-[D-Tyr$^{6}$,β Ala$^{11}$,Phe$^{13}$,Nle$^{14}$]bombesin(6–14). *Clin Cancer Res.* 2002;8:1139–1146.
10. Reubi JC, Waser B. Concomittant expression of several peptide receptors in neuroendocrine tumors: molecular basis for in vivo multireceptor tumor targeting. *Eur J Nucl Med.* 2003;30:781–793.
11. Moody TW, Carney DN, Cuttita F, Quattrocchi K, Minna JD. High affinity receptors for bombesin/GRP-like peptides on human small cell lung cancer. *Life Sci.* 1985;37:105–113.
12. Reubi JC, Körner M, Waser B, Mazzucchelli L, Guillou L. High expression of peptide receptors as novel target in gastrointestinal stromal tumours. *Eur J Nucl Med.* 2004;31:803–810.
13. Van de Wiele C, Dumont F, Van den Broecke R, et al. Technetium-99m RP527, a GRP analogue for visualisation of GRP receptor-expressing malignancies: a feasibility study. *Eur J Nucl Med.* 2000;27:1694–1699.
14. Breeman WAP, de Jong M, Erion JL, et al. Preclinical comparison of $^{111}$In-labeled DTPA- or DOTA-bombesin analogs for receptor targeted scintigraphy and radionuclide therapy. *J Nucl Med.* 2002;43:1650–1656.
15. Hoffman TJ, Gali H, Smith CJ, et al. Novel series of In-111 labeled bombesin analogs as potential radiopharmaceuticals for specific targeting of gastrin-releasing peptide receptors expressed on human prostate cancer cells. *J Nucl Med.* 2003;44:823–831.
16. Van de Wiele C, Dumont F, Dierckx RA, et al. Biodistribution and dosimetry of $^{99m}$Tc-RP 527, a gastrin-releasing peptide (GRP) agonist for the visualization of GRP receptor-expressing malignancies. *J Nucl Med.* 2001;42:1722–1727.
17. Smith CJ, Sieckman GL, Owen NK, et al. Radiochemical investigations of gastrin-releasing peptide receptor-specific [$^{99m}$Tc (X) $(CO)_3$-Dipr-Ser-Ser-Ser-Gln-Trp-Ala-Val-Gly-His-Leu-Met($NH_2$)] in PC-3, tumor-bearing, rodent models: syntheses, radiolabeling, and in vitro/in vivo studies where Dpr = 2,3-diaminopropionic acid and X = $H_2O$ or $P(CH_2OH)_3$. *Cancer Res.* 2003;63:4082–4088.
18. Nock B, Nikolopoulou A, Chiotellis E, et al. $^{99m}$Tc-Demobesin 1, a novel potent bombesin analogue for GRP receptor-targeted tumor imaging. *Eur J Nucl Med.* 2003;30:247–258.
19. Scopinaro F, DeVincentis G, Varvarigou AD, et al. $^{99m}$Tc-Bombesin detects prostate cancer and invasion of pelvic lymph nodes. *Eur J Nucl Med.* 2003;30:1378–1382.
20. Smith CJ, Sieckman GL, Owen NK, et al. Radiochemical investigations of [$^{188}$Re$(H_2O)(CO)_3$-diaminopropionic acid-SSS-bombesin(7–14) $NH_2$]: syntheses, radiolabeling and in vitro/in vivo GRP receptor targeting studies. *Anticancer Res.* 2003;23:63–70.
21. Eisenwiener KP, Prata MI, Buschmann I, et al. NODAGATOC, a new chelator-coupled somatostatin analogue labeled with $^{67/68}$Ga and $^{111}$In for SPECT, PET, and targeted therapeutic applications of somatotastin receptor (hsst2) expressing tumors. *Bioconjug Chem.* 2002;13:530–541.
22. Schuhmacher J, Maier-Borst W. A new Ge-68/Ga-68 radioisotope generator system for production of Ga-68 in dilute HCl. *Int J Appl Radiat Isot.* 1981;32:31–36.
23. Presky DH, Schonbrunn A. Somatostatin pretreatment increases the number of somatostatin receptors in $GH_4C_1$ pituitary cells and does not reduce cellular responsiveness to somatostatin. *J Biol Chem.* 1988;263:714–721.
24. Zhang H, Chen J, Waldherr C, et al. Synthesis and evaluation of bombesin derivatives on the basis of pan-bombesin peptides labeled with In-111, Lu-177 and Y-90 for targeting bombesin receptor-expressing tumors. *Cancer Res.* 2004;64:6707–6715.
25. Doll J, Henze M, Bublitz O, et al. High resolution reconstruction of PET images using the iterative OSEM algorithm. *Nuklearmedizin.* 2004;43:72–79.
26. Hoffman TJ, Quinn TP, Volkert WA. Radiometallated receptor-avid peptide conjugates for specific in vivo targeting of cancer cells. *Nucl Med Biol.* 2001;28:527–539.
27. Van de Wiele C, Dumont F, Van Belle S, Slegers G, Peers SH, Dierckx RA. Is there a role for agonist gastrin-releasing peptide receptor radioligands in tumor imaging? *Nucl Med Commun.* 2000;22:5–15.
28. Henze M, Schuhmacher J, Hipp P, et al. PET imaging of somatostatin receptors using $^{68}$Ga DOTA-DPhe$^{1}$Tyr$^{3}$ Octreotide: first results in patients with meningiomas. *J Nucl Med.* 2001;42:1053–1056.
29. Hofmann M, Mäcke HR, Börner AR, et al. Biokinetics and imaging with the somatostatin receptor PET radioligand $^{68}$Ga-DOTA TOC: preliminary data. *Eur J Nucl Med.* 2001;28:1751–1757.
30. Kowalski J, Henze M, Schuhmacher J, Mäcke HR, Hofmann M, Haberkorn U. Evaluation of positron emission tomography imaging using $^{68}$Ga DOTA-DPhe$^{1}$-Tyr$^{3}$-Octreotide in comparison to $^{111}$In DTPA OC SPECT: first results in patients with neuroendocrine tumors. *Mol Imaging Biol.* 2003;5:42–48.
31. Tsuda T, Kusui T, Hou W, et al. Effect of gastrin releasing peptide receptor number on receptor affinity, coupling, degradation and modulation. *Mol Pharmacol.* 1997;51:721–732.
32. Tseng MJ, Detjen K, Struk V, Logsdon CD. Carboxyl-terminal domains deter-

mine internalization and recycling characteristics of bombesin receptor chimeras. *J Biol Chem.* 1995;270:18858–18864.
33. Smith CJ, Gali H, Sieckman GL, Higgenbotham C, Volkert WA, Hoffman TJ. Radiochemical investigations of $^{99m}$Tc-$N_3$-S-X-BBN[7–14]$NH_2$: an in vitro/in vivo structure-activity relationship study where X = 0-, 3-, 5-, 8-, and 11-carbon tethering moieties. *Bioconjug Chem.* 2003;14:93–102.
34. Zhu WY, Göke B, Williams JA. Binding, internalization and processing of bombesin by rat pancreatic acini. *Am J Physiol.* 1991;261:G57–G64.
35. Smith CJ, Gali H, Sieckman GL, et al. Radiochemical investigations of $^{177}$Lu-DOTA-8-Aoc-BBN[7–14]$NH_2$: an in vitro/in vivo assessment of the targeting ability of this new radiopharmaceutical for PC-3 human prostate cancer cells. *Nucl Med Biol.* 2003;30:101–109.
36. Breeman WAP, DeJong M, Bernard BF, et al. Pre-clinical evaluation of [$^{111}$In-DTPA-Pro$^1$,Tyr$^4$]bombesin, a new radioligand for bombesin-receptor scintigraphy. *Int J Cancer.* 1999;83:657–663.
37. Rogers BE, Bigott HM, McCarthy DW, et al. Micro PET imaging of a gastrin-releasing peptide receptor-positive tumor in a mouse model of human prostate cancer using a $^{64}$Cu-labeled bombesin analog. *Bioconjug Chem.* 2003;14:756–763.
38. LaBella R, Garcia-Garayoa E, Langer M, Bläuenstein P, Beck-Sickinger AG, Schubiger PA. In vitro and in vivo evaluation of a $^{99m}$Tc(I)-labeled bombesin analogue for imaging of gastrin releasing peptide receptor-positive tumors. *Nucl Med Biol.* 2002;29:553–560.
39. Heppeler A, Froidevaux S, Mäcke HR, et al. Radiometal-labeled macrocyclic chelator derivatised somatostatin analogue with superb tumor targeting properties and potential for receptor mediated internal radiotherapy. *Chem Eur J.* 1999;5:1974–1981.
40. Kwekkeboom DJ, Bakker WH, Kam BL, et al. Treatment of patients with gastro-entero-pancreatic (GEP) tumours with the novel radiolabelled somatostatin analogue [$^{177}$Lu-DOTA(0),Tyr$^3$]octreotate. *Eur J Nucl Med.* 2003;30:417–422.
41. Meyer GJ, Maecke H, Schuhmacher J, Knapp WH, Hofman M. $^{68}$Ga-Labeled DOTA-derivatised peptide ligands. *Eur J Nucl Med.* 2004;31:1097–1104.

*Manuscript 1*

# Influence of Different Spacers on the Pharmacologic Profile of a Panbombesin Analogue

**Hanwen Zhang [a], Martin Walter [a], Jianhua Chen [a], Beatrice Waser [b], Jean Claude Reubi [b], Anna Seelig [c], Helmut R. Maecke[a]**

[a] Division of Radiological Chemistry, Institute of Nuclear Medicine, Department of Radiology, University Hospital, Basel, Switzerland;
[b] Division of Cell Biology and Experimental Cancer Research, Institute of Pathology, University of Berne, Berne, Switzerland
[c] Department of Biophysical Chemistry, Biocenter of the University of Basel, Basel, Switzerland.

Present status:
Manuscript in preparation.

# Influence of different spacers on the pharmacologic profile of a panbombesin analogue

Hanwen Zhang [a], Martin Walter [a], Jianhua Chen [a], Beatrice Waser [b], Jean Claude Reubi [b], Anming Tan [c], Anna Seelig [c], Helmut R. Maecke *[a]

[a] Division of Radiological Chemistry, Department of Radiology, University Hospital Basel, Petersgraben 4, CH-4031 Basel, Switzerland;

[b] Division of Cell Biology and Experimental Cancer Research, Institute of Pathology, University of Berne, PO Box 62, Murtenstrasse 31, CH-3010 Berne, Switzerland;

[c] Department of Biophysical Chemistry, Biocenter of the University of Basel, Klingelbergstrasse 70, CH-4056 Basel, Switzerland.

[1]**Abbreviations:** BN, bombesin; BZH, [(D)Tyr$^6$, βAla$^{11}$, Thi$^{13}$, Nle$^{14}$] BN(6-14); GABA, γ-aminobutyric acid; Ahx, 6-aminohexanoic acid; $PEG_2$, 8-amino-3,6-dioxaoctanoic acid; $PEG_4$, 15-amino-4,7,10,13-tetraoxapentadecanoic acid; $Sar_5$, pentasarcosine; GRP, gastrin-releasing peptide; NMB, neuromedin B; DOTA, 1,4,7,10-tetraazacyclododecane-1,4,7,10-tetraacetic acid; DIPEA, N-ethyldiisopropylamine; DIC, N,N'-diisopropylcarbodiimide; HoBt, 1-hydroxybenzotriazole; HATU, O-(7-azabenzotriazol-1-yl)-N,N,N',N'-tetramethyluroniumhexafluorophosphate; NMP, 1-methyl-2-pyrrolidone; DMF, N,N-dimethylformamide; TNBS, 2,4,6-trinitrobenzenesulfonic acid; TFA, trifluoroacetic acid. Abbreviations of the common amino acids are in accordance with the recommendations of IUPAC-IUB [IUPAC-IUB Commission of Biochemical Nomenclature (CBN), symbols for amino acid derivatives and peptides, recommendations 1971. Eur J Biochem 1972; 27:201-207].

* To whom correspondence should be addressed:
Tel: ++41 61 265 46 99; Fax: ++41 61 265 55 59
E-mail: hmaecke@uhbs.ch

**ABSTRACT**

A variety of human cancers have been shown to overexpress bombesin (BN) receptor subtypes. The universal BN ligand [D-Tyr$^{6}$, β-Ala$^{11}$, Thi$^{13}$, Nle$^{14}$] BN (6-14) (BZH) has high affinity to all three bombesin receptor subtypes (NMB-R, GRP-R, and BRS-3). This finding prompted us to develop radiolabeled BN analogues for the diagnosis and targeted radionuclide therapy of BN receptor-expressing tumors. A direct conjugation of the chelator to the peptide, however, led to a considerable loss of binding affinity. Assuming that the introduction of a spacer between the peptide and the chelator might be necessary for retaining high affinity to BN receptors, we designed DOTA-**X**-BZH conjugates (**X** = spacer: GABA, Ahx, $PEG_2$, $PEG_4$, $\beta Ala_2$, (D)Dab-βAla and $Sar_5$) and studied the influence of the spacers on the pharmacological properties of the analogues.

All conjugates were synthesized in parallel with yields of 23% to 30%, based on the removal of the first Fmoc group. All metallated ligands had high affinity within nanomolar range ($IC_{50}$: 0.8±0.1 to 6.3±1.3 nM) to the human GRP receptor and retained affinity to the other two human BN receptor subtypes. The [$^{111}$In]-DOTA-**X**-BZH analogues showed different metabolic stabilities in serum; the $t_{1/2}$-values varied from 2.3 h to 33.6 h with increasing length of the spacer. Decomposition of [$^{111}$In]-DOTA-$PEG_4$-BZH was found to be similar in PC-3 cells and in serum, the cleavage occurring at the same sites but resulting in different proportions of the metabolites. In PC-3 cells, the major metabolite of [$^{111}$In]-DOTA-$PEG_4$-BZH resulted from the cleavage between Gln$^{7}$ and Trp$^{8}$, while in serum the major metabolite was due to the cleavage of βAla$^{11}$-His$^{12}$. Rat and human GRP receptor-expressing cell lines showed different internalization rates of $^{111}$In-labeled DOTA-$PEG_4$-BZH and DOTA-$Sar_5$-BZH, respectively. The biodistribution in AR4-2J tumor-bearing rats showed a high and specific accumulation of the $^{111}$In-labeled conjugates in the tumor and GRP-R-positive organs. A fast clearance from blood and all non-target organs except the kidneys was found. Of all conjugates, [$^{111}$In]-DOTA-$PEG_4$-BZH showed the highest tumor uptake and the best tumor-to-kidney ratio.

## INTRODUCTION

Bombesin(BN)-like peptides have become attractive for more and more research groups since many severe human cancer types have been found to overexpress BN receptors [1, 2]. Among the BN receptor family (neuromedin B receptor: NMB-R, gastrin-releasing peptide receptor: GRP-R, BN receptor subtype-3: BRS-3), GRP-R is the most relevant subtype because of its high expression on prostate [3], breast [4], and gastrointestinal stromal tumors (GIST) [5]. NMB-R and BRR-3 overexpression has been observed in intestinal carcinoids and small cell lung carcinomas whereas renal cell carcinomas overexpress GRP-R and BRS-3 concomitantly [1]. These data show that each BN receptor subtype is overexpressed on different types of tumors and that the same type of tumor may co-express two BN receptor subtypes. This indicates that a universal bombesin analog has the comparative advantage to visualize these tumors with a high incidence. Although this finding opens up the possibility to apply panbombesin ligands as vehicles for delivering radionuclides [6, 7] or cytotoxics [8] into tumors, most researchers to date still focus on the development of BN analogs for diagnosis [9-21] and targeted radionuclide therapy [22, 23] of GRP-R expressing tumors only.

Compared to the known pan-BN ligand [D-Tyr$^{6}$, βAla$^{11}$, Phe$^{13}$, Nle$^{14}$] BN (6-14) [6], metallated DOTA-GABA-[D-Tyr$^{6}$, βAla$^{11}$, Thi$^{13}$, Nle$^{14}$] BN (6-14) (BZH2) was shown to bind to GRP- and NMB-receptors with a relatively high affinity and to BRS-3 with a mediate affinity. As according to our unpublished data the direct coupling of the chelate to the peptide results in a significant loss of binding affinity to the GRP-receptor, the introduction of a spacer between the peptide and the chelate seems to be necessary for retaining the biological properties of the non-chelated peptide. In our present study, different types and lengths of spacers (**X**) were therefore introduced into the prototype DOTA-**X**-BZH, which can be labeled with hard Lewis acid type metallic radionuclides such as $^{111}$In, $^{90}$Y, $^{177}$Lu, and $^{68}$Ga. These (radio)metallopeptides were evaluated with regard to their binding affinity towards BN receptors and their internalization rates into AR4-2J (rat pancreatic tumor cells expressing rat GRP-R) and PC-3 (human prostate cancer expressing human GRP-R) cells. In addition, we studied the metabolic stability in human blood serum and PC-3 cells and the biodistribution in AR4-2J tumor-bearing rats.

## RESULTS

### Synthesis and labeling

Different types of spacers (Fig. 1) were introduced into the prototype DOTA-**X**-BZH, including hydrocarbon (GABA and Ahx), poly(ethylene oxide) ($PEG_2$ and $PEG_4$), amino acids with a positive charge on the side chain ((D)Dab-βAla), and unnatural amino acids ($βAla_2$ and $Sar_5$). All

DOTA-**X**-BZH conjugates were successfully synthesized in parallel by using solid phase peptide synthesis (Fmoc strategy), affording an overall yield of approximately 23% to 30% based on the removal of the first Fmoc group after cleavage, purification and lyophilization. The purity of all conjugates was ≥97% (HPLC grade). The composition of DOTA-**X**-BZH and metallated DOTA-**X**-BZH was determined via MS, the results being commensurate with the theoretically expected values (Table 1). All DOTA-**X**-BZH analogues could be labeled with $^{111}$In and $^{177}$Lu under the ammonium acetate buffer (pH 5, 0.4 M) at elevated temperature (95°C) for 20-25 min. In all cases labeling yields of ≥98% at a specific activity of >37 GBq μmol$^{-1}$ for $^{111}$In and of >80GBq μmol$^{-1}$ for $^{177}$Lu were achieved.

**Binding affinity to GRP-receptors and affinity profiles**

Binding experiments were performed on human prostate cancer tissue expressing GRP-R. The $IC_{50}$ value of BZH was 1.0±0.2 nM. All conjugates retained high affinity to the GRP-receptors in a nanomolar range, as shown in Table 2. Compared to the affinity of BZH and with the exception of the Ahx-conjugate, which had a slightly improved affinity (0.8±0.1 nM), the spacers together with metallated DOTA caused a reduced affinity to GRP-R by a factor of 2 (GABA: 2.2±0.2 nM; $PEG_2$: 2.1±0.8 nM; $\beta Ala_2$: 2.5±0.4 nM; (D)Dab-βAla: 2.1±0.9 nM) or by a factor of 5 ($PEG_4$: 6.3±1.3 nM and $Sar_5$: 5.7±1.4 nM).

Human cancer tissue expressing NMB-R (or GRP-R or BRS-3) was used for studying the affinity. The affinity profiles of [$^{nat}$Y/$^{nat}$Ga]-DOTA-GABA-BZH and [$^{nat}$Ga]-DOTA-$PEG_2$-BZH are shown in Table 3. Similar affinities to all three receptor subtypes were observed for $^{nat}$Y- and $^{nat}$Ga-labeled DOTA-GABA-BZH: NMB-R, 4.9±1.0 nM vs. 4.7±0.4 nM; GRP-R, 1.4±0.1 nM vs. 1.3±0.2 nM; BRS-3, 10.7±4.2 nM vs. 6.6±0.6 nM. The $IC_{50}$ values of [$Ga^{III}$]-DOTA-$PEG_2$-BZH were 6.4±2.2 nM for NMB-R, 2.0±0.6 nM for GRP-R, and 8.0±0.7 nM for BRS-3, respectively.

**Stability in human serum and PC-3 cells**

Upon 4 h incubation in fresh serum, less than 5% of radioactivity (from radiolabeled peptides) was observed in the proteic fraction obtained as pellet. All [$^{111}$In]-DOTA-**X**-BZH conjugates were metabolized to the same breakdown products as [$^{111}$In]-DTPA-GABA-BZH [6], as indicated by the similar HPLC retention times (data not shown). Table 4 shows the half-lives ($t_{1/2}$) of disappearance of [$^{111}$In]-DOTA-**X**-BZH in serum, calculated according to the equation $A=A_0*\exp(-k_1*t)$ [6], the values being: GABA, 2.2±0.2h; Ahx, 3.2±0.3h; $PEG_2$, 3.6±0.2h; $PEG_4$, 6.5±h; $\beta Ala_2$, 5.8±0.4h; (D)Dab-βAla, 14.4±1.0h; $Sar_5$, 33.6±1.1h.

As a hypothesis, non-internalized radiopeptides and externalized metabolites can be observed simultaneously in the incubation medium. Therefore, the metabolism of [$^{111}$In]-DOTA-**X**-BZH in PC-3 cells should be traceable via investigation of the components remaining in medium. Of [$^{111}$In]-DOTA-PEG$_4$-BZH as leading ligand, more than 50% of radioactivity was metabolized within 2 h incubation, whereas >95% of radioactivity still remained intact upon incubation with a large excess of DOTA-GABA-BZH (Fig. 2). Furthermore, [$^{111}$In]-DOTA-PEG$_4$-BZH was decomposed by enzymes at the same peptide bond in cells and serum (Fig. 3). Cleavage between Gln$^7$ and Trp$^8$ afforded the main metabolite in cells (the highest metabolite peak in Fig. 2), and cleavage between βAla$^{11}$ and His$^{12}$ the main metabolite in serum (data not shown).

**Internalization**

All $^{111}$In-labeled ligands showed a specific and fast uptake in AR4-2J and PC-3 cells, which did not reach a plateau within 6 h of incubation at 37°C (Fig. 4); <1% of the added activity was internalized non-specifically; <7% of the added activity was surface-bound peptide (acid removable) (data not shown). All [$^{111}$In]-DOTA-**X**-BZH analogues showed similar internalization rates (Fig. 4) into PC-3 cells, whereas the internalization rates of the **βAla$_2$**, **PEG$_4$** and **Sar$_5$** derivatives into AR4-2J cells were significantly lower than those of the other analogues (Fig. 4).

**Animal biodistribution studies**

Biodistribution studies of the $^{111}$In-labeled peptides were performed on AR4-2J (pancreatic) tumor-bearing Lewis rats. The results are presented in Fig. 5 and Table 5 as percentage of injected activity per gram of tissue (% IA/g).

[$^{111}$In]-DOTA-**X**-BZH displayed a rapid clearance from blood (0.01% IA/g at 4h) and from GRP-R-negative tissues except the kidneys, resulting in high tumor-to-nontarget ratios (Table 5). It was also observed that [$^{111}$In]-DOTA-**X**-BZH highly accumulated in the AR4-2J tumor and in GRP-R-positive organs. At 4 h [$^{111}$In]-DOTA-PEG$_4$-BZH showed the highest uptake (1.55±0.25% ID/g) and [$^{111}$In]-DOTA-GABA-BZH the lowest uptake (0.82±0.06% ID/g) of the tested derivatives in the AR4-2J tumor. Co-injection of [$^{111}$In]-DOTA-**X**-BZH with DOTA-GABA-BZH caused an >90% uptake reduction in the tumor and pancreas (GRP-R-positive tissues). A high blocking dose (50 μg DOTA-GABA-BZH) did not influence the uptake in non-target organs except the kidneys (data not shown). [$^{111}$In]-DOTA-PEG$_4$-BZH showed the highest tumor-to-kidney ratio (Table 4) of all tested ligands. The kinetics of [$^{111}$In]-DOTA-Sar$_5$-BZH (Fig.5) showed higher accumulation in the AR4-2J tumor and pancreas than [$^{111}$In]-DOTA-GABA-BZH at all time points. [$^{111}$In]-DOTA-Sar$_5$-BZH, however, was released from the tumor

and pancreas with a relatively faster rate than [$^{111}$In]-DOTA-GABA-BZH. Similar accumulation in and release from the kidneys was observed for both radiolabeled ligands.

**Secondary structure in PBS buffer**

[$^{nat}$Y]-DOTA-**X**-BZH dissolved in PBS buffer was determined with UV spectra-meter, diluted to 60 μM and then measured with circular dichroism (CD) spectroscopy under room temperature. The results from the CD spectra evaluation (Fig. 6) are listed in Table 6. The main secondary structure of [$^{nat}$Y]-DOTA-**X**-BZH in PBS buffer is random coil, varying from 40.8% to 67.9%; the second main structure was β-sheet with the contents of 17.4% to 41.7%, except for the $\beta Ala_2$ analog, which might be caused by association in solution. For GABA, Ahx, $PEG_2$ and $PEG_4$ derivatives, there were practically no α-helix and β-turn structures. (D)Dab-βAla and $Sar_5$ analogues may form about 1 helical structure.

## DISCUSSION

The results show that a spacer between chelate and peptide is a determining factor for biological properties such as binding affinity, internalization rate, biodistribution and metabolic stability. Compared to similar studies [24, 25], the present study reveals that the influence of a spacer results not only from the chain length of the spacer, but also from the type of spacer.

Except from GABA, different spacers including Ahx, $PEG_2$, $PEG_4$, $\beta Ala_2$, (D)Dab-βAla and $Sar_5$ were inserted between chelate (DOTA) and the universal BN ligand, [D-Tyr$^6$, βAla$^{11}$, Thi$^{13}$, Nle$^{14}$] BN (6-14) (BZH). All conjugates showed high affinity ($IC_{50}$ value: 0.8–6.3 nM) to GRP-R-expressing human prostate cancer tissue. Various chain lengths for the same type of spacer resulted in different binding affinities. For instance 5 hydrocarbons (Ahx: 0.8±0.1 nM) afforded a better binding affinity to hGRP-R than 3 hydrocarbons (GABA: 2.2±0.2 nM), which is consistent with other published results [24, 25]. In contrast, 4 ethylene oxides ($PEG_4$: 6.3±1.3nM) led to a worse $IC_{50}$ value than 2 ($PEG_2$: 2.1±0.8nM) and 80 ethylene oxides showed almost no affinity (3.9±0.6μM) to hGRP-R [26], indicating that the longer the poly(ethylene oxide), the worse the binding affinity, which is also consistent with known properties of PEGylated protein [27].

Considering the influence of the spacer type, a longer spacer ($PEG_4$ and $Sar_5$ (5.7±1.4nM)) led to a worse affinity to hGRP-R and to a slower internalization rate into AR4-2J cells (rat GRP-R) than a shorter spacer. Of all spacer-modified BN analogues, the internalization rates into PC-3 (hGRP-R) did not differ significantly. These findings suggest that the biological properties of GRP receptors on AR4-2J (rat) cells are different from the ones on human PC-3 cells. In other words, significant differences between AR4-2J and PC-3 were observed for the internalization rates of $^{111}$In-labeled DOTA-$PEG_4$-BZH (16.2%) and DOTA-$Sar_5$-BZH (15.7%). However, there

is only a slight difference for the other spacers (GABA, Ahx, $PEG_2$, (D)Dab-βAla and $βAla_2$), varying from 0.3% to 6.6%. These findings prompted us to analyze the binding affinities towards human and mouse/rat GRP-receptors. Using [$^{nat}$Y]-DOTA-$PEG_4$-BZH as a leading ligand, the results were converse to what we expected (i.e. the faster the internalization rate, the higher the affinity): they showed a higher affinity to the rat/mouse GRP-R (0.20 to 0.46 nM) and a lower affinity to the human GRP-R (3.9 to 6.3nM) [19]. The reason for this phenomenon might be due to the expression of the MDR1 P-glycoprotein on cells, as the density of MDR1 on murine cells is higher than on human cells, and poly(sarcosine/ethylene oxide) is exported out of the cells by MDR1 [28].

[$^{111}$In]-DOTA-**X**-BZH showed different metabolic stability values in fresh human serum with $t_{1/2}$ varying from 2.3 h to 33.6 h with increasing spacer length. The weakest bond of βAla$^{11}$-His$^{12}$ could not be stabilized directly by changing the spacer. At that time, we assumed that these ligands due to different spacers might form different secondary structures in solution. After analyzing the secondary structures, the most stable ligand, [$^{111}$In]-DOTA-$Sar_5$-BZH, seems to form one helical turn although in solution it mainly exists in random coil and β-sheet, but this does not sufficiently explain the differences in metabolic stability. Therefore we studied the metabolism in the cells, based on the hypothesis that non-internalized radiopeptides and externalized metabolites from the cells would be simultaneously in the incubation medium. All [$^{111}$In]-DOTA-**X**-BZH were metabolized due to the same broken bond, as indicated by the similarity of the HPLC elution times in serum. However, the main metabolite in the cells was due to a cleavage between Gln$^7$ and Trp$^8$, whereas the main metabolite in serum was due to the cleavage between βAla$^{11}$ and His$^{12}$ [6].

Biodistribution studies showed that the [$^{111}$In]-DOTA-**X**-BZH conjugates highly accumulated in the AR4-2J tumor and GRP-R positive organs, and were released quickly from blood and GRP-R negative tissues except the kidneys. [$^{111}$In]-DOTA-$PEG_4$-BZH showed the highest tumor uptake (1.55±0.25% ID/g) at 4h, and with a value of 2 the highest tumor-to-kidney ratio as well, indicating that the PEGylation of a BN analogue is still worthwhile as it affords a better *in-vivo* performance despite the significant loss of affinity that it brings about [27]. [$^{111}$In]-DOTA-$Sar_5$-BZH (Fig.5) displayed a higher accumulation in the AR4-2J tumor and pancreas than [$^{111}$In]-DOTA-GABA-BZH at all time points despite the higher affinity (2.8 times) and faster internalization rate (1.8 times) into AR4-2J cells of the latter. The reason for this may be due to the higher stability (15 times) of [$^{111}$In]-DOTA-GABA-BZH in serum. [$^{111}$In]-DOTA-$Sar_5$-BZH was released from the tumor and pancreas relatively faster than [$^{111}$In]-DOTA-GABA-BZH as in rats the excretion of $Sar_5$ from the AR4-2J tumor is also supported by MDR1.

In conclusion, the spacer-modified BN analogues show differences in affinity to hGRP-R and metabolic stability, respectively. An adequate length of poly(ethylene oxide) such as $PEG_4$ should allow for a high tumor-to-kidney ratio and a retained affinity to the human GRP-R. A further rationale for the design of BN analogs for clinical application may benefit from these results.

## EXPERIMENTAL SECTION

**General.** All chemicals were obtained from commercial sources and used without further purification. Rink amide MBHA resin (0.6 mmol/g) and all Fmoc-protected amino acids were commercially available from NovaBiochem (Läufelfingen, Switzerland). DOTA-tris(tBu ester) was obtained from Macrocyclics (Dallas, TX, USA). Fmoc-15-amino-4,7,10,13-tetraoxapentadecanoic acid (Fmoc-$PEG_4$-OH) was purchased from Quanta BioDesign Ltd. (Powell, OH, USA) and Fmoc-$PEG_2$-OH from Neosystem (Strasbourg, France); Fmoc-$Sar_5$-OH was synthesized in our lab (Joerg Schmitt; unpublished data). [$^{111}$In]$Cl_3$ was purchased from Mallinckrodt Medical (Petten, the Netherlands). PC-3 cells were obtained from the European Collection of Cell Cultures (ECACC, Wiltshire SP4 OJG, UK). The cell culture medium was Dulbecco's minimal essential medium (DMEM) with vitamins, essential and non-essential amino acids, L-glutamine, antibiotics (penicillin/streptomycine), fungicide (amphotericin B/Fungizone®) and 10% (1%) fetal calf serum (FCS) from BioConcept (Allschwil, Switzerland). Solid phase peptide synthesis was performed on a semiautomatic peptide synthesizer commercially available from Rink Combichem (Bubendorf, Switzerland). Electrospray ionization mass spectroscopy was carried out with a Finnigan SSQ 7000 spectrometer (Brennen, Germany) and matrix-assisted laser desorption ionization (MALDI)-mass spectrometry measurements on a Voyager sSTR equipment with a Nd:YAG laser (Applied Biosystems, Framingham, NY). Analytical HPLC was performed on a Hewlett Packard 1050 HPLC system (Waldbronn 2, Germany) with a multiwavelength detector and a flow-through Berthold LB 506 Cl γ-detector (Wildbad, Germany) using a Macherey-Nagel (Oensingen, Switzerland) Nucleosil 120 $C_{18}$ column (**System 1**: flow: 0.75 ml/min; eluents: A= 0.1% TFA in water and B= acetonitrile; non-linear gradient: 0 min, 80% A; 20 min, 50% A; 21 min, 0% A; 24 min, 0% A and 25, 80% A. **System 2**: flow: 0.75 ml/min; eluents: A= 50 mM sodium acetate buffer (pH 5.4) and B= acetonitrile; non-linear gradient as in **System 1**). Preparative HPLC was performed on a Metrohm HPLC system LC-CaDI 22-14 (Herisau, Switzerland) with a Macherey-Nagel VP 250/21 Nucleosil 100-5 $C_{18}$ column (flow: 15 ml/min; eluents: A= 0.1% TFA in water and B= acetonitrile; non-linear gradient: 0 min, 70% A; 10 min, 50% A; 11 min, 0% A; 14 min, 0% A

and 15, 70% A). Quantitative γ-counting was performed on a COBRA 5003 γ-system well counter from Packard Instruments (Meriden, CT, USA). CD spectra (190-250nm) were measured on a Jasco J720 at room temperature using a quartz cell of 0.2 mm path length.

The concentrations of all tested compounds were determined (280 nm, ε=6890) with a Lambda 2 UV-visible spectrophotometer (PerkinElmer, Bodenseewerk, Germany) and the HPLC purity of all compounds used for experiments was >99%.

**Peptide Synthesis**

The peptide synthesis was performed on a semiautomatic peptide synthesizer according to a general procedure described previously [6] (Fig. 1). Standard Fmoc chemistry was used throughout; Trt, tBu and Boc were used as protecting groups of His, D-Tyr and Trp, respectively. Fmoc-D-Tyr(tBu)-Gln-Trp(Boc)-Ala-Val-βAla-His(Trt)-Thi-Nle-resin was obtained by assembling Fmoc-protected amino acids on a Rink amide MBHA resin (1 g) with an overall yield of 90% based on the removal of the first Fmoc group. The spacers and DOTA-tris(tBu ester) were coupled in parallel (20 μmol for each conjugate): three equivalents Fmoc-spacer (3 eq GABA, Ahx, $PEG_2$, $PEG_4$ and $Sar_5$) were preincubated 30 min with HATU (3.6 equivalents) in NMP and incubated with the resin-assembled peptide until the Kaiser test was negative (>3 h) except that 5 equivalents Fmoc-$PEG_4$-OH were used. $βAla_2$ and (D)Dab-βAla were coupled using standard Fmoc procedure, with Fmoc-(D)Dab(Boc)-OH being used for the latter spacer. The peptide conjugates were cleaved from the resin, deprotected concomitantly by incubation with TFA/thioanisole/water 92/6/2 at room temperature for 4-6 h, and then precipitated in cold isopropyl ether/petroleum ether (1:1). After drying in the vacuum oven under room temperature, the crude peptide-chelator conjugate was purified by preparative HPLC. MS ((±)EI, MALDI) and analytical HPLC were used to determine the composition and purity of the conjugates, respectively.

**Metallated conjugates**

The metal complex was synthesized according to the method described previously [6]. Briefly, a mixture of conjugate (0.5 μmol) in 500 μl 0.4 M ammonium-acetate-buffer (pH 5) was incubated with 1.5 μmol $Y(NO_3)_3 \cdot 5H_2O$ ($Ga(NO_3)_3 \cdot 9H_2O$) pre-dissolved in 0.04 M HCl at 95°C for 25 min, cooled down to room temperature and purified over a SepPak $C_{18}$ cartridge (Waters Corp. Milford, MA) preconditioned with 10 ml ethanol and 10 ml water. The cartridge was eluted with 10 ml water followed by 3 ml ethanol resulting in metallated conjugates after the evaporation of ethanol. The final product was analyzed by analytical HPLC (the purities were ≥99%) and identified by MALDI and MS.

**Preparation of radiotracer**

The [$^{111}$In]-conjugate was prepared by dissolving 10 µg of the conjugate in ammonium acetate buffer (300 µl, 0.4 M, pH 5); after the addition of $^{111}InCl_3$ (3-5 mCi), the solution was heated at 95° for 25 min. A 1.5 molar excess of the relative cold metal ion was added and the final solution heated again at 95°C for 15 min. Subsequently a SepPak $C_{18}$ cartridge was utilized to purify the radiolabeled peptides to afford the pure radiolabeled ligand as described in the section "Metallated Conjugates". A quality control was performed by HPLC (**System 1**). Biodistribution studies were prepared using the same method (but without addition of cold metal), diluted in 0.9% NaCl (0.1% BSA) to afford the radioligand solution.

**Metabolic stability in serum and in PC-3 cells**

The study of metabolic stability in serum was performed as described previously [6]; 0.6 nmol $^{111}$In-labeled conjugates were added to the freshly prepared serum and the mixture was incubated in a 5% $CO_2$, 37°C environment for different periods (0, 1, 4, and 8 h).
For studying the stability in PC-3 cells, the cells were prepared in six-well plates the day before: cells were washed twice with culture medium and were allowed to adjust to the medium at 37°C for 1 h. Approximately 1.8 kBq (0.25 pmol) [$^{111}$In]-DOTA-$PEG_4$-BZH, as leading compound, was added and incubated with PC-3 cells (~1 million cells) either with or without DOTA-GABA-BZH in a 37°C, 5%$CO_2$ environment for 2 h. The solution outside the cells was collected and loaded onto a SepPak $C_{18}$ cartridge preconditioned with 10 ml methanol and 10 ml water; then the peptides were released from the cartridge with 1 ml ethanol. The ethanol solution and the metabolites from the serum were analyzed on HPLC (eluents: A= 0.1% TFA in water and B= acetonitrile; gradient: 0-55 min, 90%-55% A; 56-59 min, 100% B; 59-60 min, 80% A).

**Binding affinity to human GRP-receptors**

Using [$^{125}$I-D-Tyr$^4$]BN as GRP-R preferring ligand, the $IC_{50}$ values of $^{nat}$Y-labeled peptides were measured with successive sections of human prostate cancer tissue overexpressing GRP-receptors.
The binding affinity profiles of the [$^{nat}$Y/$^{nat}$Ga]-conjugates for the three bombesin receptor subtypes were determined *in vitro* using receptor autoradiography with [$^{125}$I-D-Tyr$^6$, β-Ala$^{11}$, Phe$^{13}$, Nle$^{14}$]BN (6-14) as universal radioligand. The procedure was described in detail previously [1, 29].

**Internalization studies**

Internalization and externalization experiments were performed in 6-well plates as described previously [6]. Using DOTA-GABA-BZH as blocking agent (final concentration: 0.58 µM) to

determine nonspecific internalization, approximately 1.8 kBq (0.25 pmol) of the radioligand was used for incubation with the cells ($10^6$ cells per well). The percentage of added dose per million cells (%/total) was calculated for the internalization rate at different time points.

**Biodistribution experiments in AR4-2J tumor-bearing Lewis rats**

Biodistribution studies were performed on AR4-2J tumor-bearing male Lewis rats as described previously [6]. $^{111}$In-labeled peptides (0.1 µg) in 200 µl 0.9% NaCl solution were injected for biodistribution, and 50 µg DOTA-GABA-BZH (injected volume, 225 µl) co-injected to determine non-specific uptake. The percentage of injected activity per gram (% IA/g) was calculated for each tissue. The total counts injected per animal were determined by extrapolation from counts of an aliquot taken from the injected solution as a standard.

Kinetic studies of [$^{111}$In]-DOTA-GABA-BZH and [$^{111}$In]-Sar$_5$-BZH were carried out at different time points, including 4h, 24h, 48h and 72h post injection.

All animal experiments were performed in compliance with the Swiss regulation for animal treatment (Bundesamt für Veterinärwesen, approval no. 789).

**Analysis of secondary structure using CD**

All [$^{nat}$Y]-DOTA-**X**-BZH conjugates were dissolved in 0.1 M phosphate buffer (pH=7.4), measured with a UV spectrometer (280 nm, ε=6890) and diluted to 60 µM. CD spectra (190-250 nm) were obtained by determination on a Jasco J720 at room temperature using a quartz cell of 0.2 mm path length; 50 scans were averaged for each sample and the averaged blank spectra were subtracted.

**Statistical Analysis**

Data are expressed as mean ± SD, which were calculated on Microsoft Excel. The Student t test (origin 6, Microcal Software, Inc., Northampton, MA) was used to determine statistical significance at the 95% confidence level with $P < 0.05$ being considered significantly different.

**Acknowledgements**

We thank the Swiss National Science Foundation and the "Amt für Ausbildungsbeiträge Basel-Stadt" for financial support of this work and Novartis for analytical support.

**References**


1. Reubi JC, Wenger S, Schmuckli-Maurer J, Schaer JC, Gugger M. Bombesin receptor subtypes in human cancers: detection with the universal radioligand $^{125}$I-[D-Tyr$^{6}$, β-Ala$^{11}$, Phe$^{13}$, Nle$^{14}$] bombesin(6-14). Clin Cancer Res. 2002; 8: 1139-46.
2. Preston SR, Miller GV, Primrose JN. Bombesin-like peptides and cancer. Crit Rev Oncol Hematol. 1996; 23: 225-38.
3. Markwalder R, Reubi JC. Gastrin-releasing peptide receptors in the human prostate: relation to neoplastic transformation. Cancer Res. 1999; 59: 1152-9.
4. Gugger M, Reubi JC. Gastrin-releasing peptide receptors in non-neoplastic and neoplastic human breast. Am J Pathol. 1999; 155: 2067-76.
5. Reubi JC, Korner M, Waser B, Mazzucchelli L, Guillou L. High expression of peptide receptors as a novel target in gastrointestinal stromal tumours. Eur J Nucl Med Mol Imaging. 2004; 31: 803-10.
6. Zhang H, Chen J, Waldherr C, Hinni K, Waser B, Reubi JC, et al. Synthesis and evaluation of bombesin derivatives on the basis of pan-bombesin peptides labeled with indium-111, lutetium-177, and yttrium-90 for targeting bombesin receptor-expressing tumors. Cancer Res. 2004; 64: 6707-15.
7. Schuhmacher J, Zhang H, Doll J, Macke HR, Matys R, Hauser H, et al. GRP Receptor-Targeted PET of a Rat Pancreas Carcinoma Xenograft in Nude Mice with a $^{68}$Ga-Labeled Bombesin(6-14) Analog. J Nucl Med. 2005; 46: 691-9.
8. Moody TW, Mantey SA, Pradhan TK, Schumann M, Nakagawa T, Martinez A, et al. Development of high affinity camptothecin-bombesin conjugates that have targeted cytotoxicity for bombesin receptor-containing tumor cells. J Biol Chem. 2004; 279: 23580-9.
9. Van de Wiele C, Dumont F, Vanden Broecke R, Oosterlinck W, Cocquyt V, Serreyn R, et al. Technetium-99m RP527, a GRP analogue for visualisation of GRP receptor-expressing malignancies: a feasibility study. Eur J Nucl Med. 2000; 27: 1694-9.
10. Van de Wiele C, Dumont F, Dierckx RA, Peers SH, Thornback JR, Slegers G, et al. Biodistribution and dosimetry of $^{99m}$Tc-RP527, a gastrin-releasing peptide (GRP) agonist for the visualization of GRP receptor-expressing malignancies. J Nucl Med. 2001; 42: 1722-7.
11. Rogers BE, Bigott HM, McCarthy DW, Della Manna D, Kim J, Sharp TL, et al. MicroPET imaging of a gastrin-releasing peptide receptor-positive tumor in a mouse model of human prostate cancer using a $^{64}$Cu-labeled bombesin analogue. Bioconjug Chem. 2003; 14: 756-63.
12. Scopinaro F, De Vincentis G, Varvarigou AD, Laurenti C, Iori F, Remediani S, et al. $^{99m}$Tc-bombesin detects prostate cancer and invasion of pelvic lymph nodes. Eur J Nucl Med Mol Imaging. 2003; 30: 1378-82.
13. Smith CJ, Sieckman GL, Owen NK, Hayes DL, Mazuru DG, Kannan R, et al. Radiochemical investigations of gastrin-releasing peptide receptor-specific [$^{99m}$Tc(X)(CO)$_3$-Dpr-Ser-Ser-Ser-Gln-Trp-Ala-Val-Gly-His-Leu-Met-(NH$_2$)] in PC-3, tumor-bearing, rodent models: syntheses, radiolabeling, and in vitro/in vivo studies where Dpr = 2,3-diaminopropionic acid and X = $H_2O$ or P(CH$_2$OH)$_3$. Cancer Res. 2003; 63: 4082-8.
14. Baidoo KE, Lin KS, Zhan Y, Finley P, Scheffel U, Wagner HN, Jr. Design, synthesis, and initial evaluation of high-affinity technetium bombesin analogues. Bioconjug Chem. 1998; 9: 218-25.
15. Gali H, Hoffman TJ, Sieckman GL, Owen NK, Katti KV, Volkert WA. Synthesis, characterization, and labeling with $^{99m}$Tc/$^{188}$Re of peptide conjugates containing a dithia-bisphosphine chelating agent. Bioconjug Chem. 2001; 12: 354-63.

16. Karra SR, Schibli R, Gali H, Katti KV, Hoffman TJ, Higginbotham C, et al. $^{99m}$Tc-labeling and in vivo studies of a bombesin analogue with a novel water-soluble dithiadiphosphine-based bifunctional chelating agent. Bioconjug Chem. 1999; 10: 254-60.
17. La Bella R, Garcia-Garayoa E, Langer M, Blauenstein P, Beck-Sickinger AG, Schubiger PA. In vitro and in vivo evaluation of a $^{99m}$Tc(I)-labeled bombesin analogue for imaging of gastrin releasing peptide receptor-positive tumors. Nucl Med Biol. 2002; 29: 553-60.
18. Lin KS, Luu A, Baidoo KE, Hashemzadeh-Gargari H, Chen MK, Brenneman K, et al. A new high affinity technetium-99m-bombesin analogue with low abdominal accumulation. Bioconjug Chem. 2005; 16: 43-50.
19. Maina T, Nock B, Zhang H, Nikolopoulou A, Reubi JC, Maecke HR. Interspecies differences during comparative evaluation of [$^{111}$In]Z070 and [$^{99m}$Tc]Demobesin 1 in rat or human origin GRP-R-expressing cells and animal models. J Nucl Med. 2005; 46.
20. Nock B, Nikolopoulou A, Chiotellis E, Loudos G, Maintas D, Reubi JC, et al. [$^{99m}$Tc]Demobesin 1, a novel potent bombesin analogue for GRP receptor-targeted tumour imaging. Eur J Nucl Med Mol Imaging. 2003; 30: 247-58.
21. Nock BA, Nikolopoulou A, Galanis A, Cordopatis P, Waser B, Reubi JC, et al. Potent Bombesin-like Peptides for GRP-Receptor Targeting of Tumors with $^{99m}$Tc: A Preclinical Study. J Med Chem. 2005; 48: 100-10.
22. Smith CJ, Gali H, Sieckman GL, Hayes DL, Owen NK, Mazuru DG, et al. Radiochemical investigations of $^{177}$Lu-DOTA-8-Aoc-BBN[7-14]$NH_2$: an in vitro/in vivo assessment of the targeting ability of this new radiopharmaceutical for PC-3 human prostate cancer cells. Nucl Med Biol. 2003; 30: 101-9.
23. Lantry LE, Thomas R, Waser B, Maddalena M, Fox JS, Arunachalam T, et al. Preclinical evaluation of $^{177}$Lu-AMBA, a DOTA conjugate that targets GRP and NMB receptor expressing tumors: internalization, in vivo biodistribution, single dose radiotherapy in PC-3 tumor bearing nude mice and in vitro autoradiography in animal and human tissues. *In:* Annual Congress of the EANM, Helsinki (Finland), 2004, pp. S389.
24. Smith CJ, Gali H, Sieckman GL, Higginbotham C, Volkert WA, Hoffman TJ. Radiochemical investigations of $^{99m}$Tc-$N_3$S-X-BBN[7-14]$NH_2$: an in vitro/in vivo structure-activity relationship study where X = 0-, 3-, 5-, 8-, and 11-carbon tethering moieties. Bioconjug Chem. 2003; 14: 93-102.
25. Hoffman TJ, Gali H, Smith CJ, Sieckman GL, Hayes DL, Owen NK, et al. Novel series of $^{111}$In-labeled bombesin analogs as potential radiopharmaceuticals for specific targeting of gastrin-releasing peptide receptors expressed on human prostate cancer cells. J Nucl Med. 2003; 44: 823-31.
26. Rogers BE, Manna DD, Safavy A. In vitro and in vivo evaluation of a $^{64}$Cu-labeled polyethylene glycol-bombesin conjugate. Cancer Biother Radiopharm. 2004; 19: 25-34.
27. Veronese FM, Pasut G. PEGylation, successful approach to drug delivery. Drug Discov Today. 2005; 10: 1451-8.
28. Seelig A. A general pattern for substrate recognition by P-glycoprotein. Eur J Biochem. 1998; 251: 252-61.
29. Fleischmann A, Laderach U, Friess H, Buechler MW, Reubi JC. Bombesin receptors in distinct tissue compartments of human pancreatic diseases. Lab Invest. 2000; 80: 1807-17.

**Table 1**: Characteristic data of DOTA-**X**-BZH (**X** = **GABA**, **Ahx**, **$PEG_2$**, **$PEG_4$**, **(D)Dab-βAla**, **$(βAla)_2$**, **$Sar_5$**; BZH = [D-Tyr$^6$, βAla$^{11}$, Thi$^{13}$, Nle$^{14}$]BN(6-14)) and relative metallated ligands.

| DOTA-**X**-BZH† | Calculated MW | Measured MW | | |
|---|---|---|---|---|
| | | ESI (+) | ESI (-) | MALDI |
| **GABA** | 1610.83 | 1634.0 $[M+Na]^+$ | 1647.0 $[M+K-H]^-$ | 1610.6 $(M+H]^+$) |
| **Ahx** | 1638.89 | 839.4 $[M+K+H]^{2+}$ | 1677.4 $[M+K-H]^-$ | 1638.7 ($[M+H]^+$) |
| **$PEG_2$** | 1670.89 | 1709.7$[M+K+H]^+$ | 1707.8 $[M+K-H]^-$ | 1670.0 ($[M+H]^+$) |
| **$PEG_4$** | 1773.02 | 1811.7$[M+K+H]^+$ | 1809.7 $[M+K-H]^-$ | 1772.7 ($[M+H]^+$) |
| **(D)Dab-βAla** | 1696.93 | 1736.4 $[M+K]^+$ | 1733.5 $[M+K-H]^-$ | 1696.9 ($[M+H]^+$) |
| **$(βAla)_2$** | 1667.89 | 1707.8$[M+K+H]^+$ | 1706.7 $[M+K-H]^-$ | 1667.3 ($[M+H]^+$) |
| **$Sar_5$** | 1881.12 | 1919.7 $[M+K]^+$ | 1919.2 $[M+K-H]^-$ | 1881.2 ($[M+H]^+$) |
| [$^{nat}$Y]- **GABA** | 1696.72 | 860.0 $[M+Na+H]^{2+}$ | ND | 1696.8 ($[M+H]^+$) |
| [$^{nat}$Ga]- **GABA** | 1677.53 | ND | ND | 1677.6 ($[M+H]^+$) |
| [$^{nat}$Y]- **Ahx** | 1724.77 | 874.6 $[M+Na+H]^{2+}$ | ND | 1725.7 ($[M+H]^+$) |
| [$^{nat}$Y]- **$PEG_2$** | 1756.77 | ND | ND | 1756.8 ($[M+H]^+$) |
| [$^{nat}$Ga]- **$PEG_2$** | 1737.58 | 881.6 $[M+Na+H]^{2+}$ | 867.2 $[M-2H]^{2-}$ | 1737.8 ($[M+H]^+$) |
| [$^{nat}$Y]- **$PEG_4$** | 1858.90 | ND | ND | 1859.8 ($[M+H]^+$) |
| [$^{nat}$Y]- **(D)Dab-βAla** | 1782.81 | 892.4 $[M+2H]^{2+}$ | 1781.5 $[M-H]^-$ | 1782.9 ($[M+H]^+$) |
| [$^{nat}$Y]- **$(βAla)_2$** | 1754.75 | ND | ND | 1755.0 ($[M+H]^+$) |
| [$^{nat}$Y]- **$Sar_5$** | 1967.00 | ND | ND | 1967.9 ($[M+H]^+$) |

Note: MW, molecular weight.

**Table 2**: $IC_{50}$ values for displacement of human GRP-receptor-bound [$^{125}$I-Tyr$^{4}$]BN by increasing concentrations of BN analogues. $IC_{50}$ values (nM ± SE) are in triplicates; number of independent studies is given in brackets. BZH: [Tyr$^{6}$, βAla$^{11}$, Thi$^{13}$, Nle$^{14}$] BN (6-14).

| Compound | GRP-R |
|---|---|
| BZH | 1.0±0.2 (3) |
| [$^{nat}$Y]-DOTA-GABA-BZH | 2.2±0.2 (3) |
| [$^{nat}$Y]-DOTA-Ahx-BZH | 0.8±0.1 (3) |
| [$^{nat}$Y]-DOTA-$PEG_2$-BZH | 2.1±0.8 (3) |
| [$^{nat}$Y]-DOTA-$PEG_4$-BZH | 6.3±1.3 (5) |
| [$^{nat}$Y]-DOTA-$Sar_5$-BZH | 5.7±1.4 (3) |
| [$^{nat}$Y]-DOTA-$βAla_2$-BZH | 2.5±0.4 (3) |
| [$^{nat}$Y]-DOTA-(D)Dab-βAla-BZH | 2.1±0.9 (3) |

**Table 3**: Affinity profiles ($IC_{50}$) for human NMB-R, GRP-R and BRS-3 with displacement of bound [$^{125}$I-Tyr$^{6}$, βAla$^{11}$, Phe$^{13}$, Nle$^{14}$] BN (6-14) by increasing concentrations of BN analogues. $IC_{50}$ values (nM ± SE) are in triplicates; number of independent studies is given in brackets.

| Compound | NMB-R | GRP-R | BRS-3 |
|---|---|---|---|
| [Tyr$^{6}$, βAla$^{11}$, Phe$^{13}$, Nle$^{14}$] BN (6-14) | 1.0±0.1 (5) | 0.7±0.1 (5) | 1.7±0.6 (3) |
| [$^{nat}$Y]-DOTA-GABA-BZH | 4.9±1.0 (3) | 1.4±0.1 (3) | 10.7±4.2 (3) |
| [$^{nat}$Ga]-DOTA-GABA-BZH | 4.7±0.4 (3) | 1.3±0.2 (4) | 6.6±0.6 (4) |
| [$^{nat}$Ga]-DOTA-PEG$_2$-BZH | 6.4±2.2 (4) | 2.0±0.6 (4) | 8.0±0.7 (4) |

**Table 4**: Calculation of the metabolic stability of [$^{111}$In]-DOTA-**X**-BZH (**X** = **GABA**, **Ahx**, **$PEG_2$**, **$PEG_4$**, **(D)Dab-βAla**, **$(\beta Ala)_2$**, **$Sar_5$**; BZH = [D-Tyr$^6$, βAla$^{11}$, Thi$^{13}$, Nle$^{14}$]BN(6-14)) in human serum according to the equation: $A=A_0*\exp(-k_1*t)$.

| **X** | $k_1(h^{-1})$ | $T_{1/2}(h)$ |
|---|---|---|
| **GABA** | 0.316±0.037 | 2.2±0.2 |
| **Ahx** | 0.215±0.024 | 3.2±0.3 |
| **$PEG_2$** | 0.193±0.010 | 3.6±0.2 |
| **$PEG_4$** | 0.106±0.008 | 6.5±0.4 |
| **$\beta Ala_2$** | 0.118±0.006 | 5.8±0.4 |
| **(D)Dab-βAla** | 0.048±0.003 | 14.4±1.0 |
| **$Sar_5$** | 0.021±0.001 | 33.6±1.1 |

**Table 5:** Biodistribution (4h p.i.) and tumor-to-normal tissue ratios of [$^{111}$In]-DOTA-**X**-BZH (**X** = **GABA**, **Ahx**, **PEG$_2$**, **PEG$_4$**, **Sar$_5$**; BZH = [D-Tyr$^6$, βAla$^{11}$, Thi$^{13}$, Nle$^{14}$]BN(6-14)) in AR4-2J tumor-bearing Lewis rats. Results are the mean of groups of three or four animals.

| Site | GABA | Ahx | $PEG_2$ | $PEG_4$ | $Sar_5$ |
|---|---|---|---|---|---|
| Blood | 0.01±0.00 | 0.01±0.00 | 0.01±0.00 | 0.01±0.01 | 0.01±0.00 |
| Kidneys | 1.51±0.66 | 1.03±0.12 | 0.90±0.19 | 0.76±0.18 | 1.13±0.42 |
| Adrenals | 0.07±0.01 | 0.09±0.01 | 0.13±0.01 | 0.23±0.05 | 0.31±0.10 |
| Pancreas | 1.96±0.67 | 4.39±0.45 | 2.69±0.60 | 4.29±0.61 | 3.70±0.49 |
| Spleen | 0.04±0.00 | 0.05±0.02 | 0.05±0.01 | 0.05±0.01 | 0.06±0.01 |
| Muscle | 0.01±0.00 | 0.01±0.00 | 0.01±0.00 | 0.02±0.00 | 0.03±0.01 |
| Stomach | 0.11±0.01 | 0.24±0.04 | 0.11±0.02 | 0.15±0.03 | 0.15±0.02 |
| Bowel | 0.22±0.04 | 0.36±0.14 | 0.18±0.05 | 0.31±0.10 | 0.27±0.08 |
| Liver | 0.07±0.01 | 0.08±0.03 | 0.05±0.01 | 0.07±0.02 | 0.06±0.00 |
| Lung | 0.03±0.01 | 0.05±0.03 | 0.02±0.00 | 0.03±0.01 | 0.03±0.01 |
| Heart | 0.01±0.00 | 0.01±0.00 | 0.01±0.00 | 0.01±0.00 | 0.01±0.00 |
| Bone | 0.01±0.00 | 0.02±0.00 | 0.01±0.00 | 0.02±0.01 | 0.03±0.01 |
| Tumor | 0.82±0.06 | 1.41±0.23 | 1.11±0.31 | 1.55±0.25 | 1.21±0.13 |
| Tumor-to-normal tissue ratio | | | | | |
| Tumor/Blood | 103 | 123 | 213 | 111 | 101 |
| Tumor/Muscle | 103 | 127 | 108 | 75 | 38 |
| Tumor/Liver | 12 | 18 | 22 | 21 | 19 |
| Tumor/Kidney | 0.54 | 1.37 | 1.23 | 2.04 | 1.07 |

**Table 6:** Analysis of secondary structure with circular dichroism. [$^{nat}$Y]-DOTA-**X**-BZH (**X** = **GABA**, **Ahx**, **PEG$_2$**, **PEG$_4$**, **(D)Dab-βAla**, **(βAla)$_2$**, **Sar$_5$**; BZH = [D-Tyr$^6$, βAla$^{11}$, Thi$^{13}$, Nle$^{14}$]BN(6-14)) dissolved in 0.1 M phosphate buffer (pH=7.4); concentration (60 μM) calibrated with UV (280 nm, ε=6890).

| Spacer / % | GABA | Ahx | $PEG_2$ | $PEG_4$ | $βAla_2$ | D-Dab-βAla | $Sar_5$ |
|---|---|---|---|---|---|---|---|
| α-helix | 8.3±0.4 | 6.4±1.3 | 0.0±0.0 | 3.6±0.3 | 21.2±0.7 | 17.0±0.8 | 16.9±1.5 |
| β-sheet | 24.2±1.9 | 24.5±4.0 | 41.7±1.8 | 36.4±1.1 | 0.0±0.0 | 17.4±3.3 | 28.8±4.5 |
| Random coil | 67.6±1.3 | 54.0±2.2 | 57.7±1.7 | 60.1±0.7 | 67.9±1.1 | 65.7±2.2 | 40.8±2.5 |
| β-turn | 0.0±0.0 | 14.1±2.0 | 0.7±1.3 | 0.0±0.0 | 10.8±2.1 | 0.0±0.0 | 13.5±2.2 |

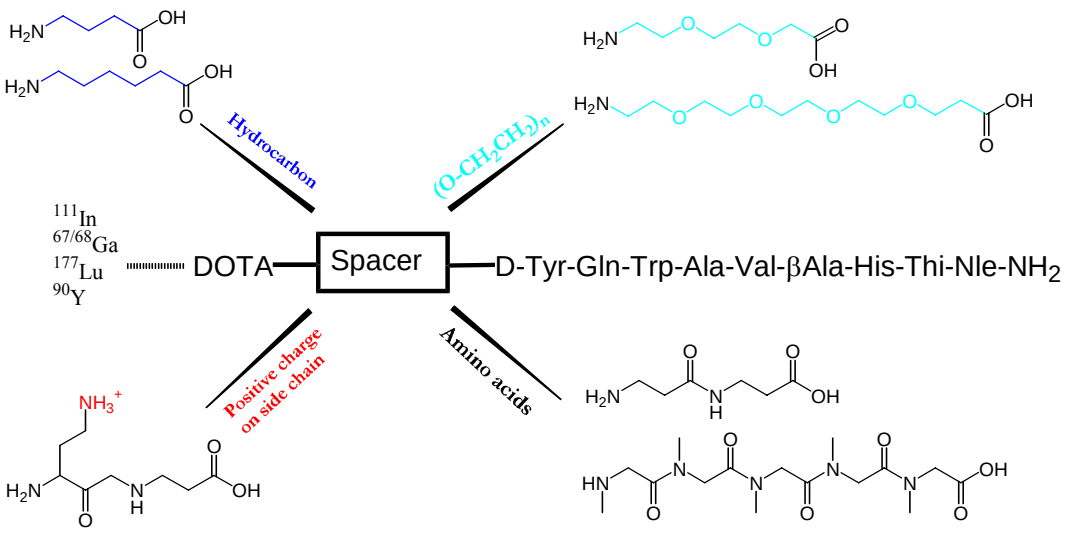


**Figure 1** Formula of spacer-modified pan-bombesin analogs (DOTA-**X**-[D-Tyr$^{6}$, βAla$^{11}$, Thi$^{13}$, Nle$^{14}$]BN(6-14), **X** = **GABA**, **Ahx**, **PEG$_2$**, **PEG$_4$**, **Dab-βAla**, **βAla$_2$ Sar$_5$**)

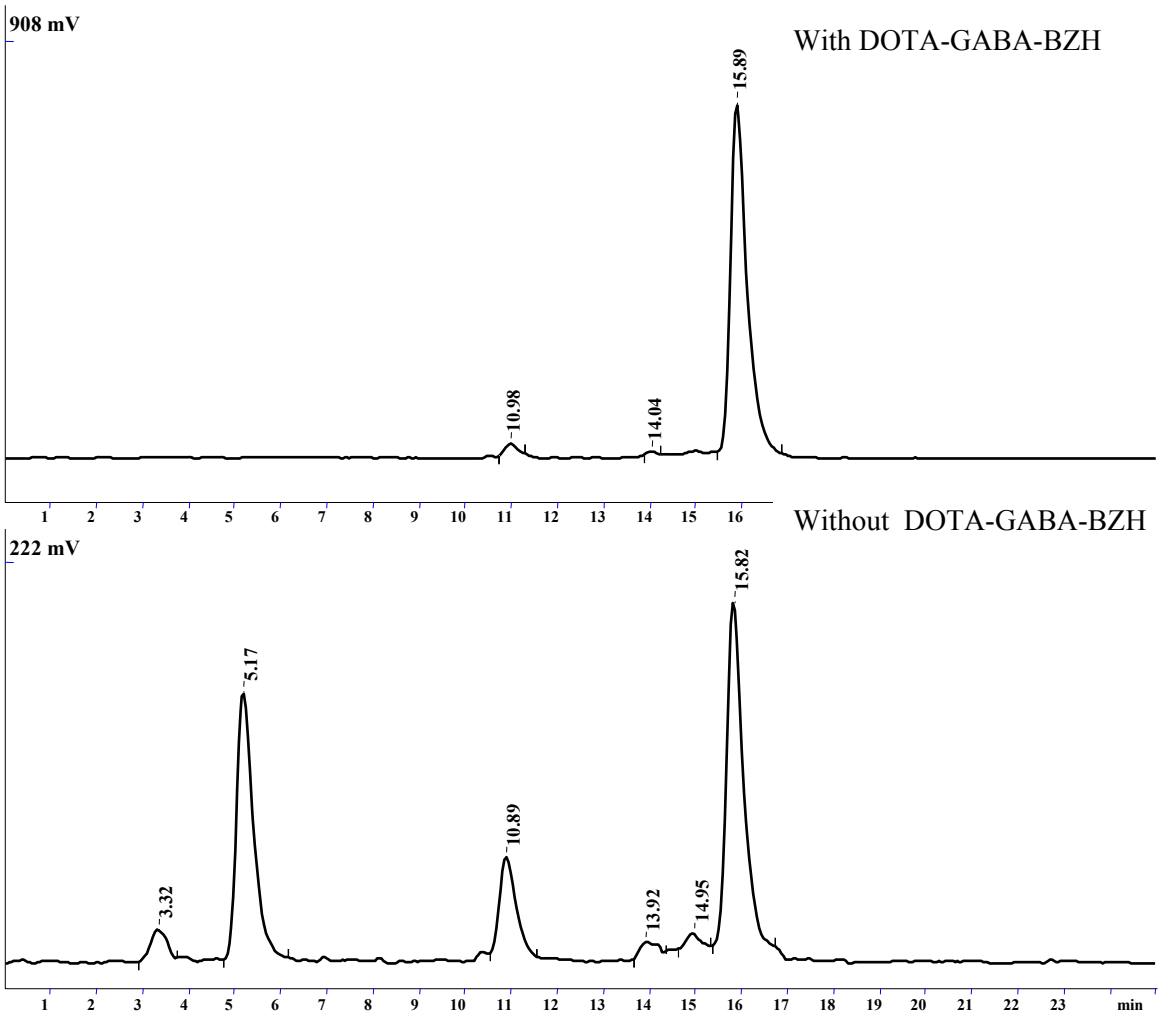


**Figure 2** HPLC elution profile of [$^{111}$In]-DOTA-PEG$_4$-BZH metabolites from culture medium after 2 h incubation with PC-3 cells

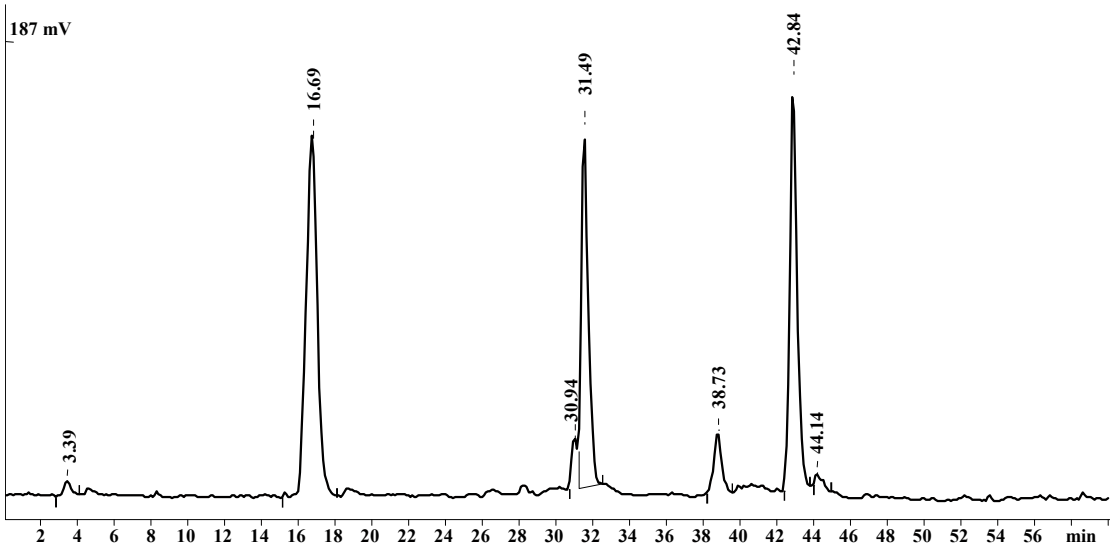


**Figure 3** HPLC elution profile of the co-injection of [$^{111}$In]-DOTA-PEG$_4$-BZH metabolites from PC-3 cells and its metabolites from serum.

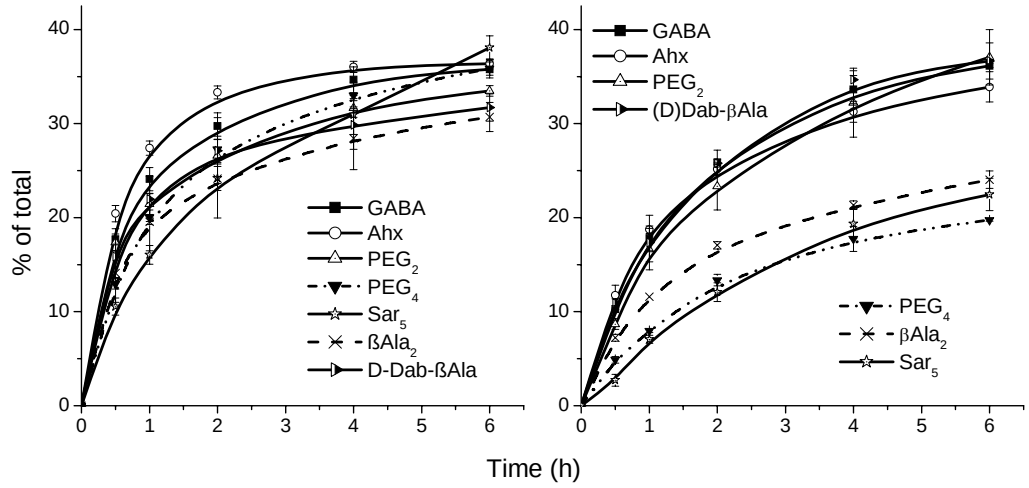


**Figure 4** Internalization rates of [$^{111}$In]-DOTA-**X**-BZH **(X = GABA**, **Ahx**, **PEG$_2$**, **PEG$_4$**, **(D)Dab-βAla**, **(βAla)$_2$**, **Sar$_5$**; BZH = [D-Tyr$^6$, βAla$^{11}$, Thi$^{13}$, Nle$^{14}$]BN(6-14)) into PC-3 (left) and AR4-2J (right) cells. Data result from two independent experiments with triplicates in each experiment and are expressed as specific internalization.

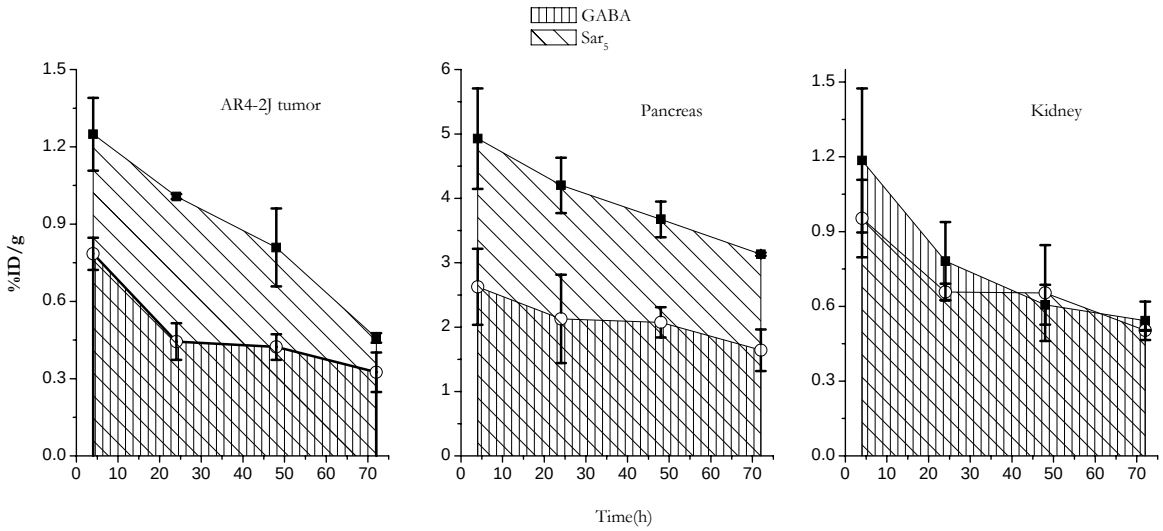


**Figure 5** Retention of [$^{111}$In]-DOTA-GABA-BZH (○) vs [$^{111}$In]-DOTA-Sar$_5$-BZH (■) in AR4-2J tumor-bearing Lewis rats. The uptake is given in percent injected activity per gram at 4h, 24h, 48h and 72h.

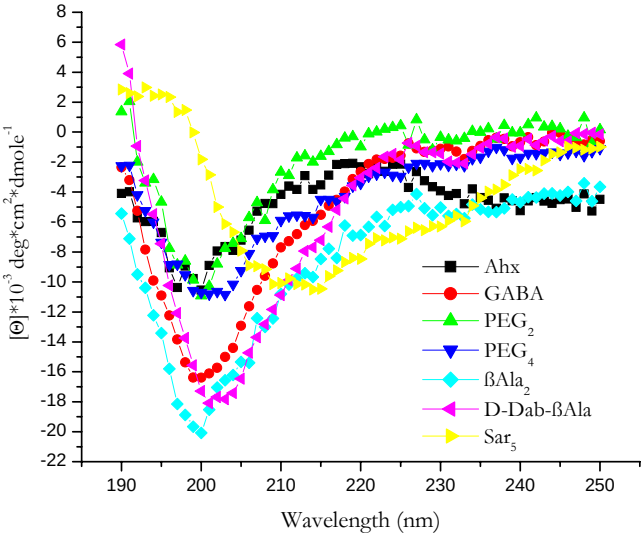


**Figure 6** Circular dichroism spectra of 60 µM [$^{nat}$Y]-DOTA-**X**-BZH (**X** = Ahx, GABA, $PEG_2$, $PEG_4$, $\beta Ala_2$, D-Dab-βAla, and $Sar_5$) in 0.1 M phosphate buffer (pH=7.4); concentration calibrated with UV (280 nm, ε=6890).

*Manuscript 2*

# Synthesis and Evaluation of Modifications at the 11$^{th}$ Position of the Prototype DOTA-GABA-[D-Tyr$^{6}$,X$^{11}$]Bombesin (6-14)

**Hanwen Zhang [a], Schmitt Jörg Simon [a], Beatrice Waser [b], Jean Claude Reubi [b], Martin Walter [a], Helmut R. Maecke [a]**

[a] Division of Radiological Chemistry, Institute of Nuclear Medicine, Department of Radiology, University Hospital, Basel, Switzerland;
[b] Division of Cell Biology and Experimental Cancer Research, Institute of Pathology, University of Berne, Berne, Switzerland

Present status:
Manuscript in preparation.

# Synthesis and Evaluation of Modifications at the 11$^{th}$ Position of the Prototype DOTA-GABA-[D-Tyr$^{6}$]Bombesin (6-14)

Hanwen Zhang [a], Jörg Simon Schmitt [a], Martin Alexander Walter [a], Beatrice Waser [b], Jean Claude Reubi [b], Helmut R. Maecke*[a]

[a] Division of Radiological Chemistry, Department of Radiology, University Hospital Basel, Petersgraben 4, CH-4031 Basel, Switzerland;
[b] Division of Cell Biology and Experimental Cancer Research, Institute of Pathology, University of Berne, PO Box 62, Murtenstrasse 31, CH-3010 Bern, Switzerland

* To whom correspondence should be addressed:
Tel: ++41 61 265 46 99; Fax: ++41 61 265 55 59
E-mail: hmaecke@uhbs.ch

**ABSTRACT**

Radiolabeled bombesin (BN) analogues have shown a promising potential for targeting GRP-receptors, which are overexpressed in a variety of human cancers. It has been indicated that the peptide bond between the $11^{th}$ and the $12^{th}$ position of BN might have an influence on the metabolic stability and subtype selectivity. On that account we substituted glycine at the $11^{th}$ position of DOTA-GABA-[D-$Tyr^{6}$,$X^{11}$] BN (6-14) (X = Gly) with three unnatural amino acids (X = Agly, βAla, and D-Ala), and investigated the influence on the biological properties of the derivatives.

All conjugates were synthesized with yields between 29% and 36%, based on the removal of the first Fmoc group, and labeled with $^{111}$In in high yields (≥37GBq μmol$^{-1}$). The [$In^{III}$]-labeled peptides showed high affinity to the mouse GRP receptor (0.5 – 5.8 nM) and mediate affinity to the human GRP receptor (11.5 – 96 nM). The metabolic stability ($t_{1/2}$) of the radiolabeled peptides in fresh human serum varied from 2.9±0.5 h ($Gly^{11}$) to 14.1±1.5 h ($Agly^{11}$). The radiolabeled peptides internalized faster into PC-3 cells (human receptor) than into AR4-2J cells (rat receptor). For [$^{111}$In]-DOTA-GABA-[D-$Tyr^{6}$, $Agly^{11}$] BN (6-14), the internalization rate into these two cell lines differed only to 3% (6 h incubation), whereas for [$^{111}$In]-DOTA-GABA-[D-$Tyr^{6}$, D-$Ala^{11}$] BN (6-14), it differed to 13.7% which was the highest difference found among the four ligands. The efflux of the radiotracers from PC-3 cells after 2 h of internalization (8 h incubation: 46.1-55.8 %, P=0.98) was similar, with the exception of the D-Ala analogue (P = 0.04). The biodistribution studies showed a specifically higher uptake in the AR4-2J tumor than in the PC-3 tumor, which correlated with the binding affinity and metabolic stability values of the conjugates.

Our results demonstrate that the $11^{th}$ position of BN analogues is crucial in regards to metabolic stability and binding affinity to GRP receptors in different species.

INTRODUCTION

A wide variety of peptides show high affinity for certain receptors that are overexpressed on a large number of human tumors [1, 2]. This finding has led to an exponential growth in the development of radiolabeled peptides for diagnostic and therapeutic application in oncology [3]. Among these radiopeptides, somatostatin analogs have shown the most promising results [4, 5] with [$^{111}$In-DTPA]octreotide (OctreoScan®) being the first FDA-approved radiopharmacon. On the other hand, bombesin (BN) analogues have become increasingly important, as gastrin-releasing peptide (GRP) receptors (the mammalian counterpart of BN receptors) were found to be highly overexpressed in prostate cancer [6] , breast tumors [7] and gastrointestinal stromal tumors (GIST) [8]. Especially, primary invasive prostatic carcinoma turned out to be GRP receptor-positive tumors in 30 tested cases; in 83% of these cases, GRP receptor-expression was found to be high or very high (>1000 dpm/mg). Interestingly, 25 of 26 (96%) patients with high-grade prostatic intraepithelial neoplasia also showed high to very high densities of GRP receptors, which provides the opportunity of diagnosis and treatment at an early stage of the disease. In addition, 4 of 7 (57%) androgen-independent prostate cancer bone metastases were GRP receptor-positive [6]. These results show that the GRP receptor is a promising target for receptor-regulated imaging and treatment. Up to now, most radiolabeled BN analogues have been designed for targeting GRP receptors [9-17] and many ligands were designed by conjugating bifunctional chelates to BN (7-14) analogues [9, 11, 14-17]. In this respect, it has been indicated that aromatic amino acids including D-Tyr or D-Phe placed at the 6$^{th}$ position might lead to a sustained high affinity [18-21].

Mantey et al [18, 22, 23] developed BRS-3 selective ligands by substituting β-alanine$^{11}$ (βAla$^{11}$) with conformationally restricted amino acids in the prototypical universal ligand ([D-Tyr$^{6}$, βAla$^{11}$, Phe$^{13}$, Nle$^{14}$] BN (6–14)). By modifying the side chain of βAla$^{11}$ they achieved high affinity to the human bombesin receptor subtype-3 (hBRS-3), but only low affinity to the human GRP receptor and the human neuromedin B receptor (hNMB-R). We have demonstrated that carnosinase is responsible for cleaving the peptide bond between βAla$^{11}$ and His$^{12}$ in [$^{111}$In]-DTPA-GABA-[D-Tyr$^{6}$, βAla$^{11}$, Thi$^{13}$, Nle$^{14}$] BN (6–14) [24]. These data indicate that a modification on βAla$^{11}$ may change the peptide conformation, and subsequently the binding affinity as well as the serum stability. Furthermore, since carnosinase is a non-specific dipeptidase known to cleave AA-His (AA: amino acid) [25], we assumed that the peptide bond (Gly$^{11}$-His$^{12}$) in BN was also decomposed by carnosinase.

Therefore, we designed and synthesized DOTA-GABA-[D-Tyr$^{6}$, **X**$^{11}$] BN (6-14) (**X** = Gly, βAla, D-Ala, and Agly) to study the influence of the different substitutes on binding affinity, metabolic

stability, internalization and efflux (externalization) as well as on biodistribution in tumor-bearing nude mice.

## RESULTS

### Synthesis and radiolabeling

DOTA-GABA-[D-Tyr$^6$, **X**$^{11}$] BN (6-14) (**X** = Gly, D-Ala, β-Ala, and Agly) were synthesized on a Rink amide MBHA resin in parallel by standard Fmoc solid phase peptide synthesis, as shown in Fig 1. Fmoc-Agly (5-((9H-fluoren-9-yl)methoxy)-1,3,4-oxadiazol-2(3H)-one) was prepared following the reported procedure [26, 27] and coupled to a $NH_2$-His(Trt)-Leu-Met-Rink amide MBHA resin via incubation for 40 min without any activating agent and base since Fmoc-Agly is a very active intermediate agent. After cleavage from the resin, purification and lyophilization, the final products (white powder) were obtained with an overall yield of 29% to 36%, based on the removal of the first Fmoc group, and characterized (Table 1) by MS and analytic HPLC. The purity of all conjugates was ≥97% (HPLC purity).

All DOTA-GABA-[D-Tyr$^6$, **X**$^{11}$] BN (6-14) analogues were successfully labeled with $^{111}$In using an ammonium acetate buffer (pH 5, 0.4 M) at elevated temperature (95°C, 20-25 min). In all cases $^{111}$In-labeling yields of ≥98% at a specific activity >37 GBq μmol$^{-1}$ were achieved.

### Binding affinity to GRP receptor

Using [$^{125}$I-Tyr$^4$] BN as competitive ligand, the binding affinities of all conjugates to GRP receptors in human cancer and mouse pancreas tissue were measured (Table 2). The $IC_{50}$ values towards the hGRP receptor were 11.5±2.6nM, 12.6±3.5nM, 41±12nM, and 96±13nM for [In$^{III}$]-**I**, **II**, **III,** and **IV,** respectively **(I,** DOTA-GABA-[D-Tyr$^6$]BN(6-14); **II,** DOTA-GABA-[D-Tyr$^6$, β-Ala$^{11}$]BN(6-14)**; III,** DOTA-GABA-[D-Tyr$^6$, D-Ala$^{11}$]BN(6-14); **IV,** DOTA-GABA-[D-Tyr$^6$, Agly$^{11}$]BN(6-14)); towards the mouse GRP receptor they were 1.2±0.5nM, 0.5±0.2nM, 5.8±2.2nM, and 1.0±0.5nM.

### Metabolic stability in human serum

As shown in Table 3, the half-lives ($t_{1/2}$) of [$^{111}$In]-**I**, **II**, **III,** and **IV** were 2.9±0.5, 7.8±1.1, 6.3±0.5, and 14.1±1.5 h, respectively. After 8 h incubation in fresh serum under the condition of 37°C and 5%$CO_2$, the radioactivity bound to the proteic fraction was <5% of the added total.

**Internalization and Externalization**

Figure 2 illustrates the specific internalization of $^{111}$In-labeled ligands into PC-3 cells (A) and AR4-2J cells (B). In both cell lines a time-dependent internalization of all four radiotracers was found, which could be blocked by DOTA-GABA-[D-Tyr$^{6}$, βAla$^{11}$, Thi$^{13}$, Nle$^{14}$] BN (6-14). In PC-3 cells, [$^{111}$In]-**IV** (Agly) showed a slower internalization rate (31.3±3.0% at 6 h) than the other three radiotracers (at 6 h, D-Ala: 38.4±1.7%, Gly: 39.8±1.5%, and βAla: 41.5±1.5%; P = 0.04). In AR4-2J cells a different tendency was observed (D-Ala: 24.7±0.5, Agly: 28.3±1.7%, Gly: 33.4±0.1%, and βAla: 34.5±1.2% at 6 h incubation). The surface-bound peptide (acid removable) was <7% of the added activity (data not shown).

Externalization rates of the radiotracers from PC-3 cells are shown in Fig. 3. All ligands were released from PC-3 cells with a similar rate (P = 0.98) with the exception of [$^{111}$In]-**III** which showed a relatively faster washout (P = 0.04).

**Animal biodistribution studies**

Biodistribution studies of the $^{111}$In-labeled peptides were performed in Lewis rats bearing an AR4-2J tumor and athymic nu/nu mice bearing a PC-3 tumor. Results are presented in Tables 4 and 5 as percentage of injected activity per gram of tissue (% IA/g).

In Lewis rats without tumors (Table 4), all $^{111}$In-labeled ligands displayed a rapid clearance from blood with 0.01% IA/g at 4 h and from GRP-R-negative tissues except from the kidneys which accumulated 0.85±0.08 %IA/g of [$^{111}$In]-**I** (Gly), 1.31±0.08 %IA/g of [$^{111}$In]-**II** (βAla), 0.79±0.17 %IA/g of [$^{111}$In]-**III** (D-Ala), and 1.36±0.16 %IA/g of [$^{111}$In]-**IV** (Agly), respectively. All derivatives showed high uptake in GRP-R-positive organs; for instance, the pancreas uptake was 4.03±0.31% IA/g for [$^{111}$In]-**I** (Gly), 6.41±0.56 %IA/g for [$^{111}$In]-**II** (βAla), 2.71±0.07 %IA/g for [$^{111}$In]-**III** (D-Ala), and 6.04±0.38 %IA/g for [$^{111}$In]-**IV** (Agly), respectively.

The biodistribution in athymic nude mice bearing AR4-2J and PC-3 tumors was similar to the one in rats (Tables 4 and 5) showing a rapid clearance from background and non-target organs and a high uptake in GRP receptor-expressing organs, including pancreas, stomach, bowel, and adrenals. The uptake in the AR4-2J tumor was also high ([$^{111}$In]-**I** (Gly): 12.22±3.95%IA/g, [$^{111}$In]-**II** (βAla): 17.56±1.51%IA/g, [$^{111}$In]-**III** (D-Ala): 7.70±1.12%IA/g, [$^{111}$In]-**IV** (Agly): 14.11±1.99%IA/g), whereas the PC-3 tumor uptake was rather poor ([$^{111}$In]-**I** (Gly): 2.36±0.70%IA/g, [$^{111}$In]-**II** (βAla): 2.56±0.42%IA/g, [$^{111}$In]-**III** (D-Ala): 1.62±0.52%IA/g, [$^{111}$In]-**IV** (Agly): 2.15±0.22%IA/g). *In vivo* competition experiments using 50 μg DOTA-GABA-[D-Tyr$^{6}$, βAla$^{11}$, Thi$^{13}$, Nle$^{14}$] BN (6–14) (BZH2) co-injected with $^{111}$In-labeled conjugates resulted in an >90% uptake reduction in the pancreas and both types of tumors (data

not shown). The injection of the blocking dose, however, had no significant influence on the uptake in non-target organs except the kidneys.

## DISCUSSION

GRP receptors have already been of considerable interest for the diagnosis and therapy of GRP receptor-expressing tumors, which has attracted many research groups to develop radiolabeled BN-based ligands [9, 28]. The 11$^{th}$ position of BN analogues seems to be an important site to modify the subtype selectivity [18, 22, 23] and metabolic stability in serum [24]. In this study, we have designed three DOTA-based peptides and evaluated the influence of modifications at the 11$^{th}$ position of the prototype [$^{111}$In]-DOTA-GABA-[D-Tyr$^{6}$] BN (6-14) on chemical and pharmacologic properties.

The study of the metabolic stability of [$^{111}$In]-DOTA-GABA-[D-Tyr$^{6}$, **X**$^{11}$] BN (6-14) (**X** = Gly, βAla, D-Ala and Agly) in fresh human serum showed the bond between His$^{12}$ and **X**$^{11}$ to be a weak site, which is consistent with the fact that the weakest peptide bond in the prototype DOTA-GABA-[D-Tyr$^{6}$, βAla$^{11}$, Thi$^{13}$, Nle$^{14}$] BN (6-14) is (βAla$^{11}$-His$^{12}$) [24]. Although many *in vivo* peptidases are responsible for hydrolyzing BN at other sites [24, 29, 30], BN can still partially be stabilized by replacing the natural amino acid (Gly$^{11}$) with unnatural amino acids. Especially, the substitution of Gly$^{11}$ by Agly (–$CH_2$– versus –NH–) led to an increased stability by a factor of 4.9 whereas the half-life of [$^{111}$In]-DOTA-GABA-[D-Tyr$^{6}$, βAla(D-Ala)$^{11}$] BN (6-14) was twice as high as that of [$^{111}$In]-DOTA-GABA-[D-Tyr$^{6}$] BN (6-14).

By using [$^{125}$I-Tyr$^{4}$] BN as GRP receptor-preferring radioligand, the affinity of metallated ligands to human GRP receptors was observed to be lower than the affinity of corresponding ligands to mouse GRP receptors. [In$^{III}$]-DOTA-GABA-[D-Tyr$^{6}$, Agly$^{11}$] BN (6-14) showed the biggest difference in affinity to human and mouse GRP receptors ($IC_{50}$ values: 96±13nM vs. 1.0±0.5nM; 96-fold) whereas the difference for the βAla, Gly and D-Ala derivatives were only 25, 9.6, and 7.1-fold, respectively.

It is known that a slight variation (<10%) of GRP receptors among different species results in significantly different biological properties [31]. Recently, we and other groups also reported on a species sensitivity to some radiolabeled BN analogs [32]. In this study we found that the Agly$^{11}$ analog has the highest sensitivity towards GRP receptors of different species. Our results indicate that the 11$^{th}$ position is an important site with regard to the affinity to human GRP receptors, whereas its effect on the affinity to mouse GRP receptors is negligible.

All $^{111}$In-labeled peptides **I-IV** were rapidly internalized by PC-3 and AR4-2J cells, which is consistent with the expected agonistic behavior of these radiotracers against the GRP receptor. The comparison of the internalization kinetics of every ligand into the two cell lines showed a minimal difference for [$^{111}$In]-DOTA-GABA-[D-Tyr$^{6}$, Agly$^{11}$] BN (6-14) although it had the highest difference in binding affinity to the GRP receptor; conversely, [$^{111}$In]-DOTA-GABA-[D-Tyr$^{6}$, D-Ala$^{11}$] BN (6-14) with its minimal difference in affinity displayed the highest difference in internalization rates. It was observed that [$^{111}$In]-DOTA-GABA-[D-Tyr$^{6}$, D-Ala$^{11}$] BN (6-14) was released from PC-3 cells with a faster rate than the other three ligands.

The *in vitro* experiments mentioned above together with published data [22, 23] indicate that a modification at the 11$^{th}$ position may influence not only the selectivity of BN receptor subtypes but also the metabolic stability in serum and the receptor affinity in different species. Therefore, it was very interesting to probe how such a modification affects the individual *in vivo* biodistribution. The biodistribution in normal rats showed a higher accumulation of the βAla and Agly derivatives in the pancreas and the kidneys than of the Gly and D-Ala analogs. As a high accumulation correlates with a high specific receptor affinity of the ligands, the high kidney uptake may be explained with an overexpression of the receptor in the rat kidney. To evaluate the influence of the species directly, rat (AR4-2J) and human (PC-3) tumors were inoculated in each flank of a mouse. The uptake of all radiotracers in the PC-3 tumor was significantly lower than in the AR4-2J tumor, which is consistent with their relative binding affinities. Although the βAla and D-Ala derivatives show a similar metabolic stability in serum, their uptake ratios differed, being 3.5 in the pancreas, 2.3 in the AR4-2J tumor (rat) and 1.6 in the PC-3 tumor (human), due to the higher binding affinity of βAla to the GRP receptor (human and mouse). [$^{111}$In]-DOTA-GABA-[D-Tyr$^{6}$, Agly$^{11}$] BN (6-14) and [$^{111}$In]-DOTA-GABA-[D-Tyr$^{6}$] BN (6-14) showed a similar accumulation in the pancreas, AR4-2J tumor and PC-3 tumor even though the latter showed a significantly worse affinity to the human GRP receptor, probably due to its higher stability in serum.

**Conclusion**

The combined experimental data indicate that the 11$^{th}$ position is important with regard to metabolic stability in serum, binding affinity to the GRP receptor, and accumulation in targeted organs which is determined by binding affinity and stability concomitantly. However, there is considerable variation between different species, which has to be taken into account in the design of successful BN analogues for clinical trials.

EXPERIMENTAL SECTION

**General**

Abbreviations: BN, bombesin; GRP, gastrin-releasing peptide; **I**, DOTA-GABA-[D-Tyr$^6$] BN (6-14); **II**, DOTA-GABA-[D-Tyr$^6$, βAla$^{11}$] BN (6-14); **III**, DOTA-GABA-[D-Tyr$^6$, D-Ala$^{11}$] BN (6-14); **IV**, DOTA-GABA-[D-Tyr$^6$, Agly$^{11}$] BN (6-14); GABA, γ-aminobutyric acid; Agly, azaglycine; DOTA, 1,4,7,10-tetraazacyclododecane-1, 4,7,10-tetraacetic acid; NMP, 1-methyl-2-pyrrolidone; TFA, trifluoroacetic acid. Abbreviations of the common amino acids are in accordance with the recommendations of IUPAC-IUB [IUPAC-IUB Commission of Biochemical Nomenclature (CBN), symbols for amino acid derivatives and peptides, recommendations 1971. Eur J Biochem 1972; 27:201-207].

All chemicals were obtained from commercial sources and used without further purification. Rink amide MBHA resin (0.6mmol/g) and all Fmoc-protected amino acids were commercially available from NovaBiochem (Läufelfingen, Switzerland). DOTA-tris(tBu ester) was purchased from Macrocyclics (Dallas, Texas). Fmoc-hydrazine was prepared according to the published protocol [33]. 5-((9H-fluoren-9-yl)methoxy)-1,3,4-oxadiazol-2(3H)-one (Fmoc-Agly) was synthesized using the reported procedure [26, 27]. [$^{111}$In]$Cl_3$ was purchased from Mallinckrodt Medical (Petten, the Netherlands). PC-3 cells were purchased from the European Collection of Cell Cultures (ECACC, Wiltshire SP4 OJG, UK). Male Lewis rats and female athymic nu/nu nude mice were obtained from Harlan (Horst, the Netherlands). The cell culture medium was Dulbecco's minimal essential medium (DMEM) with vitamins, essential and non-essential amino acids, L-glutamine, antibiotics (penicillin/streptomycine), fungicide (amphotericin B/Fungizone®) and 10% or 1% fetal calf serum (FCS) from Bioconcept (Allschwil, Switzerland). Solid phase peptide synthesis was performed on a semiautomatic peptide synthesizer commercially available from Rink Combichem (Bubendorf, Switzerland). Electrospray ionization mass spectroscopy (ESI-MS) was carried out with a Finnigan SSQ 7000 spectrometer (Brennen, Germany) and matrix-assisted laser desorption ionization (MALDI)-mass spectrometry measurements on a Voyager sSTR equipment with a Nd:YAG laser (Applied Biosystems, Framingham, USA). Analytical HPLC was performed on a Hewlett Packard 1050 HPLC system (Waldbronn 2, Germany) with a multiwavelength detector and a flow-through Berthold LB 506 Cl γ-detector (Wildbad, Germany) using a Macherey-Nagel (Oensingen, Switzerland) Nucleosil 120 $C_{18}$ column (**System 1**: flow: 0.75 ml/min; eluents: A= 0.1% TFA in water and B= acetonitrile; non-linear gradient: 0 min, 80% A; 20 min, 50% A; 21 min, 0% A; 24

min, 0% A and 25 min, 80% A. **System 2**: flow: 0.75 ml/min; eluents: A= 50 mM sodium acetate buffer (pH 5.4) and B= acetonitrile; the non-linear gradient is the same as in **system 1**). Preparative HPLC was performed on a Metrohm HPLC system LC-CaDI 22-14 (Herisau, Switzerland) with a Macherey-Nagel VP 250/21 Nucleosil 100-5 $C_{18}$ column (flow: 15 ml/min; eluents: A= 0.1% TFA in water and B= acetonitrile; non-linear gradient: 0 min, 70% A; 10 min, 50% A; 11 min, 0% A; 14 min, 0% A and 15 min, 70% A). Quantitative γ-counting was performed on a COBRA 5003 γ-system well counter from Packard Instruments (Meriden, CT, USA).

The concentrations of all tested compounds were determined (280 nm, ε=6890) with a Lambda 2 UV-visible spectrophotometer (Perkin-Elmer & Co GmbH, Bodenseewerk, Germany). The HPLC purity of all compounds used for experiments was >99%.

**Synthesis**

The conjugates were synthesized (Fig. 1) in parallel according to a procedure described previously [24]. Briefly, the peptide synthesis was performed on a semiautomatic peptide synthesizer according to standard Fmoc chemistry; Trt, tBu and Boc were used as protecting groups of His, D-Tyr, and Trp, respectively. Fmoc-protected amino acids were assembled according to the peptide sequence on a Rink amide MBHA resin (20 μmol based on the removed amount of Fmoc for each conjugate) except Fmoc-Agly. Fmoc-Agly (500 μmol) in anhydrous $CH_2Cl_2$ (3mL) was added to 20 μmol $NH_2$-His(Trt)-Leu-Met-Rink amide MBHA resin, then the reaction mixture was shaken slightly at room temperature for 40 min, washed with NMP and isopropanol and dried in a vacuum oven. Few beads were cleaved by TFA/thioanisole/water (92/6/2) to be analyzed with MS (calculated MW: 678.8, found: 679.8, $[M+H]^+$, 791.8 $[M+CF_3COO]^-$).

After loading all amino acids and the protected DOTA, the peptide-chelated conjugates were cleaved from the resin and simultaneously deprotected by incubation with TFA/thioanisole/ water (92/6/2) for 4-6 h at room temperature and then precipitated in cold diisopropyl ether/petroleum ether (1:1). After drying in the vacuum oven at room temperature, the crude peptide-chelated conjugate was purified by preparative HPLC. MS ((±)EI, MALDI) and analytical HPLC were used to determine the composition and purity of the conjugates.

**Metallated conjugates**

The metal complex was synthesized according to methods previously described [24]. Briefly, a mixture of conjugate (0.5 μmol) in 500 μL 0.4 M ammonium acetate buffer (pH 5) was

incubated with 1.5 μmol $InCl_3 \cdot 5H_2O$ pre-dissolved in 0.04 M HCl at 95°C for 25 min, cooled to room temperature and purified over a SepPak $C_{18}$ cartridge (Waters Corp. Milford, MA) preconditioned with 10 ml ethanol and 10 ml water. The cartridge was eluted with 10 ml water followed by 3 ml ethanol resulting in $In^{III}$-conjugates after evaporation of the ethanol. The final product was analyzed by analytical HPLC (purities were ≥99%) and identified by MALDI.

**Preparation of radiotracer**

The [$^{111}$In]-conjugate was prepared by dissolving 10 μg in ammonium acetate buffer (300 μl, 0.4 M, pH 5). After the addition of $^{111}InCl_3$ (3-5 mCi), the solution was heated at 95° for 25 min. A 1.5 molar excess of cold $InCl_3$ was added and the final solution heated again at 95°C for 25 min. Subsequently, the radiolabeled peptides were purified utilizing a SepPak $C_{18}$ cartridge preconditioned with 10 ml ethanol and 10 ml water. The cartridge was eluted with 3 ml water, followed by 3 ml ethanol, to afford the pure radiolabeled ligands for the internalization experiment. A quality control was performed by HPLC. Biodistribution studies were prepared using the same method as above but without addition of cold metal and diluted in 0.9% NaCl (0.1% BSA) to afford the radioligand solution.

**Internalization and efflux studies**

Internalization and externalization experiments were performed in 6-well plates as described previously [24]. The procedure was the same for both cell lines. Briefly, approximately 1.8 kBq (0.25 pmol) of the radioligand was studied in PC-3 and AR4-2J cells (0.5 to $1\times10^6$ cells per well) at 0.5 h, 1 h, 2 h, 4 h and 6 h incubation. To determine nonspecific internalization, BZH2 (150 μl of a 5.8 μM solution) was involved. The percentage of added activity per million cells (% of total) was calculated for the internalization rate at each time point.
For externalization studies, PC-3 cells were allowed to internalize the radioligands for periods of 2 h and were then exposed to an acid wash for dissociating the cell surface-bound radioligand. One ml of culture medium was added to each well, the cells were incubated at 37°C in a 5 % $CO_2$ environment and the externalization rates of the cell-incorporated radioactivity were studied at different time points. The culture medium was collected and measured for radioactivity. The percentage of totally internalized radiotracer was calculated for efflux.

**Metabolic stability in serum**

To 1 ml of freshly prepared human serum, previously equilibrated in a 5% $CO_2$ (95% air) environment at 37°C, 0.6 nmol $^{111}$In-labeled conjugates were added. The mixture was incubated in a 5% $CO_2$, 37°C environment. At different time points (0, 1, 4, and 8 h), 50 μl aliquots (in

triplicates) were removed and treated with 60 µl ethanol. Samples were then cooled (4°C) to precipitate serum proteins and centrifuged for 15 min at 500 g. Fifty µl of the supernatant were removed for activity counting in a γ-well counter, the sediment was washed twice with 1 ml of ethanol and counted; the activity in the supernatant was compared with the activity in the pellet to give the percentage of peptides not bound to proteins or radiometal transferred to serum proteins; the supernatant was also analyzed with HPLC (**system 1**). The data points were used for calculating the half-life ($t_{1/2}$) of the disappearance of intact peptide as described in a previous publication [24].

**Binding affinity to GRP receptor**

Using [$^{125}$I-D-Tyr$^{4}$] BN as GRP receptor-preferring ligand, competition binding experiments were performed with $In^{III}$-labeled conjugates in human tumors expressing GRP receptors or mouse pancreas expressing mouse GRP receptors, as described in detail previously [34].

**Biodistribution experiments in Lewis rats**

Male Lewis rats (160-200 g) were injected in the back leg vein with 0.1 µg radiolabeled peptides, diluted in NaCl (0.1% BSA, pH 7.4, total injected volume = 200 µl). Rats (in groups of 4) were sacrificed at 4 h, organs of interest collected, rinsed of excess blood, blotted, weighed and counted in a γ-counter. The percentage of injected activity per gram (% IA/g) was calculated for each tissue. The total counts injected per animal were determined by extrapolation from counts of an aliquot taken from the injected solution as a standard.

**Biodistribution experiments in AR4-2J and PC-3 tumor-bearing athymic nu/nu mice**

Biodistribution studies of the $^{111}$In-labeled conjugates were additionally performed in nude mice bearing PC-3 and AR4-2J tumors on their flanks. Female athymic nu/nu mice of 4-5 weeks of age were used for the experiments. Animals were inoculated with a 100 µl suspension of $10^7$ PC-3 cells in PBS buffer in the left flank and a 100 µl suspension of $10^7$ AR4-2J cells in PBS buffer in the right flank. Seven to 14 days later the tumors in both inoculation sites had grown to palpability and were ready for biodistribution studies. Each mouse received 100 µl, 5 µCi $^{111}$In-labeled conjugates (corresponding to 10 pmol peptide per mouse) in PBS through the lateral tail vein. After a slight isoflurane anesthesia, the animals were sacrificed with $CO_2$ gas in groups of four at 4 h post injection. Blood and interesting tissue samples were collected and weighed and the radioactivity was measured in a γ–counter. Tissue distribution data were calculated as percent injected activity per gram of tissue (%IA/g).

All animal experiments were performed in compliance with the Swiss regulations for animal treatment (Bundesamt für Veterinärwesen, approval no. 789).

**Statistical Analysis**

Data are expressed as mean ± SD, calculated on Microsoft Excel. The Student t test (Origin 6, Microcal Software, Inc., Northampton, MA) was used to determine statistical significance at the 95% confidence level with $P < 0.05$ being considered significantly different.

ACKNOWLEDGEMENTS

We thank the Swiss National Science Foundation for financial support (grant No. 3100A0-100390) and Novartis for analytical support.

**Table 1**: Characteristics of compounds **I**, **II**, **III,** and **IV** and of their relative cold metallated compounds.

| Compound† | Calculated MW | Measured MW | | | Retention time‡ (min) | |
|---|---|---|---|---|---|---|
| | | ESI (+) | ESI (-) | MALDI | **System 1** | **System 2** |
| **I** | 1574.80 | 1597.7 ($[M+Na]^+$) | 1611.4 ($[M+K-H]^-$) | 1574.5 ($[M+H]^+$) | 13.05 | 16.01 |
| **II** | 1588.83 | 1627.4 ($[M+K]^+$) | 1625.5 ($[M+K-H]^-$) | 1588.7 ($[M+H]^+$) | 12.32 | 15.54 |
| **III** | 1588.83 | 1627.7 ($[M+K]^+$) | 1625.7 ($[M+K-H]^-$) | 1588.6 ($[M+H]^+$) | 13.45 | 16.36 |
| **IV** | 1575.79 | 1614.3 ($[M+K]^+$) | 1612.5 ($[M+K-H]^-$) | 1575.8 ($[M+H]^+$) | 12.16 | 15.37 |
| $[In^{III}]$-**I** | 1686.60 | ND | ND | 1686.5 $[M+H]^+$ | 14.30 | 17.30 |
| $[In^{III}]$-**II** | 1700.62 | ND | ND | 1700.5 $[M+H]^+$ | 13.65 | 16.51 |
| $[In^{III}]$-**III** | 1700.62 | ND | ND | 1700.3 $[M+H]^+$ | 14.77 | 17.87 |
| $[In^{III}]$-**IV** | 1687.58 | ND | ND | 1687.4 $[M+H]^+$ | 13.51 | 16.34 |

Note: MW: molecular weight; †: I, **DOTA-GABA-[D-Tyr$^6$]BN(6-14)**; II, **DOTA-GABA-[D-Tyr$^6$, β-Ala$^{11}$]BN(6-14)**; III, **DOTA-GABA-[D-Tyr$^6$, D-Ala$^{11}$]BN(6-14)**; IV, **DOTA-GABA-[D-Tyr$^6$, Agly$^{11}$]BN(6-14)**. ‡ RP HPLC eluents: **System 1**, flow: 0.75 ml/min; eluents: A= 0.1% TFA in water and B= acetonitrile; non-linear gradient: 0 min, 80% A; 20 min, 50% A; 21 min, 0% A; 24 min, 0% A and 25, 80% A. **System 2**: flow: 0.75 ml/min; eluents: A= 50 mM sodium acetate buffer (pH 5.4) and B= acetonitrile; non-linear gradient as in **System 1**.

**Table 2**: $IC_{50}$ values for displacing GRP-receptor-bound [$^{125}$I-Tyr$^{4}$]BN by increasing concentrations of BN analogues. $IC_{50}$ values (nM ± SE) are in triplicates. Number of independent studies is in brackets. Human GRP-R were from human prostate cancer and mouse GRP-R were from mouse pancreas.

| Code No. | Human GRP-R | Mouse GRP-R |
|---|---|---|
| [$In^{III}$]-**I** | 11.5±2.6 (3) | 1.2±0.5 (3) |
| [$In^{III}$]-**II** | 12.6±3.5 (3) | 0.5±0.2 (3) |
| [$In^{III}$]-**III** | 41±12 (3) | 5.8±2.2 (3) |
| [$In^{III}$]-I**V** | 96±13 (5) | 1.0±0.5 (4) |

**Table 3**: Calculation of metabolic stability of [$^{111}$In-DOTA]-GABA-[D-Tyr$^{6}$, X$^{11}$]BN(6-14) in serum according to the equation: $A=A_0*\exp(-k_1*t)$.

| Ligands ($X^{11}$) | $k_1(h^{-1})$ | $T_{1/2}(h)$ |
|---|---|---|
| [$^{111}$In]-**I** (Gly) | 0.237±0.037 | 2.9±0.5 |
| [$^{111}$In]-**II** (βAla) | 0.089±0.013 | 7.8±1.1 |
| [$^{111}$In]-**III** (D-Ala) | 0.109±0.009 | 6.3±0.5 |
| [$^{111}$In]-**IV** (Agly) | 0.049±0.005 | 14.1±1.5 |

**Table 4:** Biodistribution (4 h p.i.) in male Lewis rats. Results are the mean of groups of four animals except for the Agly derivative, for which 9 animals were used.

| Site | [$^{111}$In]-**I** | [$^{111}$In]-**II** | [$^{111}$In]-**III** | [$^{111}$In]-**IV** |
|---|---|---|---|---|
| Blood | 0.028±0.003 | 0.012±0.001 | 0.014±0.002 | 0.017±0.002 |
| Muscle | 0.027±0.011 | 0.033±0.008 | 0.018±0.003 | 0.044±0.010 |
| Kidneys | 0.85±0.08 | 1.31±0.08 | 0.79±0.17 | 1.36±0.16 |
| Adrenals | 0.30±0.08 | 0.44±0.04 | 0.23±0.02 | 0.47±0.10 |
| Pancreas | 4.03±0.31 | 6.41±0.56 | 2.71±0.07 | 6.04±0.38 |
| Spleen | 0.06±0.01 | 0.07±0.02 | 0.05±0.00 | 0.07±0.01 |
| Stomach | 0.17±0.02 | 0.39±0.04 | 0.16±0.03 | 0.34±0.12 |
| Bowel | 0.33±0.05 | 0.76±0.11 | 0.31±0.04 | 0.44±0.05 |
| Liver | 0.05±0.01 | 0.04±0.00 | 0.04±0.00 | 0.05±0.00 |
| Lung | 0.03±0.01 | 0.03±0.00 | 0.04±0.01 | 0.04±0.00 |
| Heart | 0.02±0.00 | 0.01±0.00 | 0.01±0.00 | 0.01±0.00 |
| Bone | 0.03±0.01 | 0.04±0.01 | 0.02±0.00 | 0.04±0.00 |
| Pituitary | 0.31±0.09 | 0.69±0.11 | 0.54±0.19 | 0.49±0.18 |

**Table 5:** Biodistribution (4 h p.i.) of $^{111}$In-DOTA-GABA-[D-Tyr$^{6}$, X$^{11}$]BN(6-14) (X=Gly, βAla, D-Ala and Agly) in double tumor-bearing (AR4-2J and PC-3) female athymic nu/nu mice. Results are the mean of groups of four animals.

| Organ | [$^{111}$In]-**I** | [$^{111}$In]-**II** | [$^{111}$In]-**III** | [$^{111}$In]-**IV** |
|---|---|---|---|---|
| Blood | 0.029±0.002 | 0.034±0.005 | 0.024±0.002 | 0.064±0.006 |
| Muscle | 0.046±0.019 | 0.046±0.010 | 0.024±0.005 | 0.043±0.005 |
| Stomach | 0.96±0.10 | 2.70±0.41 | 0.49±0.06 | 1.49±0.30 |
| Kidneys | 3.19±0.54 | 4.25±0.92 | 2.24±0.14 | 3.09±0.99 |
| Bowel | 1.77±0.20 | 5.98±0.60 | 1.63±0.18 | 3.11±0.75 |
| Pancreas | 26.11±3.09 | 45.21±0.95 | 12.96±1.41 | 31.59±4.16 |
| Spleen | 1.15±0.15 | 1.68±0.28 | 0.63±0.09 | 1.30±0.12 |
| Liver | 0.11±0.01 | 0.15±0.02 | 0.13±0.02 | 0.14±0.02 |
| Lung | 0.08±0.01 | 0.10±0.02 | 0.06±0.01 | 0.16±0.06 |
| Heart | 0.04±0.00 | 0.05±0.01 | 0.03±0.00 | 0.05±0.01 |
| Adrenals | 11.01±1.58 | 15.22±3.60 | 5.14±0.65 | 11.86±1.85 |
| Bone | 0.11±0.01 | 0.31±0.15 | 0.06±0.01 | 0.22±0.03 |
| PC-3 | 2.36±0.70 | 2.56±0.42 | 1.62±0.52 | 2.15±0.22 |
| AR4-2J | 12.22±3.95 | 17.56±1.51 | 7.70±1.12 | 14.11±1.99 |
| | Pancreas **:** AR4-2J tumor **:** PC-3 tumor ratios | | | |
| | 11.1:5.2:1 | 17.7:6.9:1 | 8.0:4.8:1 | 14.7:6.6:1 |

DOTA-GABA-[D-Tyr$^{6}$]BN(6-14)

**I**

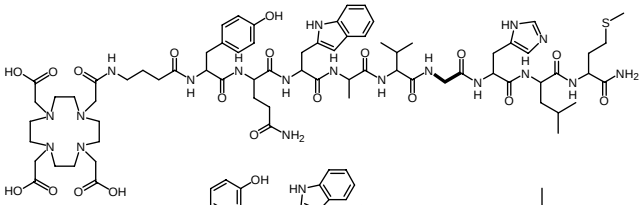

DOTA-GABA-[D-Tyr$^{6}$, βAla$^{11}$]BN(6-14)

**II**

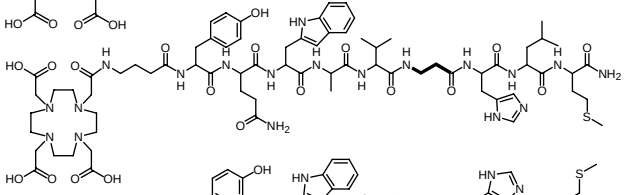

DOTA-GABA-[D-Tyr$^{6}$, D-Ala$^{11}$]BN(6-14)

**III**

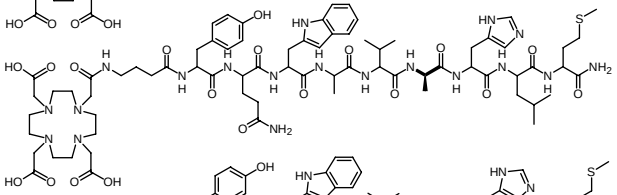

DOTA-GABA-[D-Tyr$^{6}$, Agly$^{11}$]BN(6-14)

**IV**

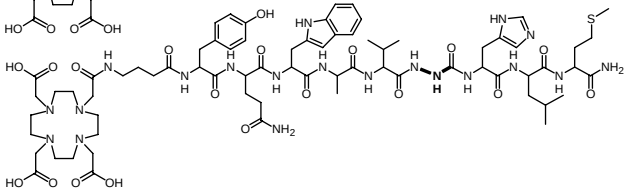

**Figure 1** Formula of DOTA-GABA-[D-Tyr6, **X**$^{11}$]BN (6-14), **X** = Gly, β-Ala, D-Ala and Agly.

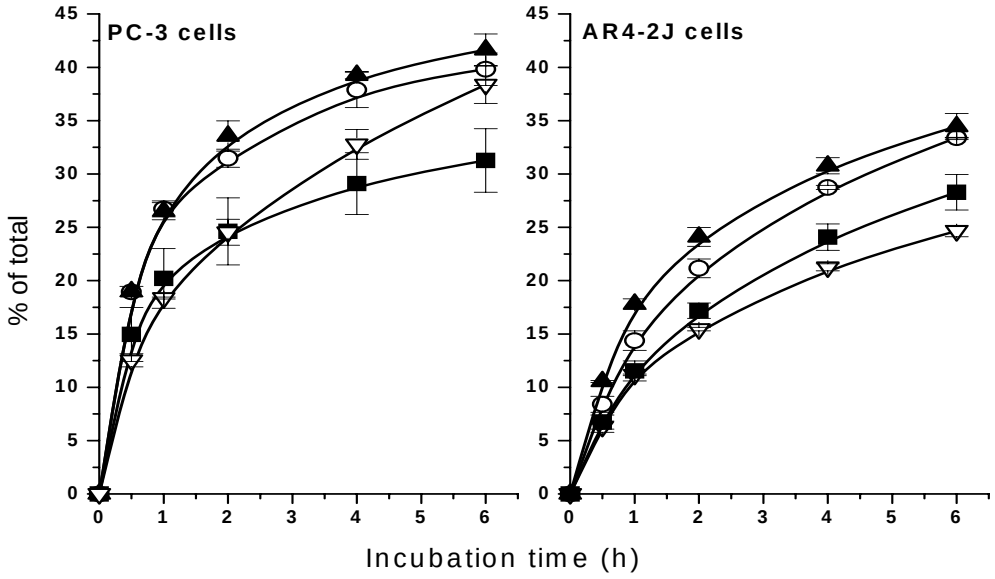


**Figure 2** Comparison of the internalization rates of [$^{111}$In]-DOTA-GABA-[D-Tyr$^{6}$, X$^{11}$] BN (6-14) into PC-3 cells (*left*) and AR4-2J cells (*right*), X=Agly (■), Gly (○), βAla (▲), and D-Ala (∇). Data result from two independent experiments with triplicates in each experiment and are expressed as specific internalization.

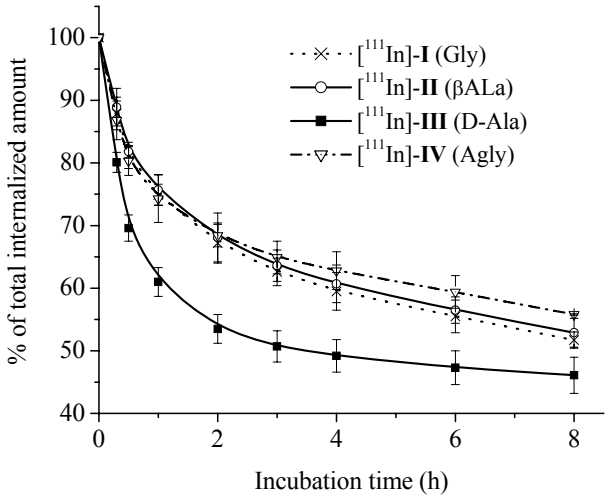


**Figure 3** Comparison of the externalization rates of [$^{111}$In]-DOTA-GABA-[D-Tyr$^{6}$, X$^{11}$] BN (6-14) from PC-3 cells, X=Agly (∇), Gly (×), βAla (○), and D-Ala (■). Data result from two independent experiments with triplicates in each experiment and are expressed as percentage of total internalized amount.

## References


1. Weiner RE, Thakur ML. Radiolabeled peptides in the diagnosis and therapy of oncological diseases. Appl Radiat Isot. 2002; 57: 749-63.
2. Reubi JC. Peptide receptors as molecular targets for cancer diagnosis and therapy. Endocr Rev. 2003; 24: 389-427.
3. Sosabowsky J, Melendez-Alafort L, Mather S. Radiolabelling of peptides for diagnosis and therapy of non-oncological diseases. Q J Nucl Med. 2003; 47: 223-37.
4. Ginj M, Maecke HR. Radiometallo-labeled peptides in tumor diagnosis and therapy. Met Ions Biol Syst. 2004; 42: 109-42.
5. Kwekkeboom D, Krenning EP, de Jong M. Peptide receptor imaging and therapy. J Nucl Med. 2000; 41: 1704-13.
6. Markwalder R, Reubi JC. Gastrin-releasing peptide receptors in the human prostate: relation to neoplastic transformation. Cancer Res. 1999; 59: 1152-9.
7. Reubi JC, Gugger M, Waser B. Co-expressed peptide receptors in breast cancer as a molecular basis for in vivo multireceptor tumour targeting. Eur J Nucl Med Mol Imaging. 2002; 29: 855-62.
8. Reubi JC, Korner M, Waser B, Mazzucchelli L, Guillou L. High expression of peptide receptors as a novel target in gastrointestinal stromal tumours. Eur J Nucl Med Mol Imaging. 2004; 31: 803-10.
9. Smith CJ, Volkert WA, Hoffman TJ. Gastrin releasing peptide (GRP) receptor targeted radiopharmaceuticals: a concise update. Nucl Med Biol. 2003; 30: 861-8.
10. Nock B, Nikolopoulou A, Chiotellis E, Loudos G, Maintas D, Reubi JC, et al. [$^{99m}$Tc]Demobesin 1, a novel potent bombesin analogue for GRP receptor-targeted tumour imaging. Eur J Nucl Med Mol Imaging. 2003; 30: 247-58.
11. Smith CJ, Gali H, Sieckman GL, Hayes DL, Owen NK, Mazuru DG, et al. Radiochemical investigations of $^{177}$Lu-DOTA-8-Aoc-BBN[7-14]$NH_2$: an in vitro/in vivo assessment of the targeting ability of this new radiopharmaceutical for PC-3 human prostate cancer cells. Nucl Med Biol. 2003; 30: 101-9.
12. Chen X, Park R, Hou Y, Tohme M, Shahinian AH, Bading JR, et al. microPET and autoradiographic imaging of GRP receptor expression with $^{64}$Cu-DOTA-[Lys$^3$]bombesin in human prostate adenocarcinoma xenografts. J Nucl Med. 2004; 45: 1390-7.
13. Breeman WA, Hofland LJ, de Jong M, Bernard BF, Srinivasan A, Kwekkeboom DJ, et al. Evaluation of radiolabelled bombesin analogues for receptor-targeted scintigraphy and radiotherapy. Int J Cancer. 1999; 81: 658-65.
14. Van de Wiele C, Dumont F, Dierckx RA, Peers SH, Thornback JR, Slegers G, et al. Biodistribution and dosimetry of $^{99m}$Tc-RP527, a gastrin-releasing peptide (GRP) agonist for the visualization of GRP receptor-expressing malignancies. J Nucl Med. 2001; 42: 1722-7.
15. Smith CJ, Sieckman GL, Owen NK, Hayes DL, Mazuru DG, Kannan R, et al. Radiochemical investigations of gastrin-releasing peptide receptor-specific [$^{99m}$Tc(X)$(CO)_3$-Dpr-Ser-Ser-Ser-Gln-Trp-Ala-Val-Gly-His-Leu-Met-($NH_2$)] in PC-3, tumor-bearing rodent models: syntheses, radiolabeling, and in vitro/in vivo studies where Dpr = 2,3-diaminopropionic acid and X = $H_2O$ or $P(CH_2OH)_3$. Cancer Res. 2003; 63: 4082-8.
16. La Bella R, Garcia-Garayoa E, Langer M, Blauenstein P, Beck-Sickinger AG, Schubiger PA. In vitro and in vivo evaluation of a $^{99m}$Tc(I)-labeled bombesin analogue for imaging of gastrin releasing peptide receptor-positive tumors. Nucl Med Biol. 2002; 29: 553-60.
17. Smith CJ, Gali H, Sieckman GL, Higginbotham C, Volkert WA, Hoffman TJ. Radiochemical investigations of $^{99m}$Tc-$N_3S$-X-BBN[7-14]$NH_2$: an in vitro/in vivo structure-activity relationship study where X = 0-, 3-, 5-, 8-, and 11-carbon tethering moieties. Bioconjug Chem. 2003; 14: 93-102.
18. Mantey SA, Weber HC, Sainz E, Akeson M, Ryan RR, Pradhan TK, et al. Discovery of a high affinity radioligand for the human orphan receptor, bombesin receptor subtype 3, which demonstrates that it has a unique pharmacology compared with other mammalian bombesin receptors. J Biol Chem. 1997; 272: 26062-71.

19. Darker JG, Brough SJ, Heath J, Smart D. Discovery of potent and selective peptide agonists at the GRP-preferring bombesin receptor (BB2). J Pept Sci. 2001; 7: 598-605.
20. Weber D, Berger C, Heinrich T, Eickelmann P, Antel J, Kessler H. Systematic optimization of a lead-structure identities for a selective short peptide agonist for the human orphan receptor BRS-3. J Pept Sci. 2002; 8: 461-75.
21. Lin JT, Coy DH, Mantey SA, Jensen RT. Comparison of the peptide structural requirements for high affinity interaction with bombesin receptors. Eur J Pharmacol. 1995; 294: 55-69.
22. Mantey SA, Coy DH, Pradhan TK, Igarashi H, Rizo IM, Shen L, et al. Rational design of a peptide agonist that interacts selectively with the orphan receptor, bombesin receptor subtype 3. J Biol Chem. 2001; 276: 9219-29.
23. Mantey SA, Coy DH, Entsuah LK, Jensen RT. Development of bombesin analogs with conformationally restricted amino acid substitutions with enhanced selectivity for the orphan receptor human bombesin receptor subtype 3. J Pharmacol Exp Ther. 2004; 310: 1161-70.
24. Zhang H, Chen J, Waldherr C, Hinni K, Waser B, Reubi JC, et al. Synthesis and evaluation of bombesin derivatives on the basis of pan-bombesin peptides labeled with indium-111, lutetium-177, and yttrium-90 for targeting bombesin receptor-expressing tumors. Cancer Res. 2004; 64: 6707-15.
25. Teufel M, Saudek V, Ledig JP, Bernhardt A, Boularand S, Carreau A, et al. Sequence identification and characterization of human carnosinase and a closely related non-specific dipeptidase. J Biol Chem. 2003; 278: 6521-31.
26. Nowick JS, Holmes DL, Noronha G, Smith EM, Nguyen TM, Huang SL. Synthesis of peptide isocyanates and isothiocyanates. J Org Chem. 1996; 61: 3929-34.
27. Gibson C, Goodman SL, Hahn D, Hoelzemann G, Kessler H. Novel solid-phase synthesis of azapeptides and azapeptoids via Fmoc-strategy and its application in the synthesis of RGD-mimetics. J Org Chem. 1999; 64: 7388-94.
28. Smith CJ, Volkert WA, Hoffman TJ. Radiolabeled peptide conjugates for targeting of the bombesin receptor superfamily subtypes. Nucl Med Biol. 2005; 32: 733-40.
29. Shipp MA, Tarr GE, Chen CY, Switzer SN, Hersh LB, Stein H, et al. CD10/neutral endopeptidase 24.11 hydrolyzes bombesin-like peptides and regulates the growth of small cell carcinomas of the lung. Proc Natl Acad Sci U S A. 1991; 88: 10662-6.
30. Chen J, Nguyen H, Metcalfe E, Eaton S, Arunachalam T, Raju N, et al. Formulation and in vitro metabolism studies with $^{177}$Lu-AMBA; a radiotherapeutic compound that targets gastrin releasing peptide receptors. *In:* Annual Congress of the EANM, Helsinki, 2004, pp. S281.
31. Giladi E, Nagalla SR, Spindel ER. Molecular cloning and characterization of receptors for the mammalian bombesin-like peptides. J Mol Neurosci. 1993; 4: 41-54.
32. Maina T, Nock B, Zhang H, Nikolopoulou A, Reubi JC, Maecke HR. Interspecies differences during comparative evaluation of [$^{111}$In]Z070 and [$^{99m}$Tc]Demobesin 1 in rat or human origin GRP-R-expressing cells and animal models. J Nucl Med. 2005; 46.
33. Carpino LA, Han GY. The 9-Fluorenylmethoxycarbonyl Amino-Protecting Group. J Org. Chem. 1972; 37: 3404-9.
34. Fleischmann A, Laderach U, Friess H, Buechler MW, Reubi JC. Bombesin receptors in distinct tissue compartments of human pancreatic diseases. Lab Invest. 2000; 80: 1807-17.

*Manuscript 3*

# Potent Bombesin-chelated Conjugates Labeled with $^{64/67}$Cu for PET Imaging and Targeted Radionuclide Therapy of GRP-receptor Expressing Tumors

**Hanwen Zhang [a], Simona Ciobanu [a], Beatrice Waser [b], Jean Claude Reubi [b], Ilse Novak-Hofer[c], Michael Honer[c], Helmut R Maecke [a]**

[a] Division of Radiological Chemistry, Institute of Nuclear Medicine, Department of Radiology, University Hospital, Basel, Switzerland;
[b] Division of Cell Biology and Experimental Cancer Research, Institute of Pathology, University of Berne, Berne, Switzerland;
[c] Center for Radiopharmaceutical Science, Paul Scherrer Institute, Villigen, Switzerland

Present status:
Manuscript in preparation.

# Potent Bombesin-chelated Conjugates Labeled with $^{64}$Cu and $^{67}$Cu for PET Imaging and Targeted Radionuclide Therapy of Bombesin Receptor-expressing Tumors

Hanwen Zhang [a], Simona Ciobanu [a], Beatrice Waser [b], Jean Claude Reubi [b], Ilse Novak-Hofer[c], Michael Honer[c], Helmut R. Maecke*[a]

[a] Division of Radiological Chemistry, Department of Radiology, University Hospital, Petersgraben 4, CH-4031 Basel, Switzerland;

[b] Division of Cell Biology and Experimental Cancer Research, Institute of Pathology, University of Berne, PO Box 62, Murtenstrasse 31, CH-3010 Berne, Switzerland;

[c] Center for Radiopharmaceutical Science, Paul Scherrer Institute, Switzerland

[1]**Abbreviations:** BN, bombesin; BZH4, DOTA-GABA-[D-Tyr$^6$, β-Ala$^{11}$, Nle$^{14}$]BN(6-14); BZH5, CPTA-[D-Tyr$^6$, β-Ala$^{11}$, Nle$^{14}$]BN (6-14); BZH6, CPTA-[D-Tyr$^6$, β-Ala$^{11}$]BN (6-14); BZH7, CPTA-[β-Ala$^{11}$]BN (7-14); BZH8, CPTA-[Gly$^6$, β-Ala$^{11}$]BN (6-14); GRP, gastrin-releasing peptide; NMB, neuromedin B; hGRP-R, human gastrin releasing peptide receptor; mGRP-R, mouse gastrin releasing peptide receptor; NMB-R, the neuromedin B receptor; BNRS-3, BN receptor subtype-3; DOTA, 1,4,7,10-tetraazacyclododecane-1,4,7,10-tetraacetic acid; CPTA, 1,4,8,11-tetraaza-cyclotetradecane-1-p-toluic acid (cyclam-p-toluic acid); HoBt, 1-hydroxybenzotriazole; PyBop, benzotriazole-1-yl-oxy-tris-pyrrolidino-phosphonium hexafluorophosphate; DIPEA, N-ethyldiisopropylamine; NMP, 1-methyl-2-pyrrolidone; TNBS, 2,4,6-trinitrobenzenesulfonic acid. Abbreviations of the common amino acids are in accordance with the recommendations of IUPAC-IUB [IUPAC-IUB Commission of Biochemical Nomenclature (CBN), symbols for amino-acid derivatives and peptides, recommendations 1971. Eur J Biochem 1972; 27:201-207].

---

* To whom correspondence should be addressed:
Tel: ++41 61 265 46 99; Fax: ++41 61 265 55 59
E-mail: hmaecke@uhbs.ch

**ABSTRACT**

A series of novel bombesin (BN) analogs were synthesized for the labeling with $^{64}Cu$ and $^{67}Cu$, which were expected to be useful for diagnosis and targeted radiotherapy of BN receptor positive tumors.

The positively charged ligands had a significantly higher affinity to human gastrin releasing peptide receptors (hGRP-R) than a negatively charged or neutral peptide. [$Cu^{II}$]-CPTA-[β-$Ala^{11}$]BN (7-14) ([$Cu^{II}$]-BZH7) showed the highest binding affinities to human and mouse GRP receptors (0.42 ± 0.13 nM versus 0.22 ± 0.07 nM). The replacement of $Met^{14}$ by Nle or the introduction of Gly or D-Tyr between [$Cu^{II}$]-CPTA and [β$Ala^{11}$]BN (7-14) led to a loss of affinity to human GRP receptors by a factor of 3.2, 4.3, and 2.4, respectively. Among these analogs [$^{64/67}Cu$]-BZH7 had the highest internalization rate into PC-3 cells, a relatively slow efflux, and was the most stable in fresh human serum.

Biodistribution studies in PC-3 tumor xenografts showed [$^{64/67}Cu$]-BZH7 to have the highest accumulation in the tumor: 11.2 ± 1.5% IA/g (% injected activity per gram), 6.63 ± 0.80% IA/g and 4.14 ± 0.55% IA/g at 1 h, 4 h and 24 h p.i., respectively. A fast clearance from blood and all non-target organs except the kidneys and liver was found. Increasing tumor-to-kidney and tumor-to-liver ratios were observed from 1 h to 24 h p.i. MicroPET imaging of [$^{64}Cu$]-BZH7 (3 h p.i.) visualized the tumor nicely.

These results indicate that the novel ligand [$^{64/67}Cu$]-BZH7 is a very promising radiopeptide for the early diagnosis and targeted radiotherapy of carcinoma overexpressing BN receptors.

INTRODUCTION

Imaging of early disease events and systemic therapy in patients suffering from cancer benefit from the definition of agents preferentially targeting biomarkers which are expressed selectively or at least preferentially on the cell surface. Promising targets in this respect are receptors of regulatory peptides which are highly overexpressed in major human tumors. The prototypic receptors and corresponding targeting radiopeptides are based on somatostatin receptors. High expression of somatostatin receptors is restricted to a relatively small group of tumors, such as neuroendocrine tumors, carcinoids, some low grade brain tumors, renal cell carcinoma, etc. A more promising family of receptors with respect to targeting major human tumors are the mammalian bombesin receptors which were found to be overexpressed by human tumors including prostate[1, 2] and breast[3, 4] cancer, SCLC[5, 6] and gastrointestinal stromal tumors (GIST)[7]. All three receptor types of the BN receptor family, including NMB-R, GRP-R and BNRS-3 were observed to be overexpressed on human tumors, GRP-R being the most relevant because of its high expression on prostate, breast and gastrointestinal stromal tumors. In addition, GRP-R are also highly overexpressed in prostatic intraepithelial neoplasia (PIN), the early stage of prostate cancer, which provides the possibility to non-invasively localize an early event in prostate carcinogenesis using imaging probes.

Therefore much activity was devoted towards the development of BN analogs radiolabeled with $^{99m}$Tc[2, 8-10] or with $^{111}$In for SPECT. Based on $^{64}$Cu[11, 12], PET tracers were also developed. Copper-64 is an interesting radionuclide as it is not only a positron- (19%, $E_{\beta^+ max}$ = 656 keV) but also a $\beta^-$-emitter (39.6%, $E_{\beta^- max}$ = 573 keV) with a half-life of 12.7 h and may therefore be used for diagnostic and therapeutic targeting of BN receptor-positive tumors. In addition, it can be produced in large amounts by small medical cyclotrons[13].

We had several goals in mind when we designed this study. 1) We aimed at developing a BN-based radiopeptide for the labeling with $^{64}$Cu ($^{67}$Cu) to be used in the imaging and potentially in radionuclide therapy of BN receptor-positive tumors. 2) We were interested in studying the influence of a charge at the N-terminus of the radiopeptides on their pharmacologic and biologic properties because we had noticed before that the replacement of a tetraamine ligand (antagonistic BN analog) for $^{99m}$Tc-labeling[14] by a negatively charged DTPA causes an affinity drop by a factor of approximately $10^3$ (Reubi, Schmitt, Maecke, unpublished results). We were wondering if the same effect can also be seen in the herein presented class of radiopeptides (agonistic BN analogs). 3) As the structure of the CPTA(4-(1,4,8,11-tetraazacyclotetradec-1-yl)-methyl benzoic acid)-ligand allows a modification with glycine to afford a hippurane-like structural spacer, we wanted to know if this structural element results in an enhanced kidney

clearance. 4) Finally, we and others[15] have recently observed that species differences may be of high importance in the development and evaluation of bombesin receptor ligands. We therefore studied modifications of BN(7-14) with regard to amino acid substitution at the 6$^{th}$ and 14$^{th}$ position of BN. Since CPTA allows high labeling yields under very mild labeling conditions, it was chosen as a bifunctional chelator for the labeling of monoclonal antibodies[16] and octreotide[17] with radiocopper. On this basis a series of BN analogs were constructed to evaluate their binding affinity to the three bombesin receptor subtypes, their internalization rates into and efflux from PC-3 cells. We also report on the comparison of biodistribution data of the $^{64/67}$Cu-labelled bombesin-based peptides in PC-3 tumor-bearing nude mice and on microPET imaging. This work is the first study of the influence of different charges at the N-terminus of BN analogs on the binding affinity, of the hippurane-like spacer molecule on kidney clearance, and of a modification at the 6$^{th}$ and 14$^{th}$ position of these (radio)metallobombesin analogs in different species with the goal to optimize radioligands for diagnosis and targeted radionuclide therapy of bombesin receptor-positive tumors.

## EXPERIMENTAL SECTION

### Materials

All chemicals were obtained from commercial sources and used without further purification. Cyclam-p-toluic acid (CPTA) was synthesized as described previously[18]. Rink amide MBHA resin and all Fmoc-protected amino acids were commercially available from NovaBiochem (Läufelfingen, Switzerland). [$^{111}$In]$Cl_3$ was purchased from Mallinckrodt Medical (Petten, The Netherlands). Electrospray ionization (ESI) mass spectroscopy was carried out with a Finnigan SSQ 7000 spectrometer, fast atom bombardment (FAB) mass spectroscopy with a VG 70SE spectrometer and MALDI-MS measurement on a Voyager sSTR equipped with an Nd:YAG laser (Applied Biosystems, Framingham, USA). Analytical HPLC was performed on a Hewlett Packard 1050 HPLC system (Waldbronn 2, Germany) with a multiwavelength detector and a flow-through Berthold LB 506 Cl γ-detector (Wildbad, Germany) using a Macherey-Nagel Nucleosil 120 $C_{18}$ column (Oensingen, Switzerland). Preparative HPLC was performed on a Metrohm HPLC system LC-CaDI 22-14 (Herisau, Switzerland) with a Macherey-Nagel VP 250/21 Nucleosil 100-5 $C_{18}$ column. Quantitative γ-counting was performed on a COBRA 5003 γ-system well counter from Packard Instruments (Meriden, CT, USA). Solid phase peptide synthesis was performed on a semiautomatic peptide synthesizer commercially available from Rink Combichem (Bubendorf, Switzerland). The cell culture medium was Dulbecco's minimal

essential medium (DMEM) with 10% fetal calf serum (FCS) from BioConcept (Allschwil, Switzerland). MicroPET imaging was performed on a dedicated small animal PET tomograph quad-HIDAC (Oxford Positron System, UK).

**Synthesis**

The peptides were synthesized as described previously[19]. The bifunctional chelator CPTA was coupled to the resin-assembled peptide as follows: 6 equivalents CPTA were mixed together with 18 equivalents PyBop, 18 equivalents HoBt and 80 equivalents DIPEA in NMP and immediately incubated with the resin-assembled peptide until the TNBS test was negative (approximately 5 h).

**Production of $^{64}$Cu and $^{67}$Cu**

$^{64}$Cu/$^{67}$Cu nuclides were produced at the 72 MeV accelerator of the Paul Scherrer Institute by irradiating $^{nat}$Zn with protons, and irradiations were modified for the preparation of $^{67}$Cu and $^{64}$Cu, respectively[20, 21]. Briefly, for $^{64}$Cu production, the proton irradiation schedule was reduced to maximally 20 h and the Zn target was processed 12 h post end of bombardment (EOB). The ratio of $^{64}$Cu/$^{67}$Cu was 20/1 with a specific activity of 1.5 GBq $^{64}$Cu/μg Cu. For $^{67}$Cu production, the irradiation time was longer and separation of the $^{64}$Cu/$^{67}$Cu mixture was postponed until most of $^{64}$Cu decayed to afford pure $^{67}$Cu with a specific activity of 112.5 MBq/μg Cu. The copper radionuclides used in the present study were radiochemically isolated according to the procedure of Schwarzbach et al[20]. For the in vitro assays and the biodistribution studies a mixture of $^{64}$Cu/$^{67}$$CuCl_2$ was used. $^{64}$Cu used for the PET imaging experiment contained approximately 10% $^{67}$Cu.

**Metallated conjugates**

A mixture of peptides (0.5 μmol) in 500 μL 0.5 M ammonium-acetate-buffer (pH 5) was incubated with 1.5 μmol $CuCl_2 \cdot 2H_2O$ pre-dissolved in 0.04M HCl for 1h at room temperature, and purified over a SepPak $C_{18}$ cartridge (Waters Corp. Milford, MA) preconditioned with 10 mL ethanol and 10 mL water. The cartridge was eluted with 10 mL water followed by 3 mL methanol resulting in $Cu^{II}$-peptide after evaporation of the methanol. The final product was analyzed by analytical HPLC and MALDI. Using 3 equivalents $InCl_3 \cdot 5H_2O$, [$In^{III}$]-BZH4 was synthesized at elevated temperature (95ºC, 20-25 min).

**Preparation of radiotracer for internalization and biodistribution studies**

[$^{64/67}$Cu]-BZH7 was prepared by dissolving 10 μg of BZH7 (7.5 nmol) in ammonium acetate buffer (300 μL, 0.5 M, pH 5.5); after the addition of $^{64/67}CuCl_2$ (about 185 MBq $^{64}$Cu and 37 MBq $^{67}$Cu), the solution was incubated at room temperature for 1 h. A 1.5 molar excess of $CuCl_2 \cdot 2H_2O$ was added and incubated again for 0.5 h. Subsequently radiolabeled peptides were purified utilizing a SepPak $C_{18}$ cartridge preconditioned with 10 mL methanol and 10 mL water; the cartridge was eluted with 3 mL water, followed by 2 mL ethanol, to afford the pure $^{64/67}$Cu-labeled ligand. For biodistribution studies, the labeling was performed accordingly without the addition of cold $CuCl_2 \cdot 2H_2O$. The solution was prepared for injection by dilution with 0.9% NaCl (0.1% BSA) to afford the radioligand solution. All $^{64/67}$Cu-labeled conjugates were prepared in the same way. The preparation of [$^{111}$In]-BZH4 was described previously[19]. All radiolabeled peptides were analyzed with HPLC (eluents: A= 0.1% TFA in water and B= acetonitrile; gradient: 0-20 min, 80%-50% A; 20-21 min, 100% B; 21-24 min, 100% B; 25 min, 80% A).

**Binding affinity and receptor subtype profile**

Using [$^{125}$I-D-Tyr$^4$]BN as GRP-R-preferring ligand, the $IC_{50}$ values of the $^{nat}$Cu/$^{nat}$In-labeled peptides were measured by in vitro autoradiography of sections of human prostate cancer tissue overexpressing GRP receptors or mouse pancreas tissue expressing mouse GRP receptors.
The binding affinity profile of [$Cu^{II}$]-BZH7 for the three bombesin receptor subtypes was determined by using [$^{125}$I-D-Tyr$^6$, β-Ala$^{11}$, Phe$^{13}$, Nle$^{14}$]BN (6-14) as universal radioligand. The procedures were described in detail previously[22, 23].

**Internalization and externalization (efflux) studies**

Internalization and externalization experiments were performed in 6-well plates as described in a previous publication[19]**.** Briefly, the cells were washed twice with internalization medium (DMEM supplemented with vitamins, essential and non-essential amino acids, L-glutamine, antibiotics (penicillin/streptomycine), fungicide (amphotericin B/Fungizone) and 1% FCS) and allowed to adjust to the medium for 1 h at 37°C. Approximately 1.3 kBq (0.25 pmol) of radioligand was added to the medium and the cells, $10^6$ cells per well, incubated (in triplicates) for 0.5, 1, 2, 4, and 6 h at 37°C, 5% $CO_2$, with or without excess BZH2 (150 μL of a 5.8 μM solution, final concentration of cold BZH2 was 0.58 μM. (BZH2: DOTA-GABA-[D-Tyr$^6$, β-Ala$^{11}$, Thi$^{13}$, Nle$^{14}$]BN (6-14)) to determine nonspecific internalization. The final volume was 1.5 mL. At appropriate time points the internalization was stopped by removing the medium,

followed by washing the cells with ice-cold phosphate buffered saline. Cells were then twice treated for 5 min with glycine buffer (0.05 M glycine solution, pH adjusted to 2.8 with 1M HCl) to distinguish between cell surface-bound (acid releasable) and internalized (acid resistant) radioligand. Finally, cells were detached from the plates by incubation for 10 min at 37°C with 1M NaOH, and the radioactivity was measured in a γ-counter.

For externalization studies, PC-3 cells were allowed to internalize the radioligands for periods of 2 h and were then exposed to an acid wash, as described in the previous section, to dissociate cell surface-bound radioligand. One mL of culture medium was added to each well, cells were incubated at 37°C in a 5% $CO_2$ environment and externalization of the cell-incorporated radioactivity was studied at different times. The culture medium was collected and measured for radioactivity.

**Serum stability**

To 1 mL of freshly prepared human serum, previously equilibrated in a 5% $CO_2$ (95% air) environment at 37°C, 0.6 nmol $^{111}$In- or $^{64/67}$Cu-labeled conjugates were added. The mixture was incubated in a 5% $CO_2$, 37°C environment. At different time points (0, 1, 4, and 8 h), 50 µL aliquots (in triplicates) were removed and treated with 60 µL ethanol. Samples were then cooled (4°C) and centrifuged for 15 min at 500 g to precipitate serum proteins. Fifty µL of supernatant were removed for activity counting in a γ well-counter. The sediment was washed twice with 1 mL ethanol and counted, and the activity in the supernatant was compared with the activity in the pellet to give the percentage of peptides not bound to proteins or radiometals transferred to serum proteins. The supernatant was also analyzed with HPLC (eluents: A= 0.1% TFA in water and B= acetonitrile; gradient: 0-20 min, 80%-50% A; 21-24 min, 100% B; 24-25 min, 80% A). The data points were used to calculate the half-life of disappearance of intact peptide as previously described[19].

**Biodistribution experiments in PC-3 tumor-bearing nude mice**

After a slight anesthesia with isoflurane in an air/oxygen mixture, female athymic nude mice were implanted subcutaneously with approximately 10 million PC-3 tumor cells, which were freshly expanded in 100 µL sterilized PBS solution.

Seven to ten days after inoculation the tumors weighed 60-130 mg and the mice were injected via a lateral tail vein with 10 pmol radiolabeled peptides (about 0.24 MBq $^{64}$Cu and 0.05 MBq $^{67}$Cu), diluted in 0.9% NaCl (0.1% BSA, pH 7.4, total injected volume = 100 µL). For the determination of non-specific uptake in the tumor or receptor-positive organs, a group of 4 animals was injected with a mixture of 10 pmol radiolabeled peptide/50 µg [$Cu^{II}$]-BZH7 in 0.9%

NaCl solution (injected volume 150 μL). At 1 h, 4 h and 24 h, mice were sacrificed, and organs of interest collected, rinsed of excess blood, blotted, weighed and counted in a γ-counter. The percentage of injected activity per gram (% IA/g) was calculated for each tissue. The total counts injected per animal were determined by extrapolation from counts of an aliquot taken from the injected solution as a standard.

**MicroPET imaging**

PET imaging was performed on a dedicated small animal PET tomograph quad-HIDAC (0.3 mm bin size, 180×280×270 matrix size). PET data were acquired in list-mode, reconstructed in a 70 min time frame using the FAIR algorithm and analyzed by using the dedicated software Pmod to afford image files. For imaging studies, an awake animal with an inoculated PC-3 tumor on each side of the body was slightly restrained and injected with 5 MBq [$^{64}$Cu]-BZH7 via a lateral tail vein. Three hours later the animal was anesthetized with isoflurane in an air/oxygen mixture and positioned in the tomograph symmetrically in the center of the field of view while anesthesia was monitored through measuring the respiratory frequency. Body temperature was kept at 37.3°C by a heated air stream. Acquisition of PET data was initiated 15 min after induction of anesthesia, scan duration was 90 min. Twenty-three hours after injection, the mouse was sacrificed, and organs of interest were collected and measured as described above in the biodistribution section. The results were calculated as percentage of injected activity per gram of tissue (%IA/g).
All animal experiments were performed in compliance with the Swiss regulations for animal treatment (Bundesamt für Veterinärwesen, approval no. 789).

**Statistical analysis**

Data are expressed as mean ± SD, calculated on Microsoft Excel. The Student's t-test (Origin 6, Microcal Software, Inc., Northampton, MA) was used to determine statistical significance at the 95% confidence level with $P < 0.05$ being considered significantly different.

## RESULTS

### Synthesis and labeling

All conjugates (Table 1) were synthesized using the Fmoc strategy affording a maximum yield of approximately 30% based on the removal of the first Fmoc group; the purity analyzed by HPLC was ≥97%. BZH4 was labeled with $^{111}$In at elevated temperature (95°C) for 20-25 min, and all conjugates were labeled with $^{64/67}$Cu at room temperature. In all cases, radiolabeling yields of ≥98% at specific activities of >24 GBq μmol$^{-1}$ were achieved for $^{64}$Cu, >5 GBq μmol$^{-1}$ for $^{67}$Cu and >37GBq μmol$^{-1}$ for [$^{111}$In]-BZH4.

**Receptor binding affinity**

Table 2 shows the binding affinities of the metallopeptides to GRP receptors of mouse and human origin. The $Cu^{II}$- and $In^{III}$-complexed peptides exhibit high to moderate affinity to the human and high affinity to the mouse GRP receptor, as demonstrated by competitive binding assays using [$^{125}$I-Tyr$^4$]bombesin as radioligand and human cancerous tissue as well as mouse pancreas tissue as a source of GRP receptors. The affinity to the human receptor varies between 0.42 ± 0.13 nM and 41.5 ± 2.5 nM whereas the affinity to the mouse receptor varies between 0.22 ± 0.07 nM and 1.1 ± 0.33 nM.

The most promising peptide, Cu-BZH7, was also studied with respect to the bombesin receptor subtype profile using human cancerous tissue shown to express predominantly one single bombesin receptor subtype. The peptide showed high binding affinity to all 3 human receptor subtypes (0.27 ± 0.16 nM to NMB-R; 0.30 ± 0.07 nM to GRP-R; 1.4 ± 0.6 nM to BNRS-3).

**Internalization and efflux studies**

The internalization kinetics of [$^{64/67}$Cu]-BZH5-8 and [$^{111}$In]-BZH4 in PC-3 cells at 37°C is summarized in Fig. 1. All radiopeptides show specific, receptor-mediated cell uptake. [$^{64/67}$Cu]-BZH5 and [$^{64/67}$Cu]-BZH7 internalize very efficiently, reaching about 80% of the total activity added to a well containing 1 million cells within 6 h. [$^{64/67}$Cu]-BZH6, [$^{64/67}$Cu]-BZH8 and [$^{111}$In]-BZH4 have internalization rates of 64%, 46%, and 36% at 6 h under the same experimental conditions. Internalization was almost completely blocked (nonspecific internalization was <1% of the added activity) in the presence of 0.57 μM unlabeled DOTA-GABA-[D-Tyr$^6$, β-Ala$^{11}$, Thi$^{13}$, Nle$^{14}$]BN (6-14). The surface-bound peptide (radioactivity removable by acid wash) was below 7% of the added radiopeptide at each time point.

The efflux kinetics was studied in PC-3 cells which were exposed to the radioligand for 2 h as described for internalization, followed by an acid wash, and then incubated with medium (1% FCS). The results are summarized in Fig. 2. Upon 8 h incubation, 36% of [$^{64/67}$Cu]-BZH7, 45% of [$^{64/67}$Cu]-BZH6, 51% and 52% of [$^{64/67}$Cu]-BZH5 and [$^{64}$Cu]- BZH8, and 60% of [$^{111}$In]-BZH4 were washed out from the PC-3 cells.

To identify the composition of the externalized peptides, [$^{111}$In]-BZH4 was used as a leading peptide. Upon 2 h of internalization and acid wash, the externalized radioactivity after 2 h already consisted of approximately 84% metabolites ($^{111}$In-DOTA: 13.8%; $^{111}$In-DOTA-GABA-D-Tyr-Gln: main peak, 63.5%; $^{111}$In-DOTA-GABA-D-Tyr-Gln-Trp-Ala-Val-βAla: 6.2%) and 16% intact peptide.

**Stability in human serum**

Serum stability was studied to determine the half-lives of disappearance of intact peptides in serum (Table 3). There was less than 3% of radiometal transfer to serum proteins during serum incubation studies. Using the equation $A=A_0*\exp(-k_1*t)$, the half-lives ($t_{1/2}$) of disappearance of intact peptides in serum were calculated[19]; they varied between 0.55 h and 5.1 h. The N-terminally attached chelate, [$^{111}$In]-DOTA in [$^{111}$In]-BZH4 and [$^{64/67}$Cu]-CPTA in [$^{64/67}$Cu]-BZH5 did not influence the metabolic stability in serum (0.61 ± 0.11 h versus 0.55 ± 0.11 h). The replacement of methionine ([$^{64/67}$Cu]-BZH5) by norleucine ([$^{64/67}$Cu]-BZH6) increased the $T_{1/2}$ by 40%; [$^{64/67}$Cu]-BZH7 and [$^{64/67}$Cu]-BZH8 reached 5.1 ± 1.7 h and 4.5 ± 1.2 h, respectively.

**Animal biodistribution studies**

Biodistribution studies were performed with the $^{64/67}$Cu-labeled peptides in female athymic nude mice bearing the PC-3 tumor. Results are presented in Tables 4 and 5 as percentage of injected activity per gram of tissue (% IA/g).

According to Table 4, [$^{64/67}$Cu]-BZH5, [$^{64/67}$Cu]-BZH7, and [$^{64/67}$Cu]-BZH8 display a similar rapid blood clearance from the PC-3 tumor-bearing mice, varying between 0.142% IA/g to 0.182% IA/g at 4h. There was also a rapid clearance from GRP-R-negative organs except the kidneys and liver. The three radiolabeled ligands showed high uptake in the human prostate tumor xenograft and in mouse GRP-R-positive organs; e.g. at 4 h the tumor uptake values were as follows: 3.47 ± 0.15% IA/g for [$^{64/67}$Cu]-BZH5, 6.63 ± 0.80% IA/g for [$^{64/67}$Cu]-BZH7, and 4.29 ± 0.70% IA/g for [$^{64/67}$Cu]-BZH8. The uptake in the pancreas corresponded to the tumor uptake (34.9 ± 1.6% IA/g versus 57.2 ± 2.7% IA/g versus 36.4 ± 3.4% IA/g). Of the three conjugates [$^{64/67}$Cu]-BZH7 showed the lowest liver uptake.

In vivo competition experiments (Table 3) using 50 µg [$Cu^{II}$]-BZH7 co-injected with [$^{64/67}$Cu]-BZH7 resulted in a >89% reduction of tumor uptake and also in a reduction of the uptake in GRP-R-positive organs, e.g. >97% in the pancreas, 96% in the adrenals, 91% in the bowel, 84% in the stomach, 76% in the spleen and bone. The co-injection of [$Cu^{II}$]-BZH7 led to a somewhat increased liver uptake, whereas the uptake in the kidneys was partially blocked. The injection of the blocking dose had no significant influence on the uptake in other non-target organs. Due to the rapid clearance of the peptides, high tumor-to-background ratios were found (Tables 2 and 3). The [$^{64/67}$Cu]-BZH7 conjugate showed the best tumor-to-background and tumor-to-liver ratio. The kinetics of [$^{64/67}$Cu]-BZH7 (Table 3) showed early localization of the tumor with high initial accumulation (11.2 ± 1.5% IA/g at 1 h p.i.), a decrease in tumor uptake to 6.63 ± 0.80% IA/g at 4

h and to 4.14 ± 0.55% IA/g at 24 h p.i., indicating a rapid initial wash out. The ratios between tumor and background (blood and muscle) were higher than 20 at 1 h p.i. and increased to more than 40 at 24 h. The ratios between tumor and liver or kidney also increased somewhat from 1 h to 24 h.

Introduction of a glycine-forming hippurane-type spacer (Fig. 3) influenced the retention of radioactivity in the kidneys. The kidney uptake of [$^{64/67}$Cu]-BZH7 and [$^{64/67}$Cu]-BZH8 differed by a factor of 1.8 at 1 h and of about 0.4 at 4 h (6.9 ± 1.2% IA/g versus 5.0 ± 0.5% IA/g, P = $1.4\times10^{-3}$). Under the condition of excessive Cu-BZH7, the kidney uptake of [$^{64/67}$Cu]-BZH8 was lower than that of [$^{64/67}$Cu]-BZH7 (2.02 ± 0.13% IA/g versus 2.44 ± 0.10%IA/g, (P = $2.9\cdot10^{-3}$).

**MicroPET imaging**

PET imaging of PC-3 tumor xenografts was performed 3 h p.i. of [$^{64/67}$Cu]-BZH7, as shown in Fig. 4. Both tumors were visible with clear contrast from the adjacent background and were also distinguished well from the other organs. A prominent uptake of radioactivity was also observed in the pancreas, liver and kidneys. The high resolution imaging displayed the cortex of one kidney. When biodistribution was measured 23 h p.i. the uptake in the PC-3 tumor was 3% IA/g and the tumor-to-kidney ratio was 2. The results of direct tissue counting and of PET imaging were consistent.

DISCUSSION

This study describes a promising modification of BN analogs for radiocopper labeling. According to the results a further design of BN ligands for targeted radiotherapy seems to be worthwhile. In fact, [$^{64}$Cu]-BZH7 has already proven promising for application in diagnosis (PET) and targeted radionuclide therapy of bombesin receptor-positive tumors such as prostate cancer.

**Binding affinity**

Different charges were introduced at the N-terminus of the BN peptides by attaching different metal-chelate complexes. Compared to the negative charge or neutral charge, the positive charge was found to significantly improve the $IC_{50}$ values of the peptides by a factor of 8.2 and 13.0, respectively, indicating that the use of DOTA as bifunctional chelator for conjugating copper-64 to BN analogs was not a good choice. These findings can explain why the positively charged [$^{99m}$Tc]-labeled bombesin analog[14] displays high affinity to the GRP receptor and high accumulation in PC-3 tumors whereas negatively charged analogs, such as $^{64}$Cu-labeled DOTA-Aoc-BN (7-14)[11] or DOTA-[Lys$^3$]BN[12] show low affinities. Interestingly, the three differently

charged peptides show but slight differences in the affinity to mouse GRP receptors, indicating that the mouse GRP receptor is not sensitive to the charge at the N-terminus.

The substitution of methionine by norleucine is expected to prevent radio-oxidation (due to oxidation of the methionine sulfide group) without affecting the binding affinity to the GRP receptor (because of the small difference (-S- vs -$CH_2$-) between these two amino acids). We previously found that the replacement of methionine by norleucine does not change the $IC_{50}$ values of our panbombesin analogs (norleucine in the 14$^{th}$ position). The data in Table 2 show that the substitution of Nle$^{14}$ ([$Cu^{II}$]-BZH5) by Met$^{14}$ ([$Cu^{II}$]-BZH6) caused the binding affinity toward hGRP receptors to increase from 3.2 ± 0.5 nM to 1.0 ± 0.2 nM whereas it had no influence on the $IC_{50}$ values for the mouse pancreas (0.6 ± 0.2 nM versus 0.8 ± 0.2 nM). We assume that this is due to the positive charge at the N-terminus.

[$Cu^{II}$]-BZH7 showed the highest affinity to human and mouse GRP receptors (0.42 ± 0.13 nM versus 0.22 ± 0.07 nM) we have found in more than 100 BN analogs. By introducing Gly (D-Tyr) between CPTA and [βAla$^{11}$]BN (7-14) the binding affinity toward the human GRP receptor dropped by a factor of 4.3 (2.4) and to the mouse GRP receptor by a factor of 3.6 (3.6), respectively, indicating that the insertion of glycine or D-Tyrosine does not improve the binding affinity when there is a metal-complexed bifunctional chelate at the N-terminus. This is not the case with D-Phe or D-Tyr in the sequence of [D-Tyr$^6$, β-Ala$^{11}$, Phe$^{13}$, Nle$^{14}$]BN (6-14)[24-27] or BN(6-14)[28] which are important to keep the binding affinity. The reason is that the BN (7-14) analog keeps its affinity to human GRP receptors only on condition that its N-terminus has been protected by an acetyl group or an amino acid or spacer molecule (our unpublished data).

[$Cu^{II}$]-BZH7 (cyclam-(4-methylbenzoyl)-[βAla$^{11}$]BN (7-14)) showed very high binding affinity to all 3 human BN receptor subtypes as do the known pan-bombesin ligand [D-Tyr$^6$, β-Ala$^{11}$, Phe$^{13}$, Nle$^{14}$]BN (6-14)[24, 26] and the metallated panbombesin peptide [$Y^{III}$-DOTA$^0$, GABA$^1$, D-Tyr$^6$, β-Ala$^{11}$, Thi$^{13}$, Nle$^{14}$]BN (6-14)[19]. Recently, Chen et al[29] reported that [$^{177}$Lu]-AMBA (DOTA-Gly-[4-aminobenzoyl]BN (7-14)) has high affinity to the NMB-R (0.9 nM) and GRP-R (0.8 nM), and almost no affinity to the BNRS-3 (>1 μM). Nock et al[8] developed a BN-based peptide with an N-terminal open-chain tetraamine framework ([($N_4$-Bzdig)$^0$]BN (7-14)) for $^{99m}$Tc-labeling, which has high affinity to the NMB-R (0.65 nM) and GRP-R (0.9 nM) but negligible affinity to the BNRS-3 (37 nM). These results point out that βAla$^{11}$ is a key factor in maintaining high affinity to BNRS-3.

**Metabolic stability**

Compared to our previously developed/synthesized ligand (BZH2: DOTA-[D-Tyr$^{6}$, β-Ala$^{11}$, Thi$^{13}$, Nle$^{14}$]BN(6-14))[19], [$^{111}$In]-BZH4 has a 3.5 times lower stability in serum than [$^{111}$In]-BZH2, which proves that the replacement of Leu$^{13}$ by an unnatural amino acid (Thi) stabilizes the ligand significantly and indicates that the peptidases (CD10 /NEP)[30] may be responsible for the cleavage of His$^{12}$-Leu$^{13}$ or His$^{12}$-Thi$^{13}$ although the weakest peptide bond in [$^{111}$In]-BZH2 was identified to be βAla$^{11}$-His$^{12}$. In the prototype of [D-Tyr$^{6}$, β-Ala$^{11}$, Nle$^{14}$]BN(6-14), DOTA-GABA and CPTA conjugated to the peptide have a similar stability. However, compared to Cu-CPTA-D-Tyr-[β-Ala$^{11}$]BN(7-14), Cu-CPTA(or Cu-CPTA-Gly)-[β-Ala$^{11}$]BN(7-14) showed an improved stability by a factor of 5. Furthermore, Met$^{14}$ ([$^{64/67}$Cu]-BZH6) afforded a higher stability than Nle$^{14}$ ([$^{64/67}$Cu]-BZH5) by a factor of 2.

**In-vivo evaluation**

Rapid internalization and efficient trapping (i.e. residualization time of radiopeptide) allow for an optimal tumor-to-background ratio for imaging and even more important for a successful targeted radionuclide therapy.

All [$^{64/67}$Cu]-labeled BN analogs show a specific uptake in the PC-3 tumor and bombesin receptor-positive organs such as the pancreas. Especially, due to its highest binding affinity among this series of ligands, [$^{64/67}$Cu]-BZH7 internalized into PC-3 cells with the fastest rate and had a relatively slow externalization rate from PC-3 cells, which correlates with the high accumulation of the conjugate in targeted organs. [$^{64/67}$Cu]-BZH7 showed the highest uptake in the PC-3 tumor (11.2 ± 1.5% IA/g at 1 h p.i., 6.63 ± 0.80% IA/g at 4 h, and 4.14 ± 0.55% IA/g at 24 h), which is consistent with its in vitro behavior. These results are comparatively better than those of negatively charged BN analogs such as [$^{64}$Cu]-DOTA-Aoc-BN (7-14)[11] and [$^{64}$Cu]-DOTA-[Lys$^{3}$]BN[12] since [$^{64/67}$Cu]-BZH7(positively charged) has a 5 times higher affinity to the GRP receptor. As a consequence of its favorable properties [$^{64}$Cu]-BZH7 localized the PC-3 tumor very well with MicroPET imaging, and liver, kidneys and pancreas were distinguished as well. These results imply that $^{64}$Cu-labeled ligands can provide a high-resolution tool in the clinical diagnosis, e.g. in the detection of small-size metastases.

The uptake of all tested [$^{64}$Cu-CPTA]BN analogs in the liver and kidneys was high; this also holds for the [$^{64}$Cu-DOTA]-conjugated BN analogs[11, 12], indicating that the charge of $^{64}$Cu-labeled BN has no influence on the excretion pathway. Reports on the metabolism of copper-labeled antibody fragments indicate that intact complexes may clear via the kidneys and disassociated copper ions via the liver, similar to the situation observed with radiocopper-labeled

antibodies[31-33]. According to the comparison of $^{64}$Cu-labeled cross-bridged macrocyclic chelators[34], positively charged (+1) peptides showed significantly lower accumulation in the liver and kidneys than negatively charged (-1) ones. All these data imply that cross-bridged macrocyclic chelators may be more preferable for radionuclide therapy with $^{64/67}$Cu-BN analogs, affording a positive charge and hence a lower liver uptake.

The blocking experiment of [$^{64/67}$Cu]-BZH7, which was competed with [$Cu^{II}$]-BZH7, showed predominantly specific accumulation in GRP receptor-positive tissues such as pancreas, adrenals and PC-3 tumor. The radioactivity uptake in the kidneys was partially blocked. This might either be due to BN receptors present in the mouse kidney, since Dumesny et al[35] reported on the identification of mRNA of the GRP receptor in the rat kidney, or because an excessive [$Cu^{II}$]-BZH7 has already blocked the metabolism and clearance of [$^{64/67}$Cu]-BZH7.

As a hippurane-type molecule might facilitate clearance through the kidney, the introduction of a glycine-forming hippurane-type spacer molecule was expected to show a similar behavior. The kidney uptake was found to be decreased significantly at 1 h and 4 h p.i.; even under the condition of excessive [$Cu^{II}$]-BZH7, [$^{64/67}$Cu]-BZH8 was excreted faster from the kidneys than [$^{64/67}$Cu]-BZH7, indicating that the "pure" excretion of [$^{64/67}$Cu]-BZH7 was not as rapid as that of [$^{64/67}$Cu]-BZH8 provided that all binding sites of the GRP receptor in mice were blocked**.** These results also demonstrate that the non-target and target accumulations contribute simultaneously to the kidney uptake. Because [$^{64/67}$Cu]-BZH7 has higher affinity to the GRP-receptor than [$^{64/67}$Cu]-BZH8, the tumor-kidney ratio of [$^{64/67}$Cu]-BZH7 (with hippurane-type spacer) was not better than that of [$^{64/67}$Cu]-BZH8 (without hippurane-type spacer).

**Comparison of radionuclides**

Copper-64 is a radionuclide with good physical properties for PET imaging. It also holds therapeutic potential, due to its low energy $\beta^-$-emission (39.6%, $E_{\beta^- max}$ = 573 keV)[36], but its therapeutic efficacy is somewhat impeded by the high energy γ-radiation associated with $^{64}$Cu. Copper-67 ($T_{1/2}$ = 61.9 h) is a low energy β-emitter (19%, $E_{\beta^- max}$ = 577, 484, and 395 keV), its therapeutic β-emissions result in a mean energy of 141 keV, similar to the mean β-energy of $^{177}$Lu, and the mean particle range of 0.2 mm makes these nuclides very suitable for irradiation of small metastases. Similar to $^{177}$Lu, $^{67}$Cu emits low energy photons, which are particularly suitable for pretherapeutic diagnostic imaging with a γ-camera. In contrast to $^{177}$Lu, $^{67}$Cu has a shorter half-life (2.6 d compared with 6 d). $^{67}$Cu-labeled antibodies have excellent tumor targeting properties and are developed for radioimmunotherapy[37]. [$^{67}$Cu]-BZH7 may thus be another option in the clinical treatment of prostate cancer if high specific or carrier-free $^{67}$Cu is

available, and it would be interesting to compare its therapeutic efficacy with that of $^{64}$Cu- and $^{177}$Lu-labeled peptides.

## Conclusion

Reubi et al and Markwalder et al[5, 38] have reported a massive GRP receptor overexpression not only in prostate cancer tissue and prostatic intraepithelial neoplasia (PIN), but also with a high percentage in neoplastic and non-neoplastic breast cancer tissues as well as in gastrinomas, small cell lung carcinomas, renal cell carcinomas, and bone metastases of androgen-independent prostate cancer. The results of our study allow for the following conclusions:

1) [$^{64, 67}$Cu]-BZH7 (CPTA-[β-Ala$^{11}$]BN (7-14)) has the potential to visualize and possibly treat the above mentioned cancer types in the clinic;

2) The charge at the N-terminus has an influence on the pharmacologic and biologic properties of human GRP receptors (with a very slight difference of mouse GRP receptors);

3) The introduction of a glycine-forming hippurane-like spacer leads to an enhanced kidney clearance;

4) Met$^{14}$ is much better than Nle$^{14}$ for retaining the pharmacological behavior of the BN analog.

## Acknowledgements

We thank the Swiss National Science Foundation (Grant No. 3100A0-100390), for financial support of this work and Novartis Basel for analytical support, and Ms. Claudine Pfister for her kind work during the preparation of the article.

**Table 1**: Characteristics of compounds BZH4, BZH5, BZH6, BZH7 and BZH8, and their corresponding cold metallated compounds.

| Compound† | Calculated MW | Measured MW | | | RP-HPLC‡ retention time (min) |
|---|---|---|---|---|---|
| | | ESI (+) | ESI (-) | MALDI | |
| BZH4 | 1570.79 | 1609.1 ($[M+K]^+$) | 1607.7 ($[M+K-H]^-$) | 1570.5 ($[M+H]^+$) | 13.61 |
| BZH5 | 1415.73 | 1416.5 ($[M+H]^+$) | 1414.8 ($[M-H]^-$) | 1415.7 ($[M+H]^+$) | 14.54 |
| BZH6 | 1433.77 | 1434.1 ($[M+H]^+$) | 1432.3 ($[M-H]^-$) | 1433.8 ($[M+H]^+$) | 12.76 |
| BZH7 | 1270.59 | 1270.9 ($[M+H]^+$) | 1269.7 ($[M-H]^-$) | 1270.5 ($[M+H]^+$) | 12.97 |
| BZH8 | 1327.64 | 1328.1 ($[M+H]^+$) | 1326.7 ($[M-H]^-$) | 1327.8 $[M+H]^+$ | 12.54 |
| $[Cu^{II}]$-BZH4 | 1632.32 | 816.5 ($[M+2H]^{2+}$) | 814.3 ($[M-2H]^{2-}$) | 1632.4 $[M+H]^+$ | 15.28 |
| $[In^{III}]$-BZH4 | 1682.58 | ND | ND | 1682.4 $[M+H]^+$ | 14.81 |
| $[Cu^{II}]$-BZH5 | 1479.27 | ND | ND | 1477.6 $[M+H]^+$ | 16.20 |
| $[Cu^{II}]$-BZH6 | 1497.31 | ND | ND | 1497.7 $[M+H]^+$ | 13.18 |
| $[Cu^{II}]$-BZH7 | 1334.14 | ND | ND | 1332.4 $[M+H]^+$ | 13.83 |
| $[Cu^{II}]$-BZH8 | 1391.19 | ND | ND | 1392.3 $[M+H]^+$ | 13.32 |

Note: †. MW: molecular weight; BZH4: **DOTA-GABA-[D-Tyr$^6$, β-Ala$^{11}$, Nle$^{14}$]BN(6-14)**; BZH5: **CPTA-[D-Tyr$^6$, β-Ala$^{11}$, Nle$^{14}$]BN(6-14)**; BZH6: **CPTA-[D-Tyr$^6$, β-Ala$^{11}$]BN(6-14)**; BZH7: **CPTA-[β-Ala$^{11}$]BN(7-14)**; BZH8: **CPTA-[Gly$^6$, β-Ala$^{11}$]BN(6-14)**. ‡ RP HPLC eluents: A= 0.1% TFA in water and B= acetonitrile; gradient: 0-20 min, 80%-50% A; 20-21 min, 100% B; 21-24 min, 100% B; 25 min, 80% A.

**Table 2**: $IC_{50}$ values for displacement of GRP receptor-bound [$^{125}$I-Tyr$^{4}$]BN by increasing concentration of BN analogs. $IC_{50}$ values (nM ± SE) are in triplicates. Number of independent studies is in brackets.

| Code No. | Peptide structure | Charge | GRP receptor | |
|---|---|---|---|---|
| | | | human | mouse |
| [$Cu^{II}$]-BZH4 | $Cu^{II}$-DOTA-GABA-[D-Tyr$^{6}$, βAla$^{11}$, Nle$^{14}$]BN(6-14) | -1 | 26.3±3.5 (3) | 1.1±0.3 (3) |
| [$In^{III}$]-BZH4 | $In^{III}$-DOTA-GABA-[D-Tyr$^{6}$, βAla$^{11}$, Nle$^{14}$]BN(6-14) | 0 | 41.5±2.5 (2) | 0.8±0.4 (2) |
| [$Cu^{II}$]-BZH5 | $Cu^{II}$-CPTA -[D-Tyr$^{6}$, βAla$^{11}$, Nle$^{14}$]BN(6-14) | +2 | 3.2±0.5 (3) | 0.6±0.2 (3) |
| [$Cu^{II}$]-BZH6 | $Cu^{II}$-CPTA-[D-Tyr$^{6}$, βAla$^{11}$]BN(6-14) | +2 | 1.0±0.2 (3) | 0.8±0.2 (3) |
| [$Cu^{II}$]-BZH7 | $Cu^{II}$-CPTA-[βAla$^{11}$]BN(7-14) | +2 | 0.42±0.13 (4) | 0.22±0.07 (3) |
| [$Cu^{II}$]-BZH8 | $Cu^{II}$-CPTA-[Gly$^{6}$, βAla$^{11}$]BN(6-14) | +2 | 1.8±0.6 (3) | 0.8±0.2 (3) |

**Table 3**: Metabolic degradation kinetics calculated according to the equation: $A=A_0*\exp(-k_1*t)$[19].

| **Conjugates** | $k_1$ ($h^{-1}$) | $T_{1/2}$ (h) |
|---|---|---|
| [$^{111}$In]-BZH4 | 1.14 ± 0.26 | 0.61 ± 0.11 |
| [$^{64/67}$Cu]-BZH5 | 1.26 ± 0.31 | 0.55 ± 0.11 |
| [$^{64/67}$Cu]-BZH6 | 0.756 ± 0.168 | 0.92 ± 0.17 |
| [$^{64/67}$Cu]-BZH7 | 0.137 ± 0.066 | 5.1 ± 1.7 |
| [$^{64/67}$Cu]-BZH8 | 0.154 ± 0.054 | 4.5 ± 1.2 |

**Table 4:** Comparison of biodistribution and tissue ratios (4 h p.i.) of [$^{64/67}$Cu]-BZH5, [$^{64/67}$Cu]-BZH6, [$^{64/67}$Cu]-BZH7, and [$^{64/67}$Cu]-BZH8 in PC-3 tumor-bearing nude mice. Results are the mean (% IA/g) of groups of eight or four animals.

| Site | [$^{64/67}$Cu]-BZH5 | [$^{64/67}$Cu]-BZH6 | [$^{64/67}$Cu]-BZH7 | [$^{64/67}$Cu]-BZH8 |
|---|---|---|---|---|
| Blood | 0.182 ± 0.011 | 0.175 ± 0.021 | 0.154 ± 0.033 | 0.142 ± 0.004 |
| Muscle | 0.087 ± 0.006 | 0.109 ± 0.025 | 0.123 ± 0.032 | 0.064 ± 0.011 |
| Kidneys | 4.59 ± 0.65 | 5.84 ± 0.55 | 6.87 ± 1.16 | 4.97 ± 0.46 |
| Adrenals | 25.7 ± 2.2 | 27.3 ± 3.7 | 30.8 ±4.1 | 25.3 ± 1.3 |
| Pancreas | 34.9 ± 1.6 | 58.0 ± 3.9 | 57.2 ± 2.7 | 36.4 ± 3.4 |
| Spleen | 2.66 ± 0.06 | 3.67 ± 0.25 | 3.77 ± 0.62 | 2.93 ± 0.40 |
| Stomach | 1.81 ± 0.17 | 3.42 ± 0.82 | 3.76 ± 0.48 | 2.81 ± 0.29 |
| Bowel | 4.62 ± 0.23 | 8.19 ± 1.06 | 7.25 ± 0.74 | 6.44 ± 0.21 |
| Liver | 10.78 ± 1.32 | 10.01 ± 1.03 | 7.31 ± 0.87 | 8.51 ± 0.44 |
| Lung | 0.48 ± 0.16 | 0.72 ± 0.12 | 0.67 ± 0.13 | 0.78 ± 0.18 |
| Heart | 0.25 ± 0.04 | 0.35 ± 0.08 | 0.22 ± 0.05 | 0.20 ± 0.02 |
| Bone | 0.34 ± 0.04 | 1.05 ± 0.23 | 0.90 ± 0.16 | 0.49 ± 0.07 |
| Tumor | 3.47 ± 0.15 | 5.05 ± 0.46 | 6.63 ± 0.80 | 4.29 ± 0.70 |
| Tumor to normal tissue radioactivity ratio | | | | |
| Tumor/Blood | 19 | 29 | 43 | 30 |
| Tumor/Muscle | 40 | 46 | 54 | 67 |
| Tumor/Liver | 0.3 | 0.5 | 0.9 | 0.5 |
| Tumor/Kidney | 0.8 | 0.9 | 1.0 | 0.9 |

**Table 5:** Kinetic studies of [$^{64/67}$Cu]-BZH7 and tissue ratios in PC-3 tumor-bearing nude mice. Results are the mean (% IA/g) of groups of eight or four animals.

| Site | 1h | 4h | 24h | 4h, Blocked |
|---|---|---|---|---|
| Blood | 0.461 ± 0.078 | 0.154 ± 0.033 | 0.102 ± 0.010 | 0.149 ± 0.013 |
| Muscle | 0.539 ± 0.384 | 0.123 ± 0.032 | 0.072 ± 0.018 | 0.082 ± 0.002 |
| Kidneys | 10.4 ± 1.2 | 6.87 ± 1.16 | 2.48 ± 0.25 | 2.44 ± 0.10 |
| Adrenals | 36.5 ± 5.7 | 30.8 ± 4.1 | 5.29 ± 0.36 | 1.39 ± 0.06 |
| Pancreas | 81.3 ± 15.2 | 57.2 ± 2.7 | 18.7 ± 1.6 | 1.30 ± 0.08 |
| Spleen | 5.03 ± 0.40 | 3.77 ± 0.62 | 2.15 ± 0.21 | 0.88 ± 0.05 |
| Stomach | 3.98 ± 0.32 | 3.76 ± 0.48 | 2.23 ± 0.39 | 0.51 ± 0.07 |
| Bowel | 10.8 ± 1.42 | 7.25 ± 0.74 | 5.14 ± 0.20 | 0.63 ± 0.16 |
| Liver | 9.89 ± 0.89 | 7.31 ± 0.87 | 3.01 ± 0.47 | 8.90 ± 0.43 |
| Lung | 1.01 ± 1.42 | 0.67 ± 0.13 | 0.64 ± 0.31 | 0.58 ± 0.02 |
| Heart | 0.34 ± 0.05 | 0.22 ± 0.05 | 0.21 ± 0.03 | 0.14 ± 0.01 |
| Bone | 1.16 ± 0.20 | 0.90 ± 0.16 | 0.43 ± 0.10 | 0.21 ± 0.06 |
| Tumor | 11.2 ± 1.5 | 6.63 ± 0.80 | 4.14 ± 0.55 | 0.71 ± 0.08 |
| Tumor to normal tissue radioactivity ratio | | | | |
| Tumor/Blood | 24 | 43 | 41 | |
| Tumor/Muscle | 21 | 54 | 58 | |
| Tumor/Liver | 1.1 | 0.9 | 1.4 | |
| Tumor/Kidney | 1.1 | 1.0 | 1.7 | |

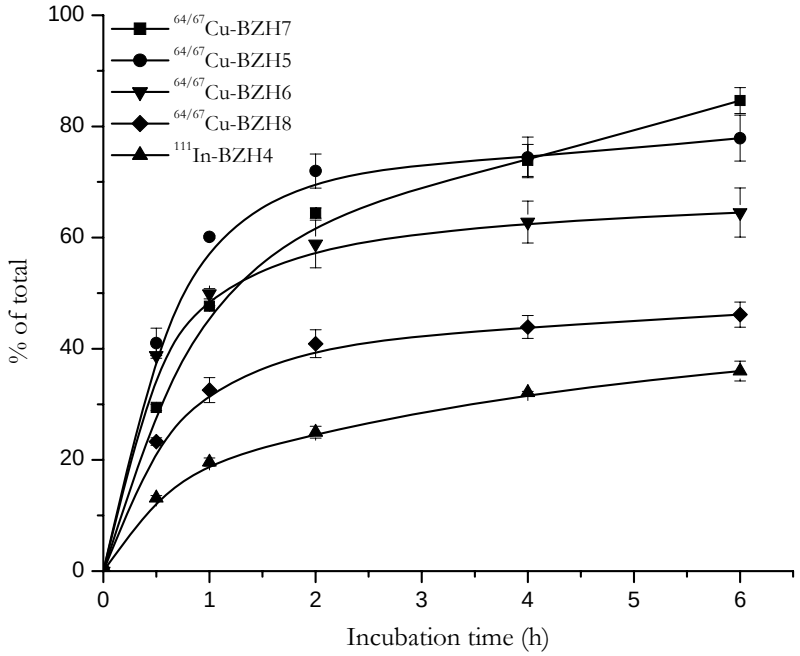


**Figure 1** Comparison of the internalization of [$^{111}$In]-BZH4 and [$^{64/67}$Cu]-labeled BZH5, BZH6, BZH7 and BZH8 into PC-3 cells. Data result from two independent experiments with triplicates in each experiment and are expressed as specific internalization.

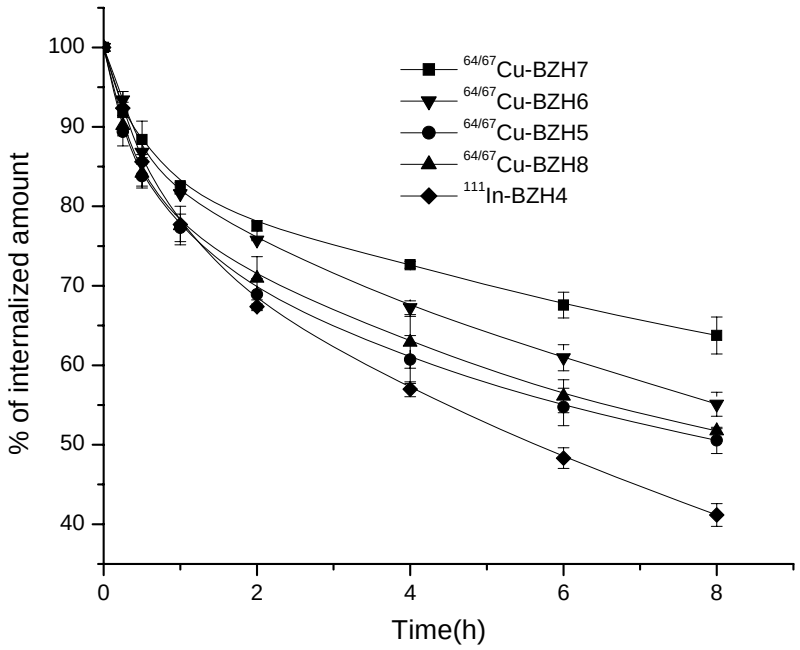


**Figure 2** Comparison of the externalization of [$^{111}$In]-BZH4, [$^{64/67}$Cu]-labeled BZH7, BZH5, BZH6 and BZH8 from PC-3 cells. Data result from two independent experiments with triplicates in each experiment.

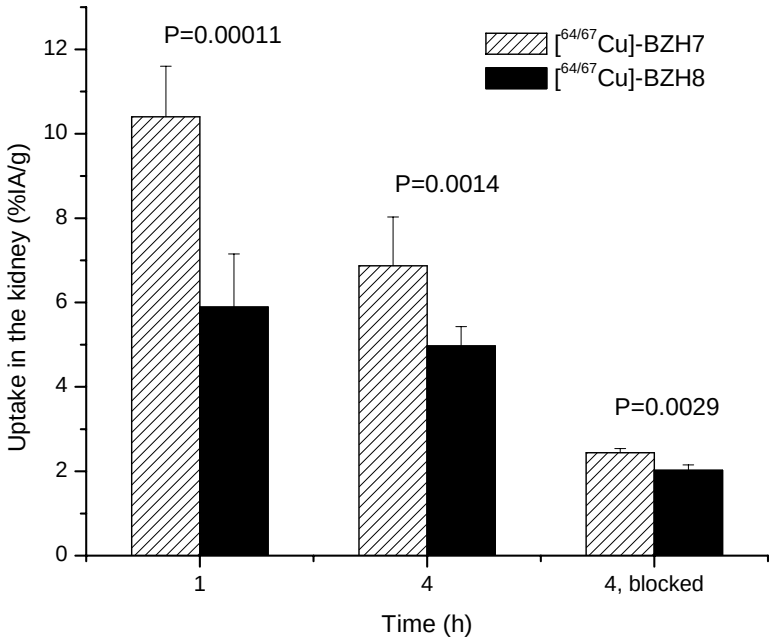


**Figure 3** Decrease of kidney uptake by introduction of a glycine forming hippurane-type spacer molecule ([$^{64/67}$Cu]-BZH8).

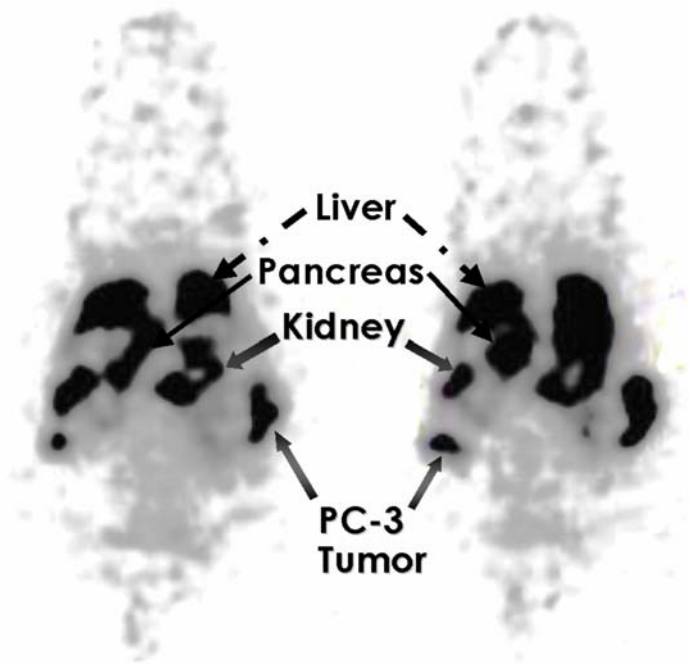


**Figure 4** MicroPET imaging of [$^{64}$Cu]-BZH7 in PC-3 tumor-bearing nude mice (5 MBq, 3 h p.i.). Both tumors inoculated in each flank of the mouse are visible with clear contrast from the adjacent background, pancreas, liver and kidneys. The high-resolution imaging displays the cortex of one kidney. The PC-3 tumor uptake was 3% IA/g, and the ratio between tumor and kidney reached 2 at 23 h p.i. The results of direct tissue counting and PET imaging were consistent.

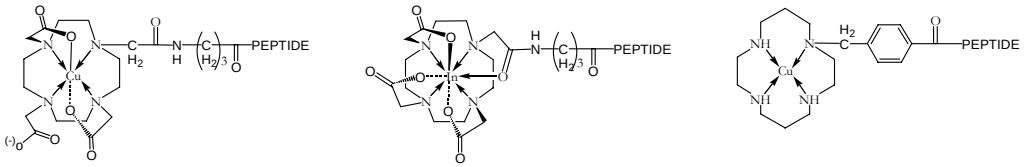


**-1** **0** **+2**

**Scheme 1** Metal-complexed conjugates with different charges at the N-terminus under the condition of pH 7.4.

BZH5: 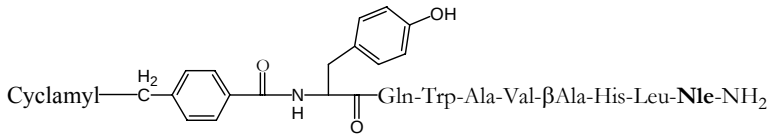


BZH6: 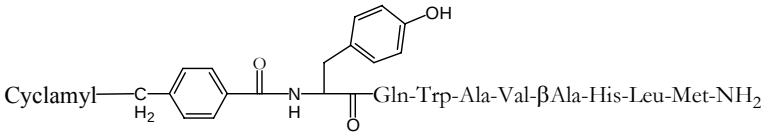


BZH7: 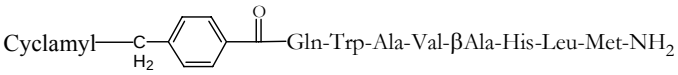


BZH8: 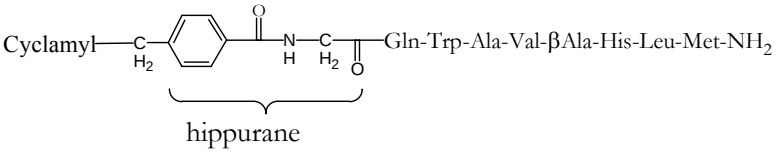


**Scheme 2** Comparison of the 14th position (Nle versus Met) and 6th position (D-Tyr, Gly and without amino acid).

**References**


1. Karra, S. R.; Schibli, R.; Gali, H.; Katti, K. V.; Hoffman, T. J.; Higginbotham, C.; Sieckman, G. L.; Volkert, W. A. *Bioconjug Chem* **1999,** 10, (2), 254-60.
2. Smith, C. J.; Volkert, W. A.; Hoffman, T. J. *Nucl Med Biol* **2003,** 30, (8), 861-8.
3. Smith, C. J.; Sieckman, G. L.; Owen, N. K.; Hayes, D. L.; Mazuru, D. G.; Kannan, R.; Volkert, W. A.; Hoffman, T. J. *Cancer Res* **2003,** 63, (14), 4082-4088.
4. Van de Wiele, C.; Dumont, F.; Dierckx, R. A.; Peers, S. H.; Thornback, J. R.; Slegers, G.; Thierens, H. *J Nucl Med* **2001,** 42, (11), 1722-1727.
5. Reubi, J. C.; Wenger, S.; Schmuckli-Maurer, J.; Schaer, J. C.; Gugger, M. *Clin Cancer Res* **2002,** 8, (4), 1139-1146.
6. Zhou, J.; Chen, J.; Mokotoff, M.; Zhong, R.; Shultz, L. D.; Ball, E. D. *Clin Cancer Res* **2003,** 9, (13), 4953-60.
7. Reubi, J. C.; Korner, M.; Waser, B.; Mazzucchelli, L.; Guillou, L. *Eur J Nucl Med Mol Imaging* **2004,** 31, (6), 803-10.
8. Nock, B. A.; Nikolopoulou, A.; Galanis, A.; Cordopatis, P.; Waser, B.; Reubi, J. C.; Maina, T. *J Med Chem* **2005,** 48, (1), 100-110.
9. Lin, K. S.; Luu, A.; Baidoo, K. E.; Hashemzadeh-Gargari, H.; Chen, M. K.; Pili, R.; Pomper, M.; Carducci, M.; Wagner, H. N., Jr. *Bioconjug Chem* **2004,** 15, (6), 1416-23.
10. Smith, C. J.; Volkert, W. A.; Hoffman, T. J. *Nucl Med Biol* **2005,** 32, (7), 733-40.
11. Rogers, B. E.; Bigott, H. M.; McCarthy, D. W.; Della Manna, D.; Kim, J.; Sharp, T. L.; Welch, M. J. *Bioconjug Chem* **2003,** 14, (4), 756-763.
12. Chen, X.; Park, R.; Hou, Y.; Tohme, M.; Shahinian, A. H.; Bading, J. R.; Conti, P. S. *J Nucl Med* **2004,** 45, (8), 1390-1397.
13. Blower, P. J.; Lewis, J. S.; Zweit, J. *Nucl Med Biol* **1996,** 23, (8), 957-80.
14. Nock, B.; Nikolopoulou, A.; Chiotellis, E.; Loudos, G.; Maintas, D.; Reubi, J. C.; Maina, T. *Eur J Nucl Med Mol Imaging* **2003,** 30, (2), 247-258.
15. Maina, T.; Nock, B. A.; Zhang, H.; Nikolopoulou, A.; Waser, B.; Reubi, J. C.; Maecke, H. R. *J Nucl Med* **2005,** 46, (5), 823-30.
16. Smith-Jones, P. M.; Fridrich, R.; Kaden, T. A.; Novak-Hofer, I.; Siebold, K.; Tschudin, D.; Maecke, H. R. *Bioconjug Chem* **1991,** 2, (6), 415-21.
17. Anderson, C. J.; Pajeau, T. S.; Edwards, W. B.; Sherman, E. L.; Rogers, B. E.; Welch, M. J. *J Nucl Med* **1995,** 36, (12), 2315-25.
18. Studer, M.; Kaden, T. A.; Maecke, H. R. *Helvetica Chimica Acta* **1990,** 73, (1), 149-53.
19. Zhang, H.; Chen, J.; Waldherr, C.; Hinni, K.; Waser, B.; Reubi, J. C.; Maecke, H. R. *Cancer Res* **2004,** 64, (18), 6707-6715.
20. Schwarzbach, R.; Zimmermann, K.; Blauenstein, P.; Smith, A.; Schubiger, P. A. *Appl Radiat Isot* **1995,** 46, (5), 329-36.
21. Zimmermann, K.; Grunberg, J.; Honer, M.; Ametamey, S.; Schubiger, P. A.; Novak-Hofer, I. *Nucl Med Biol* **2003,** 30, (4), 417-27.
22. Reubi, J. C.; Wenger, S.; Schmuckli-Maurer, J.; Schaer, J. C.; Gugger, M. *Clin Cancer Res* **2002,** 8, (4), 1139-46.
23. Fleischmann, A.; Laderach, U.; Friess, H.; Buechler, M. W.; Reubi, J. C. *Lab Invest* **2000,** 80, (12), 1807-17.
24. Mantey, S. A.; Weber, H. C.; Sainz, E.; Akeson, M.; Ryan, R. R.; Pradhan, T. K.; Searles, R. P.; Spindel, E. R.; Battey, J. F.; Coy, D. H.; Jensen, R. T. *J Biol Chem* **1997,** 272, (41), 26062-26071.
25. Darker, J. G.; Brough, S. J.; Heath, J.; Smart, D. *J Pept Sci* **2001,** 7, (11), 598-605.

26. Pradhan, T. K.; Katsuno, T.; Taylor, J. E.; Kim, S. H.; Ryan, R. R.; Mantey, S. A.; Donohue, P. J.; Weber, H. C.; Sainz, E.; Battey, J. F.; Coy, D. H.; Jensen, R. T. *Eur J Pharmacol* **1998,** 343, (2-3), 275-287.
27. Weber, D.; Berger, C.; Heinrich, T.; Eickelmann, P.; Antel, J.; Kessler, H. *J Pept Sci* **2002,** 8, (8), 461-475.
28. Lin, J. T.; Coy, D. H.; Mantey, S. A.; Jensen, R. T. *Eur J Pharmacol* **1995,** 294, (1), 55-69.
29. Chen, J.; Nguyen, H.; Metcalfe, E.; Eaton, S.; Arunachalam, T.; Raju, N.; Cappelletti, E.; Lattuada, L.; Cagnolini, A.; Maddalena, M.; Lantry, L. E.; Nunn, A.; Swenson, R. E.; Tweedle, M. F.; Linder, K. E. In *Formulation and in Vitro Metabolism Studies with $^{177}$Lu-AMBA; a Radiotherapeutic Compound that Targets Gastrin Releasing Peptide Receptors*, Annual Congress of the EANM, Helsinki, 2004; 'Ed.'^'Eds.' Helsinki, 2004; p^pp S281.
30. Shipp, M. A.; Tarr, G. E.; Chen, C. Y.; Switzer, S. N.; Hersh, L. B.; Stein, H.; Sunday, M. E.; Reinherz, E. L. *Proc Natl Acad Sci U S A* **1991,** 88, (23), 10662-6.
31. Mirick, G. R.; O'Donnell, R. T.; DeNardo, S. J.; Shen, S.; Meares, C. F.; DeNardo, G. L. *Nucl Med Biol* **1999,** 26, (7), 841-845.
32. Bass, L. A.; Wang, M.; Welch, M. J.; Anderson, C. J. *Bioconjug Chem* **2000,** 11, (4), 527-532.
33. Novak-Hofer, I.; Zimmermann, K.; Schubiger, P. A. *Cancer Biother Radiopharm* **2001,** 16, (6), 469-481.
34. Sprague, J. E.; Peng, Y.; Sun, X.; Weisman, G. R.; Wong, E. H.; Achilefu, S.; Anderson, C. J. *Clin Cancer Res* **2004,** 10, (24), 8674-82.
35. Dumesny, C.; Whitley, J. C.; Baldwin, G. S.; Giraud, A. S.; Shulkes, A. *Am J Physiol Renal Physiol* **2004,** 287, (3), F578-85.
36. Wang, M.; Caruano, A. L.; Lewis, M. R.; Meyer, L. A.; VanderWaal, R. P.; Anderson, C. J. *Cancer Res* **2003,** 63, (20), 6864-9.
37. Novak-Hofer, I.; Schubiger, P. A. *Eur J Nucl Med Mol Imaging* **2002,** 29, (6), 821-830.
38. Markwalder, R.; Reubi, J. C. *Cancer Res* **1999,** 59, (5), 1152-1159.

*Manuscript 4*

# DOTA-PESIN, a Promising Bombesin Analogue Labeled with $^{67/68}$Ga, $^{177}$Lu for GRP Receptor-expressing Tumors and their Metastases

**Hanwen Zhang [a], Jochen Schumacher[c], Michael Eisenhut[c], Jean Claude Reubi [b], Beatrice Waser [b], Damian Wild [d], Helmut R Maecke [a]**

[a] Division of Radiological Chemistry, Department of Radiology, University Hospital, Petersgraben 4, CH-4031 Basel, Switzerland;
[b] Division of Cell Biology and Experimental Cancer Research, Institute of Pathology, University of Berne, PO Box 62, Murtenstrasse 31, CH-3010 Berne, Switzerland;
[c] Department of Diagnostic and Therapeutic Radiology, German Cancer Research Center, Heidelberg, Germany;
[d] Clinic and Institute of Nuclear Medicine, Department of Radiology, University Hospital, Petersgraben 4, CH-4031 Basel, Switzerland.

Present status:
Manuscript accepted for publication in the *European Journal for Nuclear Medicine and Molecular Imaging*.

Eur J Nucl Med Mol Imaging
DOI 10.1007/s00259-006-0347-4

ORIGINAL ARTICLE

# DOTA-PESIN, a DOTA-conjugated bombesin derivative designed for the imaging and targeted radionuclide treatment of bombesin receptor-positive tumours

**Hanwen Zhang · Jochen Schuhmacher · Beatrice Waser · Damian Wild · Michael Eisenhut · Jean Claude Reubi · Helmut R. Maecke**

Received: 13 June 2006 / Accepted: 17 November 2006


**Abstract**
*Purpose* We aimed at designing and developing a novel bombesin analogue, DOTA-$PEG_4$-BN(7–14) (DOTA-PESIN), with the goal of labelling it with $^{67/68}$Ga and $^{177}$Lu for diagnosis and radionuclide therapy of prostate and other human cancers overexpressing bombesin receptors.
*Methods* The 8-amino acid peptide bombesin (7–14) was coupled to the macrocyclic chelator DOTA via the spacer 15-amino-4,7,10,13-tetraoxapentadecanoic acid ($PEG_4$). The conjugate was complexed with Ga(III) and Lu(III) salts. The GRP receptor affinity and the bombesin receptor subtype profile were determined in human tumour specimens expressing the three bombesin receptor subtypes. Internalisation and efflux studies were performed with the human GRP receptor cell line PC-3. Xenografted nude mice were used for biodistribution.
*Results* [$Ga^{III}$/$Lu^{III}$]-DOTA-PESIN showed good affinity to GRP and neuromedin B receptors but no affinity to BB3. [$^{67}$Ga/$^{177}$Lu]-DOTA-PESIN internalised rapidly into PC-3 cells whereas the efflux from PC-3 cells was relatively slow. In vivo experiments showed a high and specific tumour uptake and good retention of [$^{67}$Ga/$^{177}$Lu]-DOTA-PESIN. [$^{67}$Ga/$^{177}$Lu]-DOTA-PESIN highly accumulated in GRP receptor-expressing mouse pancreas. The uptake specificity was demonstrated by blocking tumour uptake and pancreas uptake. Fast clearance was found from blood and all non-target organs except the kidneys. High tumour-to-normal tissue ratios were achieved, which increased with time. PET imaging with [$^{68}$Ga]-DOTA-PESIN was successful in visualising the tumour at 1 h post injection. Planar scintigraphic imaging showed that the $^{177}$Lu-labelled peptide remained in the tumour even 3 days post injection.
*Conclusion* The newly designed ligands have high potential with regard to PET and SPECT imaging with $^{68/67}$Ga and targeted radionuclide therapy with $^{177}$Lu.

**Keywords** Gallium-68 · Lutetium-177 · Bombesin receptors · Targeted radiotherapy · Prostate cancer

H. Zhang · H. R. Maecke (✉)
Division of Radiological Chemistry, Department of Radiology,
University Hospital Basel,
Petersgraben 4,
4031 Basel, Switzerland
e-mail: hmaecke@uhbs.ch

J. Schuhmacher · M. Eisenhut
Department of Radiopharmaceutical Chemistry,
German Cancer Research Centre,
Heidelberg, Germany

B. Waser · J. C. Reubi
Division of Cell Biology and Experimental Cancer Research,
Institute of Pathology, University of Berne,
P.O. Box 62, Murtenstrasse 31,
3010 Berne, Switzerland

D. Wild
Clinic and Institute of Nuclear Medicine,
Department of Radiology, University Hospital,
Basel, Switzerland

## Introduction

Radionuclides coupled to receptor-specific peptides are currently under investigation in clinical trials involving different tumours [1]. They specifically localise receptors overexpressed on the plasma membrane and then internalise into cells [2–4]. The prototypes of these peptides are analogues of somatostatin [5].

In designing radiometal-based radiopeptides for cancer diagnosis and treatment, important factors to consider are

half-life, mode of decay, cost and availability of the radionuclide. In diagnostic imaging [6], $^{99m}$Tc, $^{123}$I, $^{67}$Ga and $^{111}$In are used for SPECT and $^{18}$F, $^{11}$C, $^{64}$Cu and $^{68}$Ga for positron emission tomography (PET). $^{177}$Lu-labelled peptides have become attractive in targeted radiotherapy of small tumours or metastases owing to their excellent radiophysical properties and commercial availability of the radionuclide [5, 7, 8]. $^{68}$Ga, on the other hand, is a promising metallic positron emitter ($t_{1/2}$=68 min, 89%, $E_{\beta^+ max}$=1.90 MeV) for regular use in PET imaging because of its production from a $^{68}$Ga/$^{68}$Ge generator, which allows independence from an on-site cyclotron and offers almost unlimited availability if two or three of these generators are used concomitantly as elution is possible every 3 h [9, 10]. To develop a ligand for the labelling with these two radionuclides would therefore seem promising.

In the field of radiolabelled peptides, bombesin (BN) analogues have become a promising class of ligands as gastrin-releasing peptide (GRP) receptors, a subtype of BN receptors, were found to be overexpressed on primary prostatic invasive carcinoma (and their invaded lymph nodes), breast tumours and gastrointestinal stromal tumours [11]. Up to now, many types of radiolabelled BN analogues have been designed to target GRP receptor-expressing tumours [12–24]. In particular, Van de Wiele et al. reported on a first study of prostate ($n$=4) and breast cancer ($n$=6) patients [13, 25]. Their results showed that $^{99m}$Tc-RP527 visualised four of six breast and one of four prostate carcinomas. This radiopeptide showed inferior properties to many other radiopeptides in the PC-3 tumour-bearing nude mouse model [26]. As $^{99m}$Tc-Demobesin 1 ([$^{99m}$Tc-N4$^{0-1}$, bzlg$^{0}$,(D)Phe$^{6}$,Leu-NHEt$^{13}$,*des*-Met$^{14}$]BN(6–14)) has shown higher affinity to the GRP receptor and a higher tumour accumulation in PC-3 tumour-bearing mice [27] than $^{99m}$Tc-RP527, it may be a superior candidate for studying in patients.

We have recently developed DOTA (1,4,7,10-tetraazacyclododecane-1,4,7,10-tetraacetic acid)- and DTPA-modified (pan)BN radioligands having high affinity to all three human BN receptors [i.e. neuromedin B receptor (NMB-R), GRP-R and BN receptor subtype-3 (BB3)] [17]. Preliminary results in clinical studies of two of these radiopeptides have shown occasional uptake in the pancreas and relatively fast washout from lesions when labelled with $^{111}$In. The fast washout may be due to a low metabolic stability of these radiopeptides. Therefore, we set up a programme to synthesise BN-based radiopeptides with improved metabolic stability, an optimised tumour-to-kidney ratio and lack of affinity to BB3. From a series of peptides evaluated, DOTA-PEG$_4$-BN(7–14) (DOTA-PESIN) looked particularly promising in our preclinical studies.

Here we present data on the synthesis and labelling of this peptide with the positron emitter $^{68}$Ga, the $\gamma$- and Auger electron emitter $^{67}$Ga and the $\beta(\gamma)$-emitter $^{177}$Lu. In addition, we studied the receptor subtype affinity profile and the in vivo biodistribution of radiolabelled DOTA-PESIN with regard to BN receptor subtypes. PET imaging and scintigraphy were also performed.

## Materials and methods

All chemicals were obtained from commercial sources and used without further purification. Rink amide 4-methylbenzhydrylalanine (MBHA) resin and all Fmoc-protected amino acids are commercially available from NovaBiochem (Laeufelfingen, Switzerland). [$^{67}$Ga]Cl$_3$ was purchased from Mallinckrodt Medical (Petten, the Netherlands) and [$^{177}$Lu]Cl$_3$ from IDB (Petten, the Netherlands). Fmoc-15-amino-4,7,10,13-tetraoxapentadecanoic acid (Fmoc-PEG$_4$-OH) was obtained from Quanta BioDesign (Powell, Ohio, USA) and 1,4,7,10-tetraazacyclododecane-1,4,7-*tris*(acetic acid-t-butyl ester)-10-acetic acid [DOTA-*tris*($^{t}$Bu ester)] from Macrocyclics (Dallas, Texas, USA). Electrospray ionisation mass spectroscopy was carried out with a Finnigan SSQ 7,000 spectrometer (Bremen, Germany) and MALDI-MS measurement on a Voyager sSTR equipped with an Nd:YAG laser (Applied Biosystems, Framingham, USA). Ten milligrams of 3,5-dimethoxy-4-hydroxycinnamic acid were dissolved in 0.05% TFA of acetonitrile/water (1:1) and used as matrix. Analytical high-performance liquid chromatography (HPLC) was performed on a Hewlett Packard 1050 HPLC system with a multiwavelength detector and a flow-through Berthold LB 506 Cl $\gamma$-detector (Regensdorf, Switzerland) using a Macherey-Nagel Nucleosil 120 C$_{18}$ column (Oensingen, Switzerland) (eluents: A=0.1% TFA in water and B=acetonitrile; gradient: 0–20 min, 80%–50% A; 21–24 min, 100% B; 24–25 min, 80% A). Preparative HPLC was performed on a Metrohm HPLC system LC-CaDI 22–14 (Herisau, Switzerland) with a Macherey-Nagel VP 250/21 Nucleosil 100–5 C$_{18}$ column (eluents: A=0.1% TFA in water and B=acetonitrile; gradient: 0–10 min, 70%–52% A; 11–14 min, 100% B; 14–15 min, 70% A). Quantitative $\gamma$-counting was performed on a COBRA 5003 $\gamma$-system well counter from Packard Instruments (Meriden, CT, USA). Solid phase peptide synthesis was performed on a semiautomatic peptide synthesiser commercially available from Rink Combichem Technologies (Bubendorf, Switzerland). The cell culture medium was Dulbecco's minimal essential medium (DMEM) with 10% or 1% foetal calf serum (FCS) from BioConcept (Allschwil, Switzerland). PET imaging was performed on a Siemens ECAT EXACT HR$^{+}$ scanner (Siemens/CTI, Knoxville, TN, USA), and scintigraphic imaging was carried out on a PRISM 2000 XP camera (Philips, the Netherlands). $^{68}$Ga was obtained from a

$^{68}$Ge/$^{68}$Ga generator which consists of a column containing a self-made phenolic ion exchanger loaded with $^{68}$Ge and coupled in series with a small anion exchanger column (AG 1×8 Cl-1, mesh 200–400; Bio-Rad, Munich, Germany) to concentrate $^{68}$Ga during elution [28].

## Synthesis

DOTA-PESIN was synthesised on solid support as described previously [17]. In brief, the peptide was assembled on a Rink amide MBHA resin according to classical Fmoc chemistry on a semi-automatic peptide synthesiser. Trityl and *tert*-butoxycarbonyl were used as side chain-protecting groups of His and Trp, respectively. Fmoc-$PEG_4$-OH (four equivalents) and DOTA-*tris*(tBu) ester (three equivalents) were consecutively coupled to the peptide with HATU [1.2 equivalents based on Fmoc-$PEG_4$-OH or DOTA-*tris*(tBu) ester] as activating agent. Cleavage from the resin and deprotection as well as product purification and identification were performed according to a previously described protocol [17]. Calculated MW: 1573.81; MS-ES(−): 1610.3 $[M+K-H]^-$, 804.8 $[M+K-2H]^{2-}$; MS-ES(+): 806.8 $[M+K+2H]^{2+}$; MALDI, m/z (%): 1573.7 (100, $[M+H]^+$), 1594.7 (5, $[M+Na]^+$); HPLC $t_R$: 12.5 min on analytical HPLC (purity: >98%).

*[$Ga^{III}$/$Lu^{III}$]-DOTA-PESIN* A mixture of DOTA-PESIN (0.5 μmol) in 500 μl 0.5 mol/l ammonium acetate buffer (pH 5) was incubated with 1.5 μmol $Ga(NO_3)_3{\cdot}9H_2O$ or $Lu(NO_3)_3{\cdot}5H_2O$ (in 0.04 mol/l HCl) at 95°C for 25 min, and purified over a SepPak $C_{18}$ cartridge (Waters Corp., Milford, MA) preconditioned with 10 ml ethanol and 10 ml water. The cartridge was eluted with 10 ml water followed by 3 ml methanol, resulting in the metal$^{III}$-DOTA-peptide after evaporation of methanol. The final product was analysed by analytical HPLC and MALDI. *[$Ga^{III}$-DOTA-PESIN* (calculated MW): 1640.51; MALDI, m/z (%): 1641.7 (100, $[M+H]^+$), 1663.6 (20, $[M+Na]^+$); HPLC $t_R$: 13.8 min. Purity: >99%. *[$Lu^{III}$]-DOTA-PESIN* (calculated MW): 1745.76; MALDI, m/z (%): 1745.8 (100, $[M+H]^+$), 1767.7 (10, $[M+Na]^+$); HPLC $t_R$: 14.1 min. Purity: >99%.

## Preparation of radiotracer for in vitro and in vivo studies

[$^{177}$Lu]-DOTA-PESIN was prepared by dissolving 10 μg of the peptide (6.35 nmol) in ammonium acetate buffer (300 μl, 0.5 mol/l, pH 5.5); after addition of $^{177}LuCl_3$ (2 mCi), the solution was incubated for 15 min at 95°C. A 1.5 molar excess of $Lu(NO_3)_3{\cdot}5H_2O$ was added and incubated again for 15 min. Subsequently, [$^{177}$Lu]-DOTA-PESIN was purified utilising a SepPak $C_{18}$ cartridge preconditioned with 10 ml methanol and 10 ml water; the cartridge was eluted with 3 ml water, followed by 2 ml ethanol to yield pure [$^{177}$Lu]-DOTA-PESIN. For biodistribution studies, the labelling was performed accordingly without the addition of cold $Lu(NO_3)_3{\cdot}5H_2O$. Oxidation of C-terminal $MetNH_2$ was suppressed by the addition of methionine. The solution for injection was prepared by dilution with 0.9% NaCl (0.1% BSA) to provide the radioligand solution. [$^{67}$Ga]-DOTA-PESIN was prepared in the same way. All radiolabelled peptides were analysed with analytical HPLC and showed a radiochemical purity of >97%.

## Preparation of [$^{68}$Ga]-DOTA-PESIN for PET imaging

The generator eluate containing ~0.5 GBq $^{68}$Ga in 0.2 ml/0.5 mol/l HCl was evaporated to dryness and redissolved in 0.2 ml acetate buffer (pH 4.8, 0.1 mol/l). After addition of 5 μl of a 1 mmol/l aqueous DOTA-PESIN solution, the mixture was kept for 10 min at 90°C. The uncomplexed $^{68}$Ga was separated by adsorption onto a SepPak $C_{18}$ cartridge that was equilibrated with 0.1 mol/l acetate buffer (pH 6.2), whereas [$^{68}$Ga]-DOTA-PESIN was eluted with 1.5 ml ethanol. After evaporation of the organic solvent, the radiotracer was redissolved in 0.01 mol/l phosphate-buffered saline (pH 7.4) containing 0.5 mg/ml human serum albumin. The preparations were checked for bound and free $^{68}$Ga by paper chromatography using Whatman No.1 and methanol/0.01 mol/l acetate buffer (pH 6.2) at a ratio of 55:45. $^{68}$Ge contamination of the [$^{68}$Ga]-DOTA-PESIN preparation was determined by gamma counting after a decay period of ≥30 h.

## Binding affinity and receptor subtype profile

Using [$^{125}$I-D-Tyr$^4$]BN as a GRP-R preferring ligand, the $IC_{50}$ values of [$^{nat}$Ga/$^{nat}$Lu]-DOTA-PESIN were measured in competitive binding experiments performed with increasing concentrations of $^{nat}$Ga/$^{nat}$Lu-labelled peptides in successive tissue sections containing tumours expressing GRP-R [29].

The binding affinity profile for the three BN receptor subtypes was determined as described in detail previously [11, 30]. Human tumours were selected that have previously been shown to express predominantly one single BN receptor subtype. $IC_{50}$ values were determined in competitive binding experiments performed with increasing amounts of $^{nat}$Ga/$^{nat}$Lu-DOTA-PESIN using [$^{125}$I-D-Tyr$^6$, β-Ala$^{11}$, Phe$^{13}$, Nle$^{14}$]BN(6–14) as universal radioligand.

## Cell culture

PC-3 cells (ECACC, Wiltshire SP4 OJG, UK) were cultured in DMEM. DMEM was supplemented with vitamins,

essential and non-essential amino acids, L-glutamine, antibiotics (penicillin/streptomycin), fungicide [amphotericin B (Fungizone)] and 10% FCS.

### Internalisation and efflux studies

Internalisation and externalisation experiments were performed in six-well plates as described previously [17]. Briefly, approximately 3 kBq (0.25 pmol) of [$^{177}$Lu/$^{67}$Ga]-DOTA-PESIN was added to PC-3 cell-containing incubation medium ($0.5–1\times10^6$ cells per well) and incubated at 37°C in a 5% $CO_2$ environment at different time points (0.5, 1, 2, 4 and 6 h). A large excess of [$Ga^{III}$]-DOTA-PESIN (0.4 μmol/l, 150 μl) was used to determine non-specific internalisation. At each time point, the internalisation was stopped by removal of the medium followed by washing the cells with ice-cold solution composed of 0.9% NaCl/0.01 mol/l $Na_2HPO_4$/0.01 mol/l $KH_2PO_4$ (pH 7.2). Cells were then treated (twice) with glycine buffer (0.05 mol/l glycine solution, pH adjusted to 2.8 with 1 mol/l HCl) for 5 min to distinguish between cell surface-bound (acid buffer removable) and internalised (acid-resistant) radioligand. Finally, cells were detached from the plates by incubation with 1 mol/l NaOH for 10 min at 37°C, and the radioactivity was measured in a gamma counter. The percentage of added activity per million cells (% of total) was calculated for internalisation at each time point.

For externalisation studies, PC-3 cells were allowed to internalise [$^{177}$Lu/$^{67}$Ga]-DOTA-PESIN for 2 h; they were then exposed to an acid wash, as described in the internalisation experiments, to dissociate the cell surface-bound radioligand. Then 1 ml of culture medium (1% FCS) was added to each well, the cells were incubated at 37°C in a 5% $CO_2$ environment and the externalisation of the cell-incorporated radioactivity was studied at different times. The culture medium was collected and measured for radioactivity. The percentage of total internalised radiotracer was calculated for efflux.

### Biodistribution experiments in PC-3 tumour-bearing nude mice

After a slight anaesthesia with isoflurane in an air/oxygen mixture, athymic nude female mice (Harlan, the Netherlands) were implanted subcutaneously on the right flank with about 10 million PC-3 tumour cells, which were freshly expanded in 100 μl sterilised PBS solution.

Seven to ten days after inoculation the tumours weighed 60–130 mg and the mice were injected via the tail vein with 10 pmol radiolabelled peptide (about 0.12 MBq [$^{67}$Ga]-DOTA-PESIN), diluted in 0.9% NaCl (0.1% BSA, pH 7.4, total injected volume 100 μl). For the determination of non-specific uptake in the tumour and receptor-positive organs, a group of four animals was injected with a mixture of 10 pmol radiolabelled peptide/50 μg [$Ga^{III}$]-DOTA-PESIN in 0.9% NaCl solution (injected volume, 150 μl). To study the biodistribution of [$^{67}$Ga]-DOTA-PESIN, mice were sacrificed at 1, 4 and 24 h post injection; the organs of interest were collected, rinsed of excess blood, blotted, weighed and counted in a γ-counter. The percentage of injected activity per gram (%IA/g) was calculated for each tissue. The total counts injected per animal were determined by extrapolation from counts of an aliquot taken from the injected solution as a standard. For the biodistribution study of [$^{177}$Lu]-DOTA-PESIN, mice were sacrificed at 4, 24, 48 and 72 h post injection.

To study the influence of lysine, 15 mg lysine was co-injected with 10 pmol [$^{67}$Ga]-DOTA-PESIN in 150 μl, and the animals were sacrificed at 4 h post injection.

Biodistribution studies with [$^{67}$Ga]-DOTA-PESIN were also performed at the German Cancer Research Centre under conditions of PET imaging with [$^{68}$Ga]-DOTA-PESIN. Six- to 8-week-old female Swiss CD1 *nu*/*nu* mice were inoculated with a PC-3 tumour in the right flank. Eleven to thirteen days later, tumours weighing 70–175 mg were ready for experiment. Fifteen pmol (0.61 MBq) [$^{67}$Ga]-DOTA-PESIN was injected into the lateral tail vein. Mice were sacrificed at 1 h p.i. and organs of interest collected for measurement as described previously [31].

### PET imaging with [$^{68}$Ga]-DOTA-PESIN

PET imaging was performed on a Siemens ECAT EXACT $HR^+$ scanner (Siemens/CTI, Knoxville, TN, USA), and PET data were acquired in 3D mode and reconstructed iteratively with a full 3D algorithm from a $256\times256$ matrix for viewing transaxial, coronal and sagittal slices of 0.57 mm thickness. Pixel size was 1.14 mm and transaxial resolution obtained was 2.8 mm. For imaging studies, an awake female CD1 *nu*/*nu* mouse that was inoculated with a PC-3 tumour on the right flank was lightly restrained and injected with 1.94 MBq, 15 pmol [$^{68}$Ga]-DOTA-PESIN via a lateral tail vein. One hour later the mouse was anaesthetised with isoflurane in an air/oxygen mixture and sacrificed, then positioned in the tomograph symmetrically in the centre of the field of view. Acquisition of PET data was obtained with a 30-min emission and a 10-min transmission scan.

### Scintigraphy with [$^{177}$Lu]-DOTA-PESIN

Scintigraphic imaging of PC-3 tumour xenografts was performed on a PRISM 2000 XP camera. Two mice were inoculated with a PC-3 tumour on the right hind leg. After 16 days the tumours had grown enough for imaging. Both

animals were lightly restrained and injected with 13.5 MBq, 0.32 nmol [$^{177}$Lu]-DOTA-PESIN via a lateral tail vein; one of them was co-injected with 50 μg [$Ga^{III}$]-DOTA-PESIN. Four hours after injection, the animals were anaesthetised with isoflurane in an air/oxygen mixture and positioned on the head of the camera symmetrically in the centre of the field of view while anaesthesia was monitored by observing the breath frequency. Scans were taken 15 min after anaesthesia at 4, 24, 48 and 72 h post injection.

All animal experiments were performed in compliance with the Swiss regulations for animal treatment (Bundesamt für Veterinärwesen, approval no. 789), or with the German laws for the protection of animals.

### Statistical analysis

Data are expressed as mean ± SD, which were calculated on Microsoft Excel. Student's *t* test (Origin 6, Microcal Software, Inc., Northampton, MA) was used to determine statistical significance at the 95% confidence level with $p<0.05$ being considered significantly different.

## Results

### Synthesis and radiolabelling

DOTA-PESIN (Fig. 1) was synthesised using Fmoc strategy, affording yields of 45% based on the removal of the first Fmoc group; the purity analysed by HPLC was ≥97%. DOTA-PESIN and [$Ga^{III}$/$Lu^{III}$]-DOTA-PESIN were characterised by electrospray and MALDI TOFF mass spectrometry. Radiolabelled DOTA-PESIN was prepared by incubation with $^{67/68}GaCl_3$ or $^{177}LuCl_3$ at elevated temperature. The labelling yield of [$^{67/68}$Ga]-DOTA-PESIN was ≥98% at specific activities of >129 GBq μmol$^{-1}$ for $^{68}$Ga and >12 GBq μmol$^{-1}$ for $^{67}$Ga, respectively. The radiolytic oxidation of methionine in [$^{177}$Lu]-DOTA-PESIN was about 2% when the specific activity was ≤11.6 GBq μmol$^{-1}$ and reached 26% at 60 GBq μmol$^{-1}$. With optimisation of the labelling conditions, labelling yields of ≥95% of [$^{177}$Lu]-DOTA-PESIN were achieved at a specific activity of >85 GBq μmol$^{-1}$ in the presence of 400 μg methionine per 370 MBq $^{177}$Lu.

### Receptor binding affinity and profile

Table 1 shows the GRP-R binding affinities of DOTA-PESIN and its respective metallopeptides to human cancer tissue overexpressing GRP-R, as determined by a competitive binding assay using [$^{125}$I-Tyr$^4$]BN as radioligand. On the human GRP-R, the $IC_{50}$ values were 9.5±3.4 nmol/l for DOTA-PESIN and 6.1±3.0 nmol/l and 6.6±0.1 nmol/l for the $Lu^{III}$- and $Ga^{III}$-complexed peptides, respectively. There was no significant difference on the mouse GRP-R.

[$Ga^{III}$]-DOTA-PESIN and [$Lu^{III}$]-DOTA-PESIN were also studied with respect to the BN receptor subtype profile using human cancer tissue shown to express predominantly a single BN receptor subtype. Using [$^{125}$I-D-Tyr$^6$, β-Ala$^{11}$, Phe$^{13}$, Nle$^{14}$]BN(6–14) as radioligand, the binding studies showed good binding affinities to NMB-R and GRP-R, and no affinity to BB3-R.

### Internalisation and efflux studies

Internalisation of both radiopeptides was followed for 6 h. Both $^{177}$Lu- and $^{67}$Ga-labelled DOTA-PESIN showed specific and time-dependent cell uptake, reaching 39.1±1.1% and 43.7±1.8% of the total amount added to the medium, respectively, after 6 h of incubation at 37°C (Fig. 2). Within the first 2 h of incubation [$^{177}$Lu]-DOTA-PESIN internalised somewhat faster than [$^{67}$Ga]-DOTA-PESIN but after 4 h there was no statistical difference. The efflux kinetics (Fig. 3) showed a cellular retention of 52.5±1.6% of the total internalised activity 20 h after start of efflux for both radiopeptides.

### Animal biodistribution studies

Biodistribution studies using the $^{67}$Ga/$^{177}$Lu-labelled peptides were performed with athymic nude female mice bearing the PC-3 human prostate tumour; the results are presented in Tables 2 and 3 as percentage of injected activity per gram of tissue (%IA/g).

According to Table 2, [$^{67}$Ga]-DOTA-PESIN and [$^{177}$Lu]-DOTA-PESIN (data in parentheses in the following) displayed rapid blood clearance from the PC-3-bearing mice, with 0.47±0.06 %IA/g at 1 h and 0.11±0.04 (0.04±0.01) %IA/g at 4 h post injection. Both radiotracers were

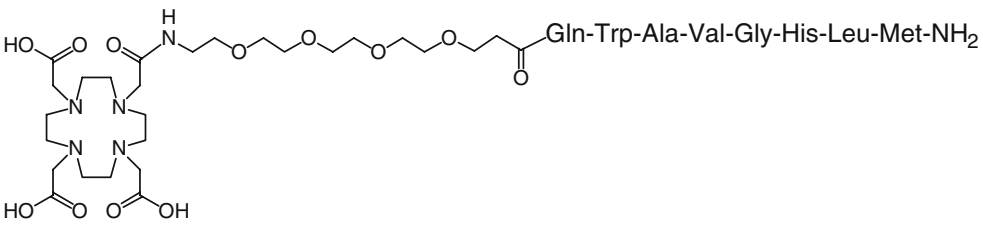


**Fig. 1** Structural formula of DOTA-PESIN

**Table 1** $IC_{50}$ values for metallated DOTA-PESIN when competed with [$^{125}$I-Tyr$^4$]BN against the human and mouse GRP-R and affinity profiles using [$^{125}$I-Tyr$^6$, β-Ala$^{11}$, Phe$^{13}$, Nle$^{14}$]BN(6–14)

| Compound | Human GRP-R | Mouse GRP-R | BN receptor subtypes | | |
|---|---|---|---|---|---|
| | | | NMB-R | GRP-R | BB3-R |
| DOTA-PESIN | 9.5±3.4 (3) | ND | ND | ND | ND |
| [Lu$^{III}$]-DOTA-PESIN | 6.1±3.0 (3) | ND | 15.0±4.0 (2) | 8.3±1.7 (2) | >1,000 (2) |
| [Ga$^{III}$]-DOTA-PESIN | 6.6±0.1 (3) | 7.0±1.2 (3) | 12.5±0.5 (2) | 10.0±0.0 (2) | >1,000 (2) |

$IC_{50}$ values (nmol/l±SE) are in triplicates. Numbers of independent studies are listed in parentheses
*ND* not determined

quickly washed out from the GRP-R-negative tissues except the kidneys. [$^{67}$Ga/$^{177}$Lu]-DOTA-PESIN also showed high uptake in the human prostate tumour xenograft and in the mouse GRP-R-positive organs, e.g. at 4 h the tumour uptake was 8.77±1.88 (7.46±1.64) %IA/g and the pancreas uptake 43.8±6.9 (39.0±4.9) %IA/g. In vivo competition experiments (Table 2) involving co-injection of 50 μg [Ga$^{III}$]-DOTA-PESIN with [$^{67}$Ga]-DOTA-PESIN resulted in a >94% reduction of uptake in the tumour and also in a reduction of uptake in other GRP-R-positive organs, e.g. >95% in the pancreas and 97% in the pituitary, 83–85% in the adrenals, spleen and bowel, and 78% in the stomach, showing specific receptor-mediated uptake in these tissues. The injection of the blocking dose had no significant influence on the uptake in other non-target organs whereas it led to a somewhat decreased kidney uptake. Co-injection of lysine did not reduce the kidney uptake, and the ratio between tumour and kidney remained almost unchanged. The impact of the blocking dose on biodistribution of [$^{177}$Lu]-DOTA-PESIN can be seen from the scans shown in Fig. 6.

Due to the rapid clearance from the body, high tumour-to-background ratios were found (Table 3). These ratios increased with time. For instance, the ratios of [$^{67}$Ga]-DOTA-PESIN between tumour and blood (muscle) varied from 31 (62) to 211 (237) during 1 h to 24 h post injection; for [$^{177}$Lu]-DOTA-PESIN, the respective ratios were 201 (147) at 4 h, 215 (387) at 24 h and 715 (486) at 72 h post injection. Both radiotracers also displayed high tumour-to-kidney and tumour-to-liver ratios (in parentheses): 2.4–2.6 (22–23) for the $^{67}$Ga-labelled and 1.7–3.6 (36–52) for the $^{177}$Lu-labelled peptide.

The pharmacokinetics (Fig. 4) of [$^{67}$Ga]-DOTA-PESIN shows the potential to visualise the tumour very early owing to the high initial accumulation, which reached 14.8±2.4 % IA/g at 1 h p.i. (9.40±1.39 %IA/g with an injected dose of 15 pmol and a different mouse strain), decreased to 8.77± 1.88 %IA/g at 4 h and was still 6.76±0.29 %IA/g at 24 h. [$^{177}$Lu]-DOTA-PESIN also displayed a high uptake in the tumour and a relatively slow washout: 7.46±1.64 %IA/g at 4 h, 5.81±0.40 %IA/g at 24 h, 4.05±0.23 %IA/g at

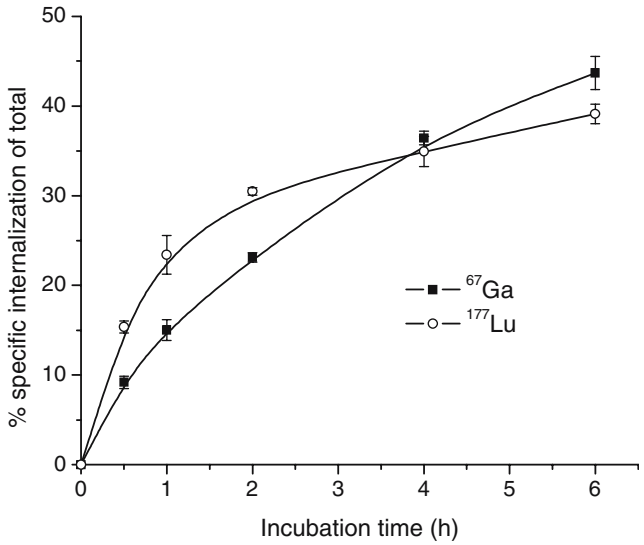


**Fig. 2** Internalisation of $^{67}$Ga-labelled (■) and $^{177}$Lu-labelled (○) DOTA-PESIN into PC-3 cells. Data are from two independent experiments with triplicates in each experiment and are expressed as % specific internalisation of total activity added to the medium

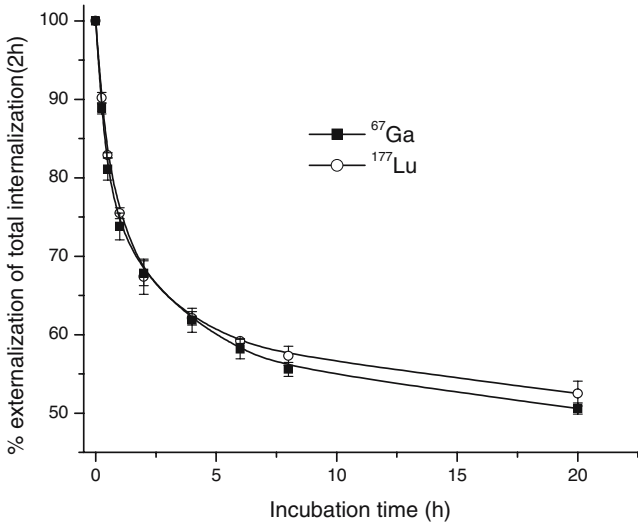


**Fig. 3** Externalisation of $^{67}$Ga-labelled (■) and $^{177}$Lu-labelled (○) DOTA-PESIN from PC-3 cells. Cells were allowed to internalise for 2 h. Data are from two independent experiments with triplicates in each experiment and are expressed as % specifically externalised of total activity internalised added to the medium

**Table 2** Biodistribution analysis (%IA/g ± SD) of $^{67}$Ga and $^{177}$Lu-labelled DOTA-PESIN in PC-3 tumour-bearing nude mice

| Site | $^{67}$Ga[a] | $^{67}$Ga[b] | | | | $^{177}$Lu[b] |
|---|---|---|---|---|---|---|
| | 1 h | 1 h | 4 h | 4 h blocked[c] | 4 h lysine[d] | 4 h |
| Blood | 0.556±0.120 | 0.471±0.060 | 0.108±0.041 | 0.103±0.029 | 0.235±0.012 | 0.037±0.011 |
| Muscle | 0.160±0.046 | 0.243±0.170 | 0.042±0.008 | 0.043±0.004 | 0.068±0.014 | 0.051±0.015 |
| Adrenals | NC | 20.6±2.1 | 15.8±3.2 | 2.80±2.59 | 16.1±2.4 | 15.3±3.4 |
| Pancreas | 47.7±4.7 | 65.3±8.7 | 43.8±6.9 | 2.26±2.00 | 54.8±8.3 | 39.0±4.9 |
| Spleen | 2.62±0.28 | 2.67±0.47 | 2.25±0.16 | 0.48±0.05 | 2.36±0.10 | 2.55±0.55 |
| Kidney | 4.27±0.66 | 6.27±0.94 | 3.36±0.47 | 2.09±0.27 | 4.67±0.97 | 4.67±0.78 |
| Stomach | NC | 4.77±0.65 | 1.72±0.86 | 0.39±0.28 | 2.39±0.21 | 1.68±0.43 |
| Bowel | 7.23±0.66 | 7.41±0.79 | 3.65±1.55 | 0.57±0.47 | 5.75±1.21 | 3.77±1.30 |
| Liver | 0.50±0.10 | 0.64±0.15 | 0.41±0.06 | 0.44±0.15 | 0.37±0.03 | 0.21±0.04 |
| Lung | 0.60±0.12 | 0.69±0.16 | 0.41±0.16 | 0.19±0.05 | 0.22±0.03 | 0.10±0.04 |
| Heart | NC | 0.31±0.08 | 0.06±0.01 | 0.06±0.01 | 0.12±0.01 | 0.06±0.01 |
| Bone | 0.35±0.06 | 0.60±0.20 | 0.40±0.14 | 0.22±0.10 | 0.62±0.07 | 0.48±0.06 |
| Pituitary | NC | 18.7±9.8 | 3.35±1.62 | 0.09±0.08 | 3.07±0.77 | 3.44±0.53 |
| Tumour | 9.40±1.39 | 14.8±2.5 | 8.77±1.88 | 0.52±0.21 | 8.87±1.1 | 7.46±1.63 |

Results are the mean of groups of four to eight mice
*NC* not collected
[a] PC-3 tumour-bearing CD nude mice were used for the biodistribution of 15 pmol (0.61 MBq) [$^{67}$Ga]-DOTA-PESIN
[b] 10 pmol [$^{67}$Ga/$^{177}$Lu]-DOTA-PESIN was injected to PC-3 tumour-bearing athymic nude mice
[c] Blocked by co-injection of 50 μg [Ga$^{III}$]-DOTA-PESIN
[d] Co-injection of 15 mg lysine per mouse

48 h and 2.43±0.12 %IA/g at 72 h. In the pancreas, [$^{177}$Lu]-DOTA-PESIN was released faster than the $^{67}$Ga-labelled peptide. In addition, the release of [$^{177}$Lu]-DOTA-PESIN from the pancreas and kidneys was faster than from the tumour, leading to an increasing tumour-to-organ ratio with time.

## PET imaging

Iteratively reconstructed PET images of PC-3 tumour xenografts with [$^{68}$Ga]-DOTA-PESIN (1.94 MBq, 15 pmol) were performed at 1 h post injection (Fig. 5). The PC-3 tumour was located in the thoracic wall, and was perceptible with clear contrast from the adjacent background in the transaxial slices. Coronal slices distinctly show the tumour and kidneys. Sagittal slices demonstrate that [$^{68}$Ga]-DOTA-PESIN accumulates predominantly in the PC-3 tumour, pancreas and kidneys. The results of direct tissue counting and of PET imaging were consistent.

## Scintigraphy

Figure 6 shows the scintigraphic imaging of PC-3 tumour xenografts with [$^{177}$Lu]-DOTA-PESIN (left: unblocked; right: blocked with 50 μg [Ga$^{III}$]-DOTA-PESIN). Imaging was performed at 4, 24, 48 and 72 h after injection. In the blocked mouse the tumour could not be visualised and only the kidneys were visible, whereas the PC-3 tumour of the non-blocked mouse was visualised with clear contrast from the adjacent background at all time points. Prominent uptake was also observed in the pancreas and kidneys. The imaging kinetics showed that [$^{177}$Lu]-DOTA-PESIN was preferably retained in the tumour rather than in the

**Table 3** Radioactivity ratios between PC-3 tumour and other organs of $^{67}$Ga- and $^{177}$Lu-labelled DOTA-PESIN in PC-3 tumour-bearing female athymic nude mice [8≥*n*≥4]

| Time (h) | Blood | | Muscle | | Kidney | | Liver | |
|---|---|---|---|---|---|---|---|---|
| | $^{67}$Ga | $^{177}$Lu | $^{67}$Ga | $^{177}$Lu | $^{67}$Ga | $^{177}$Lu | $^{67}$Ga | $^{177}$Lu |
| 1 | 31 | | 62 | | 2.4 | | 23 | |
| 4 | 81 | 201 | 209 | 147 | 2.6 | 1.7 | 22 | 36 |
| 24 | 211 | 215 | 237 | 387 | 2.4 | 2.5 | 23 | 43 |
| 48 | | 476 | | 488 | | 3.1 | | 52 |
| 72 | | 715 | | 486 | | 3.6 | | 48 |

Tumour-to-blocked tumour ratio (4 h)=16.9

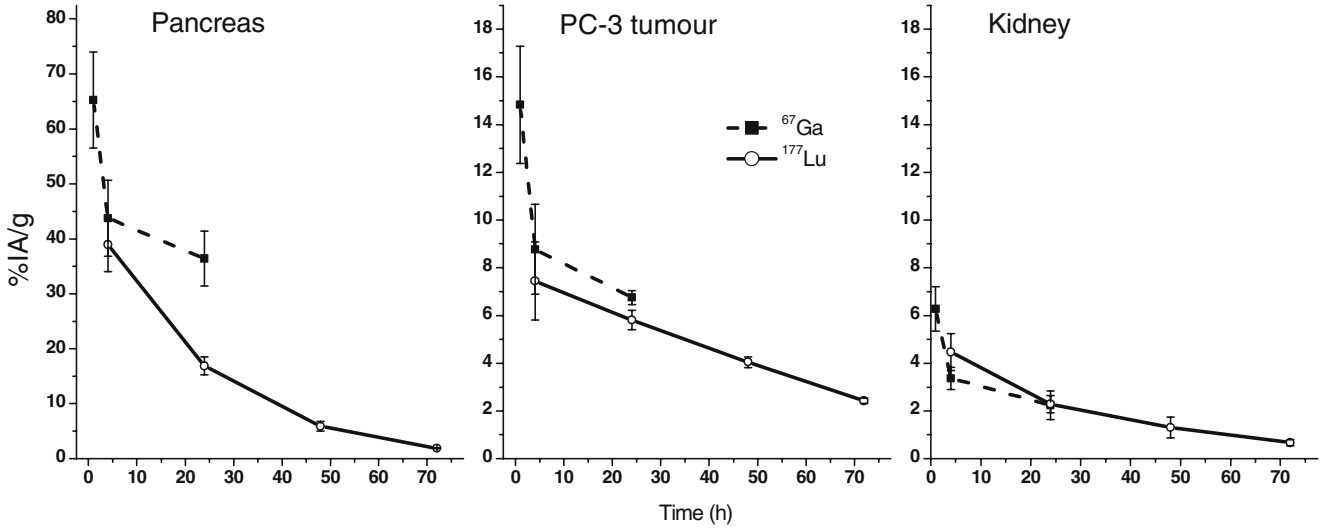


**Fig. 4** Kinetics of $^{67}$Ga-labelled (■) and $^{177}$Lu-labelled (○) DOTA-PESIN in PC-3 tumour-bearing mice (*left*, pancreas; *middle*, PC-3 tumour; *right*, kidney)

pancreas and kidneys. These imaging results are consistent with biodistribution data (Fig. 4).

## Discussion

We report on the development of a radiopeptide which can be used in SPECT ($^{67}$Ga), PET ($^{68}$Ga) and targeted radionuclide therapy ($^{177}$Lu) of BN receptor-positive tumours such as prostate and breast cancer or gastrointestinal stromal tumours. As part of a small library of peptides, which differ by the spacer between the chelate and the pharmacophoric peptide, DOTA-$PEG_4$-BN(7–14) appeared to have promising properties in terms of a relatively high tumour-to-kidney and tumour-to-liver ratio. Therefore we decided to study this peptide in depth after labelling with $^{67}$Ga, $^{68}$Ga and $^{177}$Lu with the aim of introducing these radiopeptides into the clinic. DOTA (1,4,7,10-tetraazacyclododecane-1,4,7,10-tetraacetic acid) was chosen as chelator since it forms $M^{3+}$ complexes with high in vitro and in vivo stability [32]. $PEG_4$ (15-amino-4,7,10,13-tetraoxapentadecanoic acid) was chosen as spacer and pharmacokinetic modifier. Very long PEG-based spacers (>3,000 D) coupled to peptides or antibodies appear to decrease the binding affinity of these biomolecules to their receptors and to lower the rate of internalisation significantly, as shown by Rogers et al. using a [$^{64}$Cu]-DOTA-PEG-BN (7–14) derivative [33]. Smaller versions do not seem to have a sufficient influence on the pharmacokinetics and hydrophilicity [31, 33].

The presented peptide was synthesised on solid phase with an overall yield of >45%. $^{68}$Ga labelling was straight-

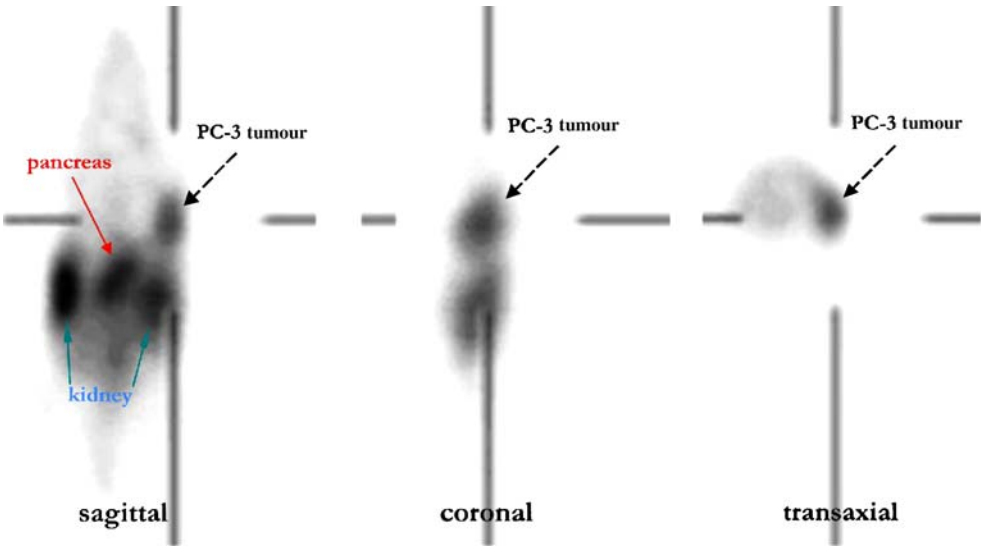


**Fig. 5** Iteratively reconstructed PET images of PC-3 tumour xenograft with [$^{68}$Ga]-DOTA-PESIN (1.94 MBq, 15 pmol) performed at 1 h post injection. The transaxial slice shows the PC-3 tumour (right flank) to be located in the thoracic wall. The coronal slice shows a clear distinction between tumour and kidneys. The sagittal slice demonstrates that [$^{68}$Ga]-DOTA-PESIN accumulates predominantly in the PC-3 tumour, pancreas and kidneys

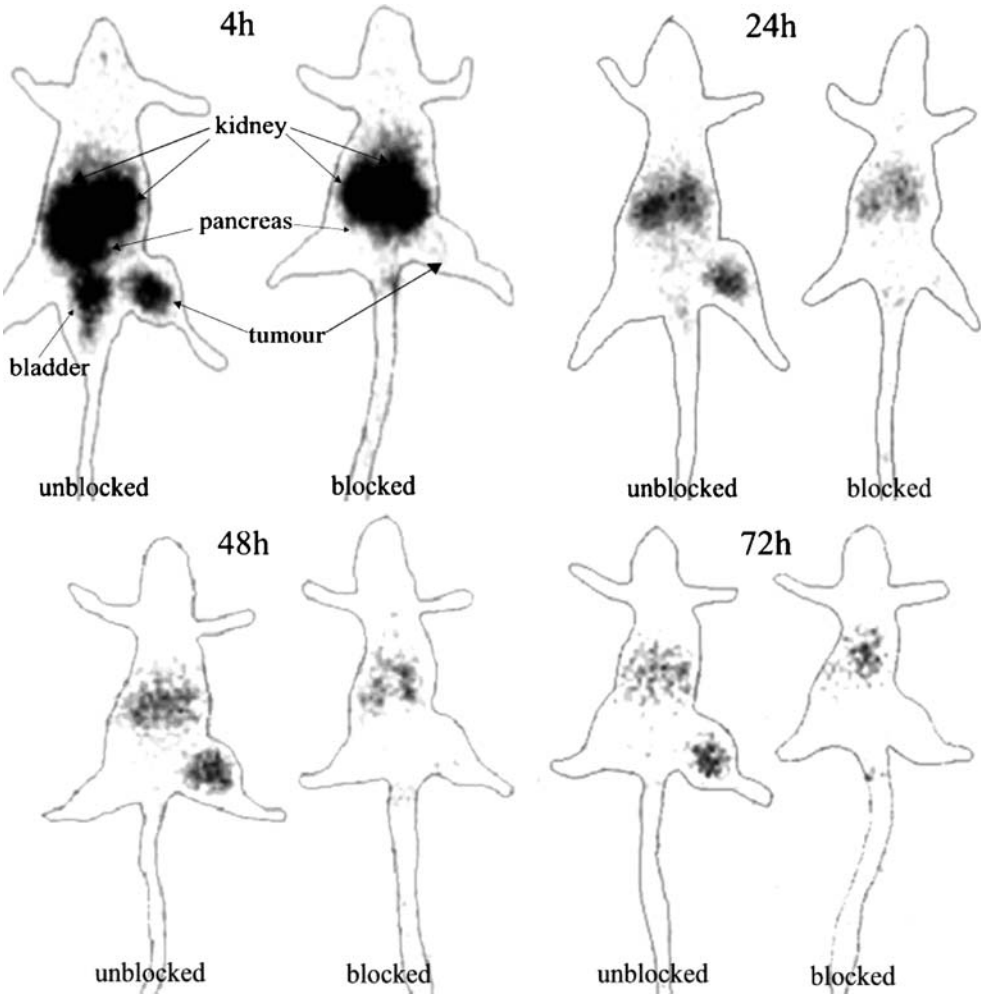


**Fig. 6** Scintigraphic images of [$^{177}$Lu]-DOTA-PESIN in PC-3 tumour-bearing mice at 4, 24, 48 and 72 h post injection (13.5 MBq, blocked with 50 μg [$Ga^{III}$]-DOTA-PESIN. *Left*, unblocked; *right*, blocked)

forward and afforded high radiochemical yields at a reasonable specific activity of ≥130 GBq μmol$^{-1}$, which allowed production of good PET images at 1 h post injection. Sagittal slices clearly showed that [$^{68}$Ga]-DOTA-PESIN mainly localises the PC-3 tumour, the GRP receptor-positive pancreas and the kidneys.

Binding studies using the GRP receptor ligand [$^{125}$I-$Tyr^4$]BN revealed medium affinity of [$Ga^{III}$]-DOTA-PESIN and [$Lu^{III}$]-DOTA-PESIN to the human GRP receptor and no difference between human and mouse GRP receptors, at least for [$Ga^{III}$]-DOTA-PESIN. The affinity to the three human BN receptor subtypes using the universal radioligand [$^{125}$I-D-$Tyr^6$, β-$Ala^{11}$, $Phe^{13}$, $Nle^{14}$]BN(6–14) showed that both metallopeptides have good to moderate affinity to the GRP and the NMB receptor and no affinity to the BB3 receptor. The affinities are about ten times lower than those of truncated BN(7–14) and intact BN derivatives coupled to bifunctional tetra-amines, which show $IC_{50}$ values between 0.2 and 2 nmol/l to the GRP receptor and, with one exception, also to the NMB receptor. The best of the $^{99m}$Tc-labelled compounds have $K_d$ values and $IC_{50}$ values below 1 nmol/l [19]. There was no significant difference in affinity between the peptides metallated with $Ga^{3+}$ or $Lu^{3+}$. This is in contrast to DOTA-octreotide derivatives; these conjugates show a distinctly improved binding affinity when labelled with radiogallium [32, 34].

The rate of internalisation into PC-3 cells was similar for the two radiopeptides and somewhat more efficient than the internalisation of the panbombesin ligands studied previously in the same assay and under the same conditions [17]. This similarity does not reflect the distinct difference in binding affinity. The high rate of internalisation of the two radiopeptides indicates that they are agonists.

Efflux curves of [$^{67}$Ga]-DOTA-PESIN and [$^{177}$Lu]-DOTA-PESIN from the PC-3 cells after 2 h of internalisation are essentially identical and their half-lives are ≥20 h, which is much longer than those of the panbombesin derivatives. Efflux studies were also performed with [$^{177}$Lu-DOTA-Aoc]BN(7–14) but only up to 2 h [18]. Within this time period the two compounds behave similarly. [$^{67}$Ga-$DOTA^0$-$PEG_2$, D-$Tyr^6$, β-$Ala^{11}$, $Thi^{13}$, $Nle^{14}$]BN(7–14) and the corresponding $^{177}$Lu-labelled radiopeptide externalise

with a somewhat different rate ($t_{1/2}$ ($^{67}$Ga)=16.5±2.4 h; $t_{1/2}$ ($^{177}$Lu)=12.8±1.4 h) [31]. A prolonged intracellular retention is of importance if long-lived radionuclides are to be used in therapy studies.

After administration of [$^{67}$Ga/$^{177}$Lu]-DOTA-PESIN, clearance from the circulation was fast and whole body clearance proceeded via the urinary system, unlike the positively charged $^{99m}$Tc-$N_4$-labelled BN analogues, which are partly excreted via the hepatobiliary tract [19, 27]. Clearance from GRP receptor-negative tissues was also rapid except from the kidneys.

Initially, tumour uptake was very high (14.8% IA/g at 1 h), approaching the uptake of the best radiopeptides studied so far in the PC-3 tumour model [27]. This new radiopeptide has a high tumour-to-liver ratio which may make it even somewhat superior to the best $^{99m}$Tc-labelled peptides [19]. The uptake in tumour, pancreas, intestine and pituitary was specific and receptor mediated, as shown by the co-injection of cold peptide, indicating that these organs are also GRP receptor positive. Unlike others [16, 35, 36] we also found a decrease in the kidney uptake when a peptide-blocking dose was administered, whereas a substantial reduction in kidney uptake upon blocking was also shown recently by use of an $^{18}$F-labelled Lys$^3$-BN derivative [37]. The fast background clearance of the radiogallium peptide renders [$^{68}$Ga]-DOTA-PESIN an ideal radiotracer for PET imaging. The relatively fast initial washout from the tumour may be explained by radioligand not being internalised and being metabolised during its presence in the tumour compartment.

The structural entities which confer the suitable pharmacokinetic properties to this molecule most likely reside in the $PEG_4$ spacer. Preliminary data using shorter and longer spacers indicate that $PEG_4$ has an optimal length. The lack of affinity to the BB3 receptor may be advantageous as this orphan receptor is expressed in the human pancreas.

## Conclusion

Despite the relatively low binding affinity of [$Lu^{III}$, $Ga^{III}$]-DOTA-PESIN the corresponding radiopeptides show suitable pharmacokinetics in the PC-3 tumour-bearing mouse model, with high tumour uptake and relatively slow washout from the tumour. The radiopeptides show superior tumour-to-liver and suitable tumour-to-kidney ratios in comparison with our earlier published radiopeptides and even with the best $^{99m}$Tc-labelled BN analogues. This renders the new peptides suitable for clinical studies.

**Acknowledgements** We thank the Swiss National Science Foundation (Grant No. 3100A0-100390) and the European Network of Excellence 'EMIL' (European Molecular Imaging Laboratories, Grant No. 503569) for financial support of this work and Novartis Basel for analytical support.

## References

1. Reubi JC. Peptide receptors as molecular targets for cancer diagnosis and therapy. Endocr Rev 2003;24:389–427.
2. Behr TM, Behe M, Becker W. Diagnostic applications of radiolabeled peptides in nuclear endocrinology. Q J Nucl Med 1999;43:268–80.
3. Heppeler A, Froidevaux S, Eberle AN, Maecke HR. Receptor targeting for tumor localisation and therapy with radiopeptides. Curr Med Chem 2000;7:971–94.
4. Breeman WA, de Jong M, Kwekkeboom DJ, Valkema R, Bakker WH, Kooij PP, et al. Somatostatin receptor-mediated imaging and therapy: basic science, current knowledge, limitations and future perspectives. Eur J Nucl Med 2001;28:1421–9.
5. De Jong M, Kwekkeboom D, Valkema R, Krenning EP. Radiolabelled peptides for tumour therapy: current status and future directions. Plenary lecture at the EANM 2002. Eur J Nucl Med Mol Imaging 2003;30:463–9.
6. Anderson CJ, Welch MJ. Radiometal-labeled agents (non-technetium) for diagnostic imaging. Chem Rev 1999;99:2219–34.
7. Schmitt A, Bernhardt P, Nilsson O, Ahlman H, Kolby L, Maecke HR, et al. Radiation therapy of small cell lung cancer with $^{177}$Lu-DOTA-Tyr$^3$-octreotate in an animal model. J Nucl Med 2004;45:1542–8.
8. Kwekkeboom DJ, Bakker WH, Kooij PP, Konijnenberg MW, Srinivasan A, Erion JL, et al. [$^{177}$Lu-DOTA$^0$Tyr$^3$]octreotate: comparison with [$^{111}$In-DTPA$^0$]octreotide in patients. Eur J Nucl Med 2001;28:1319–25.
9. Maecke HR, Hofmann M, Haberkorn U. $^{68}$Ga-labeled peptides in tumor imaging. J Nucl Med 2005;46 Suppl 1:172S–8S.
10. Meyer GJ, Maecke H, Schuhmacher J, Knapp WH, Hofmann M. $^{68}$Ga-labelled DOTA-derivatised peptide ligands. Eur J Nucl Med Mol Imaging 2004;31:1097–104.
11. Reubi JC, Wenger S, Schmuckli-Maurer J, Schaer JC, Gugger M. Bombesin receptor subtypes in human cancers: detection with the universal radioligand $^{125}$I-[D-Tyr$^6$, beta-Ala$^{11}$, Phe$^{13}$, Nle$^{14}$] bombesin(6–14). Clin Cancer Res 2002;8:1139–46.
12. Breeman WA, Hofland LJ, de Jong M, Bernard BF, Srinivasan A, Kwekkeboom DJ, et al. Evaluation of radiolabelled bombesin analogues for receptor-targeted scintigraphy and radiotherapy. Int J Cancer 1999;81:658–65.
13. Van de Wiele C, Dumont F, Vanden Broecke R, Oosterlinck W, Cocquyt V, Serreyn R, et al. Technetium-99m RP527, a GRP analogue for visualisation of GRP receptor-expressing malignancies: a feasibility study. Eur J Nucl Med 2000;27:1694–9.
14. Smith CJ, Volkert WA, Hoffman TJ. Gastrin releasing peptide (GRP) receptor targeted radiopharmaceuticals: a concise update. Nucl Med Biol 2003;30:861–8.
15. Hoffman TJ, Gali H, Smith CJ, Sieckman GL, Hayes DL, Owen NK, et al. Novel series of $^{111}$In-labeled bombesin analogs as potential radiopharmaceuticals for specific targeting of gastrin-releasing peptide receptors expressed on human prostate cancer cells. J Nucl Med 2003;44:823–31.
16. Chen X, Park R, Hou Y, Tohme M, Shahinian AH, Bading JR, et al. microPET and autoradiographic imaging of GRP receptor expression with $^{64}$Cu-DOTA-[Lys$^3$]bombesin in human prostate adenocarcinoma xenografts. J Nucl Med 2004;45:1390–7.
17. Zhang H, Chen J, Waldherr C, Hinni K, Waser B, Reubi JC, et al. Synthesis and evaluation of bombesin derivatives on the basis of pan-bombesin peptides labeled with indium-111, lutetium-177, and yttrium-90 for targeting bombesin receptor-expressing tumors. Cancer Res 2004;64:6707–15.
18. Smith CJ, Gali H, Sieckman GL, Hayes DL, Owen NK, Mazuru DG, et al. Radiochemical investigations of $^{177}$Lu-DOTA-8-Aoc-BBN[7–14]$NH_2$: an in vitro/in vivo assessment of the targeting

ability of this new radiopharmaceutical for PC-3 human prostate cancer cells. Nucl Med Biol 2003;30:101–9.
19. Nock BA, Nikolopoulou A, Galanis A, Cordopatis P, Waser B, Reubi JC, et al. Potent bombesin-like peptides for GRP-receptor targeting of tumors with $^{99m}$Tc: a preclinical study. J Med Chem 2005;48:100–10.
20. Baidoo KE, Lin KS, Zhan Y, Finley P, Scheffel U, Wagner HN Jr. Design, synthesis, and initial evaluation of high-affinity technetium bombesin analogues. Bioconjug Chem 1998;9:218–25.
21. Scopinaro F, De Vincentis G, Varvarigou AD, Laurenti C, Iori F, Remediani S, et al. $^{99m}$Tc-bombesin detects prostate cancer and invasion of pelvic lymph nodes. Eur J Nucl Med Mol Imaging 2003;30:1378–82.
22. La Bella R, Garcia-Garayoa E, Langer M, Blauenstein P, Beck-Sickinger AG, Schubiger PA. In vitro and in vivo evaluation of a $^{99m}$Tc(I)-labeled bombesin analogue for imaging of gastrin releasing peptide receptor-positive tumors. Nucl Med Biol 2002;29:553–60.
23. Smith CJ, Sieckman GL, Owen NK, Hayes DL, Mazuru DG, Kannan R, et al. Radiochemical investigations of gastrin-releasing peptide receptor-specific [$^{99m}$Tc(X)$(CO)_3$-Dpr-Ser-Ser-Ser-Gln-Trp-Ala-Val-Gly-His-Leu-Met-$(NH_2)$] in PC-3, tumor-bearing, rodent models: syntheses, radiolabeling, and in vitro/in vivo studies where Dpr = 2,3-diaminopropionic acid and X = $H_2O$ or P $(CH_2OH)_3$. Cancer Res 2003;63:4082–8.
24. Chen J, Nguyen H, Metcalfe E, Eaton S, Arunachalam T, Raju N. Formulation and in vitro metabolism studies with $^{177}$Lu-AMBA; a radiotherapeutic compound that targets gastrin releasing peptide receptors. Eur J Nucl Med Mol Imaging 2004;31 Suppl 2:S281.
25. Van de Wiele C, Dumont F, Dierckx RA, Peers SH, Thornback JR, Slegers G, et al. Biodistribution and dosimetry of $^{99m}$Tc-RP527, a gastrin-releasing peptide (GRP) agonist for the visualization of GRP receptor-expressing malignancies. J Nucl Med 2001;42:1722–7.
26. Hoffmann T, Simpson S, Smith C, Simmons J, Sieckman G, Higginbotham C, et al. Accumulation and retention of Tc-99 m-RP527 by GRP receptor expressing tumors in scid mice. J Nucl Med 1999;40:104P (Abstract No. 419).
27. Nock B, Nikolopoulou A, Chiotellis E, Loudos G, Maintas D, Reubi JC, et al. [$^{99m}$Tc]Demobesin 1, a novel potent bombesin analogue for GRP receptor-targeted tumour imaging. Eur J Nucl Med Mol Imaging 2003;30:247–58.
28. Schuhmacher J, Maier-Borst W. A new $^{68}$Ge/$^{68}$Ga radioisotope generator system for production of $^{68}$Ga in dilute HCl. Int J Appl Radiat Isot 1981;32:31–6.
29. Markwalder R, Reubi JC. Gastrin-releasing peptide receptors in the human prostate: relation to neoplastic transformation. Cancer Res 1999;59:1152–9.
30. Fleischmann A, Laderach U, Friess H, Buechler MW, Reubi JC. Bombesin receptors in distinct tissue compartments of human pancreatic diseases. Lab Invest 2000;80:1807–17.
31. Schuhmacher J, Zhang H, Doll J, Maecke HR, Matys R, Hauser H, et al. GRP receptor-targeted PET of a rat pancreas carcinoma xenograft in nude mice with a $^{68}$Ga-labeled bombesin(6–14) analog. J Nucl Med 2005;46:691–9.
32. Heppeler A, Froidevaux S, Mäcke HR, Jermann E, Béhé M, Powell P, et al. Radiometal-labelled macrocyclic chelator-derivatised somatostatin analogue with superb tumour-targeting properties and potential for receptor-mediated internal radiotherapy. Chemistry A European Journal 1999;5:1016–23.
33. Rogers BE, Manna DD, Safavy A. In vitro and in vivo evaluation of a $^{64}$Cu-labeled polyethylene glycol-bombesin conjugate. Cancer Biother Radiopharm 2004;19:25–34.
34. Reubi JC, Schar JC, Waser B, Wenger S, Heppeler A, Schmitt JS, et al. Affinity profiles for human somatostatin receptor subtypes SST1–SST5 of somatostatin radiotracers selected for scintigraphic and radiotherapeutic use. Eur J Nucl Med 2000;27:273–82.
35. Lin KS, Luu A, Baidoo KE, Hashemzadeh-Gargari H, Chen MK, Brenneman K, et al. A new high affinity technetium-99m-bombesin analogue with low abdominal accumulation. Bioconjug Chem 2005;16:43–50.
36. Rogers BE, Bigott HM, McCarthy DW, Della Manna D, Kim J, Sharp TL, et al. MicroPET imaging of a gastrin-releasing peptide receptor-positive tumor in a mouse model of human prostate cancer using a $^{64}$Cu-labeled bombesin analogue. Bioconjug Chem 2003;14:756–63.
37. Zhang X, Cai W, Cao F, Schreibmann E, Wu Y, Wu JC, et al. $^{18}$F-labeled bombesin analogs for targeting GRP receptor-expressing prostate cancer. J Nucl Med 2006;47:492–501.